

Holocene sedimentary development and
event sedimentation of a mid-ocean atoll
lagoon, Maldives, Indian Ocean

Dissertation
zur Erlangung des Doktorgrades
der Naturwissenschaften

vorgelegt beim Fachbereich Geowissenschaften der
Goethe-Universität
in Frankfurt am Main

von
Lars Klostermann
aus Mainz
Frankfurt am Main, (2014)

(D30)

vom Fachbereich 11 der

Goethe-Universität Frankfurt am Main als Dissertation
angenommen.

Dekan: Prof. Dr. Ulrich Achatz

Gutachter: Prof. Dr. Eberhard Gischler
Prof. Dr. Christian Betzler

Datum der Disputation: 18. Mai 2015

Table of contents

Abbreviations	I
List of figures	III
List of tables	VIII
Chapter 1. Introduction	- 1 -
1.1 Geology of the Maldives	- 1 -
1.2 Aims and structure of the PhD thesis	- 2 -
Chapter 2. Holocene sedimentary evolution of a mid-ocean atoll lagoon, Maldives, Indian Ocean	- 5 -
2.1 Introduction	- 6 -
2.2 Setting/Study area.....	- 8 -
2.3 Methods	- 9 -
2.4 Results	- 13 -
2.4.1 Sedimentary facies	- 13 -
2.4.2 Facies distribution.....	- 19 -
2.4.3 Mineralogy.....	- 23 -
2.4.4 Sedimentation rates.....	- 24 -
2.5 Discussion	- 24 -
2.5.1 Interpretation of facies	- 24 -
2.5.2 Lagoonal sedimentation.....	- 26 -
2.5.3 Filled accommodation space versus empty bucket.....	- 30 -
2.6 Conclusions	- 31 -
Chapter 3. Sedimentary record of late Holocene event beds in a mid-ocean atoll lagoon, Maldives, Indian Ocean: potential for deposition by tsunamis.....	- 34 -
3.1 Introduction	- 35 -
3.2 Regional setting.....	- 36 -
3.3 Methods	- 37 -
3.4 Results and interpretation	- 40 -

3.5 Discussion	- 45 -
3.5.1. Tsunamis versus storms	- 45 -
3.5.2 Limitations of the study	- 46 -
3.6 Conclusions	- 48 -
Chapter 4. Changes in diversity and assemblages of foraminifera through the Holocene in an atoll from the Maldives, Indian Ocean.....	- 49 -
4.1 Introduction	- 50 -
4.2 Study area	- 53 -
4.2.1. Geomorphology, sedimentology and benthic foraminifera	- 53 -
4.2.2 Hydrology and climate.....	- 56 -
4.3 Material and Methods.....	- 57 -
4.3.1 Sediment core collection, age determination, sea level reconstruction and sedimentology	- 57 -
4.3.2 Foraminiferal analysis.....	- 58 -
4.4 Results	- 60 -
4.4.1 Sedimentology and occurrence of benthic foraminifera.....	- 60 -
4.4.2 Foraminiferal assemblages and diversity in Core #16.....	- 62 -
4.4.3 Foraminiferal assemblages and diversity in Core #19	- 68 -
4.5 Discussion	- 72 -
4.5.1. Foraminiferal assemblages and diversity.....	- 74 -
4.5.2 Foraminiferal diversity and changes in the bottom water circulation of the lagoon.....	- 78 -
4.6 Conclusions	- 79 -
Chapter 5. Summary and conclusion	- 81 -
Zusammenfassung.....	- 84 -
References	- 89 -
Danksagung/Acknowledgements	- 99 -
Appendix	

Abbreviations

AMS	accelerated mass spectroscopy
BP	before present (present = 1950)
DCA	Detrended Correspondence Analysis
e.g.	<i>exempli gratia</i> (for example)
et al.	<i>et alii/aliae</i> (und andere)
Fig.	figure
HST	highstand systems tract
HMC	high magnesium calcite
i.e.	<i>id est</i> (that is / to say)
IDH	Intermediate Disturbance Hypothesis
kyrs	kilo years (1000 years)
LGM	Last Glacial Maximum
LMC	low magnesium calcite
LST	lowstand systems tract
mcaFR	mollusk-coral-algal floatstone to rudstone
mcaWF	mollusk-coral-algal wackestone to floatstone
mcMW	mollusk-coral mudstone to wackestone
mcrR	mollusk-coral-red algae rudstone
mcW	mollusk-coral wackestone
mM	mollusk mudstone
ODP	Ocean Drilling Program
PAST	Palaeontological Statistics
PCA	Principal Component Analysis
pers. comm.	personal comment
psu	practical salinity unit
RV	research vessel
sp.	species
spp.	species (plural)
SST	sea surface temperature

Abbreviations

TST	transgressive systems tract
wt. %	percentage by weight
XRD	X-ray diffractometry
yr	year
yrs	years

List of figures

Fig. 1.1 Surface facies map of Rasdhoo Atoll. From: Gischler (2006). - 2 -

Fig. 2.1 a Location of the Maldivian archipelago and Rasdhoo Atoll in the Indian Ocean; **b** locations of the seventeen investigated cores and the four transects (A-D) within Rasdhoo Atoll lagoon. - 9 -

Fig. 2.2 Core photos; **a** the soil and peat layer toward the base of core 16; **b** a coarse-grained 1-cm-thick sediment layer marking a sedimentary event in core 12; **c** a big foliaceous coral in core 31; **d, e** a coarse-grained sandy layer toward the top and transition to coral rubble sediments toward the base of core 26. - 14 -

Fig. 2.3 Tree diagram of cluster analyses (Ward's method) of sediment data illustrating six carbonate facies and a soil/peat facies. Variables: Relative abundances of mollusk, coral, foraminifera, echinoderms, Halimeda, red algae, crustacean, peloids, opaque grains, grain-size fraction < 125 μm and > 2 mm, and mineralogy. - 16 -

Fig. 2.4 Transect A through southern Rasdhoo Atoll including cores 8, 11, 12, and 13 with detailed facies description. According to radiometric age measurements isochrones are drawn. The ages are calendar-calibrated with a two-sigma probability in yrs BP and kyrs BP (in green). Core 11 has not been dated. Branched corals are *Acropora* sp., *Seriatopora* sp., and *Caulastrea* sp.; foliaceous corals are *Leptoseris* sp., *Porites* sp., *Cyphastrea* sp., *Merulina* sp., *Pachyseris* sp., and *Echinophyllia* sp.; massive corals are *Porites* sp., *Favia* sp., *Goniopora* sp., and *Faviidae*; solitary corals are *Fungia* sp. and *Caryophyllia* sp.. HST highstand systems tract..... - 20 -

Fig. 2.5 Transect B through central Rasdhoo Atoll including cores 1, 24, 27, and 29 with detailed facies description. According to radiometric age measurements isochrones are drawn. The ages are calendar-calibrated with a two-sigma probability in yrs BP and kyrs BP (in green). The base of core 1 has not been dated. Branched corals are *Acropora* sp., *Seriatopora* sp., and *Caulastrea* sp.; foliaceous corals are *Leptoseris* sp., *Porites* sp.,

Cyphastrea sp., *Merulina* sp., *Pachyseris* sp., and *Echinophyllia* sp.; massive corals are *Porites* sp., *Favia* sp., *Goniopora* sp., and *Faviidae*; solitary corals are *Fungia* sp. and *Caryophyllia* sp.. *HST* highstand systems tract..... - 21 -

Fig. 2.6 Transect C through central Rasdhoo Atoll including cores 16, 18, 30, 31, and 34 with detailed facies description. According to radiometric age measurements isochrones are drawn. The ages are calendar-calibrated with a two-sigma probability in yrs BP and kyrs BP (in green). Branched corals are *Acropora* sp., *Seriatopora* sp., and *Caulastrea* sp.; foliaceous corals are *Leptoseris* sp., *Porites* sp., *Cyphastrea* sp., *Merulina* sp., *Pachyseris* sp., and *Echinophyllia* sp.; massive corals are *Porites* sp., *Favia* sp., *Goniopora* sp., and *Faviidae*; solitary corals are *Fungia* sp. and *Caryophyllia* sp.. *LST* lowstand systems tract, *TST* transgressive systems tract, *HST* highstand systems tract. ... - 22 -

Fig. 2.7 Transect D through northern Rasdhoo Atoll including cores 2, 19, 25, and 26 with detailed facies description. According to radiometric age measurements isochrones are drawn. The ages are calendar-calibrated with a two-sigma probability in yrs BP and kyrs BP (in green). Cores 2 and 25 have not been dated. Branched corals are *Acropora* sp., *Seriatopora* sp., and *Caulastrea* sp.; massive corals are *Porites* sp., *Favia* sp., *Goniopora* sp., and *Faviidae*; solitary corals are *Fungia* sp. and *Caryophyllia* sp.. *TST* transgressive systems tract, *HST* highstand systems tract..... - 23 -

Fig. 2.8 Reconstructed sedimentary paleo-water depth of eleven cores in comparison to two sea-level curves from the Maldives. Due to insufficient age-data cores 1, 2, 11, 25, 27, and 30 are not shown. The depths in cores are corrected for vertical compaction. *LST* lowstand systems tract, *TST* transgressive systems tract, *HST* highstand systems tract. ... - 26 -

Fig. 2.9 Schematic transects (vertically exaggerated) through a mid-ocean atoll (Rasdhoo Atoll) showing Holocene reef growth and lagoonal sediment accumulation. **a** Sea-level lowstand >10 kyrs BP, subaerial exposure and erosion (karst) of a Pleistocene atoll reef and soil formation; **b** Sea-level rise to lagoon base ca. 10 kyrs BP, swamp development in the lagoon with mangroves depositing peat; **c** Sea-level reaches modern

level ca. 4.5 kyrs BP, marginal reef keeping up and lagoonal reef growth catching up sea-level, carbonate sediments accumulate in the lagoon; **d** Modern situation ca. 1 kyr BP, marginal and lagoonal reefs at mean sea-level, lagoonal sediment accumulation and sand apron progradation filling up the lagoon. *LST* lowstand systems tract, *TST* transgressive systems tract, *HST* highstand systems tract..... - 30 -

Fig. 3.1 A. Location of the Maldivian archipelago and Rasdhoo Atoll in the Indian Ocean; **B.** Locations of ten investigated core stations within Rasdhoo Atoll lagoon. - 37 -

Fig. 3.2 Ten core logs highlighting six sedimentary events. Core logs are arranged so that event layers may be correlated in a clearly laid-out manner. The age range and mean of each event are shown in the table within the figure. The ages are calendar-calibrated with a two-sigma probability in yrs BP. The branched coral symbols mark the redeposited corals (e.g., *Acropora* sp., *Seriatopora* sp.) and the solid coral symbols mark the insitu corals that have not been transported (e.g., *Porites* sp., *Leptoseris* sp.). Close-ups of the first three cores showing event 2 in detail are displayed in Fig. 3.3. Average lagoonal background sedimentation rate amounts to 0.92 m/kyrs, based on 53 calculations between dated samples (not shown)..... - 40 -

Fig. 3.3 Close-up of the topmost 60 cm of three marginal cores 1, 12, and 26. Sedimentation rates and the composition of the coarser layers show a change in sedimentation and facies types. The dashed line is the statistical mean; the gray area is the standard deviation ($\pm 1\sigma$). - 45 -

Fig. 4.1 a The location of the Maldives in the Indian Ocean. **b** The Maldives archipelago with Rasdhoo Atoll including all-year predominant wind directions. - 54 -

Fig. 4.2 a The modern distribution of sediment facies after Gischler (2006). **b** Lagoon assemblages of benthic foraminifera defined by Parker and Gischler (2011). Red dots indicate the sampling location of Core #16 (4°17'56 N/72°57'47 E) and Core #19 (4°19'34 N/72°59'35 E). **c** Location of the Cores #16 and #19 in the lagoon profile.- 56 -

Fig. 4.3 Sedimentological descriptions for (a) Core #16 and (b) Core #19. Carbonate facies were defined based on the limestone classifications of Dunham (1962) and the

extended classification by Embry and Klovan (1971). Point counting data of thin sections of the most common components in the grain-size fraction >125 μm . Note that the percentages of components were converted into percentages of the bulk weight of the sample. - 59 -

Fig. 4.4 Abundances in % of the 5 most common species, the highly diverse genus *Quinqueloculina* and *Triloculina* in Core #16, the foraminiferal accumulation rate and the estimation of the paleo water depth through time (Gischler et al., 2008) for (a) Core #16 and (b) Core #19. - 62 -

Fig. 4.5 Detrended Correspondence Analysis of the foraminiferal fauna of Core #16 to define foraminiferal assemblages through time. The species abundances were log-normal transformed prior to analysis. - 64 -

Fig. 4.6 Principal Component Analysis of the foraminiferal fauna of Core #16 showing principal components 1 and 2 and 1 and 3. Symbols refer to the assemblages defined in Fig. 4.5 - 66 -

Fig. 4.7 Diversity indices for the samples of Core #16 and Core #19 to illustrate the diversity trend in the samples through the cores. - 67 -

Fig. 4.8 Triplots of the proportion of Agglutinated, Hyaline and Miliolid foraminifera in the foraminiferal assemblages for (a) Core #16 and (b) Core #19. Black circles indicate core samples of this study, and white circles indicate surface samples from Rasdhoo Atoll (Parker and Gischler, 2011). Gray arrows in (a) indicate the path of the samples throughout the Holocene. - 68 -

Fig. 4.9 Detrended Correspondence Analysis of the foraminiferal fauna of Core #19 to define foraminiferal assemblages through time. The species abundances were log-normal transformed prior to analysis. - 69 -

Fig. 4.10 Principal Component Analysis of the foraminiferal fauna of Core #16 showing principal components 1 and 2 and 1 and 3. Symbols refer to the assemblages defined in Fig. 4.9. The species abundances were log-normal transformed prior to analysis. - 71 -

Fig. 4.11 Schematic illustration of the van Arx’s (1954) model of restricted circulation applied for Rasdhoo Atoll. **(a)** Lagoon circulation before the sand spit development in the Late Holocene after 4.0 kyrs BP. **(b)** Lagoon circulation after the development of the sand spit in the northwestern lagoon. - 79 -

List of tables

Table 2.1 Investigated cores drilled in the Rasdhoo Atoll lagoon	- 10 -
Table 2.2 Mineralogy of the clay minerals in the soil facies of core 16	- 11 -
Table 2.3 Radiocarbon and AMS ages of all samples.....	- 11 -
Table 2.4 Mineralogy of core 16	- 15 -
Table 3.1 Radiometric ages in years before present (BP) of coral, shell, and bulk sediment samples.	- 39 -
Table 3.2 List of identified corals with redeposited, shallow-water taxa marked....	- 41 -
Table 4.1 The averaged abundances of the most common species >2% of the assemblages defined in Fig. 4.5. Distances in cm are given from the core top.	- 67 -
Table 4.2 The averaged abundances of the most common species >2% of the assemblages defined in Fig. 4.9. Distances are given from the core top.	- 70 -
Plate 4.1 Scanning Electron Microscope images (1-15) and light micrographs (16-17) of selected benthic foraminifera. 1-3. <i>Ammonia</i> sp, 1 (SMFXXVII7605). 4,5. <i>Quinqueloculina</i> cf. <i>Q. oblonga</i> (SMFXXVII7586). 6-8. <i>Cymbaloporeta bradyi</i> (SMFXXVII7603). 9-11. <i>Spiroloculina nummiformis</i> (SMFXXVII7581). 12-15. <i>Textularia foliacea</i> (12: SMFXXVII7575; 13: SMFXXVII7576; 14: SMFXXVII7575; 15: SMFXXVII7574). 16-17. <i>Operculina ammonoides</i> (SMFXXVII7616). Note the different scale for images 16 and 17. SMF = Senckenberg Museum Frankfurt. The specimen derives from E. Gischler's collection of surface samples from Radhoo and Ari Atoll.	- 63 -

Chapter 1. Introduction

1.1 Geology of the Maldives

The Maldivian archipelago is among of the largest carbonate platforms on Earth. It is part of the submarine volcanic Chagos-Laccadive Ridge plateau located in the northern central Indian Ocean, southwest of India (7°N to 1°S at 73°E). The Maldivian reefs started to grow on an Early Eocene volcanic basement (Duncan and Hargraves, 1990) and to date an approximately 3 km thick carbonate limestone framework was built up (Belopolsky and Droxler, 2004). The Paleogene and Neogene development of the Maldivian carbonate succession is completely recorded by different explorations wells, seismic surveys, and the ODP Site 716 (Aubert and Droxler, 1992; Purdy and Bertram, 1993; Aubert and Droxler, 1996; Belopolsky and Droxler, 2003, 2004; Betzler et al., 2009, 2012, 2013; Lüdmann et al., 2013). Based on Pleistocene glacial and interglacial periods sea-level was fluctuating (Paul et al., 2012; and references therein). Periodically, the Pleistocene reefs were subaerially exposed and erosion (karst) took place, recognizable by large hiatus under atolls (Aubert and Droxler, 1992; Purdy and Bertram, 1993; Aubert and Droxler, 1996; Gischler et al., 2008; Betzler et al., 2012). Since the Last Glacial Maximum (LGM) sea-level rose to around 60 m below modern mean sea-level, some 12 kyrs BP (Camoin et al., 2004). Between 11 and 10 kyrs BP the carbonate platform and atoll lagoons were flooded by the continuously rising sea-level marking the Holocene transgression (Camoin et al., 1997; Dullo et al., 1998; Zinke et al., 2003, Gischler, 2003).

Rasdhoo Atoll is located in the central part of the archipelago, has a diameter of 9.25 km, and covers an area of 62 km². The lagoon harbors numerous patch reefs and three channels, up to 10 m deep, connect the interior lagoon with the open ocean. Modern reef facies are coralgall grainstones and lagoonal facies include wackestone, mudstone, and hardgrounds in the vicinity of channels (Fig. 1.1; Gischler, 2006). Between the reef margin and the atoll lagoon, sand aprons are found that are widest on the western (windward) side of the atoll. A sand spit parallel to the northern and northeastern atoll reef margin divides the lagoon in a shallow enclosed area with water depth <15 m and a deep lagoon with water depth up to 40 m.

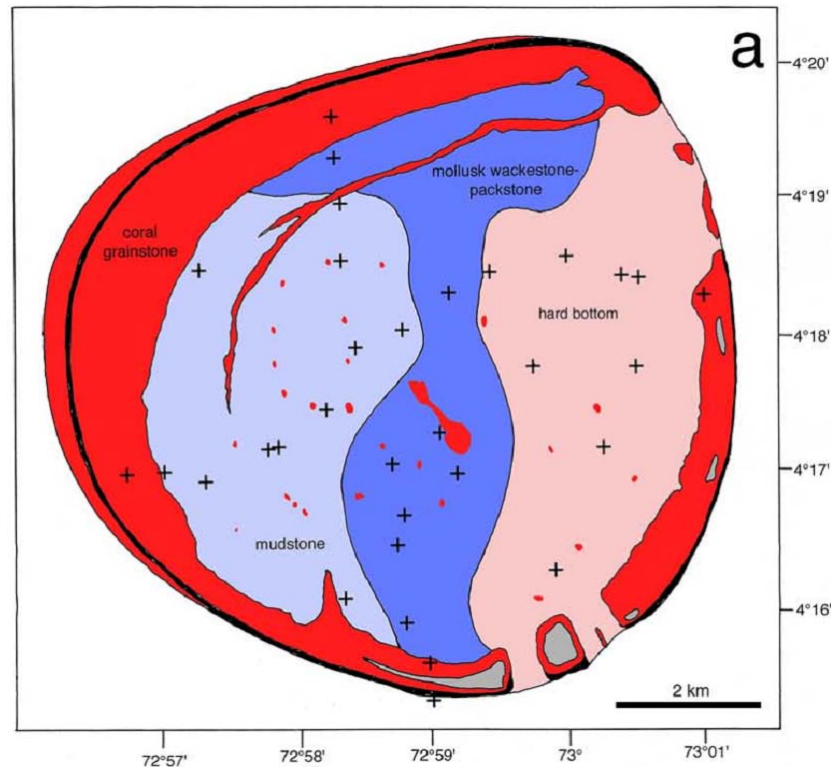


Fig. 1.1 Surface facies map of Rasdhoo Atoll. From: Gischler (2006).

1.2 Aims and structure of the PhD thesis

Based on Holocene sea-level curves from the Maldives at Rasdhoo Atoll (Gischler et al., 2008) and at Maalhosmadulu Atoll (Kench et al., 2009), considering growth rates of reef and patch reefs, Holocene lagoonal sediments of Rasdhoo Atoll were further investigated. In particular, atoll lagoon sediment cores can provide important information regarding (1) the development and natural infill of carbonate sediment successions of an atoll lagoon, (2) the response of low-lying land areas to sea-level rise, and (3) the history of tsunamis in the recent geologic past.

During an expedition from 12 November until 4 December 2010, forty-two stations in the Rasdhoo Atoll lagoon were selected for coring with a Rossfelder electrical vibracorer. At thirty-nine stations, cores were recovered and seventeen cores were chosen for sedimentological, mineralogical, and chronological analyses. Among these, nine cores are located in the center and eight cores derive from the margin of the lagoon. Water depths range from 10.7-20.0 m at the marginal coring sites (1, 2, 11, 12, 18, 19,

25, and 26) and from 21.6-37.6 m at the central coring sites (8, 13, 16, 24, 27, 29, 30, 31, and 34). No cores were collected from sand aprons and lagoonal carbonate shoals, because the Rossfelder coring system may only be used in water depths >10 m.

In the home laboratory, cores were opened, described, and samples were collected within one half of the core. The other half was saved as archive. A total of 296 sediment samples were collected and analyzed. Forty-nine samples were dated radiometrically with accelerated mass spectroscopy (AMS) and nine corals were dated using the standard radiocarbon ^{14}C -method by Beta Analytic Inc., Miami, Florida (Bard, 1998).

This PhD thesis is based on three manuscripts. Two manuscripts have been published in peer-reviewed journals (Chapters 3 and 4) and one is accepted for publication by the *Int. J. Earth Sci. (Geol. Rundsch.)* (Chapter 2).

In the first manuscript (Chapter 2), entitled "Holocene sedimentary evolution of a mid-ocean atoll lagoon, Maldives, Indian Ocean" the development of lagoonal sediments during the Holocene transgression from 10 kyrs BP until today is described. Seventeen cores were chosen for sedimentological, mineralogical, and chronological analyses covering the entire lagoon of Rasdhoo Atoll. Eight sediment facies have been classified including mineralogy and sedimentation rates. Considering local sea-level curves and reconstructed growth rates of reef and patch reefs, the Holocene lagoonal deposition history from about 10 kyrs BP until today is described.

In the second manuscript (Chapter 3), entitled "Sedimentary record of late Holocene event beds in a mid-ocean atoll lagoon, Maldives, Indian Ocean: potential for deposition by tsunamis" coarse-grained sediment layers in ten lagoonal sediment cores of Rasdhoo Atoll, are interpreted as tsunami deposits. Six event layers can be correlated among several cores within the last 6.5 kyrs. Five of the six layers may be correlated to previously published tsunami events at adjacent coastal research sites. Although, the mid-late Holocene atoll lagoon archive is incomplete based on the assumption that major earthquakes at the Indonesian subduction zone generated more than six major tsunamis, the importance of such record is clearly shown.

In the third manuscript (Chapter 4), entitled "Changes in diversity and assemblages of foraminifera through the Holocene in an atoll from the Maldives, Indian

Ocean" the temporal variation of benthic foraminiferal diversity and assemblages through the Holocene within the sediments of two cores from Rasdhoo Atoll is explored. Only few studies have examined changes in benthic foraminiferal assemblages and diversity through the Holocene in tropical reef environments (Schultz et al., 2010; Cheng et al., 2012). In the Indian Ocean, no such studies have been conducted. Complementary to the study of Parker and Gischler (2011) who investigated spatial patterns of distribution, diversity and assemblages in surface sediments from Rasdhoo and Ari Atolls at the Maldives, this study interpret distinct faunal changes around 4.0 kyrs BP and 1.4 kyrs BP to changing bottom water circulation related to the formation of a sand spit.

In Chapter 5 the main conclusions from chapters 2-4 are summarized.

Chapter 2. Holocene sedimentary evolution of a mid-ocean atoll lagoon, Maldives, Indian Ocean

Lars Klostermann, Eberhard Gischler

Institut für Geowissenschaften, Goethe-Universität Frankfurt, Altenhoferallee 1, 60438 Frankfurt am Main, Germany

Keywords: Carbonate sediment, Sediment facies, Lagoon, Holocene, Maldives, Indian Ocean

Accepted by the Int. J. Earth Sci. (Geol. Rundsch.), DOI 10.1007/s00531-014-1068-8.

Abstract: Based on detailed analyses of cores covering the lagoon of Rasdhoo Atoll, Maldives, six carbonate facies, one soil, and one peat facies have been identified. The abundance of carbonate and rare opaque grains was quantified with a point counter. X-ray diffractometry was used to measure mineralogical composition of samples. The statistical delineation of facies using cluster analysis was based on point-count, mineralogical, and textural analyses. In decreasing abundance, the six carbonate facies are classified as mollusk-coral-algal floatstone to rudstone (30%), mollusk-coral-red algae rudstone (23%), mollusk-coral-algal wackestone to floatstone (23%), mollusk-coral wackestone (13%), mollusk-coral mudstone to wackestone (9%), and mollusk mudstone (2%). The carbonate facies represent lagoonal background sedimentation, mostly consisting of fine sediments, and event sedimentation depositing transported coarse-grained reefal components. Fifty-seven carbonate samples and one peat sample were dated radiometrically, covering the Holocene transgression from 10 kyrs BP until today. Comparing the sediment accumulation data of the lagoon with two reconstructed local sea-level curves, three systems tracts can be identified: (1) a lowstand systems tract (LST) characterized by karst and soil deposition >10 kyrs BP, (2) a transgressive systems tract (TST) with peat and carbonate separated by hiatus 10-6.5 kyrs BP, and (3) a highstand systems tract (HST) dominated by carbonate sedimentation 6.5-0 kyrs BP,

further divided into three stages (6.5-3, 3-1, 1-0 kyrs BP). During the Holocene transgression, sedimentation rates increased continuously to a maximum of 1.4 m/kyr during 3-1 kyrs BP. Modern (1-0 kyrs BP) mean sedimentation rates average 0.6 m/kyr. A simple calculation suggests that two processes (background sedimentation, sand apron progradation) will probably fill up the accommodation space of the lagoon during the Holocene highstand, but these processes will not suffice to fill the larger atoll lagoons of the archipelago.

2.1 Introduction

Sedimentation in mid-ocean atoll and barrier reef lagoons is an ongoing process and has a widely spread community of interests. Scientific and economic research is focused on carbonate production, deposition, distribution, and dissolution, not only because carbonate reefs and platforms have the ability of being reservoir rocks for hydrocarbons, but also because of possible help in deciphering future climate change and the understanding of the carbon cycle by means of using lagoon deposits as archives of environmental change.

Still, the number of atoll lagoon core studies is limited. Tudhope (1989) found an up to 10 m thick Holocene sediment package in the lagoon of Davies Reef, Great Barrier Reef. Skeletal muddy sands were interpreted to be produced largely at atoll reef margin. Smithers et al. (1992) collected cores in the lagoon of Cocos (Keeling) Atoll, eastern Indian Ocean, distinguished three skeletal facies, and identified sand apron progradation as important lagoonal infill process. Yamano et al. (2002) investigated tropical Holocene lagoonal sedimentation processes in the Pacific. They analyzed surface and core sediments from three Pacific atoll lagoons in Palau and the Marshall Islands and distinguished three lagoonal carbonate facies, mainly based on the occurrence of two species of benthic foraminifera. Gischler (2003) analyzed lagoonal sediment cores from atolls off Belize in the Caribbean Sea. Pleistocene limestone bedrock was superposed by >6 m thick Holocene sediment successions of soil, peat, and lagoonal carbonate sediment mainly classified as wackestone and packstone. In the South China Sea, Yu et al. (2009) investigated sediments of the Late Holocene (4-0 kyrs BP) in the lagoon of Yongshu Reef. They measured the content of coarse-grained sediment fraction along a

lagoon core and dated wave-transported coral blocks in order to detect high energy (storm, tsunami) events.

Like in atolls, core studies in oceanic barrier reef systems are rare. In the Indian Ocean, Zinke et al. (2003b, 2005) analyzed sediment facies and faunal assemblages during Holocene transgression in the Lagoon of Mayotte, Comoro Archipelago. Due to the existence of a central volcanic island, the occurrence of Early Holocene terrigenous muddy to sandy sediments distinguish the barrier lagoon from atoll lagoon successions. Based on both core and seismic data, Zinke et al. (2001, 2003a) also interpreted lagoonal successions in terms of sequence stratigraphy and differentiated lowstand, transgressive, and highstand deposits. In a French Polynesian barrier reef system, Toomey et al. (2013) measured grain-size variation along lagoon cores in order to identify high-energy event (storm) layers during the Holocene (5-0 kyrs BP).

Although the Maldivian Archipelago is among the largest carbonate platforms, built up by numerous atolls, lagoons, patch reefs, and faroes (characteristic ring-shaped reefs), only few studies focused on modern lagoonal sediments (Gardiner and Murray, 1906; Ciarapica and Passeri, 1993; Bianchi et al., 1997; Gischler, 2006). There are a limited number of investigations of atoll reef development recording Holocene sea-level change (Woodroffe, 1992; Gischler et al., 2008; Kench et al., 2009). Kench et al. (2005) and Perry et al. (2013) used cores from sand keys and faroes to reconstruct island and lagoonal faro development. Results of the German RV METEOR cruise of 2007 in the Maldives suggest that current and sea level were major driving forces of Neogene carbonate platform development (Betzler et al., 2009, 2012, 2013; Paul et al., 2012; Lüdmann et al., 2013). Still, these studies are largely based on core and seismic data from deeper water off-reef areas; no data were collected on top of modern atoll lagoons and reefs. In the wider framework of this study, sediment cores from atoll lagoons were used to reconstruct Holocene sedimentary events and benthic foraminifera assemblages and diversity (Klostermann et al., 2014; Storz et al., 2014).

The purpose of this study is to detail, for the first time, facies, chronology, and sedimentation rates of a Maldivian atoll lagoon during the Holocene from 10 kyrs BP until today based on sediment cores covering the deep platform interior. We interpret

sedimentary succession in terms of sequence stratigraphy, and discuss the question as to whether or not available accommodation space will be filled.

2.2 Setting/Study area

The Maldives are located in the northern central Indian Ocean, southwest of India (1°S to 7°N at 73°E) and cover an area of 107,500 km² including 1,300 small islands on 21 atolls and four reef-fringed islands (Gischler et al., 2014) (Fig. 2.1a). The atolls are built up by coral reefs encircling lagoons with numerous patch reefs. Marginal and lagoonal reefs often form circular entities known as faroes. Islands are made of carbonate sand with a maximum elevation of 5 m above sea-level and are situated on marginal and lagoonal reefs (Kench et al., 2005). The interior lagoons are connected with the Indian Ocean by channels and passes through the marginal reefs. Rasdhoo Atoll (4°N/73°W) is located in the central western part of the archipelago (Fig. 2.1b), has a diameter of 9.25 km, and covers an area of 62 km². The almost continuous, shallow reef margin encircles an interior lagoon. Between the reef margin and the atoll lagoon, sand aprons are found that are widest on the western (windward) side of the atoll. A sand spit parallel to the northern and northeastern atoll reef margin divides the lagoon in a shallow enclosed area with water depth <15 m and a deep lagoon with water depth up to 40 m. Three channels, up to 10 m deep, connect the interior lagoon with the open ocean.

Along the Maldivian archipelago, precipitation increases from 1650 mm/yr in the north to 2400 mm/yr in the south (Purdy and Bertram, 1993). The seasonal rain fall and wind directions are driven by the northeast monsoon with low wind intensities from October–April and by a southwest monsoon with relative strong prevailing winds from May–September (Storz and Gischler, 2011). Strong swells approach the archipelago predominantly from the southwest (Kench and Brander, 2006). The close position to the equator causes the Maldives to be largely free of cyclones (Woodroffe, 1992; Sing et al., 2000; Webster et al., 2005; Gischler et al., 2008), but strong tsunami waves generated at the northeastern coast of the Indian Ocean have impacted the Maldives, thereby depositing lagoonal sedimentary event layers (Klostermann et al., 2014).

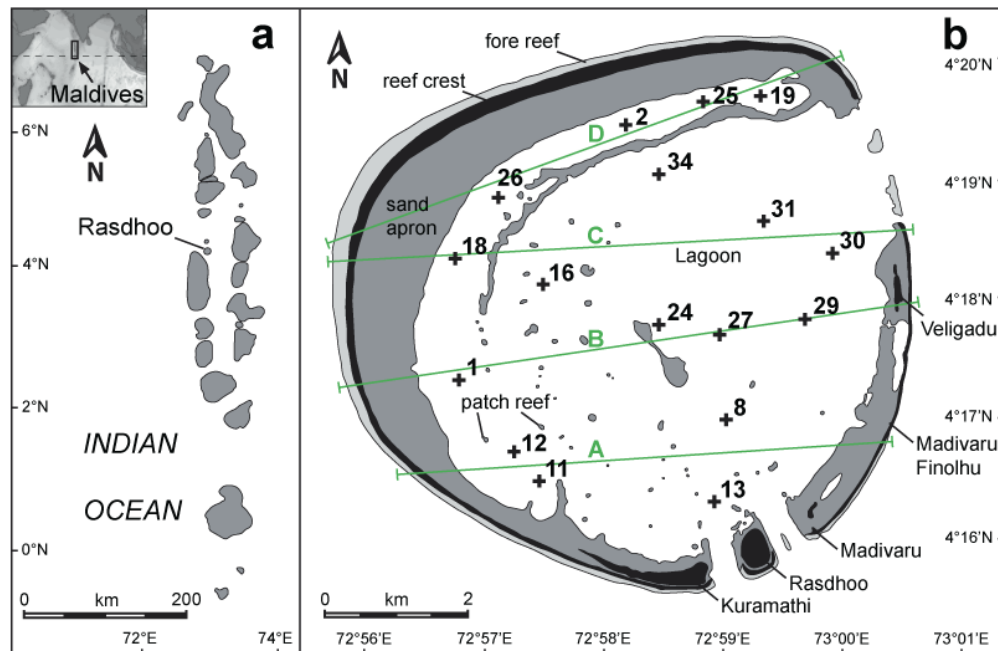


Fig. 2.1 **a** Location of the Maldivian archipelago and Rasdhoo Atoll in the Indian Ocean; **b** locations of the seventeen investigated cores and the four transects (A-D) within Rasdhoo Atoll lagoon.

2.3 Methods

During an expedition from 12 November until 4 December 2010, forty-two stations in the Rasdhoo Atoll lagoon were selected for coring with a Rossfelder electrical vibracorer connected with aluminum pipes measuring a diameter of 7.5 cm and a length of 6 m. At thirty-nine stations, cores were recovered with an average core length of 2.22 m. The longest core is 5.04 m, the shortest core spans 0.59 m. The total core length is 93.24 m. Sediment compaction during drilling was estimated to 10-53%, averaging 32%. Seventeen cores were chosen for sedimentological, mineralogical, and chronological analyses (Table 2.1). Among these, nine cores are located in the center and eight cores derive from the margin of the lagoon (Fig. 2.1). Water depths range from 10.7-20.0 m at the marginal coring sites (1, 2, 11, 12, 18, 19, 25, and 26) and from 21.6-37.6 m at the central coring sites (8, 13, 16, 24, 27, 29, 30, 31, and 34). No cores were collected from sand aprons and lagoonal carbonate shoals, because the Rossfelder coring system may only be used in water depths >10 m.

Table 2.1 Investigated cores drilled in the Rasdhoo Atoll lagoon

Core no.	Local Date	Local Time	Coordinates		Water Depth [m]	Penetration [m]	Core length [m]
			Latitude (N)	Longitude (E)			
1	11.20.2010	10:25	04°17'11	72°57'03	15.0	4.30	2.70
2	11.21.2010	10:05	04°19'20	72°58'28	10.7	4.25	2.00
8	11.24.2010	11:40	04°16'51	72°59'18	36.8	2.23	2.01
11	11.24.2010	16:15	04°16'20	72°57'43	18.0	0.87	0.64
12	11.24.2010	17:20	04°16'35	72°57'31	20.0	3.58	2.44
13	11.25.2010	09:35	04°16'10	72°59'12	29.5	2.37	1.65
16	11.25.2010	14:50	04°17'56	72°57'47	34.5	5.49	4.56
18	11.26.2010	09:00	04°18'12	72°57'01	14.3	5.67	3.37
19	11.26.2010	10:30	04°19'34	72°59'35	13.6	5.18	3.28
24	11.27.2010	14:15	04°17'39	72°58'44	28.5	2.64	1.52
25	11.27.2010	16:10	04°19'32	72°59'06	11.7	?	1.86
26	11.27.2010	17:30	04°18'43	72°57'23	12.6	3.03	2.01
27	11.28.2010	09:45	04°17'34	72°59'14	21.6	1.49	0.92
29	11.28.2010	13:25	04°17'42	72°59'58	37.5	2.27	1.42
30	11.30.2010	10:20	04°18'15	73°00'12	37.6	0.70	0.59
31	11.30.2010	11:40	04°18'31	72°59'37	37.0	2.04	1.26
34	11.30.2010	16:35	04°18'55	72°58'44	30.0	5.80	4.01

In the home laboratory, cores were opened, described, and samples were collected within one half of the core. The other half was saved as archive. Cores 1, 2, 11, 25, 27, and 30 were sampled with varying sample distance depending on the facies. Cores 8, 12, 13, 16, 18, 19, 24, 26, 29, 31, and 34 were sampled at 10 cm-intervals. A total of 296 sediment samples were collected and sieved through 0.125 mm and 2 mm sieves. Two to three grams of bulk carbonate sediment of each sample were pulverized to quantify the mineralogy using X-ray diffractometry (Milliman, 1974). X-ray diffractometry of the grain-size fraction $\leq 2 \mu\text{m}$ with vaporized ethylene glycol were used to quantify clay minerals in the soil unit of core 16 (Table 2.2). Depending on the sediment facies within each core, a split of 208 samples, using the grain-size fraction 0.125-2 mm, was embedded in epoxy resin in order to prepare thin-sections. Two-hundred grains per thin-section were identified using a point counter (van der Plas and Tobi, 1965). Forty-six samples of bulk sediment, one peat sample, and two shell samples were dated radiometrically with accelerated mass spectroscopy (AMS) and nine corals were dated using the standard radiocarbon ^{14}C -method by Beta Analytic Inc., Miami, Florida (Bard, 1998) (Table 2.3).

Table 2.2 Mineralogy of the clay minerals in the soil facies of core 16

Sample no.	Al Chlorite [rel.%]	Mixed Layer [rel.%]	Kaolinite [rel.%]	Pyrite [rel.%]	Goethite [rel.%]
#16 415-420	36,2	21,1	38,2	3,6	0,9
#16 425-430	25,0	33,3	37,4	0,0	4,3
#16 435-440	44,6	25,2	24,9	0,0	5,3
#16 445-450	39,5	24,2	26,2	0,0	10,1

Relative abundance of clay minerals measured in the grain-size fraction <2 μm sum up to 100%

Based on visual inspection and point-counting results, preliminary facies were defined based on the classification of limestones by Dunham (1962) and the extended classification by Embry and Klovan (1972). Component and matrix supported textures were differentiated based on either more or less than 50% fines (<0.125 mm). The final statistical delineation of facies including all point-count data, as well as the abundances of the grain-size fraction <0.125 mm and >2 mm was made using cluster analyses (Ward's method) provided by the software tool PAST, version 2.17c (Hammer et al., 2001). Four transects were drawn to compare the different units and classified facies of each core.

Table 2.3 Radiocarbon and AMS ages of all samples

Core #	Sampling depth [cm]	Description	Beta No.	Conventional ^{14}C -age [BP]	Calendar calibrated age (2σ) [BP]	After Day/Before Christ (2σ)	Sed.rate [cm/ka]
16	95-100	bulk (AMS)	304914	1930 \pm 40	1370 \pm 130	580 \pm 130 AD	73,0
16	185-190	bulk (AMS)	304915	2680 \pm 40	2195 \pm 155	245 \pm 155 BC	109,1
16	275-280	bulk (AMS)	304916	3550 \pm 40	3285 \pm 155	1308 \pm 155 BC	82,6
16	355-360	bulk (AMS)	304917	4990 \pm 40	5135 \pm 185	3185 \pm 185 BC	43,2
16	405-410	bulk (AMS)	298986	7530 \pm 40	7850 \pm 140	5900 \pm 140 BC	18,4
16	412-415	peat (AMS)	297652	9140 \pm 50	10320 \pm 100	8370 \pm 100 BC	2,0
19	95-100	bulk (AMS)	304918	1670 \pm 30	1090 \pm 160	860 \pm 160 AD	91,7
19	215-220	bulk (AMS)	304919	2870 \pm 30	2495 \pm 195	545 \pm 195 BC	85,4
19	255-260	bulk (AMS)	304920	3500 \pm 30	3215 \pm 165	1265 \pm 165 BC	55,6
19	318	shell (AMS)	297654	6990 \pm 50	7375 \pm 135	5425 \pm 135 BC	13,9
34	70-80	bulk (AMS)	325021	1820 \pm 30	1235 \pm 125	715 \pm 125 AD	64,8
34	145	coral (^{14}C)	308133	2980 \pm 30	2550 \pm 190	600 \pm 190 BC	49,4
34	160-170	bulk (AMS)	345363	3000 \pm 30	2590 \pm 170	640 \pm 170 BC	625,0
34	260-270	bulk (AMS)	317609	4210 \pm 30	4125 \pm 205	2175 \pm 205 BC	65,1
34	340-350	bulk (AMS)	345364	5400 \pm 30	5620 \pm 140	3670 \pm 140 BC	53,5
34	400	bulk (AMS)	309062	6180 \pm 40	6465 \pm 165	4515 \pm 165 BC	59,2

Table 2.3 continued

12	19-20	bulk (AMS)	309059	2640 ± 30	2150 ± 170	200 ± 170 BC	16,4
12	21	bulk (AMS)	320751	1870 ± 30	1280 ± 120	670 ± 120 AD	
12	110-120	bulk (AMS)	317606	2250 ± 30	1690 ± 170	260 ± 170 AD	241,5
12	242	bulk (AMS)	309060	2480 ± 30	1970 ± 160	20 ± 160 BC	435,7
8	20-30	bulk (AMS)	317605	1040 ± 30	525 ± 105	1425 ± 105 AD	57,1
8	56-75	coral (¹⁴ C)	308129	2040 ± 30	1455 ± 155	495 ± 155 AD	48,4
8	123-132	coral (¹⁴ C)	308130	2890 ± 30	2500 ± 190	550 ± 190 BC	54,5
8	150-160	bulk (AMS)	345350	3280 ± 30	2950 ± 190	1000 ± 190 BC	62,2
8	176-189	coral (¹⁴ C)	308131	3670 ± 30	3435 ± 145	1485 ± 145 BC	59,8
13	10-23	bulk (AMS)	345351	820 ± 30	350 ± 120	1600 ± 120 AD	65,7
13	50-60	bulk (AMS)	345352	1290 ± 30	735 ± 125	1215 ± 125 AD	96,1
13	80-90	bulk (AMS)	345353	1640 ± 30	1065 ± 155	885 ± 155 AD	90,9
13	160	bulk (AMS)	309061	2030 ± 30	1445 ± 155	505 ± 155 AD	184,2
29	10-20	bulk (AMS)	345357	1350 ± 30	755 ± 135	1175 ± 135 AD	26,5
29	30-35	bulk (AMS)	317607	1800 ± 30	1205 ± 135	745 ± 135 AD	33,3
29	61-66	bulk (AMS)	345358	1690 ± 30	1105 ± 155	845 ± 155 AD	600,0
29	73-80	bulk (AMS)	345359	1870 ± 30	1280 ± 120	670 ± 120 AD	
29	90-98	bulk (AMS)	317608	2680 ± 30	2190 ± 150	240 ± 150 BC	19,8
29	110-120	bulk (AMS)	325019	3100 ± 30	2740 ± 130	790 ± 130 BC	40,0
29	135-142	coral (¹⁴ C)	308132	3460 ± 30	3460 ± 150	1510 ± 150 BC	30,6
18	20-30	bulk (AMS)	325014	1470 ± 30	875 ± 155	1075 ± 155 AD	34,3
18	275-280	bulk (AMS)	325015	3920 ± 30	3725 ± 175	1775 ± 175 BC	87,7
18	300-310	bulk (AMS)	345354	4210 ± 30	4125 ± 205	2170 ± 210 BC	75,0
18	330-337	coral (¹⁴ C)	320766	5310 ± 30	5540 ± 120	3590 ± 120 BC	19,1
24	21-24	bulk (AMS)	325016	1200 ± 30	625 ± 105	1325 ± 105 AD	38,4
24	40-50	bulk (AMS)	325017	1520 ± 30	925 ± 145	1025 ± 145 AD	86,7
24	60-70	bulk (AMS)	345355	2000 ± 30	1420 ± 140	540 ± 140 AD	40,4
24	100-105	bulk (AMS)	325018	2760 ± 30	2305 ± 175	355 ± 175 BC	39,5
24	105-112	bulk (AMS)	345356	2690 ± 30	2200 ± 150	250 ± 150 BC	60,6
24	136-145	coral (¹⁴ C)	320767	3300 ± 30	2965 ± 195	1015 ± 195 BC	
31	30-40	bulk (AMS)	345360	208 ± 30	1510 ± 170	440 ± 170 AD	26,5
31	50-60	bulk (AMS)	325020	2910 ± 30	2515 ± 195	565 ± 165 BC	19,9
31	60-70	bulk (AMS)	345361	3210 ± 30	2875 ± 155	925 ± 155 BC	27,8
31	100-110	bulk (AMS)	345362	4190 ± 30	4085 ± 195	2135 ± 195 BC	47,4
31	125	bulk (AMS)	320753	4110 ± 30	3985 ± 175	2035 ± 175 BC	
27	70-77	coral (¹⁴ C)	320768	1120 ± 30	575 ± 95	1375 ± 95 AD	133,9
30	50-59	bulk (AMS)	320752	1820 ± 30	1235 ± 125	715 ± 125 AD	47,8
1	52-55	bulk (AMS)	338666	1930 ± 30	1365 ± 135	585 ± 135 AD	40,3
26	46-49	bulk (AMS)	338667	1610 ± 30	1030 ± 140	920 ± 140 AD	47,6
26	128-130	bulk (AMS)	338668	1890 ± 30	1300 ± 130	650 ± 130 AD	300,0
26	185-195	coral (¹⁴ C)	345365	3760 ± 30	3525 ± 165	1575 ± 165 BC	29,2

Calculated sedimentation rates between each date are based on calendar calibrated years before present (BP)

2.4 Results

2.4.1 Sedimentary facies

The entire Holocene lagoonal deposition is represented in the 4.56 m long core 16, which is located in the central-western part of the lagoon collected at a water depth of 34.5 m (Fig. 2.1). At this site, fine sediments (mudstone) have accumulated (Gischler, 2006) and the recovered core represents the longest Holocene section recorded in the Rasdhoo Atoll lagoon. The base of core 16 is composed of brownish Pleistocene soil (Fig. 2.2a), made of ~86% clay and ~14% quartz (Table 2.4). With sharp boundary, a 3 cm thick peat layer superposes the soil and is dated to $10,320 \pm 100$ yrs BP (Table 2.3). Between the peat and the oldest carbonate sediments a hiatus of about 2,500 yrs exist. An age of $7,850 \pm 140$ yrs BP has been measured for the oldest carbonate sediments. These are relative fine sediments composed of fragments of mollusk shells, coral fragments, foraminifera, crustacean shells, as well as *Halimeda* chips, echinoderm debris, fecal pellets, and reworked organic material. Further upcore, carbonate sediment becomes even finer and the amounts of components decrease. This pattern may be observed in most of the cores from Rasdhoo Atoll lagoon (Fig. 2.2).

Statistical comparison of composition, texture, and mineralogy of all sediment samples in each core (Table 2.5 - Appendix), as well as cluster analyses allow the classification of eight sedimentary facies, including six carbonate facies, a soil, and a peat facies (Fig. 2.3). In decreasing abundance, the six carbonate facies are classified as mollusk-coral-algal floatstone to rudstone, mollusk-coral-red algae rudstone, mollusk-coral-algal wackestone to floatstone, mollusk-coral wackestone, mollusk-coral mudstone to wackestone, and mollusk mudstone. For analyzing general trends in chronological occurrence and spatial distribution of facies within the lagoon, west-to-east orientated transects were drawn.

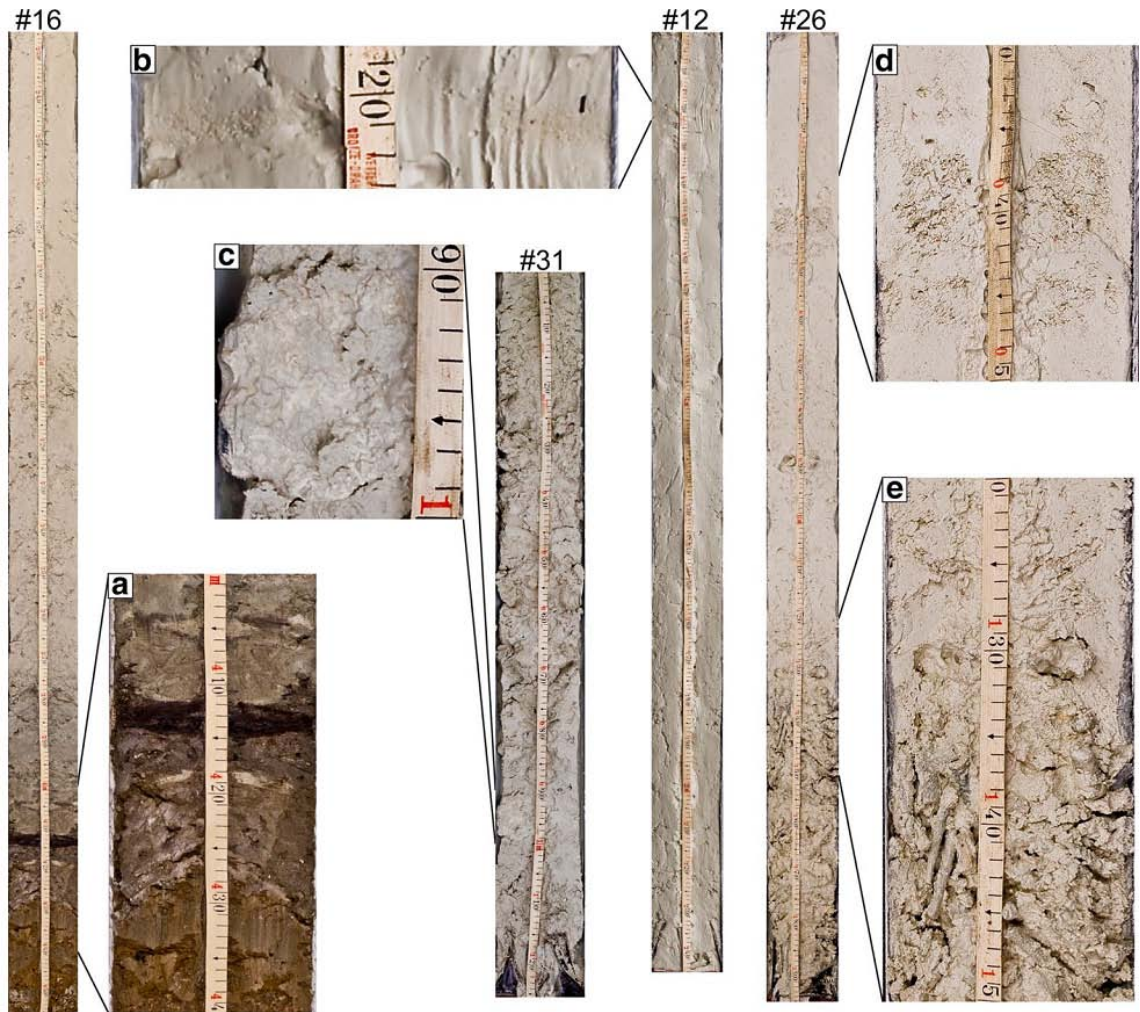


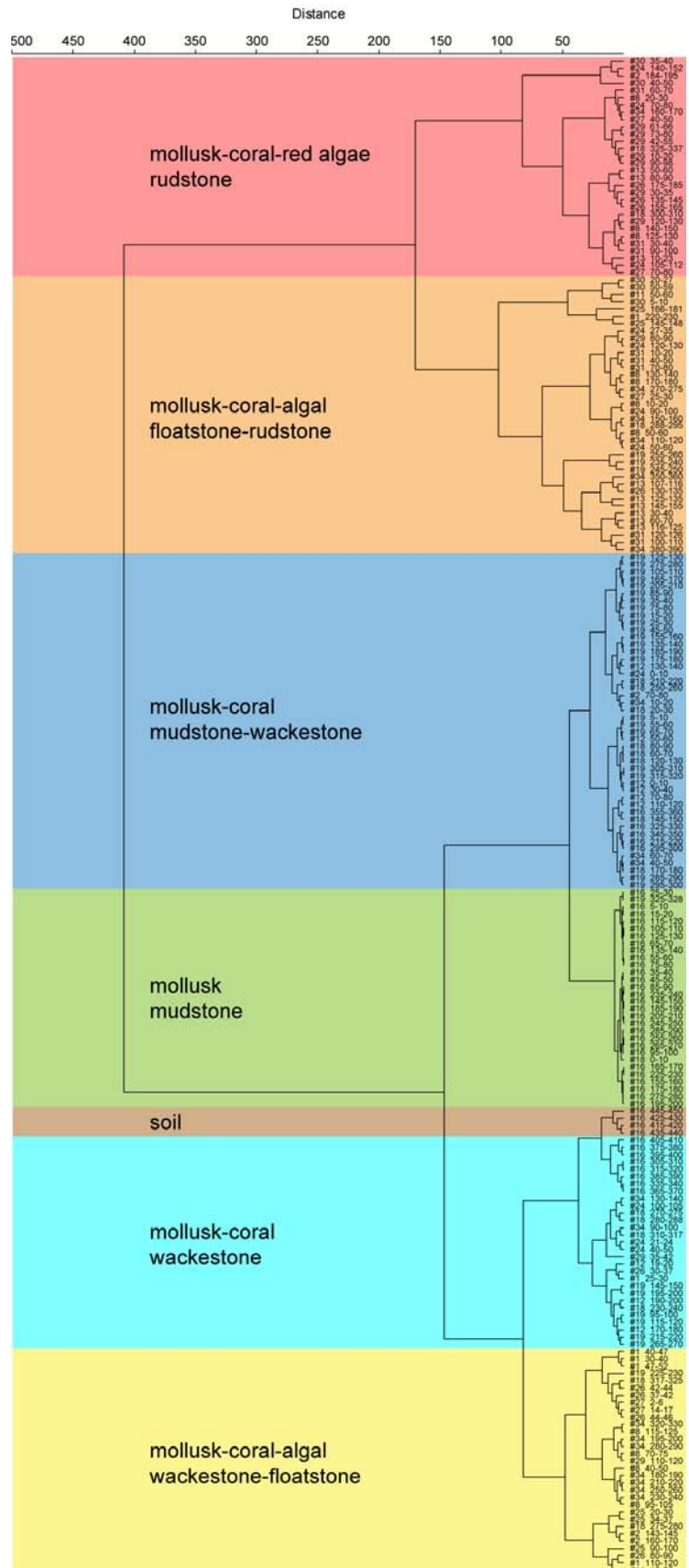
Fig. 2.2 Core photos; **a** the soil and peat layer toward the base of core 16; **b** a coarse-grained 1-cm-thick sediment layer marking a sedimentary event in core 12; **c** a big foliaceous coral in core 31; **d, e** a coarse-grained sandy layer toward the top and transition to coral rubble sediments toward the base of core 26.

Table 2.4 Mineralogy of core 16

Sample no.	Quartz [wt.%]	Clay min. [wt.%]	ARA [wt.%]	LMC [wt.%]	HMC [wt.%]
#16 005-010	0,0	0,0	85,5	3,4	11,1
#16 015-020	0,0	0,0	86,1	3,0	10,9
#16 025-030	0,0	0,0	84,9	3,3	11,8
#16 035-040	0,0	0,0	84,6	3,5	11,9
#16 045-050	0,0	0,0	84,6	3,4	11,9
#16 055-060	0,0	0,0	84,2	3,6	12,2
#16 065-070	0,0	0,0	84,6	3,2	12,2
#16 075-080	0,0	0,0	84,0	4,8	11,2
#16 085-090	0,0	0,0	84,7	3,2	12,1
#16 095-100	0,0	0,0	84,3	3,4	12,3
#16 105-110	0,0	0,0	84,8	3,4	11,8
#16 115-120	0,0	0,0	84,6	3,6	11,8
#16 125-130	0,0	0,0	84,9	3,3	11,8
#16 135-140	0,0	0,0	84,8	3,5	11,7
#16 145-150	0,0	0,0	84,4	4,3	11,3
#16 155-160	0,0	0,0	85,3	3,3	11,4
#16 165-170	0,0	0,0	84,6	3,4	12,0
#16 175-180	0,0	0,0	84,9	3,7	11,4
#16 185-190	0,0	0,0	86,5	3,2	10,4
#16 195-200	0,0	0,0	85,6	3,0	11,4
#16 205-210	0,0	0,0	85,1	3,4	11,5
#16 215-220	0,0	0,0	84,9	4,3	10,8
#16 225-230	0,0	0,0	85,7	3,1	11,2
#16 235-240	0,0	0,0	85,5	3,5	11,0
#16 245-250	0,0	0,0	85,6	3,4	11,0
#16 255-260	0,0	0,0	86,0	3,8	10,2
#16 265-270	0,0	0,0	85,3	3,3	11,4
#16 275-280	0,0	0,0	85,2	3,8	11,1
#16 285-290	0,0	0,0	84,5	3,4	12,1
#16 295-300	0,0	0,0	85,1	2,7	12,2
#16 305-310	0,0	0,0	86,9	3,0	10,1
#16 315-320	0,0	0,0	87,0	2,8	10,2
#16 325-330	0,0	0,0	88,1	3,3	8,6
#16 335-340	0,0	0,0	87,7	2,8	9,5
#16 345-350	0,0	0,0	86,8	3,2	10,0
#16 355-360	0,0	0,0	88,0	2,7	9,3
#16 365-370	0,0	0,0	87,6	3,7	8,7
#16 375-380	0,0	0,0	87,9	4,3	7,7
#16 385-390	2,3	2,6	81,9	3,6	9,7
#16 395-400	1,8	2,3	86,4	2,8	6,7
#16 405-410	2,8	6,4	81,9	3,2	5,7
#16 415-420	9,9	13,6	70,4	2,7	3,4
#16 425-430	24,2	40,0	32,9	2,0	0,9
#16 435-440	33,2	66,8	0,0	0,0	0,0
#16 445-450	13,6	86,4	0,0	0,0	0,0

XRD measurements of bulk sediment samples calibrated with added aluminum oxide (carbonate method) for all samples, and additional full angle XRD measurements for samples below 385 cm core depth

Fig. 2.3 Tree diagramm of cluster analyses (Ward's method) of sediment data illustrating six carbonate facies and a soil/peat facies. Variables: Relative abundances of mollusk, coral, foraminifera, echinoderms, Halimeda, red algae, crustacean, peloids, opaque grains, grain-size fraction < 125 µm and > 2 mm, and mineralogy.



Soil (s)

The light brownish to brownish soil is composed on average of 82% of the grain-size fraction <0.125 mm ("mud") (Table 2.6 - Appendix). The abundance of opaque components, of grains >2 mm, and root fragments reaches an average of 11%. Remaining components comprise carbonate detritus like mollusk shells, red algae, and crustacean shell fragments. Soil was recovered only in core 16.

Peat (p)

The black peat layer is composed of organic matter with only minor remains of reworked carbonate and clay-sized sediments originating from below and above the layer. The thickness of 3 cm and the foliaceous shape of the organic matter lead to the assumption of relative strong compaction. Due to the preservation, the identification of mangrove taxa was not possible. Peat was recovered only in core 16.

Mollusk-coral-algal floatstone to rudstone (mcaFR)

The relative coarse-grained facies is composed of ca. 24% components >2 mm (Table 2.7 - Appendix). The mud content (<0.125 mm) yields values of about 50%. Samples with <50% mud are characterized as rudstone, samples with >50% mud are defined as floatstone. Most abundant components are mollusk shells with an average abundance of about 10%. Corals, encrusting red algae, *Halimeda*, and foraminifera taken together reach an abundance of 16%. This coarse-grained facies has been found in most of the cores, except for cores 2, 12, and 16. It represents the most abundant facies and makes up ~30% of the recovered core material.

Mollusk-coral-red algae rudstone (mcrR)

The facies consists of ca. 47% components >2 mm on average (Table 2.8 - Appendix). The mud content (<0.125 mm) has an average abundance of around 38%. Most common components are mollusk shells, corals, and encrusting red algae, together with an abundance of ca. 8%. Foraminifera and *Halimeda* are uncommon with an abundance of <1.5% each. This facies occurs in cores 2, 8, 13, 18, 24, 26, 27, 29, 30, 31, and 34. It represents the second most abundant facies (23% of the core material).

Mollusk-coral-algal wackestone to floatstone (mcaWF)

The facies is characterized by an average abundance of about 68.5% mud (grain-size fraction <0.125 mm) and of around 8% components >2 mm (Table 2.9 - Appendix). Samples with >10% components >2 mm are characterized as floatstone and samples with <10% components >2 mm are wackestone. Most common components are mollusk shells with an average abundance of 10%, corals and algal components (*Halimeda* and red algae) counting ~5.5% each and foraminiferas occur with an average abundance of 2%. This facies occurs in cores 1, 2, 8, 11, 18, 25, 26, 27, 29, 31, and 34 (23% of the core material).

Mollusk-coral wackestone (mcW)

The facies is composed of an average of 81% mud (grain-size <0.125 mm) and of around 6% components >2 mm (Table 2.10 - Appendix). Major components include mollusk shells with an average abundance of 8% and corals with an average abundance of 3%. Remaining particles are red algae, foraminifera, and *Halimeda* with very low abundance. Mollusk-coral wackestone was found in cores 1, 12, 16, 18, 19, 24, 26, and 34 (13% of the core material).

Mollusk-coral mudstone to wackestone (mcMW)

The grain-size of the facies is mainly mud (<0.125 mm) with an average of 89.6% (Table 2.11 - Appendix). Samples with >10% components >0.125 mm are characterized as wackestones and samples containing <10% components >0.125 mm are mudstone. The most common components are mollusk shells and corals together with an abundance of about 6.8%. *Halimeda*, foraminiferas, and incrusting red algae occur in low abundance of <1% on average. This facies occurs in cores 2, 12, 16, 18, 19, 24, and 34 (9% of the core material).

Mollusk mudstone (mM)

The facies is characterized by a high abundance of mud (grain-size <0.125 mm) content of 96.8% on average (Table 2.12 - Appendix). The most abundant components are mollusk shells, with an abundance of about 2.5% on average. Foraminifera and

peloids occur in low abundance of about 0.3% each. Mollusk mudstone occurs in cores 18 and 16 (2% of the core material).

2.4.2 Facies distribution

Temporal and spatial trends of facies distribution may be recognized in the seventeen cores during 4-0 kyrs BP (Figs. 2.4-2.7). Facies in the majority of cores become finer towards the modern, together with a decrease in abundance of algal components. Most abundant facies from 4-2 kyrs BP include mollusk-coral-algal floatstone to rudstone and mollusk-coral-red algae rudstone. During 2-1.5 kyrs BP, mollusk-coral-algal wackestone to floatstone is most common. From 1.5-1 kyrs BP mollusk-coral-algal floatstone to rudstone is abundant; from 1-0 kyrs BP mollusk-coral mudstone to wackestone. There are four cores with sediments older than 4 kyrs BP: Cores 16 and 19 have relative fine sediments with facies of mollusk-coral wackestone and mollusk-coral mudstone to wackestone. Cores 18 and 34 consist of coarser grained facies (mollusk-coral-algal wackestone to floatstone, mollusk-coral-algal floatstone to rudstone, and mollusk-coral-red algae rudstone). According to the grain-size distribution of core 16 (Fig. 2.6), facies are getting finer (wackestone to mudstone) upcore. The statistical classification of core 16 combines the wackestone and floatstone units to one facies (mollusk-coral wackestone) (Fig. 2.3). Generally, the older sediments (4-10 kyrs BP) have coarser grain-sizes (e.g., cores 16, 18, and 34) as compared to younger sediments (<4 kyrs BP).

In transects A and B, cores 8, 24, and 29 show ages exceeding 2 kys BP. Facies >2 kyrs BP are coarse-grained with relative high abundance of algal components and coral rubble. From 2-0 kyrs BP, facies in the western marginal part of the lagoon are relative fine (mollusk-coral mudstone to wackestone and mollusk-coral-algal wackestone to floatstone), whereas those in the eastern central part of the lagoon are coarse-grained algal facies (mollusk-coral-algal floatstone to rudstone and mollusk-coral-red algae rudstone).

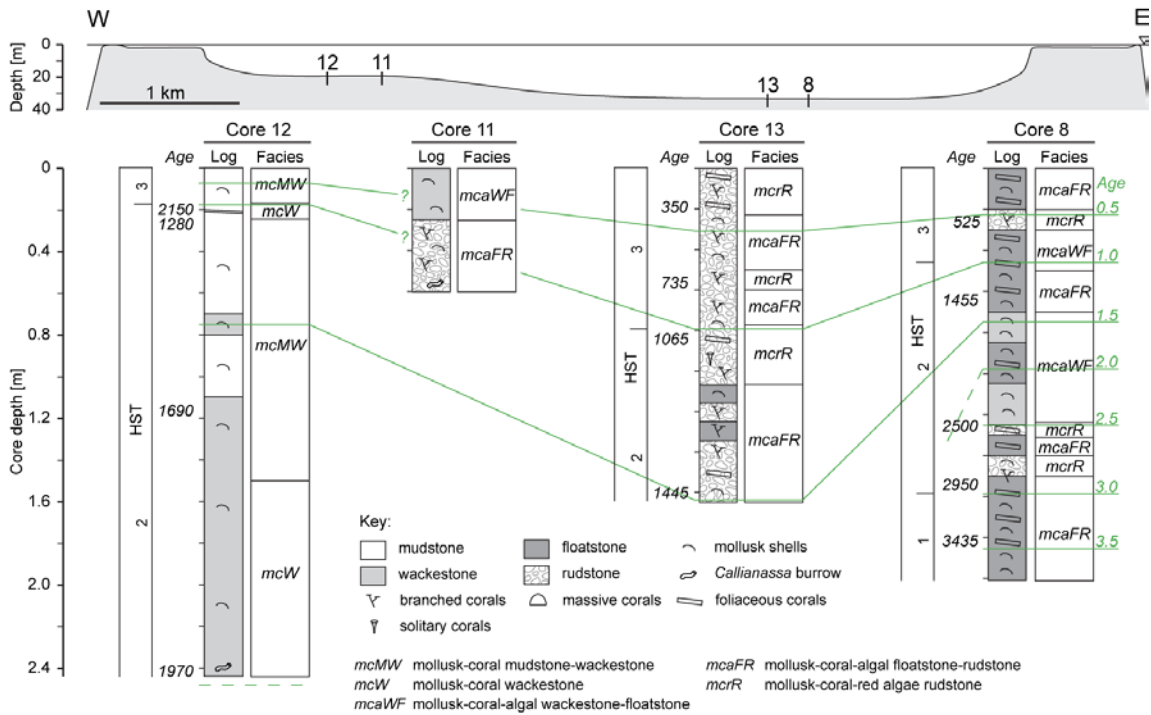


Fig. 2.4 Transect A through southern Rasdhoo Atoll including cores 8, 11, 12, and 13 with detailed facies description. According to radiometric age measurements isochrones are drawn. The ages are calendar-calibrated with a two-sigma probability in yrs BP and kyrs BP (in green). Core 11 has not been dated. Branched corals are *Acropora* sp., *Seriatopora* sp., and *Caulastrea* sp.; foliaceous corals are *Leptoseris* sp., *Porites* sp., *Cyphastrea* sp., *Merulina* sp., *Pachyseris* sp., and *Echinophyllia* sp.; massive corals are *Porites* sp., *Favia* sp., *Goniopora* sp., and *Faviidae*; solitary corals are *Fungia* sp. and *Caryophyllia* sp. HST highstand systems tract.

In transect C, sections <4 kyrs BP of mudstone to wackestone (mollusk mudstone, mollusk-coral mudstone to wackestone, and mollusk-coral-algal wackestone to floatstone) occur in the western part of the lagoon (cores 16, 18, and 34) and coarse-grained coral and algal rich sediments (mollusk-coral-algal floatstone to rudstone and mollusk-coral-red algae rudstone) in the eastern part of the lagoon (cores 30 and 31). Cores 16, 18, and 34 contain sediments >4 kyrs BP and core 16 reaches an age of 10 kyrs BP. Sedimentary facies dated 10-4 kyrs BP in cores 16, 18, and 34 are characterized by coarse-grained facies with increased algal components.

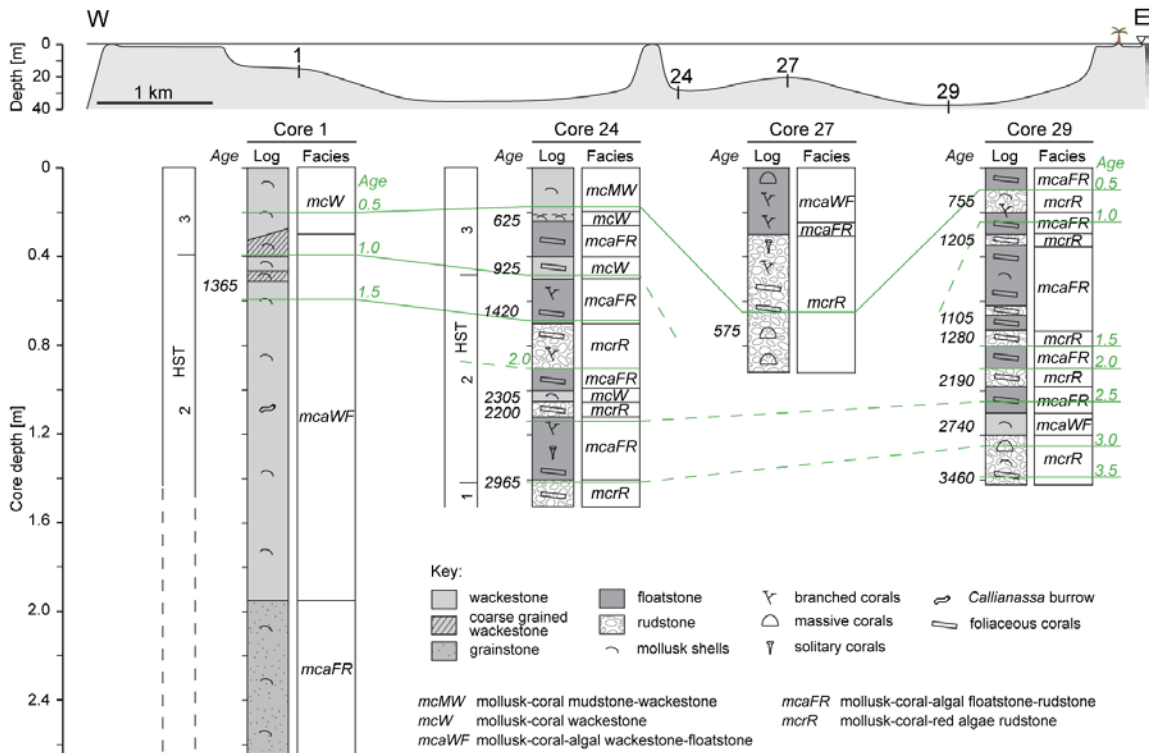


Fig. 2.5 Transect B through central Rasdhoo Atoll including cores 1, 24, 27, and 29 with detailed facies description. According to radiometric age measurements isochrones are drawn. The ages are calendar-calibrated with a two-sigma probability in yrs BP and kyrs BP (in green). The base of core 1 has not been dated. Branched corals are *Acropora* sp., *Seriatopora* sp., and *Caulastrea* sp.; foliaceous corals are *Leptoseris* sp., *Porites* sp., *Cyphastrea* sp., *Merulina* sp., *Pachyseris* sp., and *Echinophyllia* sp.; massive corals are *Porites* sp., *Favia* sp., *Goniopora* sp., and *Faviidae*; solitary corals are *Fungia* sp. and *Caryophyllia* sp.. HST highstand systems tract.

In transect D, carbonate sediments have mud-supported textures (mollusk-coral mudstone to wackestone, mollusk-coral wackestone, and mollusk-coral-algal wackestone to floatstone). Cores 2, 25, and 26 exhibit fining upward, with facies of mollusk-coral-algal floatstone to rudstone and mollusk-coral-red algae rudstone ranging from 4-2 kyrs BP. In core 19, a coarse layer of mollusk-coral-algal floatstone to rudstone occurs between 2.3-2.6 m, dated to $3,215 \pm 165$ yrs BP. Sediments below (mollusk-coral mudstone to wackestone) and above (mollusk-coral-algal wackestone to floatstone, mollusk-coral mudstone to wackestone) this layer are fine-grained.

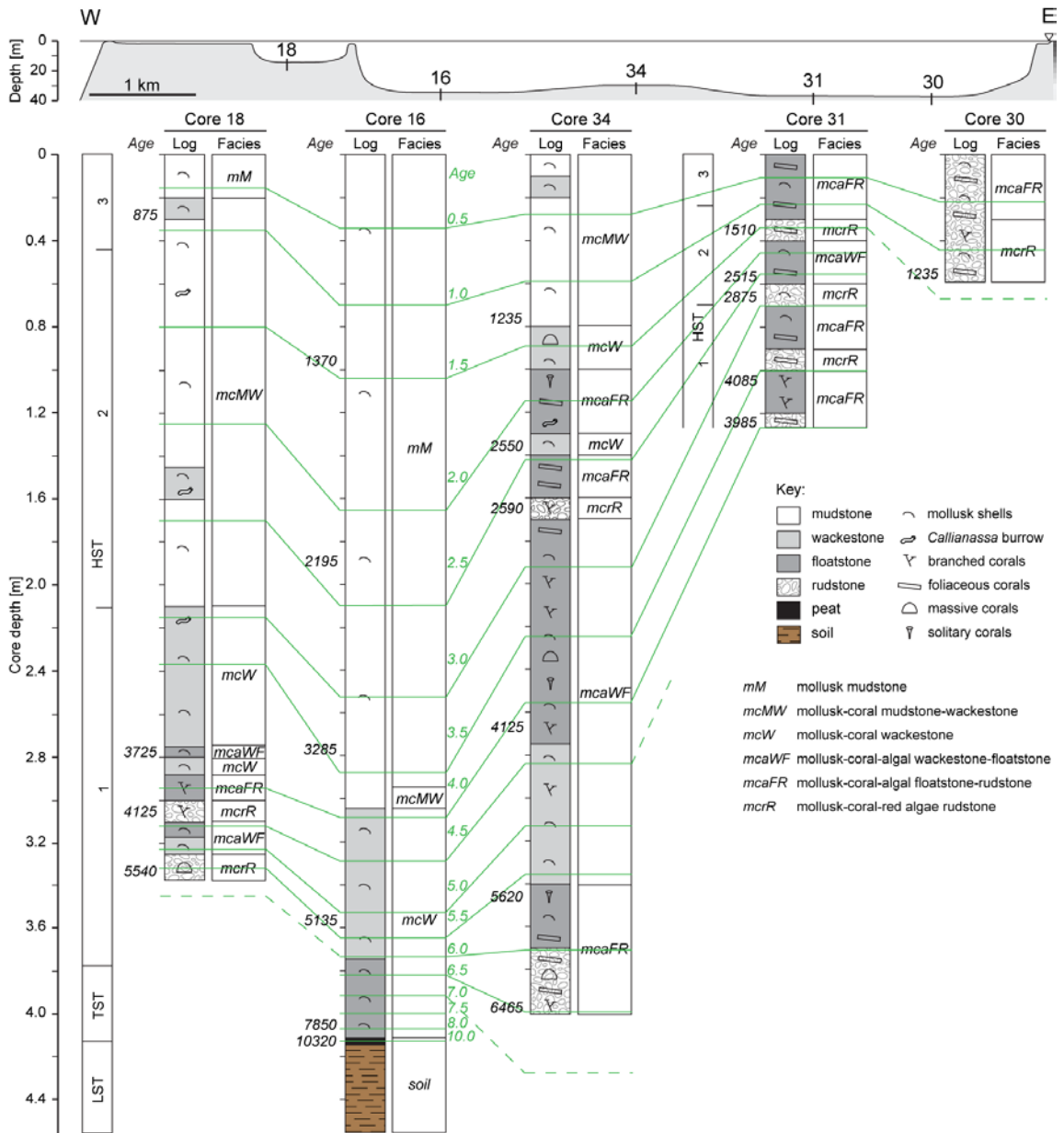


Fig. 2.6 Transect C through central Rasdhoo Atoll including cores 16, 18, 30, 31, and 34 with detailed facies description. According to radiometric age measurements isochrones are drawn. The ages are calendar-calibrated with a two-sigma probability in yrs BP and kyrs BP (in green). Branched corals are *Acropora* sp., *Seriatopora* sp., and *Caulastrea* sp.; foliaceous corals are *Leptoseris* sp., *Porites* sp., *Cyphastrea* sp., *Merulina* sp., *Pachyseris* sp., and *Echinophyllia* sp.; massive corals are *Porites* sp., *Favia* sp., *Goniopora* sp., and *Faviidae*; solitary corals are *Fungia* sp. and *Caryophyllia* sp.. LST lowstand systems tract, TST transgressive systems tract, HST highstand systems tract.

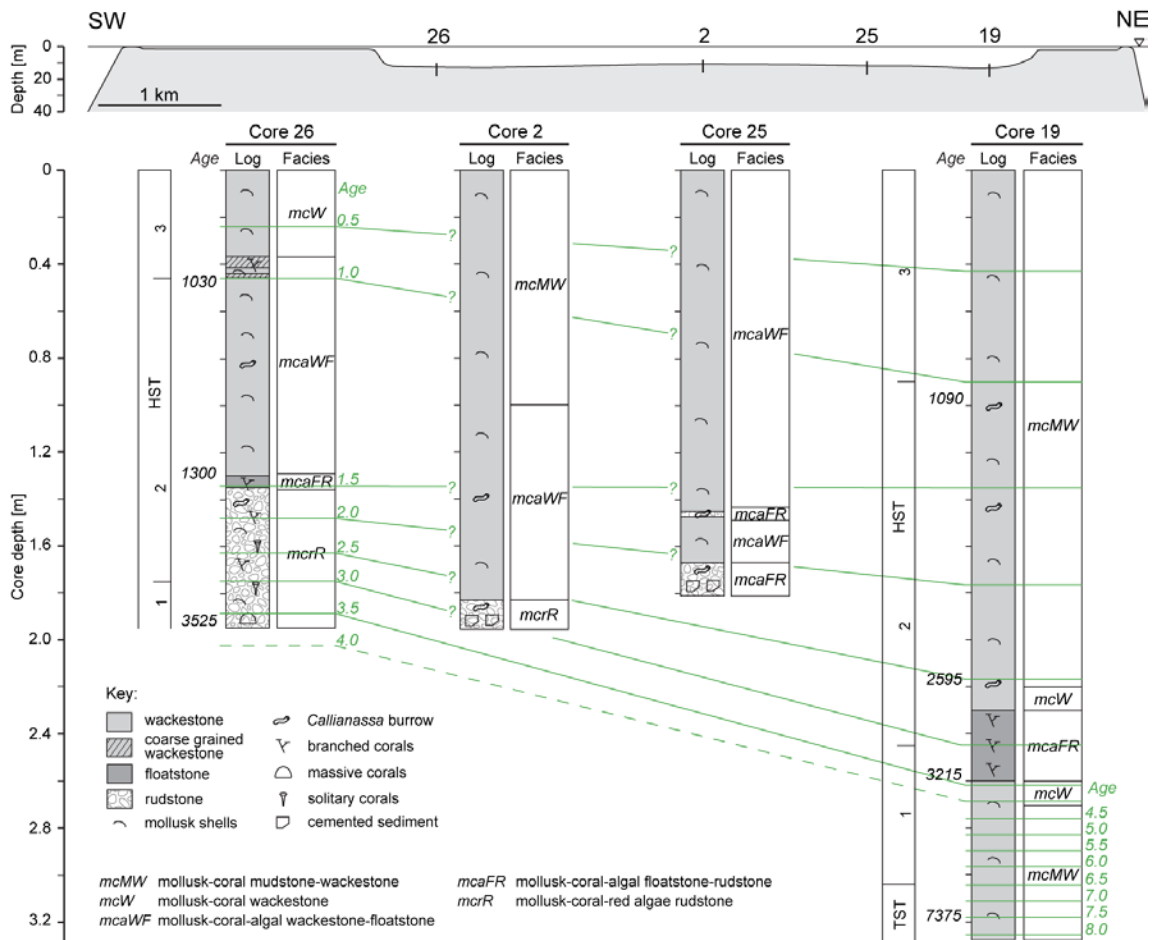


Fig. 2.7 Transect D through northern Rasdhoo Atoll including cores 2, 19, 25, and 26 with detailed facies description. According to radiometric age measurements isochrones are drawn. The ages are calendar-calibrated with a two-sigma probability in yrs BP and kyrs BP (in green). Cores 2 and 25 have not been dated. Branched corals are *Acropora* sp., *Seriatopora* sp., and *Caulastrea* sp.; massive corals are *Porites* sp., *Favia* sp., *Goniopora* sp., and *Faviidae*; solitary corals are *Fungia* sp. and *Caryophyllia* sp.. TST transgressive systems tract, HST highstand systems tract.

2.4.3 Mineralogy

Aragonite is most abundant in all the carbonate sediments measuring mean values of 86 wt.%. The average abundance of low-magnesium calcite amounts to 3.0 wt.% and of high-magnesium calcite to 11 wt.%.

There are only minor differences in mean abundance of aragonite, low-magnesium calcite, and high-magnesium calcite. The wackestone facies (mollusk-coral mudstone to wackestone, mollusk-coral wackestone, and mollusk-coral-algal wackestone to floatstone) have the highest abundances of aragonite (mean values of 88 wt.%) with lower average values of low-magnesium calcite (~2 wt.%) and high-

magnesium calcite (~10 wt.%) (Table 2.9, 2.10, and 2.11). The mudstone facies (mollusk mudstone) and rudstone facies (mollusk-coral-algal floatstone to rudstone and mollusk-coral-red algae rudstone) consist of 85 wt.% aragonite on average, of 3.5 wt.% low-magnesium calcite, and of 11.5 wt.% high-magnesium calcite (Tables 2.7, 2.8, and 2.12).

Full angle XRD analyses of the soil unit in core 16 yielded values of increasing quartz and clay minerals in abundance with decreasing values of aragonite and calcite (LMC and HMC) minerals (Table 2.4). The abundance of quartz and clay minerals within the overlying carbonate sediments, as well as the occurrence of aragonite and calcite minerals within the soil unit indicates reworking by burrowing organisms. XRD measurements of the clay (grain-size <0.02 mm) define an average abundance of 36% aluminum chlorite, 32% kaolinite, and 26% mixed layer clay minerals (Table 2.2). Towards the base of core 16, decreasing amounts of pyrite and increasing amounts of goethite make up the remainder within the soil unit.

2.4.4 Sedimentation rates

Calendar calibrated radiocarbon ages and related sediment depths allow calculating and reconstructing sedimentation rates (Table 2.3). From 10-8 kyrs BP, very low sedimentation rates of 0.02 m/kyr are observed, recognizable in core 16. From 8-6.5 kyrs BP, the mean carbonate sedimentation rate increases to 0.2 m/kyr. Continuously, the sedimentation rate increases to 0.55 m/kyr from 6.5-3 kyrs BP. From 3-1 kyrs BP, the sedimentation rate reaches a maximum of 1.4 m/kyr. Modern (1-0 kyrs BP) mean sedimentation rates average 0.6 m/kyr.

2.5 Discussion

2.5.1 Interpretation of facies

For soil deposition, aeolian transport of quartz and clay minerals like aluminum chlorite and kaolinite from adjacent coastal arid regions, together with the accumulation of organic matter and bedrock dissolution are crucial (Goldberg and Griffin, 1970). Goldberg and Griffin (1970) mentioned that the chlorites of northeastern Madagascar

might be associated with volcanic activity on the Indian Ocean ridge system, but they could not explain the source of high kaolinite in this area. Subaerial exposure of coastal shelves during sea-level lowstand was presumably conducive for clay mineral transport to the Maldives by prevailing winds. Soil was recovered only in one core; however, like in other examples soil is a common and ubiquitous formation in subaerially exposed reef lagoons (Zinke et al., 2001, 2003a, b, 2005; Gischler, 2003).

A thin peat layer superposes the soil and marks the first inundation by the rising Holocene sea-level. Marine inundation of the Rasdhoo lagoon occurred presumably via karst conduits and reef passes in the surrounding Pleistocene limestone (Gischler et al., 2008). Mangroves developed in a brackish, swampy lagoon environment thereby accumulating organic matter. Peats also mark the Holocene flooding of lagoons and coastal shelves in cores from Mayotte (Elmoutaki et al., 1992; Zinke et al., 2001, 2003a, b, 2005), Belize (Shinn et al., 1982; Gischler, 2003), the Bahamas (Newell et al., 1959), South Florida (Scholl, 1964; Dodd and Siemers, 1971) and the Great Barrier Reef (Larcombe and Carter, 1998).

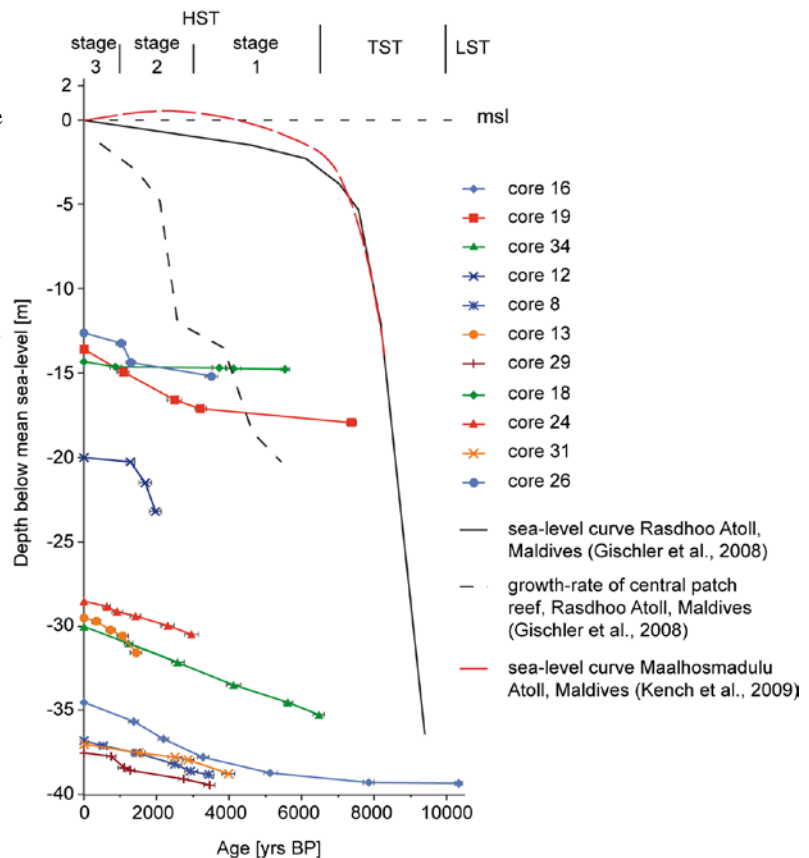
The Holocene carbonate facies can be divided into lagoonal background sedimentation, mostly consisting of fine sediments, and event sedimentation depositing transported coarse-grained reefal components. The mollusk-coral-algal floatstone to rudstone facies including in situ foliaceous and massive corals are related to lagoonal background sedimentation (e.g., cores 8, 29, and 31), because corals like *Porites* sp. and *Leptoseris* sp. occur in relatively deep water environments (Klostermann et al., 2014). The same facies including branched corals represent event sedimentation (e.g., cores 19, 24, 27, and 31), because corals like *Acropora* sp. and *Seriatopora* sp. prefer shallow water environments and were transported from the marginal reef into the lagoon (Klostermann et al., 2014). Mostly, the layers of mollusk-coral-red algae rudstone are composed of branched corals and are related to event sedimentation, but the rudstone units at the bases of cores 18, 24, 27, 29, and 30 consisting of massive or foliaceous in situ corals are part of early Holocene background sedimentation. The "sandy" facies of mollusk-coral wackestone, mollusk-coral-algal wackestone to floatstone, and mollusk-coral mudstone to wackestone, as well as the mollusk mudstone facies represent background sedimentation, except for the thin wackestone layer in core 12 and the

coarse-grained wackestone layers in cores 1 and 26, which mark a depositional tsunami event (Klostermann et al., 2014).

2.5.2 Lagoonal sedimentation

Comparing the lateral facies distribution and sedimentation rates in the lagoon with local sea-level curves (Gischler et al., 2008; Kench et al., 2009) allows for the reconstruction of the history of lagoonal infill during the Holocene. According to the specified time intervals of the sea-level curve from Mayotte (Zinke et al., 2005) and the four sea-level phases of Maalhosmadulu Atoll in the Maldives (Kench et al., 2009), three sequence stratigraphical system tracts are indicated: (1) a lowstand systems tract (LST) >10 kyrs BP, (2) a transgressive systems tract (TST) 10-6.5 kyrs BP, and (3) a highstand systems tract (HST) 6.5-0 kyrs BP (Fig. 2.8). The highstand was further divided into three stages (6.5-3, 3-1, 1-0 kyrs BP).

Fig. 2.8 Reconstructed sedimentary paleo-water depth of eleven cores in comparison to two sea-level curves from the Maldives. Due to insufficient age-data cores 1, 2, 11, 25, 27, and 30 are not shown. The depths in cores are corrected for vertical compaction. *LST* lowstand systems tract, *TST* transgressive systems tract, *HST* highstand systems tract.



Lowstand Systems Tract

The time interval of the LST to 10 kyrs BP can be recognized by an accumulation of Pleistocene brownish soil at the base of core 16 (Fig. 2.6). The soil was deposited before the rising Holocene sea inundated the Pleistocene atoll platform, but no age data is available (Fig. 2.9a). Likewise, no Pleistocene limestone bedrock was recovered in the vibracores from Rasdhoo Atoll lagoon. However, it was recovered by rotary drilling on the western marginal reef of the atoll, 13.5 m below modern sea level. U-series ages of three acroporid corals ranged from 114-137 kyrs BP, indicating deposition during marine isotope stage 5e (Gischler et al. 2008). Generally, Pleistocene bedrock covers wide areas of the Maldivian archipelago, but with large hiatus under atolls due to subaerial exposure and erosion (Purdy and Bertram 1993; Aubert and Droxler, 1996; Gischler et al., 2008; Betzler et al., 2012).

Transgressive Systems Tract

Directly above the soil, a peat layer marks the beginning of the rising sea-level and the TST of Rasdhoo Atoll lagoon. The peat layer consists of mangrove deposits, which grew close to mean sea-level within the tidal range (Fig. 2.9b). In core 16, the peat is dated to $10,320 \pm 100$ yrs BP coinciding with age measurements of the mangrove peat in core 89028 from Mayotte lagoon, dated to $10,775 \pm 270$ yrs BP (Zinke et al., 2003b), and to the basal soil in core G5 off Belize, which is dated to $10,595 \pm 45$ yrs BP and $9,600 \pm 820$ yrs BP (Gischler, 2003).

The oldest carbonate sediments were deposited above the peat at 7850 ± 140 yrs BP with very low sedimentation rates of 0.02 m/kyr. There is a considerable hiatus of several thousand years between the peat and the first lagoonal carbonates, which was also observed in other Holocene atoll lagoons (Gischler, 2003; Schultz et al., 2010). Apparently, time is a crucial factor, which is necessary for the establishment of the carbonate factory after sub aerial exposure (e.g., Tipper, 1997; and references therein). Possibly, this mechanism may be used to explain the formation of asymmetrical cycles in carbonate platforms in the fossil record. In Rasdhoo Atoll, the oldest carbonate facies is a mollusk-coral wackestone. This facies would have to be classified as floatstone, because of the high abundance of components >2 mm, but due to

similar abundances of mollusks and corals the sediments were assigned to the mollusk-coral wackestone facies. For comparison, a mollusk rudstone has been identified directly above the peat in core G5 off Belize (Gischler, 2003) indicating the deposition of coarse grained carbonate sediments at the beginning of the Holocene reef growth. At Rasdhoo Atoll, the Holocene reef started to grow around 8.6 kyrs BP (Gischler et al., 2008) and accumulated the first Holocene carbonate sediments during the onset of the TST. At Mauritius and Reunion, Holocene fringing reefs started to grow about 8 kyrs BP (Camoin et al., 1997), the barrier reef of Mayotte some 9.6 kyrs BP (Camoin et al., 1997; Dullo et al., 1998; Zinke et al., 2001, 2003a, b, 2005), and reefs in western Australia (Eisenhauer et al., 1993) and in the Indo-Pacific Ocean (Montaggioni, 1988) ca. 9.8 kyrs BP. Marginal reefs of Rasdhoo Atoll grew very fast, up to 15 m/kyr from 9-7 kyrs BP, keeping up with sea-level during the TST (Gischler et al. 2008). Sedimentation rates in Rasdhoo atoll lagoon were 0.23 m/kyr from 10-6.5 kyrs BP during lagoonal flooding. During this time interval, mollusk-coral wackestone was deposited in the deep lagoon, only recovered in core 16, with reconstructed water depth of 38 m below present sea-level (Fig. 2.6).

Highstand Systems Tract

Some 6.5 kyrs BP, a slowdown of sea-level rise marks the beginning of the HST (Zinke et al., 2001, 2003a, b; Camoin et al., 2004; Gischler et al., 2008; Kench et al., 2009). Based on variation in lagoonal sedimentation rates, accretion rates of the central patch reef in Rasdhoo Atoll lagoon (Gischler et al., 2008), and the supposed sea-level highstand above present mean sea level (Kench et al., 2009), the HST has been divided into three stages (Fig. 2.8). HST stage 1 marks the continuous slow sea-level rise, only a few meters below modern mean sea-level, and moderate sedimentation rates of 0.55 m/kyr from 6.5-3 kyrs BP (Fig. 2.9c). For comparison, in the Turneffe Island lagoon and Lighthouse Reef off Belize, similar sedimentation rates of 0.82 m/kyr and 0.53 m/kyr from 7-2.7 kyrs BP have been measured (Gischler, 2003). The accretion-rate of the central patch reef was between 3-4 m/kyr, which started to grow 5.5 kyrs BP (Gischler et al., 2008). Sedimentary facies were coarse-grained throughout the lagoon, except at the sites of core 16 and core 19, where fine sediments accumulated. At the

northeastern corner of the lagoon, towards the base of core 19, the "sandy" facies of the mollusk-coral mudstone to wackestone marks the Early Holocene (7.5-3.5 kyrs BP) sediment accumulation of the sand spit (Storz et al., 2014), which has been proceeding along the northeastern margin within the lagoon (Fig. 2.1b). Due to the development of the long lagoonal sand spit, some 4 kyrs BP, the water circulation in the deep central western area of the lagoon (core 16) became increasingly restricted (Storz et al., 2014) and mollusk-bearing mudstone accumulated. In core 19, the coarse-grained and coral-rich layer of mollusk-coral-algal floatstone to rudstone represents a potential paleo-tsunami event deposited at the boundary of HST stage 1 and HST stage 2 (Klostermann et al., 2014).

Highstand stage 2 ranging from 3-1 kyrs BP, is characterized by the proposed sea-level high stand of up to 0.5 m above present mean sea-level (Kench et al., 2009), by a high accretion-rate (ca. 10 m/kyr) of the central patch reef (Gischler et al., 2008), and by high deep lagoonal sedimentation rates of 1.4 m/kyr on average. In the lagoon of Mayotte, maximum sedimentation rates of 0.8-1.2 m/kyr have been measured during 7-1.5 kyrs BP (Zinke et al., 2001, 2003a, b), which fits to our sedimentation rates of 0.55-1.4 m/kyr during HST stages 1 and 2. High amounts of sediment have been accumulated especially at the western and northern margin of the Rasdhoo lagoon, where thick units of mainly fine-grained wackestone facies were deposited. Coarse-grained coral and algal-rich sediments have accumulated towards the southeastern area of the lagoon, due to stronger water circulation through channels connecting the lagoon with the open ocean (Gischler, 2006). Generally, sediments are fining upwards during HST stage 2, confirming most of the results from the Belize atolls (Gischler, 2003). In contrast, Yu et al. (2009) measured a weakly increasing trend in coarse-grained sediment fraction over the last 4 kyrs BP in sediments of the Yongshu Reef lagoon, South China Sea. However, they mentioned this weak trend may imply increasing local storminess towards modern time in this region, but also morphological changes of the reef-lagoon may be reasonable.

Highstand stage 3 defines the time range from 1-0 kyrs BP presented by the modern distribution of lagoon sediments in Rasdhoo Atoll (Fig. 2.9d), confirming the results of Gischler (2006). The transition zone between HST stages 2 and 3 is marked by

a potential paleo-tsunami event dated to 1280 ± 120 yrs BP in core 12 (Fig. 2.2) (Klostermann et al., 2014). Sea-level was close to the present level (Gischler et al., 2008; Kench et al., 2009), and moderate sedimentation rates of around 0.6 m/kyr prevailed. Such rates seem to be common for modern sedimentation of carbonate sediments in atoll lagoons. In the Pacific Ocean, Yamano et al. (2002) investigated three atoll lagoons and estimated a mean sedimentation rate of 0.65 m/kyr. Modern sedimentary facies in the western and central part of Rasdhoo Atoll lagoon are fine-grained with >50% mud. Facies of wackestone and floatstone built up the enclosed area between the northern sand apron and the sand spit, and relative coarse-grained, coral and algal-rich facies accumulated in the eastern and southern areas of the lagoon, due to stronger currents through the channels (Gischler, 2006).

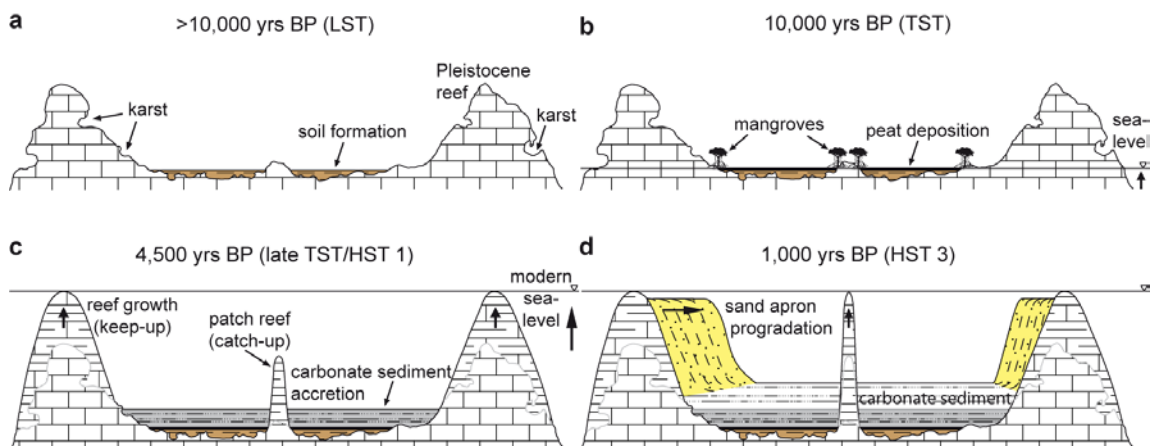


Fig. 2.9 Schematic transects (vertically exaggerated) through a mid-ocean atoll (Rasdhoo Atoll) showing Holocene reef growth and lagoonal sediment accumulation. **a** Sea-level lowstand >10 kyrs BP, subaerial exposure and erosion (karst) of a Pleistocene atoll reef and soil formation; **b** Sea-level rise to lagoon base ca. 10 kyrs BP, swamp development in the lagoon with mangroves depositing peat; **c** Sea-level reaches modern level ca. 4.5 kyrs BP, marginal reef keeping up and lagoonal reef growth catching up sea-level, carbonate sediments accumulate in the lagoon; **d** Modern situation ca. 1 kyr BP, marginal and lagoonal reefs at mean sea-level, lagoonal sediment accumulation and sand apron progradation filling up the lagoon. *LST* lowstand systems tract, *TST* transgressive systems tract, *HST* highstand systems tract.

2.5.3 Filled accommodation space versus empty bucket

In the eastern lagoon and in the marginal reef passes, the Holocene sediment cover is very low and non-existent, presumably due to strong tidal currents (Gischler, 2006). Vibracoring in these areas was therefore unsuccessful. Also, no vibracores were collected on shallow sand aprons due to the fact that the Rossfelder core system can be

used only in water depth exceeding 10 m. Sand aprons are crucial in atoll lagoon infilling by lateral progradation of reefal sediment (Marshall and Davies, 1982; Tudhope, 1989; Smithers et al., 1992; Woodroffe et al., 1994; Kench, 1998; Purdy and Gischler, 2005; Rankey and Garcia-Pérez, 2012). Based on a calculated average lagoonal background sedimentation rate of 0.65 m/kyr during the late HST and an average lagoon depth of 24 m (calculated from water depths at 17 core stations) would take some 37 kyrs to completely fill the accommodation space. Based on the length of late Quaternary interglacials, and ignoring sea-level rise due to global warming, background sedimentation alone will not suffice to fill accommodation space during the Holocene highstand. This would lead to the maintenance of the empty bucket geomorphology (Purdy and Gischler, 2005; Schlager and Purkis, 2013). Lateral infilling of the Rasdhoo Atoll lagoon by sand apron progradation would be a faster process. Based on the fact that the sand apron prograded up to 1 km since sea level reached present level some 4.5 kyrs BP, and a required progradation of ca. 3 km to the center of the lagoon, some 13.5 kyrs would be necessary for lagoonal infill. During this time span, background sedimentation would have accumulated close to 9 m of sediment. This simple calculation provides a minimum duration, and ignores the increase in lagoonal water depth from the atoll margin to the lagoon center though, i.e., a slowdown of the sand apron progradation process with time. Still, these numbers suggest that a filling of the accommodation space in such a small atoll during the Holocene highstand could be possible. However, it will not be possible in the larger atolls of the archipelago and other large atolls further afield. Timing and duration of reef lagoon infill was recently analyzed in lagoonal faroes in the Maldives (Perry et al., 2013). At smaller scale, these authors could show quantitatively that lagoon size and duration of infill are indeed negatively correlated.

2.6 Conclusions

The sediments of the Maldivian Rasdhoo Atoll lagoon were used to reconstruct the Holocene lagoonal deposition history from about 10 kyrs BP until today. A Late Pleistocene soil and an early Holocene peat layer are the oldest sediments, recovered in core 16. The soil consists of aeolian quartz and clay minerals including aluminum

chlorite, kaolinite, and mixed layer clay minerals. The peat layer is composed of mangrove deposits and marks the beginning inundation of the atoll lagoon by the rising Holocene sea-level at $10,320 \pm 100$ yrs BP, also recognizable in reefal sediment cores worldwide. The oldest carbonate sediments are dated to 7850 ± 140 yrs BP. The transition from peat to carbonate is characterized by a considerable hiatus. Carbonate facies become finer towards the modern with decreasing abundance of algal components. Therefore, Holocene lagoonal carbonate cycles can be characterized as being asymmetrical.

Six carbonate facies are classified by statistical analyses, listed in decreasing abundance: (1) mollusk-coral-algal floatstone to rudstone (mcaFR, 30%), (2) mollusk-coral-red algae rudstone (mcrR, 23%), (3) mollusk-coral-algal wackestone to floatstone (mcaWF, 23%), (4) mollusk-coral wackestone (mcW, 13%), (5) mollusk-coral mudstone to wackestone (mcMW, 9%), and (6) mollusk mudstone (mM, 2%). Based on grain-sizes in combination with coral identification, the facies represent both lagoonal background sedimentation (e.g., mcaWF, mcW, mcMW, and mM) and event sedimentation (e.g., mcaFR and mcrR), respectively.

The Rasdhoo Atoll lagoon can be divided into two areas: (1) a central to marginal deep lagoon with a lateral west-to-east textural gradient of sediment facies distribution, visible in sections <4 kyrs BP with sedimentary facies of mudstone to wackestone (mM, mcMW, and mcaWF) in the western part (e.g., cores 16, 18, and 34) and coarse-grained coral and algal-rich sediments (mcaFR and mcrR) in the eastern part of the lagoon (e.g., cores 30 and 31). The sedimentary facies >4 kyrs BP do not exhibit a lateral west-to-east textural trend (e.g., cores 16, 18, and 34). (2) A northern enclosed and shallow area between the sand apron and the sand spit accumulated "sandy" sediments of wackestone facies (mcMW, mcW, and mcaWF) without a lateral west-to-east textural gradient (cores 2, 19, 25, and 26).

Comparing the sediment accumulation data of the lagoon with two local sea-level curves, three sequence-stratigraphical system tracts may be distinguished: (1) a lowstand systems tract (LST) >10 kyrs BP. Pleistocene brownish soil superposing subaerially exposed Pleistocene reef limestone. (2) A transgressive systems tract (TST) 10-6.5 kyrs BP. A peat layer marks the beginning of inundation, and the carbonate

sedimentation starts with very low sedimentation rates of 0.02 m/kyr. (3) A highstand systems tract (HST) 6.5-0 kyrs BP, further divided into three stages (6.5-3, 3-1, 1-0 kyrs BP). During the Holocene, sea-level rise slowed down, sedimentation rates increased continuously up to a maximum of 1.4 m/kyr, the sand spit developed some 4 kyrs BP, lagoonal circulation got restricted, and the west-to-east textural gradient developed. From 1-0 kyrs BP, sedimentation rates slowed down to modern mean values of 0.6 m/kyr.

Chapter 3. Sedimentary record of late Holocene event beds in a mid-ocean atoll lagoon, Maldives, Indian Ocean: potential for deposition by tsunamis

Lars Klostermann ^{a,*}, Eberhard Gischler ^a, David Storz ^b, J. Harold Hudson ^c

^a *Institut für Geowissenschaften, Goethe-Universität Frankfurt, Altenhoferallee 1, 60438 Frankfurt am Main, Germany*

^b *Biodiversity and Climate Research Center (BiK-F) Frankfurt, Senckenberganlage 25, 60325 Frankfurt am Main, Germany*

^c *ReefTech Inc., 8325 SW 68th Street, Miami, Florida 33143, USA*

Keywords: Maldives; Holocene; atoll lagoon; tsunami; storm; event

Published in Marine Geology 348, 37–43.

Abstract: Six Holocene sedimentary events (ranging in age from 420-890, 890-1560, 2040-2340, 2420-3380, 3890-4330, and 5480-5760 yrs BP) have been identified in the lagoon of Rasdhoo Atoll (Maldives; 4°N, 73°W), thereby underlining the importance of atoll lagoons as potential archives of environmental change. Holocene coastal sediments have been studied as archives for past tsunami and storm events but comparable sedimentological studies of mid-ocean atoll lagoons are rare. In ten vibracores covering the past 6.5 kyrs that are characterized by mudstone, wackestone, and floatstone background sedimentation, we found two types of event deposits. (1) Several cm thick rudstone layers with redeposited corals like *Acropora* sp. and *Seriatopora* sp., which derive from the marginal and/or lagoonal reefs and have been transported into the lagoon. (2) Thin (several mm) layers of wackestone, floatstone, and rudstone consisting of reef-derived components like coralline red algae, reef foraminifera (e.g., *Amphistegina* spp., *Calcarina* sp.), and redeposited coral fragments. Both types of event layers may be correlated among several cores, which we interpret as tsunami deposits.

Five of the six events have temporal counterparts identified at the coasts of Thailand, Sumatra, and India. In the Maldives, close to the equator, no category 1-5 typhoons were recorded, but only tropical depressions and storms as potential triggers of event sedimentation have occurred rarely. Major earthquakes off western Indonesia and generated tsunamis, which potentially reach most parts of the Indian Ocean, are common.

3.1 Introduction

In the eastern Indian Ocean off Sumatra and the Andaman Islands, earthquakes are common due to the subduction of the Indian Plate beneath the Eurasian Plate (e.g., Newcomb and McCann, 1987). Strong earthquakes are generating tsunami waves that threaten human lives and ecosystems at the coastlines around and in the Indian Ocean. Kan et al. (2007) and Kench et al. (2008) described the effect of the tsunami on Maldivian islands generated by the catastrophic 9.2 magnitude Sumatra earthquake of 26 December 2004, which triggered wave heights of up to 1.8 m in the Maldives. Tsunami waves induce enough energy to transport and deposit grain sizes from clay to even boulders (Dawson and Stewart, 2007; Bahlburg and Spiske, 2012; Goff et al., 2012). Impacts of tsunami waves on atolls cause the transport of coarse skeletal material like coral fragments, coralline algae, and typical reef foraminifera from shallow marginal and lagoonal reefs to the deeper lagoon floor (Gischler and Kikinger, 2006). In a similar way, storms may cause reefal material to overtop reef margins and deposit coarse sediment in back-reef lagoons (Scoffin, 1993; Harmelin-Vivien, 1994; and references therein). However, evidence of tsunami and/or storm events have only been identified rarely in atoll lagoon cores. Yu et al. (2009) investigated sediment cores of an atoll lagoon in the South China Sea and dated several sedimentary events over the past 4 kyrs using redeposited coral blocks, but could not distinguish between tsunami and storm deposits. Based on grain-sizes variability in mid-late Holocene lagoon cores from a south Pacific reef lagoon, Toomey et al. (2013) identified two phases of increased storm activity during the past 5 kyrs.

Previous studies of Holocene tsunami or storm events at coastal sediment sites around the Indian Ocean focused on the west coast of Thailand (Harper, 2005; Jankaew

et al., 2008; Fujino et al., 2009; Brill et al., 2011), northern Sumatra (Monecke et al., 2008), eastern India (Rajendran et al., 2006), and the Andaman Islands (Malik et al., 2010) and documented several events during the last 2 kyrs.

Differences between depositional events like gravity mass movements, storms, and tsunamis are discussed by Einsele et al. (1996) and Morton et al. (2007), nevertheless, robust criteria to distinguish storm and tsunami deposits are lacking. Einsele et al. (1996) explained that gravity mass movements were induced by storm and tsunami waves, but especially tsunami waves produce slope failures.

In contrast to many other tropical reef areas, the cyclone activity in the northern Indian Ocean, especially in the Arabian Sea, is relatively low (Singh et al., 2000; Webster et al., 2005). The location close to the equator prevents major parts of the Maldives from being hit by strong cyclones (e.g., Woodroffe, 1992), which largely excludes storms as triggers of coarse-grained event layer formation. Therefore, the objectives of this study are to identify coarse-grained event layers in fine-grained lagoonal successions of a Maldivian atoll, relate these layers to paleo-tsunamis, and evaluate the quality of this tsunami archive.

3.2 Regional setting

The Maldivian archipelago, located in the Indian Ocean southwest of India (7°N to 1°S at 73°E), forms an elongated chain of twenty-one atolls and four reef-fringed islands (Fig. 3.1). The entire Maldives carbonate platform covers an area of 107,500 km² including reefs, lagoons, seaways, and some 1,200 islands with a maximum elevation of 5 m above sea level. Rasdhoo Atoll is located in the central part of the archipelago, has a diameter of 9.25 km, and covers 62 km². The lagoon is up to 40 m deep and harbors numerous patch reefs. Three channels interrupt the marginal reef, connecting the interior lagoon with the open ocean. Modern reef facies are coralgall grainstones and lagoonal facies include wackestone, mudstone, and hardgrounds in the vicinity of channels (Gischler, 2006).

Climate and hydrography in the Maldives is strongly influenced by the Indian Monsoon (Storz and Gischler, 2011). During May to September, strong winds from the southwest, increased precipitation and storms predominate, whereas from November to

March, weaker winds from the NE with lower rainfall frequency characterize the study area. Two tropical storms (1991, 2006) and three tropical depressions (1992, 1993) have crossed the northern part of the Maldives archipelago since 1945 according to the Joint Typhoon Warning System (<http://www.usno.navy.mil/JTWC>) and the tropical cyclone dataset (<http://www.nhc.noaa.gov/> data).

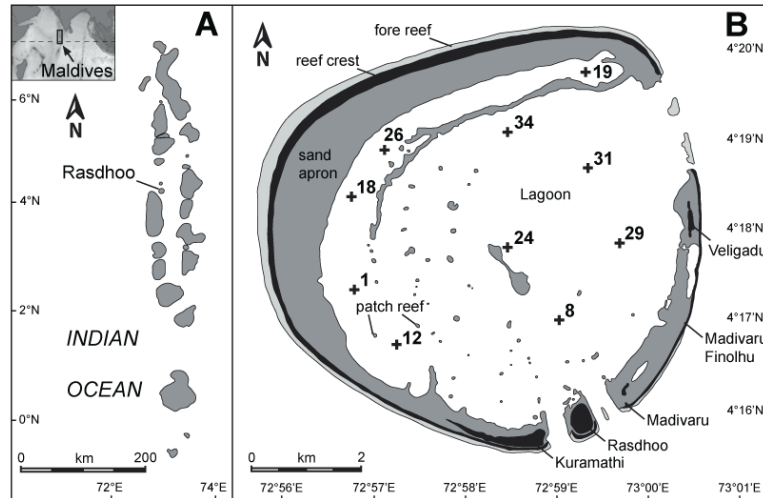


Fig. 3.1 A. Location of the Maldivian archipelago and Rasdhoo Atoll in the Indian Ocean; B. Locations of ten investigated core stations within Rasdhoo Atoll lagoon.

3.3 Methods

During an expedition in November - December 2010, forty-two stations in the Rasdhoo Atoll lagoon were selected for coring with a Rossfelder electrical vibracorer connected to 6 m-long aluminum pipes. The ten cores investigated here are located along the margin and in the center of the lagoon. Water depths range from 12.6-20 m at the marginal coring sites (1, 12, 18, 19, and 26) and from 28.5-37.5 m at the central coring sites (8, 24, 39, 31, and 34). Cores 8, 12, 18, 19, 24, 29, 31, and 34 were sampled at 10 cm-intervals and cores 1 and 26 with varying sample distance. All samples ($n=203$) were sieved through 0.125 mm and 2 mm sieves. Thin-sections ($n=133$) of the 2-0.125 mm grain-size fraction were investigated with a polarization microscope and the composition was quantified by point-counting two-hundred components per section (van der Plas and Tobi, 1965). We described the sediments according to the carbonate nomenclature of Dunham (1962), which was extended by Embry and Klován (1972).

Even though the nomenclatures were developed for rocks, they have been commonly used in sediments among carbonate sedimentologists since several decades. We chose 50% "mud" (grain-size fraction $<63 \mu\text{m}$) as the boundary between mud-supported and grain-supported textures. Facies were defined based on a cluster analysis of the composition and texture data (dendrogram not shown; detailed sedimentological results will be published elsewhere). Corals were identified using the reports of Pillai and Scheer (1976), Ciarapica and Passeri (1993), and the compendium of Veron (2000). Thirty-six samples of bulk sediment and one shell sample were dated radiometrically with accelerated mass spectroscopy (AMS) and eight corals were dated using the standard radiocarbon ^{14}C -method by Beta Analytic Inc., Miami, Florida (Table 3.1).

Table 3.1 Radiometric ages in years before present (BP) of coral, shell, and bulk sediment samples.

Core #	Sampling depth [cm]	Description	Beta No.	Conventional ^{14}C -Age (not calendar calibrated)	Calendar Calibrated Age (2 Sigma Calibration)
1	52-55	bulk (AMS)	338666	1930 ± 30 BP	1365 ± 135 BP
8	20-30	bulk (AMS)	317605	1040 ± 30 BP	525 ± 105 BP
8	56-75	coral (^{14}C)	308129	2040 ± 30 BP	1455 ± 155 BP
8	123-132	coral (^{14}C)	308130	2890 ± 30 BP	2500 ± 190 BP
8	150-160	bulk (AMS)	345350	3280 ± 30 BP	2950 ± 190 BP
8	176-189	coral (^{14}C)	308131	3670 ± 30 BP	3435 ± 145 BP
12	19-20	bulk (AMS)	309059	2640 ± 30 BP	2150 ± 170 BP
12	21	bulk (AMS)	320751	1870 ± 30 BP	1280 ± 120 BP
12	110-120	bulk (AMS)	317606	2250 ± 30 BP	1690 ± 170 BP
12	242	bulk (AMS)	309060	2480 ± 30 BP	1970 ± 160 BP
18	20-30	bulk (AMS)	325014	1470 ± 30 BP	875 ± 155 BP
18	275-280	bulk (AMS)	325015	3920 ± 30 BP	3725 ± 175 BP
18	300-310	bulk (AMS)	345354	4210 ± 30 BP	4125 ± 205 BP
18	330-337	coral (^{14}C)	320766	5310 ± 30 BP	5540 ± 120 BP
19	95-100	bulk (AMS)	304918	1670 ± 30 BP	1090 ± 160 BP
19	215-220	bulk (AMS)	304919	2870 ± 30 BP	2495 ± 195 BP
19	255-260	bulk (AMS)	304920	3500 ± 30 BP	3215 ± 165 BP
19	318	shell (AMS)	297654	6990 ± 50 BP	7375 ± 135 BP
24	21-24	bulk (AMS)	325016	1200 ± 30 BP	625 ± 105 BP
24	40-50	bulk (AMS)	325017	1520 ± 30 BP	925 ± 145 BP
24	60-70	bulk (AMS)	345355	2000 ± 30 BP	1420 ± 140 BP
24	100-105	bulk (AMS)	325018	2760 ± 30 BP	2305 ± 175 BP
24	105-112	bulk (AMS)	345356	2690 ± 30 BP	2200 ± 150 BP
24	136-145	coral (^{14}C)	320767	3300 ± 30 BP	2965 ± 195 BP
26	46-49	bulk (AMS)	338667	1610 ± 30 BP	1030 ± 140 BP
26	128-130	bulk (AMS)	338668	1890 ± 30 BP	1300 ± 130 BP
26	185-195	coral (^{14}C)	345365	3760 ± 30 BP	3525 ± 165 BP
29	10-20	bulk (AMS)	345357	1350 ± 30 BP	755 ± 135 BP
29	30-35	bulk (AMS)	317607	1800 ± 30 BP	1205 ± 135 BP
29	61-66	bulk (AMS)	345358	1690 ± 30 BP	1105 ± 155 BP
29	73-80	bulk (AMS)	345359	1870 ± 30 BP	1280 ± 120 BP
29	90-98	bulk (AMS)	317608	2680 ± 30 BP	2190 ± 150 BP
29	110-120	bulk (AMS)	325019	3100 ± 30 BP	2740 ± 130 BP
29	135-142	coral (^{14}C)	308132	3460 ± 30 BP	3460 ± 150 BP
31	30-40	bulk (AMS)	345360	208 ± 30 BP	1510 ± 170 BP
31	50-60	bulk (AMS)	325020	2910 ± 30 BP	2515 ± 195 BP
31	60-70	bulk (AMS)	345361	3210 ± 30 BP	2875 ± 155 BP
31	100-110	bulk (AMS)	345362	4190 ± 30 BP	4085 ± 195 BP
31	125	bulk (AMS)	320753	4110 ± 30 BP	3985 ± 175 BP
34	70-80	bulk (AMS)	325021	1820 ± 30 BP	1235 ± 125 BP
34	145	coral (^{14}C)	308133	2980 ± 30 BP	2550 ± 190 BP
34	160-170	bulk (AMS)	345363	3000 ± 30 BP	2590 ± 170 BP
34	260-270	bulk (AMS)	317609	4210 ± 30 BP	4125 ± 205 BP
34	340-350	bulk (AMS)	345364	5400 ± 30 BP	5620 ± 140 BP
34	400	bulk (AMS)	309062	6180 ± 40 BP	6465 ± 165 BP

3.4 Results and interpretation

We identified six event horizons (Fig. 3.2) with age ranges of 420-890 yrs BP (event 1), 890-1560 yrs BP (event 2), 2040-2340 yrs BP (event 3), 2420-3380 yrs BP (event 4), 3890-4330 yrs BP (event 5), and 5480-5760 yrs BP (event 6) that are characterized by (1) mm-thin coarse-grained, reef-derived layers within finer-grained background sedimentation and by (2) cm-thick layers of allochthonous shallow-water corals such as *Acropora* sp., *Pachyseris* sp., *Seriatopora* sp., *Merulina* sp., *Cyphastrea* sp., *Goniopora* sp., and fungiids (Table 3.2). Spatial patterns of distribution of event layers in the Rasdhoo lagoon are limited. Event layers 1 and 4 cover the eastern and northeastern parts of the lagoon, respectively. Event layers 1 and 4 have the greatest lateral extents (Figs. 3.1, 3.2). We interpret these event horizons as tsunami deposits.

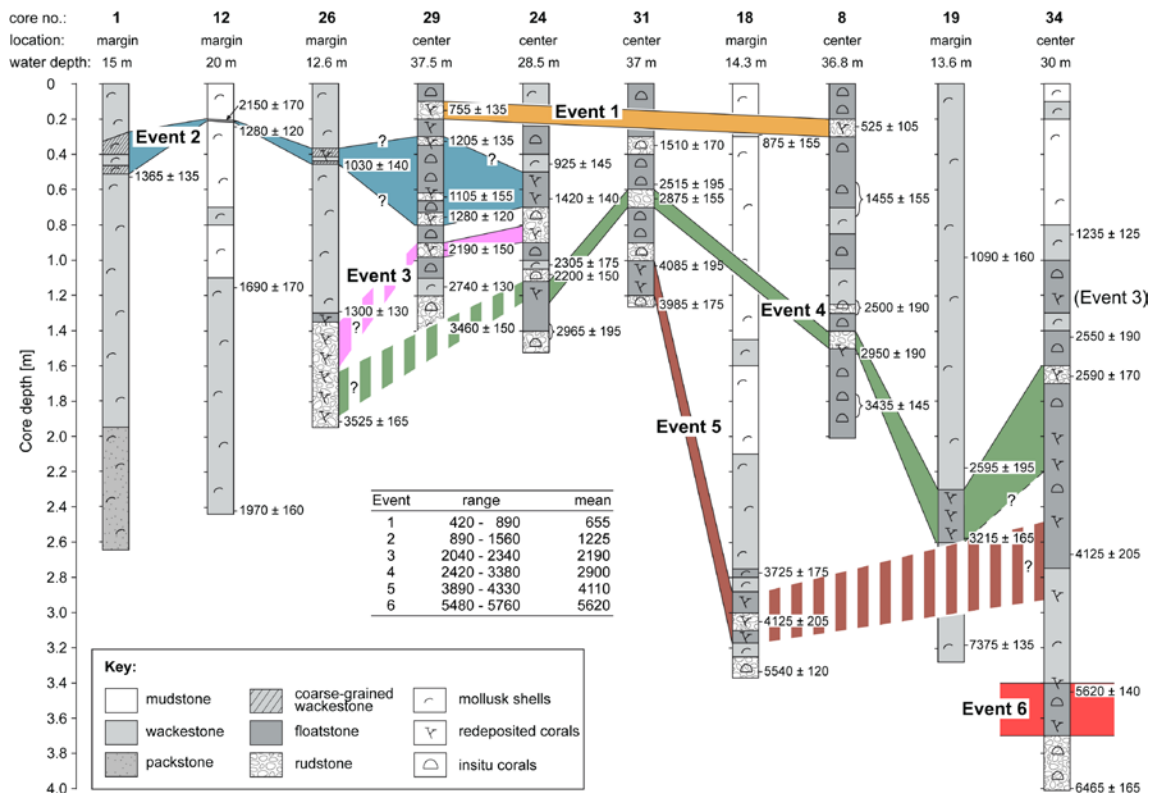


Fig. 3.2 Ten core logs highlighting six sedimentary events. Core logs are arranged so that event layers may be correlated in a clearly laid-out manner. The age range and mean of each event are shown in the table within the figure. The ages are calendar-calibrated with a two-sigma probability in yrs BP. The branched coral symbols mark the redeposited corals (e.g., *Acropora* sp., *Seriatopora* sp.) and the solid coral symbols mark the insitu corals that have not been transported (e.g., *Porites* sp., *Leptoseris* sp.). Close-ups of the first three cores showing event 2 in detail are displayed in Fig. 3.3. Average lagoonal background sedimentation rate amounts to 0.92 m/kyrs, based on 53 calculations between dated samples (not shown).

Table 3.2 List of identified corals with redeposited, shallow-water taxa marked.

Core #	Sample depth [cm]	Coral genus	Potentially redeposited
8	3	<i>Leptoseris sp.</i>	no
8	5	<i>Leptoseris sp.</i>	no
8	15	<i>Leptoseris sp.</i>	no
8	26	<i>Goniopora sp.</i>	yes
8	35	<i>Leptoseris sp.</i>	no
8	86	<i>Porites sp.</i>	no
8	90	<i>Leptoseris sp.</i>	no
8	127	<i>Porites sp.</i>	no
8	155	<i>Acropora sp.</i>	yes
8	163	<i>Porites sp.</i>	no
8	170	<i>Porites sp.</i>	no
8	175	<i>Porites sp.</i>	no
8	178	<i>Porites sp.</i>	no
8	185	<i>Porites sp.</i>	no
18	290	<i>Acropora sp.</i>	yes
18	310	<i>Acropora sp.</i>	yes
18	335	<i>Porites sp.</i>	no
19	235	<i>Acropora sp.</i>	yes
19	245	<i>Acropora sp.</i>	yes
19	250	<i>Acropora sp.</i>	yes
19	258	<i>Acropora sp.</i>	yes
24	30	<i>Acanthastrea sp.</i>	no
24	32	<i>Leptoseris sp.</i>	no
24	45	<i>Leptoseris sp.</i>	no
24	58	<i>Acropora sp.</i>	yes
24	58	<i>Echinophyllia sp.</i>	no
24	62	<i>Acropora sp.</i>	yes
24	67	<i>Pachyseris sp.</i>	yes
24	75	<i>Porites sp.</i>	no
24	95	<i>Porites sp.</i>	no
24	130	<i>Fungia sp.</i>	yes
24	142	<i>Porites sp.</i>	no
26	39	<i>Seriatopora sp.</i>	yes
26	43	<i>Seriatopora sp.</i>	yes
26	132	<i>Seriatopora sp.</i>	yes
26	133	<i>Acropora sp.</i>	yes
26	140	<i>Acropora sp.</i>	yes
26	143	<i>Acropora sp.</i>	yes
26	146	<i>Acropora sp.</i>	yes
26	150	<i>Favia sp.</i>	yes
26	154	<i>Seriatopora sp.</i>	yes
26	157	<i>Acropora sp.</i>	yes
26	160	<i>Caryophyllia sp.</i>	no
26	163	<i>Porites sp.</i>	no
26	164	<i>Seriatopora sp.</i>	yes
26	165	<i>Acropora sp.</i>	yes

Table 3.2 continued

26	170	<i>Acropora sp.</i>	yes
26	175	<i>Fungia sp.</i>	yes
26	180	<i>Seriatopora sp.</i>	yes
26	182	<i>Favia sp.</i>	yes
26	183	<i>Acropora sp.</i>	yes
26	186	<i>Seriatopora sp.</i>	yes
26	192	<i>Favia sp.</i>	yes
29	5	<i>Coscinaraea sp.</i>	no
29	18	<i>Leptoseris sp.</i>	no
29	22	<i>Acropora sp.</i>	yes
29	30	<i>Pachyseris sp.</i>	yes
29	40	<i>Leptoseris sp.</i>	no
29	50	<i>Leptoseris sp.</i>	no
29	59	<i>Cyphastrea sp.</i>	yes
29	75	<i>Merulina sp.</i>	yes
29	91	<i>Pachyseris sp.</i>	yes
29	109	<i>Porites sp.</i>	no
29	122	<i>Porites sp.</i>	no
31	3	<i>Echinophyllia sp.</i>	no
31	12	<i>Leptoseris sp.</i>	no
31	23	<i>Leptoseris sp.</i>	no
31	31	<i>Acanthastrea sp.</i>	no
31	82	<i>Porites sp.</i>	no
31	83	<i>Leptoseris sp.</i>	no
31	102	<i>Porites sp.</i>	no
31	103	<i>Leptoseris sp.</i>	no
31	106	<i>Acropora sp.</i>	yes
31	115	<i>Acropora sp.</i>	yes
34	105	<i>Alveopora sp.</i>	no
34	108	<i>Caryophyllia sp.</i>	no
34	112	<i>Pachyseris sp.</i>	yes
34	140	<i>Alveopora sp.</i>	no
34	146	<i>Porites sp.</i>	no
34	155	<i>Porites sp.</i>	no
34	162	<i>Acropora sp.</i>	yes
34	190	<i>Porites sp.</i>	no
34	202	<i>Seriatopora sp.</i>	yes
34	218	<i>Acropora sp.</i>	yes
34	222	<i>Acropora sp.</i>	yes
34	225	<i>Caryophyllia sp.</i>	no
34	230	<i>Porites sp.</i>	no
34	247	<i>Fungia sp.</i>	yes
34	250	<i>Acropora sp.</i>	yes
34	285	<i>Cyphastrea sp.</i>	yes
34	295	<i>Cyphastrea sp.</i>	yes
34	298	<i>Acropora sp.</i>	yes
34	342	<i>Seriatopora sp.</i>	yes
34	347	<i>Caryophyllia sp.</i>	no
34	363	<i>Stylophora sp.</i>	yes

Event 1 occurs in the uppermost parts of cores 8 and 29 and ranges in age from 420-890 yrs BP. These layers are characterized by redeposited shallow-water corals within coarse-grained sediment facies (rudstone layers). Event 1 may be correlated to paleo-tsunami layers identified at the coast of Thailand ranging in age from 550-700 yrs BP (Jankaew et al., 2008) and 500-700 yrs BP (Brill et al., 2011). Monecke et al. (2008) have reported a paleo-tsunami layer from the coast of Sumatra ranging from 550-660 yrs BP, which also covers the age range of event 1.

Event 2 was identified in five cores and is most clearly recognized in core 12. It consists of distinct, coarser-grained layers in the eastern lagoon cores 1, 12, and 26, and contains redeposited corals in cores 24, 26 and 29. It may be seen at high-resolution sampling that the abundance of corals (10-13%), coralline red algae (2.5-4.0%), and reef foraminifera (1.0-2.5%) significantly increases within the coarser layers of cores 1, 12, and 26 (Fig. 3.3). The identified foraminifera (e.g., *Amphistegina* spp. and *Calcarina* sp.) are characteristic of the shallow-water (1-2 m) Reef Assemblage 1 of benthic foraminifera at Ari and Rasdhoo Atoll (Parker and Gischler, 2011). The thin coarse-grained layer in core 12 is dated to 2150 ± 170 yrs BP and is significantly older than the surrounding material. This redeposited layer contains typical reef-constituting particles, and is therefore interpreted as an event layer, deposited at 1280 ± 120 yrs BP (date from directly below the event layer). Related dates in core 29 suggest high sedimentation rates and more than one depositional sequence in these time intervals that prevent us to pin down event 2 to one individual layer. The age range of this event, when taking the other four cores into consideration, is 890-1560 yrs BP. The deposits of an extreme wave event ("layer C") dated to 1265 ± 85 yrs BP at the southwestern coast of Thailand (Brill et al., 2011) falls within the age range of event 2. Event deposits of the same age range were also recognized by Rajendran et al. (2006) at the east coast of India dated to ca. 1.5 kyrs BP, and by Monecke et al. (2008) at the northern coast of Sumatra ranging from 960-1170 yrs BP.

Event 3, characterized by transported shallow-water corals within rudstone layers, was identified in three cores (24, 26, and 29). The age range is 2040-2340 yrs BP. This horizon can be correlated to a paleo-tsunami event identified by Jankaew et al. (2008) at the Thailand coast, which has an age range of 2200-2400 yrs BP.

Event 4 is found in six cores, has an age range of 2420-3380 yrs BP, and mostly occurs as a coral-rich rudstone layer in central lagoon cores (Fig. 3.2). A high abundance of redeposited *Acropora* corals characterizes this event in core 19. It is questionable whether the rudstone layer in core 31 represents event 4, because no redeposited corals were found. Event 4 has time-equivalent counterparts in Thailand (2.7-4.3 kyrs BP) and in India (3.7 kyrs BP), which were interpreted as paleo-tsunami layers (Rhodes et al., 2011).

Event 5, ranging in age from 3890-4330 kyrs BP, was identified in three cores and is also characterized by redeposited shallow-water corals within floatstone and rudstone layers. Like event 4, it may potentially be correlated to events identified along the coast of Thailand (2.7-4.3 kyrs BP) and possibly at the southwestern coast of India (3.7 kyrs BP) (Rhodes et al., 2011).

Event 6 is found only in core 34 and has an age of 5620 ± 140 yrs BP. The occurrence of allochthonous shallow-water corals within a floatstone unit characterizes this event. There are no reports on paleo-tsunami layers from adjacent coasts around the Indian Ocean with the same age range.

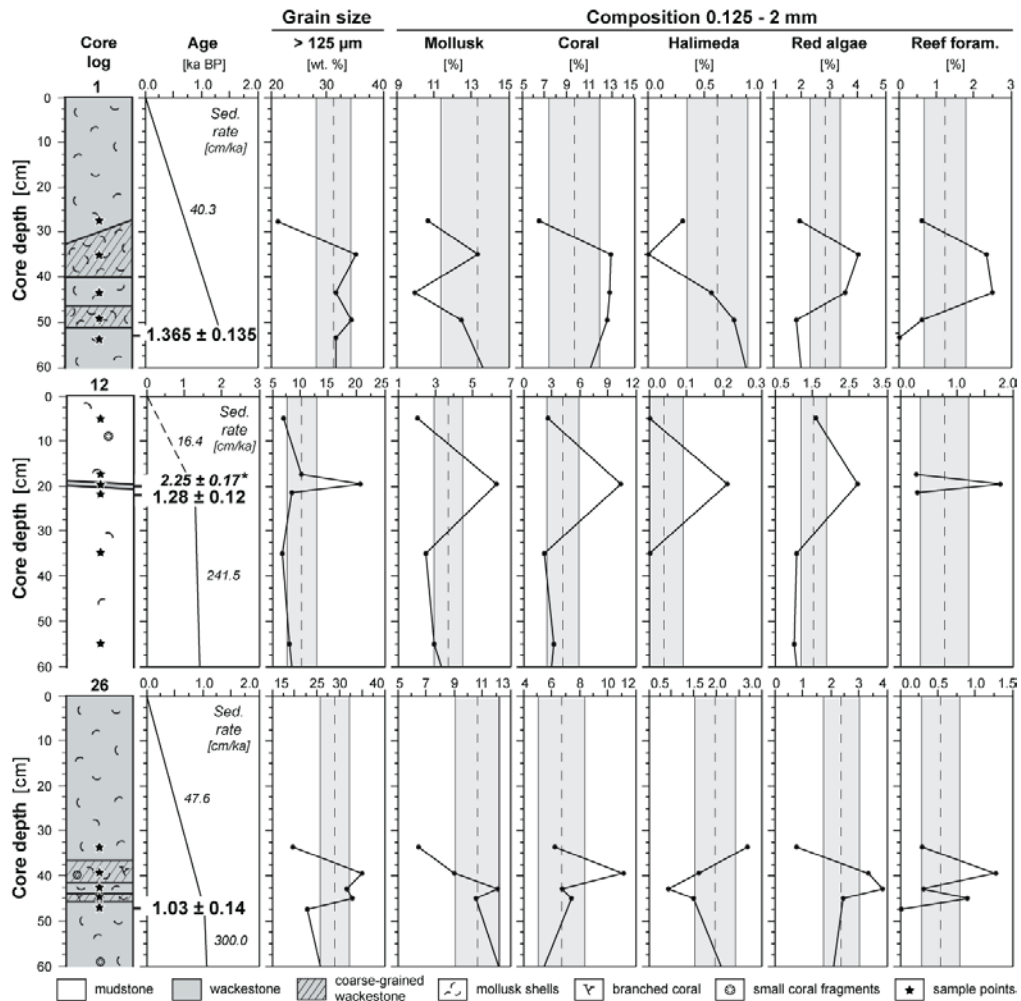


Fig. 3.3 Close-up of the topmost 60 cm of three marginal cores 1, 12, and 26. Sedimentation rates and the composition of the coarser layers show a change in sedimentation and facies types. The dashed line is the statistical mean; the gray area is the standard deviation ($\pm 1\sigma$).

3.5 Discussion

3.5.1. Tsunamis versus storms

To distinguish between tsunami and storm deposits, Morton et al. (2007) and Goff et al. (2012) listed typical characteristics of tsunami deposits in coastal environments. Coastal tsunami deposits are usually single homogeneous or graded sand beds with grain-sizes decreasing landward, mud laminae and rip-up mud clasts, and thicknesses <25 cm. Coastal boulder deposits may be common. In atoll lagoons, wave and gravity-induced slides from the back reef sand apron and lagoonal patch reefs into the lagoon can result in deposition of coarse-grained material. Likewise, larger fragments of shallow water reef-dwelling corals, such as *Acropora* sp., may be

transported from the marginal and/or lagoonal reefs into the deep lagoon environment (Scoffin, 1993). Einsele et al. (1996) pointed out that tsunami and storm waves may trigger gravity mass movements. He explained that the long wavelength and the changes in water pressure as well as the earthquake-induced stress are the most important processes causing slope failure. Gischler and Kikinger (2006) documented the impacts of the tsunami event on Rasdhoo Atoll in December 2004 including coral rubble slides at reef slopes in water depth of up to 7 m and substantial marginal sand erosion and transport towards the fore reef slope and lagoon. Reef-derived sands did not cover the lagoon floor completely but formed sand lobes spatially limited to the reef vicinity. It has to be admitted though that evidence for the identification of tsunami deposits, even when applying a multi-proxy approach, might be missing (Goff et al., 2012). This is especially relevant in 7.5-cm-diameter cores and a lack of outcrops in this study.

Storms as triggers of the six event beds cannot be excluded; however, the study area is situated in a virtually cyclone-free latitude. Only two tropical storms and three tropical depressions have been recorded crossing the Maldives since 1945. Wind speeds ranged between only 36-72 km/h (<http://www.nhc.noaa.gov/data>). No category 1-5 typhoons were recorded over the Maldives in the 68-year time window. Tropical storms and depressions passed the northern part of the archipelago. For comparison, Holocene storm data from Belize, Caribbean Sea, suggests that only category 4 and 5 hurricanes left event beds in the Lighthouse Reef Atoll lagoon whereas weaker hurricanes and tropical storms and depressions remained sedimentologically undetected (Gischler et al., 2008, 2013). Holocene cyclone records around the Indian Ocean are not as numerous as in the Atlantic and Pacific Oceans, but data from western Australia suggest elevated storm activity during 3.5-0.5 kyrs BP (Nott and Forsyth, 2012) and low activity from 5.4-3.7 kyrs BP (Nott, 2011). Events 1-4 would fall within this Holocene time window of increased storm activity; events 5 and 6 are situated in the apparent storm gap.

3.5.2 Limitations of the study

Event deposits apparently do not cover the entire lagoon floor investigated, and therefore only portions of these deposits were identified in Rasdhoo Atoll lagoon successions. For example, the 2004 tsunami did not produce a continuous event layer in

the lagoon (Gischler and Kikinger, 2006). Weaker, previous tsunamis possibly did not even trigger sediment redeposition from reefs to the lagoon floor. The frequency of major earthquakes (magnitude 8 and higher) at the Indonesian subduction zone is probably one per century according to historical data of Natawidjaja et al. (2006) and Verma and Bansal (2013). In the eastern Pacific, Araoka et al. (2013) estimated the major tsunami frequency to 150-400 years using age dates from redeposited coastal coral boulders. Based on these numbers, in the observed time window since 6.5 kyrs BP, tens (16-65) of major tsunami events occurred. However, only six events left identifiable traces in the atoll lagoon.

Time averaging via bioturbation and bulk sediment age dating cannot be excluded completely. Tudhope and Scoffin (1984) have shown how burrowing crustaceans may rework the upper ca. 60 cm of atoll lagoon sediments. Characteristic traces of *Callianassa* such as indurated burrow linings and its claws were found in all cores, but the abundance of crustacean remains were less than 2% throughout all samples. No mounds of *Callianassa* were observed during Scuba diving in the Rasdhoo Atoll lagoon, which supports the contention of only limited bioturbation.

Age dating of bulk sediments means that many different carbonate particles including mollusk shells, foraminifera, corals, and calcareous algae were analyzed, which have different taphonomic histories and ages. Flessa and Kowalewski (1994) have demonstrated that the mean age of 128 modern nearshore shells (compiled from the literature) may be as high as 2400 years. Modern sediment ages in atoll environments are significantly younger. Calibrated radiocarbon ages of modern bulk sediments in atoll lagoons of Belize ranged only from 255 yrs BP to modern (Gischler and Lomando, 2000, their table 1). Marginal bulk sediment samples from the back reef produced the oldest ages of up to 1045 yrs BP. Reef margin and fore reef samples were intermediate between the lagoon and the back reef samples.

The shallow-water origin of some of the corals identified, which were used as an indicator of redeposition, may be questioned. First, identifications of coral fragments could in many cases only be made to the genus level. Second, there exist different opinions among coral specialists regarding the depth range for some of the taxa (D. Potts, pers. comm.), and are often given in units of tens of meters. Likewise, depth

ranges of typical coralgall assemblages may be as high as 10 m (Cabioch et al., 1999). According to Scuba observations and sediment grab sampling, abundant coral growth on the deep lagoon floor of Rasdhoo Atoll is rather rare (Gischler, 2006). Sea-level data confirms that water depth in the Rasdhoo Atoll lagoon were >35 m during the past 6.5 kyrs. Due to rapid sea-level rise during the early Holocene, sea level was only 3 m below present level some 6.5 kyrs BP (Gischler et al., 2008). Therefore, we are convinced that common shallow-water corals, such as acroporids from the lagoon floor, have been redeposited and originate from shallow-water reef environments.

3.6 Conclusions

Six coarser grained layers in muddy background sediments of a Maldivian atoll lagoon were interpreted as Holocene tsunami events, based on the increase of allochthonous skeletal material with shallow-water reef affinity such as fragments of shallow-water coral species, coralline red algae, and reef-dwelling foraminifera in these layers, as well as AMS dating. Five of the six layers may be correlated to previously published tsunami events at adjacent coastal research sites. The mid-late Holocene atoll lagoon archive is incomplete though based on the assumption that major earthquakes at the Indonesian subduction zone generated more than six major tsunamis during the past 6.5 kyrs.

Chapter 4. Changes in diversity and assemblages of foraminifera through the Holocene in an atoll from the Maldives, Indian Ocean

David Storz^{1*}, Eberhard Gischler², Justin Parker³, Lars Klostermann²

¹ *Biodiversity and Climate Research Center (BiK-F) Frankfurt, Senckenberganlage 25, 60325 Frankfurt am Main, Germany*

² *Institut für Geowissenschaften, J.W. Goethe-Universität, Altenhoferallee 1, 60438 Frankfurt am Main, Germany*

³ *School of Earth and Environmental Sciences, University of Western Australia, Crawley, Perth, WA 6009, Australia*

Keywords: benthic foraminifera; Holocene; Maldives; biodiversity

Published in Marine Micropaleontology 106, 40–54.

Abstract: This study presents the first high-resolution Holocene records of diversity and assemblages of benthic foraminifera from tropical reef environments in the Indian Ocean. Two 3.2 m and 4.4 m long cores from the lagoon of Rasdhoo Atoll (4°N/73°W) in the central Maldives, were sampled at ~250 yr intervals. Core #16 covers most of the Holocene (10.32.0 kyrs BP) and was taken in the deep lagoon of the atoll (35 m water depth). Core #19 covers the time span 7.375-0 kyrs BP and is from a sublagoon (14 m water depth) on the northern margin of the atoll. In Core #16, an early colonization phase during Holocene sea-level rise is characterized by an *Ammonia* sp. 1 dominated assemblage until ~7 kyrs BP. The slowdown of sea-level rise in the Mid Holocene (~4 kyrs BP) marks the onset of a phase of stable environmental conditions in the deep lagoon with high diversity. A shift toward lower diversity and the dominance of *Textularia foliacea* has occurred from ~4-1 kyrs BP, which may be explained with the Intermediate Disturbance Hypothesis. An environmental change at ~1.4 kyrs BP has

caused a distinct faunal change, the decrease of *T. foliacea* and an increased recovery in diversity. In Core #19, a significant faunal change at ~4.0 kyrs BP from an *Ammonia* sp. 2 dominated fauna to a fauna with *Ammonia* sp. 1, miliolid taxa and a higher diversity might be related to the formation of a sand spit that separates the sublagoon from the main lagoonal basin. The westward extension of the sand spit during the Late Holocene could have changed the restricted bottom water circulation in the main lagoon and caused longer residence times of water and the build-up of lower oxygen and higher nutrient concentrations. This study underlines the importance of the factor time on diversity and the significance of lagoon circulation and bottom water residence times on assemblages and diversity of benthic foraminifera.

4.1 Introduction

A better understanding of temporal and spatial variations in natural biodiversity in the vulnerable tropical coral reef environment will be crucial when attempting to estimate future loss of biodiversity due to natural and anthropogenic environmental change (Hoegh-Guldberg, 2011). In present-day coral reefs, benthic foraminifera are the most important carbonate sediment producers besides corals and calcareous algae (Langer et al., 1997; Yamano et al., 2001). They have a great significance for ecological, sedimentological and stratigraphic studies (Scott et al., 2001; Yamano et al., 2001; Murray, 2006; Boudagher-Fadel, 2008; Langer 2008). Numerous studies have used benthic foraminifera as facies indicators of fossil and modern carbonate depositional environments (Yamano et al., 2001; Langer and Lipps, 2003; Beavington-Penney and Racey 2004), of Holocene sea level change (Horton, 2006), of environmental stress in modern reef environments (Alve, 1995; Cockey et al., 1996) and for the interpretation of storm deposits (Mamo et al., 2009). The investigation of differences between foraminiferal assemblages and diversities in fossil and modern reef environments also contributes to a better understanding of the long-term influence of environmental factors on the biodiversity in modern coral reefs and associated faunas on glacial/interglacial scales (Mossadegh et al., 2012; Parker et al., 2012).

Studies on the distribution of modern benthic foraminifera in shallow-water reef and carbonate platform environments in the Indo-Pacific mainly focus on the central

Indo-Pacific and the western Pacific (Langer and Lipps, 2003; Langer and Hottinger, 2000; Bicchi et al., 2002; Parker, 2009; Makled and Langer, 2011 and references within). Existing surveys of benthic foraminifera in surface sediments from the Western Indian Ocean region (including the Red Sea) show many differences in faunal composition, compared to those from the central Indo-Pacific (e.g. compare Heron-Allen and Earland, 1915, Chasens, 1981 and Hottinger et al., 1993 with Loeblich and Tappan, 1994, Parker, 2009). In the Maldives, Parker and Gischler (2011) identified taxa of Indo-Pacific provenance co-occurring with taxa only recorded from coastal regions in the Red Sea and western Indian Ocean.

These studies show that a variety of environmental and sedimentological parameters control the distribution, assemblages and diversity of benthic foraminifera in reef environments. Bicchi et al. (2002) and Gischler et al. (2003) found highest foraminiferal diversity in Pacific and Caribbean atoll lagoons that have open circulation. Habitat size can also influence diversity, by virtue of habitat diversity (Schultz et al., 2010). Schultz et al. (2010) also observed highest diversity in an atoll lagoon with high levels of nutrient availability and abundant fine-grained substrate. Haig (1988, 1993) found diversity of miliolid and buliminid foraminifera in a Papuan lagoon related with mud content and depth. Parker and Gischler (2011) also showed water depth to have a significant influence on diversity and assemblages of benthic foraminifera in the Maldives. They found a positive correlation between water depth and diversity ($r = 0.63$; $p < 0.0001$; Shannon's H) and highest diversity in water depth at 30-50 m. All these environmental factors have an impact on the number of available microhabitats in reef environments that influence diversity and distribution of benthic foraminifera in modern surface sediments (Langer and Lipps, 2003).

Few studies have examined changes in benthic foraminiferal assemblages and diversity through the Holocene in tropical reef environments (Schultz et al., 2010; Cheng et al., 2012). In the Indian Ocean, no such studies have been conducted. Cheng et al. (2012) studied Holocene and historical changes in species richness, diversity and assemblages of benthic foraminifers in Florida Bay to infer anthropogenic-induced environmental stress during the last 100 yrs, and Late Holocene salinity and sea level changes.

Habitat age has been reported as a factor that could influence benthic foraminiferal diversity in atoll reefs and lagoons. Bicchi et al. (2002) found higher species richness in deeper lagoons that were flooded earlier during the post glacial transgression as compared to shallower lagoons that were inundated later. These authors suggested the longer colonization period as a possible cause, but could not rule out the influence of a greater variety of available biotopes in the deeper lagoons (Bicchi et al., 2002).

Over deep geological time, i.e., millions of years, factors such as plate tectonics and the opening/closing of seaways may explain species richness and diversity changes in certain biogeographical regions (Langer and Lipps, 2003). On smaller time frames, several hypotheses have been suggested to account for modern species richness in terrestrial and marine habitats (Sanders, 1969; Connell, 1978 and references therein). According to the Intermediate Disturbance Hypothesis (IDH) of Connell (1978), local diversity reaches its maximum, when ecological and/or physical disturbance is neither too rare, nor too frequent, or occurs neither too soon nor too long after a certain disturbance. The applicability of the IDH was tested for different communities in various environments (e.g., Aronson and Precht, 1995 for coral reefs) and its validity is subject of debate (e.g., Hughes, 2010 and references therein). This idea opposes older hypotheses such as theories that assume highest diversity in an equilibrium state of a community (i.e. the Time Stability Hypothesis of Saunders, 1969) suggesting that diversity is higher in less disturbed and older environments. Richardson-White and Walker (2011) found that the IDH could not explain all encountered diversity patterns in different environments of encrusting foraminifera. Schultz et al. (2010) suggested that an increase in foraminiferal diversity in Belizian atolls during the Holocene was a diversification phase. However, a higher temporal resolution was needed to analyze the effects of disturbance events on diversity and assemblages.

Complementary to the study of Parker and Gischler (2011) that investigated spatial patterns of distribution, diversity and assemblages in surface sediments from Rasdhoo and Ari Atolls at the Maldives, this study investigates the temporal variation of diversity and assemblages through the Holocene. Sediment cores from two different lagoon sites are chosen for this study. They are well suited for such a study: they offer

continuous sedimentation records through the Holocene and enable high temporal resolution sampling. Both cores represent two lagoonal sites that experienced environmental changes during the Holocene sea-level rise (Lambeck, 1990; Gischler et al., 2008). To date, most research on effects of Holocene environmental change on biodiversity has been conducted in coastal environments, which is sensitive to changes in sea level as compared to mid-oceanic reefal settings that are considered more stable. The aim of this study is to contribute to knowledge of the factors that forced Holocene changes in the distribution, assemblages and diversity of benthic foraminifera in the center of the Indian Ocean.

4.2 Study area

4.2.1. Geomorphology, sedimentology and benthic foraminifera

The Maldives archipelago consists of 1,300 small sand islands on 21 atolls in the central Indian Ocean (Gischler et al., 2013). They extend from just below the equator about 1,000 km north toward India. The archipelago is up to 150 km wide and encompasses an area of 107,500 km². The Maldives are among the largest carbonate platform areas in the world. Rasdhoo Atoll (4°N/73°W) is located in the western row of the Maldivian atolls (Fig. 4.1). It is almost circular with a maximum diameter of 9.25 km and an area of ~62 km². The reef rim is continuous and surface breaking and almost completely surrounds the 40 m deep lagoon that contains numerous coral patch reefs. Three channels through the marginal reef connect the interior lagoon to the ocean. The fore-reef slope is very narrow except on the western side of the atoll, and ends in a near vertical drop-off (Gischler, 2006). Coral grainstone dominates the reef crest facies. Carbonate facies in the lagoon include a hard bottom in the east, mollusk wackestone to packstone in the center, and mudstone in the west (Fig. 4.2a). This asymmetric distribution reflects the hydrodynamic gradient created by tidal currents, which enter and exit the lagoon through the channels. A further consequence of this gradient is the sand spit-like continuation of the northern reef margin westwards from the NE channel into the lagoon (Gischler, 2006).

Gischler et al. (2008) provided the first comprehensive data on Holocene reef anatomy and sea-level rise in the Maldives at Rasdhoo. They identified four Holocene

reef facies: robust-branching coral facies, coralline algal facies, domal coral facies and detrital sand and rubble facies. The Holocene reefs started to grow at ~8.6 kyrs BP and developed to a thickness of between 14.5 and >22 m. Marginal reefs accreted in the keep-up mode with high rates >15 m/kyr from 9-7 kyrs BP. Due to sea-level slowdown, accretion-rates decreased significantly from 7-6 kyrs BP to values of <1 m/kyr. Kench et al. (2009) suggested slightly (50 cm) higher than present sea levels from 4-0 kyrs BP, while Gischler et al. (2008) found no evidence for such a highstand at Rasdhoo and suggested that the present day sea level was reached ~4.0 kyrs BP (Gischler et al., 2008). Gischler et al. (2008) also showed that the Pleistocene atoll was asymmetrical in shape with a highly elevated rim in the western part and weakly developed or somewhat deeper water margins in the south and east.

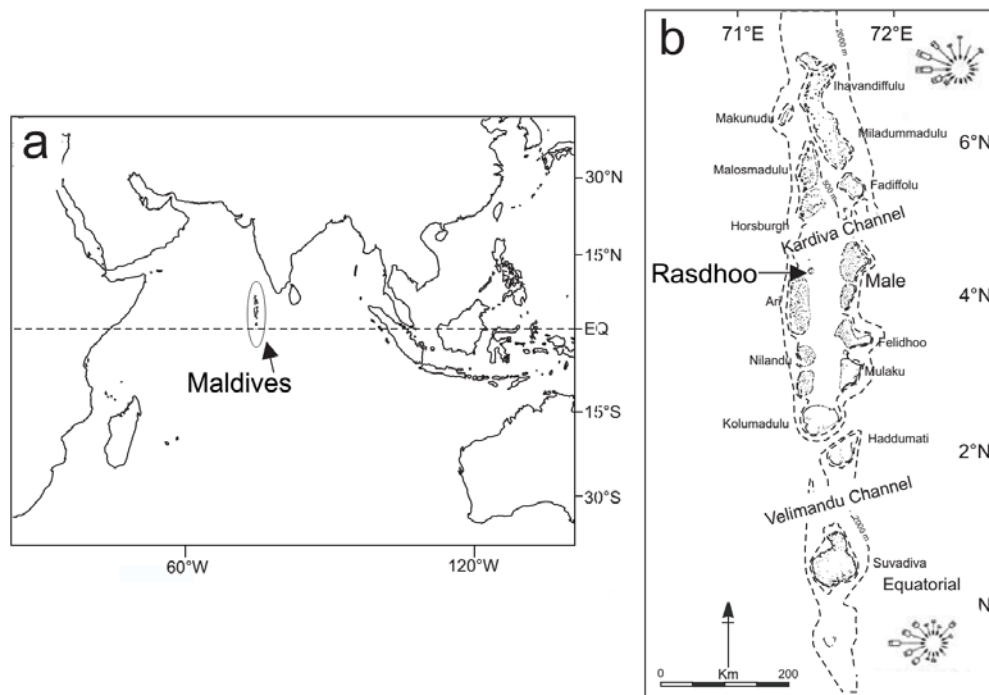


Fig. 4.1 a The location of the Maldives in the Indian Ocean. b The Maldives archipelago with Rasdhoo Atoll including all-year predominant wind directions.

Parker and Gischler (2011) conducted the first detailed study on benthic foraminifera in the Maldives, encompassing a variety of reef and lagoon environments. They analyzed surface sediment samples from the adjacent Rashoo and Ari atolls and characterized the lagoons by benthic foraminiferal assemblages including three reef crest

and back reef assemblages, and five lagoonal assemblages. Their assemblages compare well with the sedimentological characteristics of the lagoons (Gischler, 2006), and their species compositions are largely controlled by depth. In this study, 270 species were identified, which is moderate compared to the central Indo-Pacific lagoons (e.g., Langer and Lipps, 2003; Parker, 2009) and Parker and Gischler (2011) interpreted this as a consequence of lower habitat diversity. Epiphytic species typical of algal and seagrass communities, such as *Cibicides*, are sparse in the Maldives as and were found only as a minor component in the samples from Rasdhoo Atoll (Parker and Gischler, 2011). The distribution of seagrass meadows is known from the Maldives, but their distribution is patchy (Miller and Sulka, 1999). Shallow reef assemblages in Rasdhoo are characterized by *Amphistegina* and *Calcarina*, while textularid and miliolid taxa are abundant in the lagoon. No correlation was found between mud content and foraminiferal diversity, which could have been attributed to eutrophication of the muddy substrate. Consequently, most benthic foraminifera in the lagoon have an epifaunal to shallow infaunal life mode (Parker and Gischler, 2011).

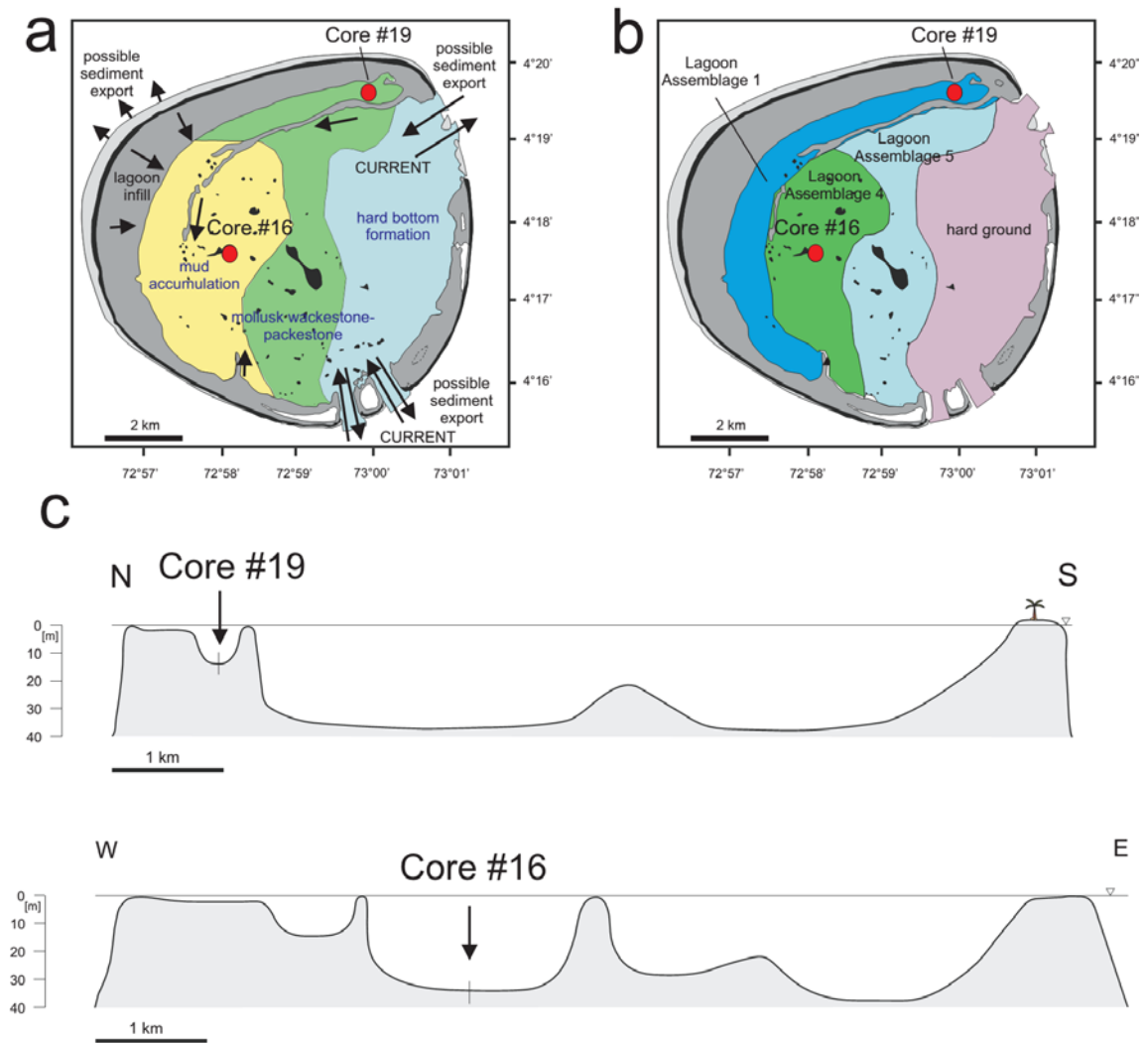


Fig. 4.2 **a** The modern distribution of sediment facies after Gischler (2006). **b** Lagoon assemblages of benthic foraminifera defined by Parker and Gischler (2011). Red dots indicate the sampling location of Core #16 ($4^{\circ}17'56''$ N/ $72^{\circ}57'47''$ E) and Core #19 ($4^{\circ}19'34''$ N/ $72^{\circ}59'35''$ E). **c** Location of the Cores #16 and #19 in the lagoon profile.

4.2.2 Hydrology and climate

The climate of the Maldives is humid and hot, with $\sim 2,000$ mm of rainfall per year. The sea surface temperatures (SST) fluctuate between 24°C in February to 30°C in April. The temperatures remain constant below a depth of 70 m. Salinity varies between 33.8-34.7‰ (Purdy and Bertram, 1993). The predominant annual wind direction is west (Fig. 4.2b). The central Maldives are influenced by the Indian monsoon, which blows from the southwest in summer (May to September) and from the northeast in winter (November to March). This seasonal pattern causes the seasonal reversal of the Indian

monsoon currents, which flow westward in summer and eastward in winter (Schott and McCready, 2001; Storz and Gischler, 2011a, b). The Indian monsoon currents also induce upwelling that causes increased nutrient supply at the Maldives (Preu and Engelbrecht, 1991; Betzler et al., 2009). The location in proximity to the Equator prevents cyclones from passing large parts of the Maldives. Holocene SST reconstructions over the NW Indian Ocean are rare and of low temporal resolution. The available proxy-based reconstructions from the Eastern Arabian Sea indicate no significant SST changes during the Holocene (Bard et al., 1997, Saraswat et al. 2005; Banakar et al., 2010). Banakar et al. (2010) suggested that for most of the Holocene SST (28-29°C) and sea surface salinity (35.5 and 36.5 psu) variation was low. A significant cooling event occurred at ~8.0 kyrs BP (Banakar et al., 2010). This event is marked by a SST decrease of ~1°C and sea surface salinity decrease of 0.5 psu and was caused by a phase of a more intense summer monsoon.

4.3 Material and Methods

4.3.1 Sediment core collection, age determination, sea level reconstruction and sedimentology

Cores #16 and #19, collected with an electrical vibracorer during November - December 2010, were selected for the systematic analysis of the benthic foraminifera (Fig. 4.2). The surface sediment of cored site #16 consists of mollusk mudstone facies and at cored site #19 it consists of wackstone facies (Fig. 4.2a; Gischler, 2006). These sediments contain foraminiferal Lagoon Assemblages 1 and 4 (Fig. 4.2b; Parker and Gischler, 2011), respectively. Lagoon Assemblage 1 is restricted to water depths of 10-27 m and is dominated by *Ammonia* sp. 1 and small miliolid taxa. The most abundant foraminifera of Lagoon Assemblage 3, restricted to water depth of 30-40 m, are *Textularia foliacea* and *Spiroloculina nummiformis*. Core #16 has a length of 4.4 m and was collected in a water depth of 35 m. Core #19 has a length of 3.2 m and comes from a water depth of 14 m, close to the marginal reef. All core sample depths reported in the text are measured with respect to top of each core. For the construction of an age model, five radiometric age determinations (accelerated mass spectroscopy, Beta Analytic Inc.) were conducted for each core. Bulk sediments were used for dating, except for the base

of Core #19, where a bivalve shell was chosen for age determination. These data show that Core #16 and #19 cover most of the Holocene (Fig. 4.3). The paleo-water depth of each of the ten dated samples was estimated by measuring the distance of each sample to the sea-level curve for the Maldives (Gischler et al., 2008).

4.3.2 Foraminiferal analysis

Seventy-four 5-cm-long sections were taken from the core halves. The sample from the base of Core #16 is from a 2-cm-long base section, as it contained 3 centimeters of a well-separated peat layer. Due to the homogeneity of the sediment, sample resolution along core was one sample per 10 cm. Samples were wet sieved through a 125 μm sieve, dried and sieved again through a 2 mm sieve. The fraction 0.125 to 2 mm was chosen for picking, to avoid problems with identification of juvenile foraminifera and to exclude large fragments. From each sample a subsample for archive was taken. Samples were split, and from every split 300 to 450 foraminifera were picked, which is appropriate to provide representative and statistically significant results for species that occur in abundances of $>1\%$ (Dennison and Hay, 1967).

The specimens were glued on Plummer cells. Species identifications were based on Ellis and Messina (1940, et seq.) in comparison of specimens with the collections of Maldivian foraminifera identified by J. Parker and to published illustrations of species from the Indian Ocean region (Chasens, 1981; Ciarapica, 1995; Hottinger et al., 1993; Levy et al., 1996; Loeblich and Tappan, 1994; Parker, 2009; and Parker and Gischler, 2011). Specimens with significant test damage, i.e. destroyed tests, were excluded from picking and were not quantified.

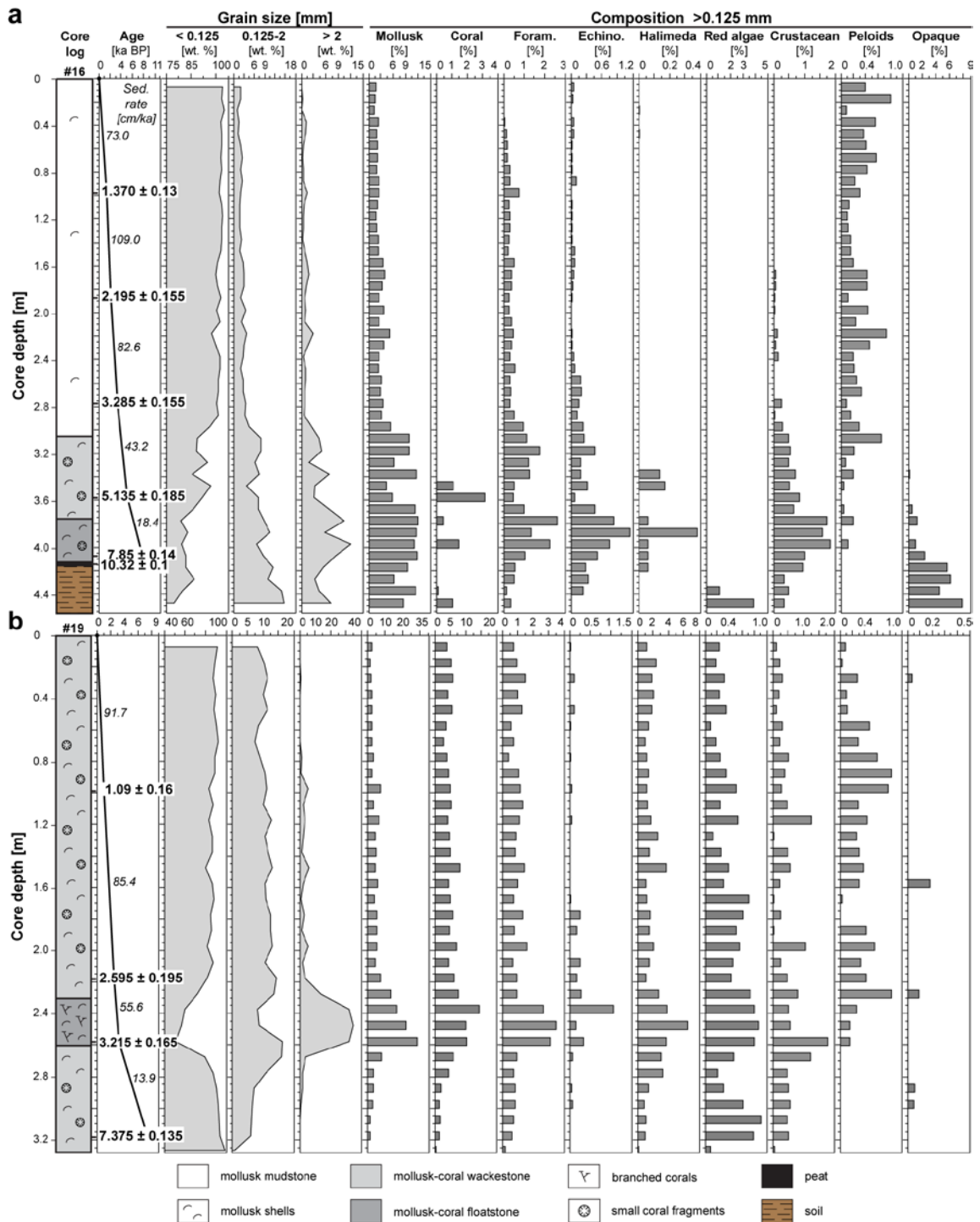


Fig. 4.3 Sedimentological descriptions for (a) Core #16 and (b) Core #19. Carbonate facies were defined based on the limestone classifications of Dunham (1962) and the extended classification by Embry and Klovan (1971). Point counting data of thin sections of the most common components in the grain-size fraction >125 μm. Note that the percentages of components were converted into percentages of the bulk weight of the sample.

For statistical analyses (Principal Component Analysis [PCA], Detrended Correspondence Analysis [DCA], calculation of diversity), the program PAST 2.17c (Hammer et al., 2001) was used. Prior to statistical analysis, species data were transformed to percentages abundance. Log-normal transformation was applied in order to reduce influence of abundant taxa in the sample faunas. The accumulation rate of benthic foraminifera was estimated based on the point counting data of thin sections of the samples (see Fig. 4.3), the dried weights of the samples and the assumption of a linear sedimentation rate between two dated samples.

4.4 Results

4.4.1 Sedimentology and occurrence of benthic foraminifera

At ~4 m core depth (10.3 kyrs BP), Core #16 features a distinct peat layer that superposes Pleistocene soil and marks the first inundation of the lagoon by the rising sea in the Early Holocene before the onset of marine carbonate sedimentation (Fig. 4.3a). The estimation of the paleo-water depths reveals for the sampling site of Core #16 a rapid rise of the paleo-water depth to 34.5 m in the Early Holocene, caused by the accelerated sea level rise from 10.3 kyrs BP until 7.0 kyrs BP.

After sea level slowdown, changes of paleo-water depths were only small. The sedimentation rate has increased through time, and has been highest in the Late Holocene (Fig. 4.3a). In the upper part of Core #16, the amount of most components decreases. Apart from mollusks, foraminifera and echinoderms are the most common components in the grain size fraction >125 μm . Foraminifera occur with a mean abundance of 0.6%. Typical fragments of the reef margin such as corals, *Halimeda*, and red coralline algae are rare and occur with low percentages only at core base.

The paleo-water depth of Core #19 from the marginal reef was estimated to be 12 m in the Middle Holocene, and was 15 m in the Late Holocene. Core #19 covers the last 8 kyrs BP, and shows an increase of sedimentation rate through time from 13.9 to 91.7 cm/kyr. It consists mainly of wackestone, which was interrupted in the lower part of the record by a coarser layer of mollusk-coral floatstone and rudstone with branched *Acropora* fragments (Fig. 4.3b). This layer was dated to 3,215 +/- 160 kyrs BP. No indications of aragonite neomorphism and formation of secondary aragonite were found

in the thin sections of the samples. The most common components $>125\ \mu\text{m}$ are coral fragments and mollusks. Foraminifera are more abundant in the samples of Core #19 than in Core #16 and average 1.2%.

Specimens with significant test damage occurred in negligible numbers in the core samples. Benthic foraminifera with neomorphism, secondary discoloration or infilled tests are uncommon. A total of 200 species were identified in the samples of both cores (Appendix 4.1 and 4.2). Eighteen agglutinated, 74 hyaline and 102 porcelaneous species were identified in the deep lagoon Core #16. In the marginal reef Core #19, 8 agglutinated, 70 hyaline and 114 porcelaneous species were identified.

Thirty-four species of benthic foraminifera occur in abundances $>2\%$ and 15 species occur in abundances $>5\%$ in samples of Core #16. In Core #19, 36 species occur in abundances $>2\%$, and 15 species occur in abundances $>5\%$.

Species from Parker and Gischler's (2011) shallow Reef Assemblage 1 (e.g. *Calcarina* sp., *Amphistegina lobifera*, *Elphidium crispum*, *Neorotalia calcar*) that characterize the western reef flat of Rasdhoo are rare in Core #16, rarely exceeding 0.3%. They are found in the core between 350-370 cm (5-5.5 kyrs BP) with 0.3 to 1.8%, indicating transport from the reef flat. In Core #19, shallow reef species associated to Reef Assemblage 1 are slightly more common, with abundances of up to 3% in a few samples in the lower part of the core between 240 and 320 cm (4.2-5.5 kyrs BP). The coarse mollusk-coral floatstone and rudstone layer in the lower part of Core #19 does not feature an increase of species that could have been transported down-slope from the shallower reef.

The estimated accumulation rate of benthic foraminifera in Core #16 is low in the Early Holocene and increases after the onset of marine sedimentation and is highest in the Middle Holocene (Fig. 4.4a). The rate fluctuates until ~ 1.5 kyrs BP around a constant value, but then decreases significantly in the samples until core top. In Core #19, the accumulation rate is in a similar range (Fig. 4.4b). It is low until ~ 4.0 kyrs BP, rises afterwards and is fluctuating and slightly decreasing until today.

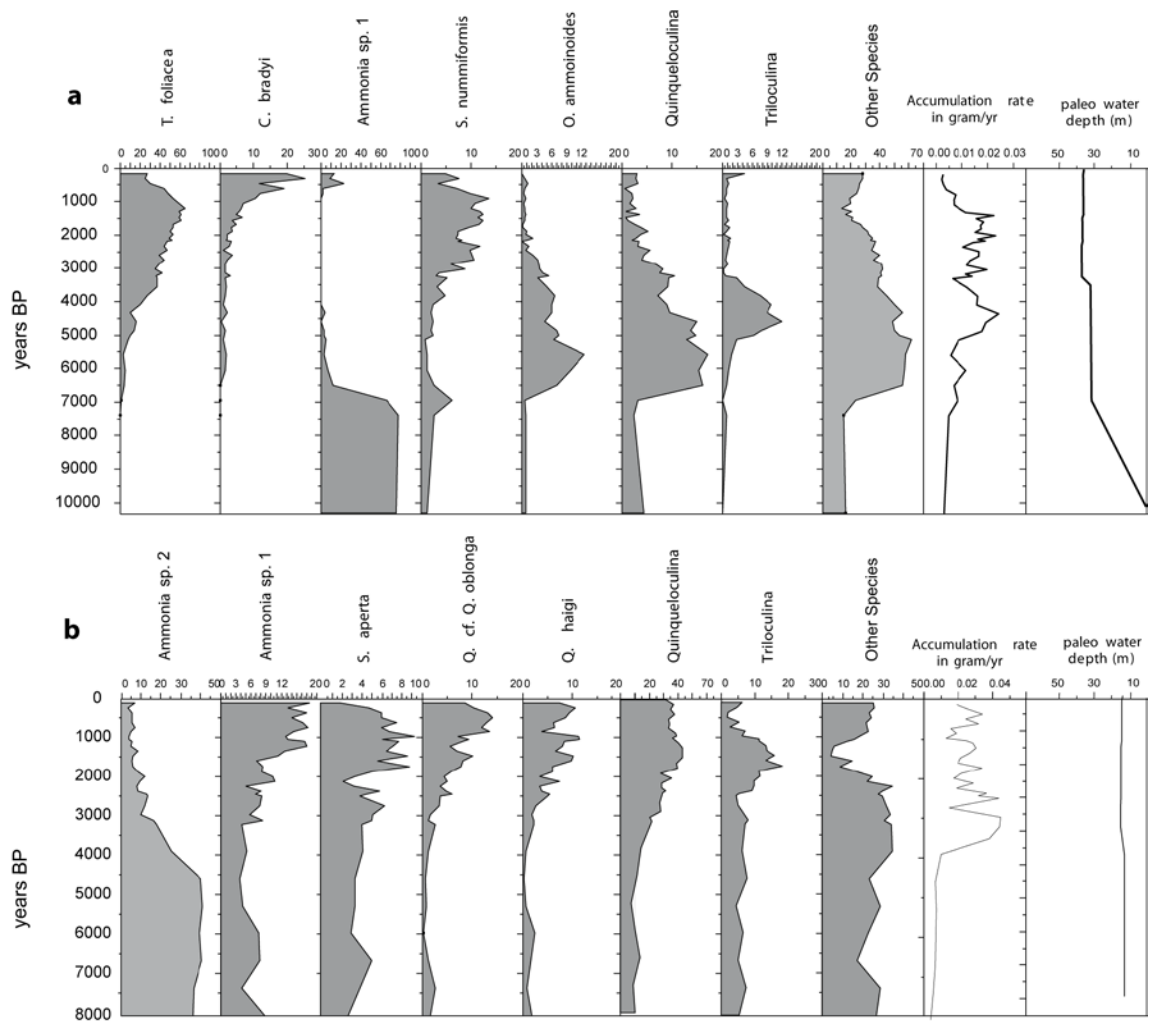


Fig. 4.4 Abundances in % of the 5 most common species, the highly diverse genus *Quinqueloculina* and *Triloculina* in Core #16, the foraminiferal accumulation rate and the estimation of the paleo water depth through time (Gischler et al., 2008) for (a) Core #16 and (b) Core #19.

4.4.2 Foraminiferal assemblages and diversity in Core #16

The five most abundant species in Core #16 are *T. foliacea*, *Ammonia sp.1*, *S. nummiformis*, *Cymbaloporeta bradyi* and *Operculina ammonoides* (Fig. 4.4a, Plate 4.1). They comprise ~60% of all species in this core. The most diverse genus is *Quinqueloculina* with 51 identified species. *Ammonia sp. 1* dominates the assemblage (up to 80%) in Early Holocene samples to ~7 kyrs BP. At this point its abundance decreases rapidly and it is absent or very rare until reappearance in the Late Holocene with a peak abundance of 25% at ~0.5 kyrs BP (20-25 cm core depth). The test sizes of specimens in the core are distinctly smaller than specimens from the modern samples of Parker and Gischler (2011).

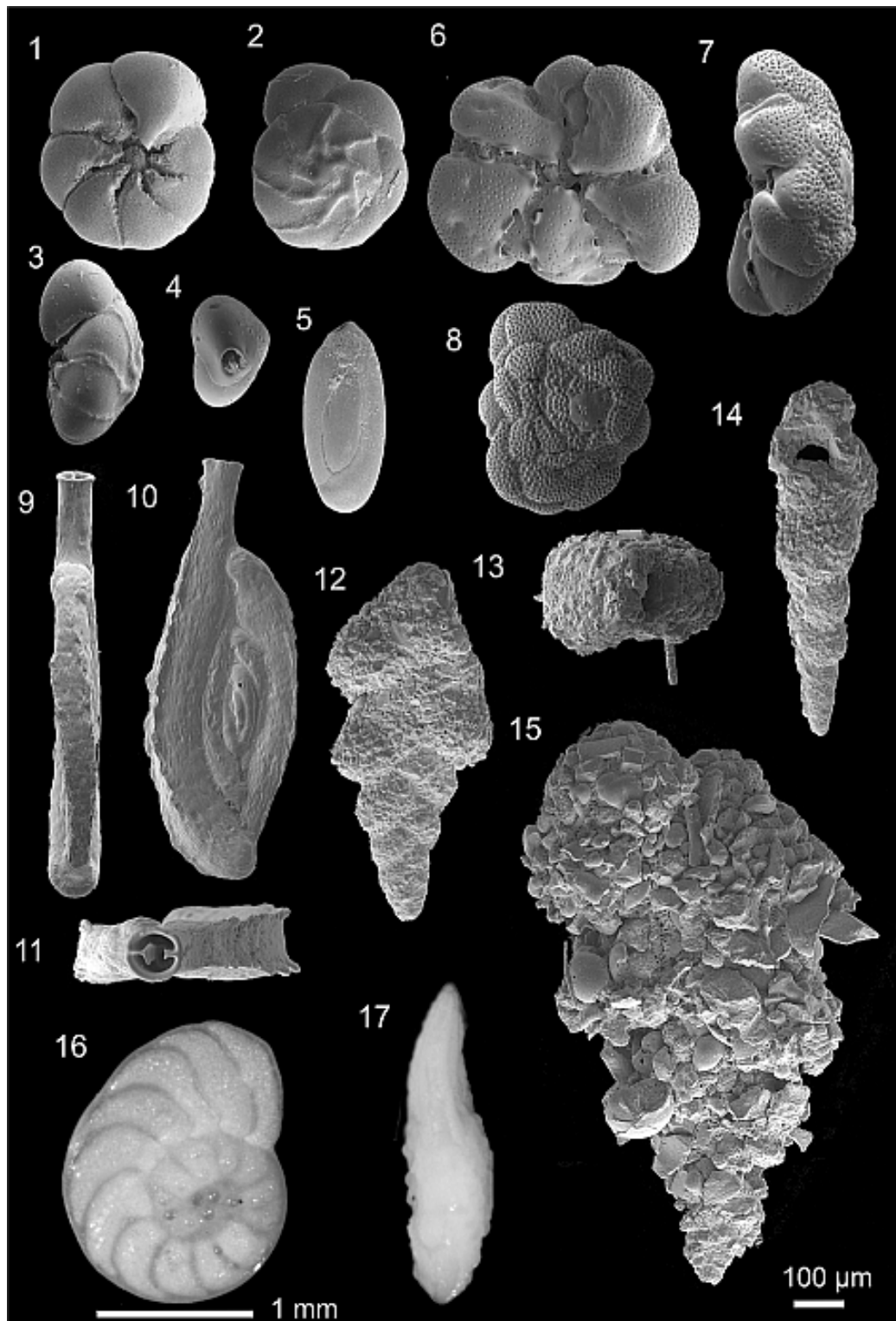


Plate 4.1 Scanning Electron Microscope images (1-15) and light micrographs (16-17) of selected benthic foraminifera. 1-3. *Ammonia* sp, 1 (SMFXXVII7605). 4,5. *Quinqueloculina* cf. *Q. oblonga* (SMFXXVII7586). 6-8. *Cymbaloporeta bradyi* (SMFXXVII7603). 9-11. *Spiroloculina nummiformis* (SMFXXVII7581). 12-15. *Textularia foliacea* (12: SMFXXVII7575; 13: SMFXXVII7576; 14: SMFXXVII7575; 15: SMFXXVII7574). 16-17. *Operculina ammonoides* (SMFXXVII7616). Note the different scale for images 16 and 17. SMF = Senckenberg Museum Frankfurt. The specimen derives from E. Gischler's collection of surface samples from Radhoo and Ari Atoll.

The abundance of agglutinating *T. foliacea* increased through the Holocene to a maximum of 65% in the Late Holocene (~1.4 kyrs BP) and decreased toward the present. *Cymbaloporetta bradyi* becomes common toward the top of the core and reaches highest abundance at the core top (up to 25%). *Operculina ammonoides* and species of *Quinqueloculina* and *Triloculina* reach their highest abundances in samples from the Middle Holocene. *Triloculina* shows a normal distribution with a peak in the Middle Holocene (Fig. 4.4a) and is dominated by *Triloculina* sp. 1. The *Triloculina* abundance peak coincides in shape and timing with the Middle Holocene peak in accumulation rate.

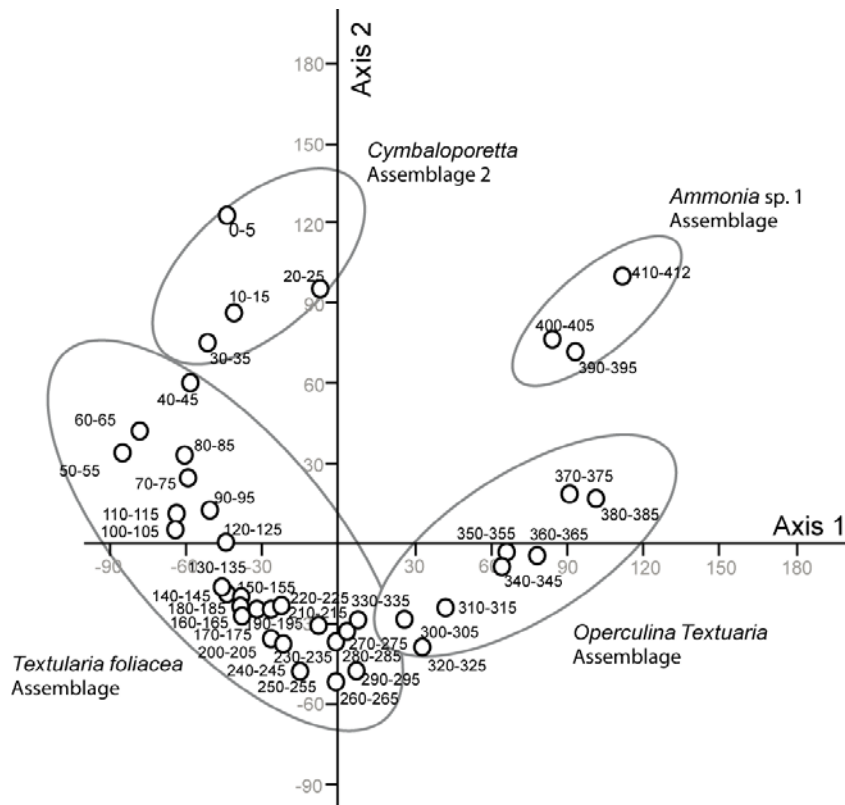


Fig. 4.5 Detrended Correspondence Analysis of the foraminiferal fauna of Core #16 to define foraminiferal assemblages through time. The species abundances were log-normal transformed prior to analysis.

To investigate trends in the dataset, a DCA was conducted (Fig. 4.5) and the principle species controlling the groupings and defining the assemblages were determined using PCA (Fig. 4.6). The foraminiferal assemblages cluster by depth. Four foraminiferal assemblages were defined (Fig. 4.5; Table 4.1). Samples from the base of

the core (3.90-4.12 m: base to ~7.0 kyrs BP) consist of dominant *Ammonia* sp. 1 and plot separate from other studied samples in this core. The other assemblages form a continuum and represents a transition through the mid-late Holocene from ~7.0 kyrs BP on the DCA plot, including the *Operculina-Textularia* (2.90-3.85 m), *Textularia foliacea* (0.30-2.85 m) and *Cymbaloporetta* (0-0.25 m) Assemblages.

The first assemblage in the transition is influenced by *Textularia* cf. *T. cushmani* and *O. ammonoides* (Fig. 4.6). The latter species occurs with the less common *Nummulites* cf. *N. venosa*. The assemblage is also characterized by the occurrence of miliolids that have a strong reef affinity (e.g., *Quinqueloculina agglutinans*, *Q. exsculpta*, *Q. kerimbatica*, *Q. philippinensis*, *Q. parkeri*, and *Pseudomassilina* sp. 1), and deeper water species (e.g., *Spirosigmoilina parri*).

The second assemblage in the transition is marked by the disappearance of *Operculina* and small miliolid taxa, and the replacement of *Textularia* cf. *T. cushmani* and other less abundant textularids by *T. foliacea*. Near the top of the core *Cybamloporretta bradyi* and *Spiroloculina nummiformis* become abundant (Fig. 4.4a).

These changes in assemblage are reflected in changes in the diversity through the core (Fig. 4.7). Foraminiferal diversity is lowest (Shannon's $H \approx 1.3$) in the *Ammonia* sp. 1 assemblage, which is almost monospecific (Fig. 4.4a). The diversity increases sharply with the disappearance of this species and the change in facies to wackestone at ~7 krs BP. Samples from the *Operculina-Textularia* Assemblage have the highest species richness and diversity of all assemblages in addition to high evenness (Figs 4.4a, 4.7). A decrease in diversity through the *Textularia foliacea* Assemblage corresponds to the increasing dominance of *T. foliacea*. The subsequent recovery of diversity coincides with the decline of *T. foliacea* and introduction of abundant *Cymbaloporetta*. The diversity indices were recalculated using only the 30 statistically most significant species and applying a log-normal transformation to test the robustness of the diversity signal. Both show the same features and the similar timing of a diversity minimum in the upper record at 1.4 kyrs BP (not shown).

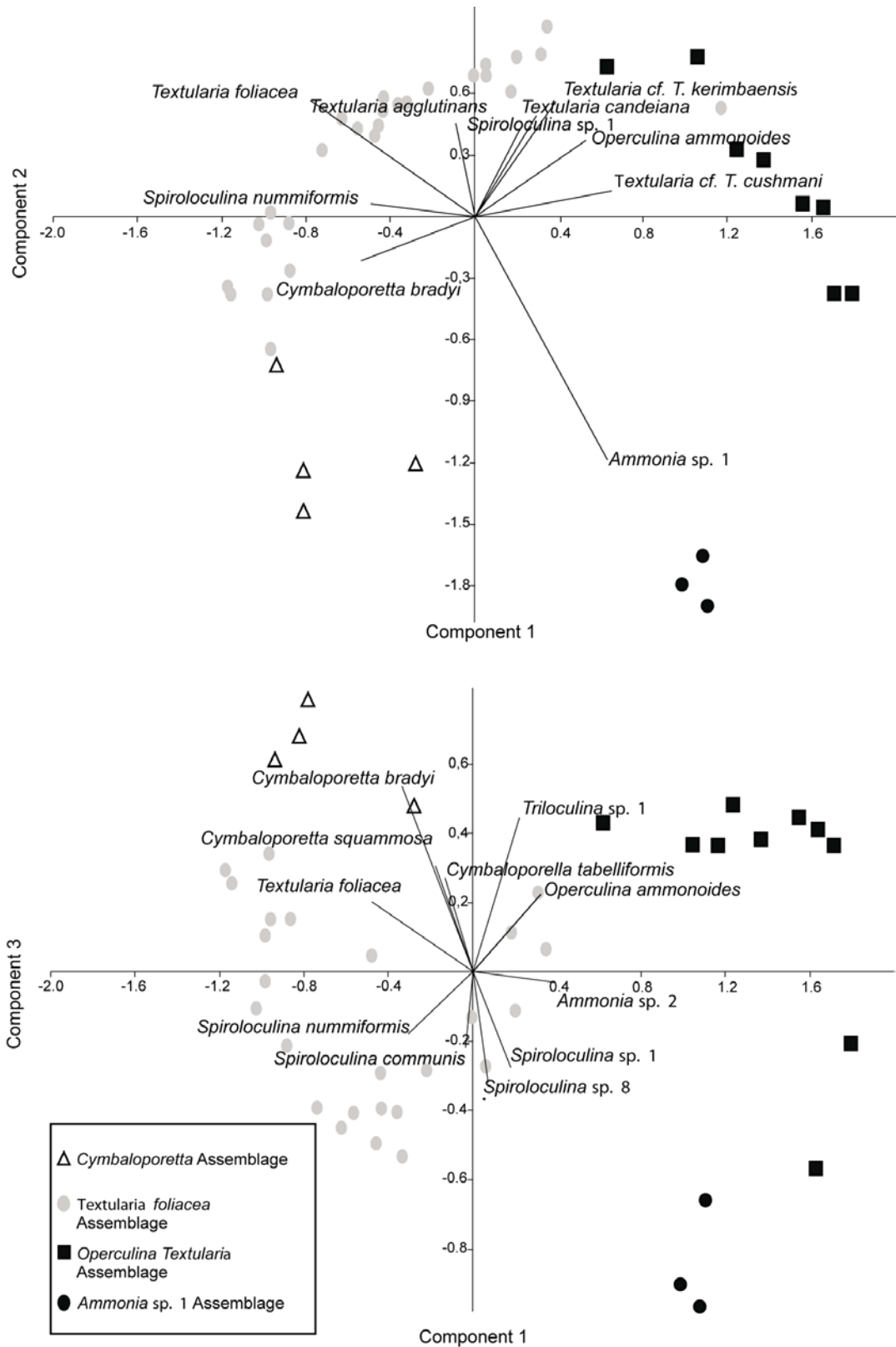


Fig. 4.6 Principal Component Analysis of the foraminiferal fauna of Core #16 showing principal components 1 and 2 and 1 and 3. Symbols refer to the assemblages defined in Fig. 4.5

Murray's (2006) triplot of agglutinated, hyaline and porcelaneous species of benthic foraminifera links samples to broad paleoenvironmental fields (Fig. 4.8a). The *Ammonia* sp. 1 Assemblage plots towards the hyaline corner in the field of hyposaline marshes or hyposaline lagoons. In the *Operculina-Textularia* Assemblage, the proportion of agglutinated, hyaline and porcelaneous species is balanced, and the samples plot in the area of normal marine marshes. Due to the increasing dominance of *T. foliacea*, the samples move toward the agglutinated corner until 0.7 kyrs BP, but remain in the area of normal marine marshes. The samples from the *Cymbaloporeta* Assemblage plot in the shelf sea area of the triplot, due to high abundances of the hyaline *C. bradyi* and *Ammonia* sp. 1.

Table 4.1 The averaged abundances of the most common species >2% of the assemblages defined in Fig. 4.5. Distances in cm are given from the core top.

Cymbaloporeta Assemblage	
0 – 35 cm; 0 – 0.5 kyrs BP	
<i>Textularia foliacea</i>	35.5
<i>Cymbaloporeta bradyi</i>	17.2
<i>Ammonia</i> sp. 1	10.0
<i>Spiroloculina nummiformis</i>	6.6
<i>Cymbaloporeta squamosa</i>	4.3
<i>Cymbaloporella tabelliformis</i>	2.8
Textularia foliacea Assemblage	
40 – 285 cm; 0.5 – 4.0 kyrs BP	
	%
<i>Textularia foliacea</i>	48.7
<i>Spiroloculina nummiformis</i>	8.9
<i>Cymbaloporeta bradyi</i>	4.0
<i>Textularia agglutinans</i>	2.8
<i>Spiroloculina</i> sp. 1	2.8
<i>Textularia candeiana</i>	2.1
Operculina-Textularia Assemblage	
285 – 385 cm; 4.0 – 7.0 kyrs BP	
	%
<i>Textularia foliacea</i>	10.8
<i>Textularia</i> cf. <i>T. cushmani</i>	8.0
<i>Operculina ammonoides</i>	7.5
<i>Triloculina</i> sp. 1	4.7
<i>Textularia candeiana</i>	4.6
<i>Ammonia</i> sp. 1	4.5
<i>Textularia kerimbaensis</i>	4.1
<i>Spiroloculina</i> sp. 1	3.6
<i>Textularia</i> sp. 1	2.7
<i>Textularia cushmani</i>	2.6
<i>Quinqueloculina cuvieriana</i>	2.3
<i>Textularia agglutinans</i>	2.2
<i>Spiroloculina</i> cf. <i>S. hadai</i>	2.1
<i>Spiroloculina nummiformis</i>	2.0
<i>Sahulia barkeri</i>	2.0
Ammonia sp. 1 Assemblage	
390 – 412 cm; 7.0 – 10.3 kyrs BP	
	%
<i>Ammonia</i> sp. 1	72.7
<i>Spiroloculina nummiformis</i>	3.4
<i>Textularia</i> cf. <i>T. cushmani</i>	2.8

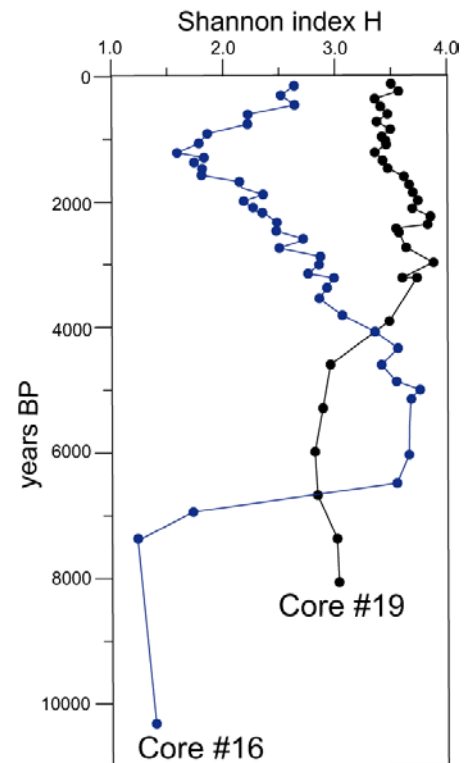


Fig. 4.7 Diversity indices for the samples of Core #16 and Core #19 to illustrate the diversity trend in the samples through the cores.

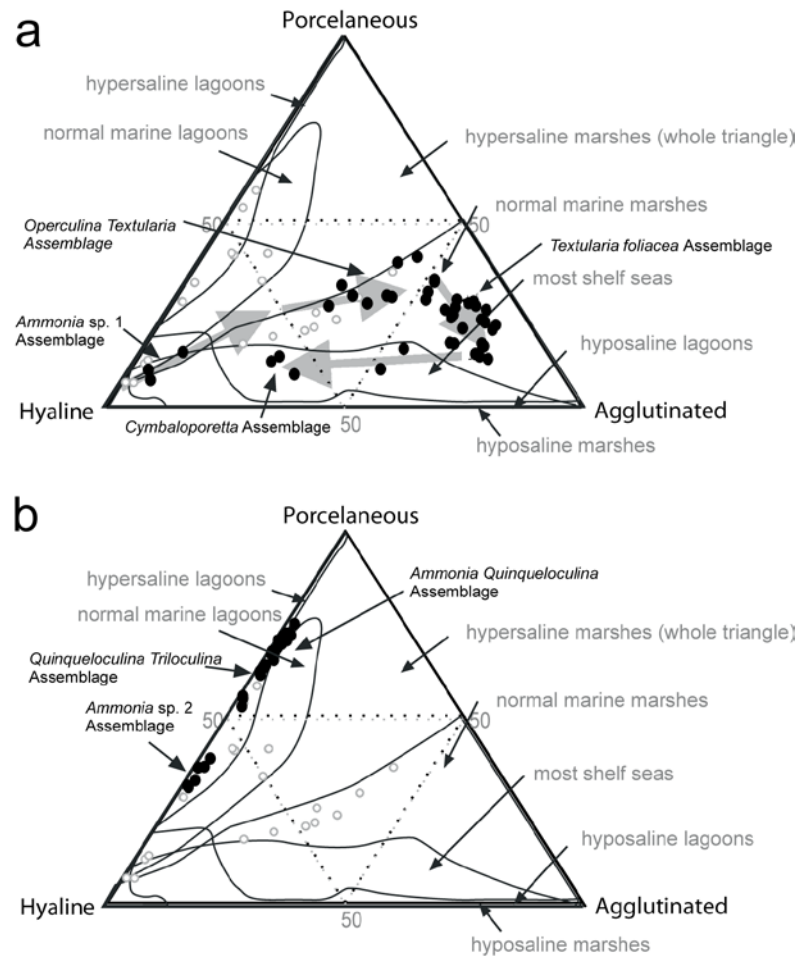


Fig. 4.8 Triplots of the proportion of Agglutinated, Hyaline and Miliolid foraminifera in the foraminiferal assemblages for (a) Core #16 and (b) Core #19. Black circles indicate core samples of this study, and white circles indicate surface samples from Rasdhoo Atoll (Parker and Gischler, 2011). Gray arrows in (a) indicate the path of the samples throughout the Holocene.

4.4.3 Foraminiferal assemblages and diversity in Core #19

The faunal composition of the marginal reef Core #19 differs distinctly from Core #16; in particular agglutinated species are very rare. *Ammonia* sp. 1, *Ammonia* sp. 2, *Spiroloculina aperta* and the small miliolids (e.g. *Quinqueloculina* cf. *Q. oblonga*, *Quinqueloculina haigi*) are the most abundant taxa in the core (Fig. 4.4b).

Ammonia sp. 2 reaches in the Middle Holocene abundances between 35% and 40%. (Fig. 4.4b). The decline of *Ammonia* sp. 2 coincides with the rise of the foraminiferal accumulation rate at ~4.0 kyrs BP. *Ammonia* sp. 1 shows an opposing trend: it increases through the record and becomes the most abundant species in the Late Holocene (up to 17%). The genus *Quinqueloculina* is represented by 50 species

(Appendix). Its abundance rises until the Late Holocene where it makes up to 40-50% in the samples. The miliolid species *Quinqueloculina* cf. *Q. oblonga* and *Quinqueloculina haigi*, which are frequent in the upper core, start to increase steadily after the onset of a higher foraminiferal accumulation. Species of the genus *Triloculina* feature highest abundances in samples from the Late Holocene (2-3 kyrs BP). Similar to Core #16, *Triloculina* shows a peak with close-to-normal distribution in this interval that, however, does not coincide with the peak of this genus in Core #16 in the Middle Holocene (3-4.5 kyrs BP).

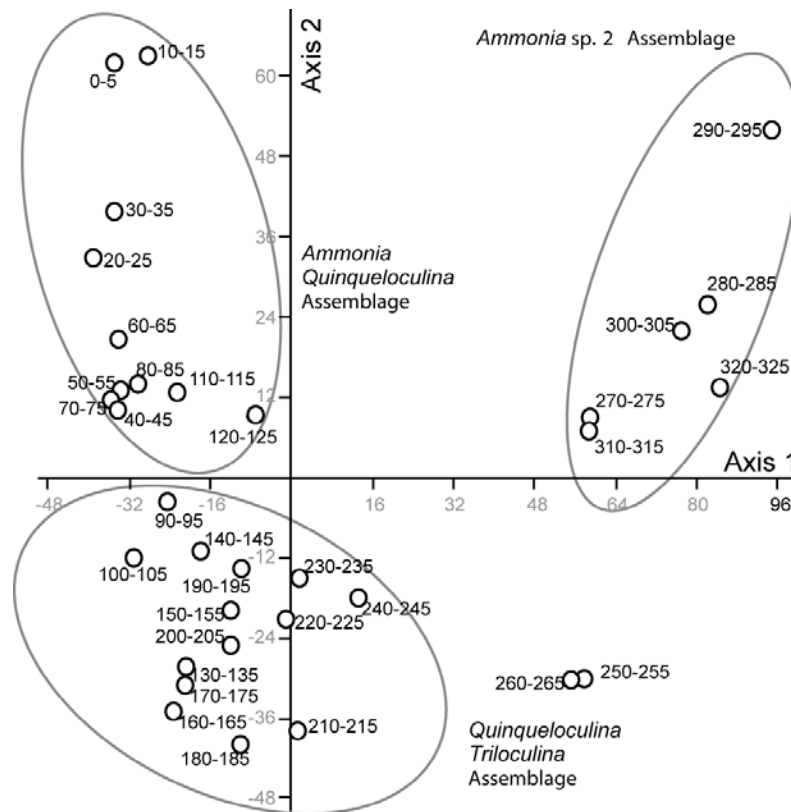


Fig. 4.9 Detrended Correspondence Analysis of the foraminiferal fauna of Core #19 to define foraminiferal assemblages through time. The species abundances were log-normal transformed prior to analysis.

Similarly to the record of Core #16, a DCA was applied (Fig. 4.9). Three assemblages were defined (Table 4.2). The first assemblage consists of the samples that are dominated by *Ammonia* sp. 2 of the lower core (2.60-3.25 m). It plots separately from the other assemblages that form, similarly to Core #16, a continuum: the

Quinqueloculina-Triloculina (1.30-2.55 m) and the *Ammonia-Quinqueloculina* assemblages (0.00-1.25 m) (Table 4.2). Two samples from 250-255 cm and 260-265 cm from the core top are plotting in distance to these assemblages and derive from the mollusk-coral floatstone and rudstone layer (Fig. 4.3b). These samples reflect the transition of the *Ammonia* sp. 2 Assemblage to the *Quinqueloculina-Triloculina*, but do not yield a significant allochthonous faunal component: tests belonging to species typical for the shallow reef are rare.

Table 4.2 The averaged abundances of the most common species >2% of the assemblages defined in Fig. 4.9. Distances are given from the core top.

<i>Ammonia-Quinqueloculina</i> Assemblage		<i>Quinqueloculina-Triloculina</i> Assemblage	
0 - 125 cm; 0 - 1.5 kyrs BP		130 - 260 cm; 1.5 - 4.0 kyrs BP	
	%		%
<i>Ammonia</i> sp. 1	13.6	<i>Ammonia</i> sp. 2	10.9
<i>Quinqueloculina</i> cf. <i>Q. oblonga</i>	9.6	<i>Ammonia</i> sp. 1	8.0
<i>Quinqueloculina haigi</i>	8.0	<i>Quinqueloculina</i> sp. 26	4.7
<i>Spiroloculina aperta</i>	6.6	<i>Quinqueloculina</i> cf. <i>Q. oblonga</i>	4.4
<i>Ammonia</i> sp. 2	5.9	<i>Triloculina</i> cf. <i>T. plicata</i>	4.4
<i>Quinqueloculina</i> sp. 26	4.6	<i>Triloculina</i> cf. <i>T. serrulata</i>	4.4
<i>Quinqueloculina eburnea</i>	2.7	<i>Quinqueloculina haigi</i>	4.4
<i>Quinqueloculina</i> sp. 4	2.4	<i>Spiroloculina aperta</i>	4.3
<i>Quinqueloculina cuivieriana</i>	2.2	<i>Quinqueloculina</i> sp. 2	3.1
<i>Cymbaloporeta bradyi</i>	2.0	<i>Quinqueloculina</i> sp. 4	2.9
<i>Quinqueloculina</i> sp. 2	2.0	<i>Quinqueloculina neostriatula</i>	2.4
		<i>Triloculina trigonula</i>	2.4
		<i>Ammonia convexa</i>	2.1
<i>Ammonia</i> sp. 2 Assemblage			
260 - 326 cm; 4.0- 8.0 kyrs BP			
	%		
<i>Ammonia</i> sp. 2	38.6		
<i>Ammonia</i> sp. 1	6.5		
<i>Ammonia convexa</i>	3.9		
<i>Spiroloculina antillarum</i>	3.8		
<i>Spiroloculina aperta</i>	3.7		
<i>Pararotalia</i> sp. 1	3.0		

The PCA illustrates that the *Quinqueloculina-Triloculina* Assemblage is controlled by the influence of *Quinqueloculina* sp. 26, *Quinqueloculina subpolygona*, *Triloculina* cf. *T. plicata* and *Triloculina* cf. *T. serrulata*. The *Ammonia-Quinqueloculina* Assemblage is influenced by *Ammonia* sp. 1 and the small miliolid taxa *Q. haigi* and *Q. cf. Q. oblonga* (Fig. 4.10).

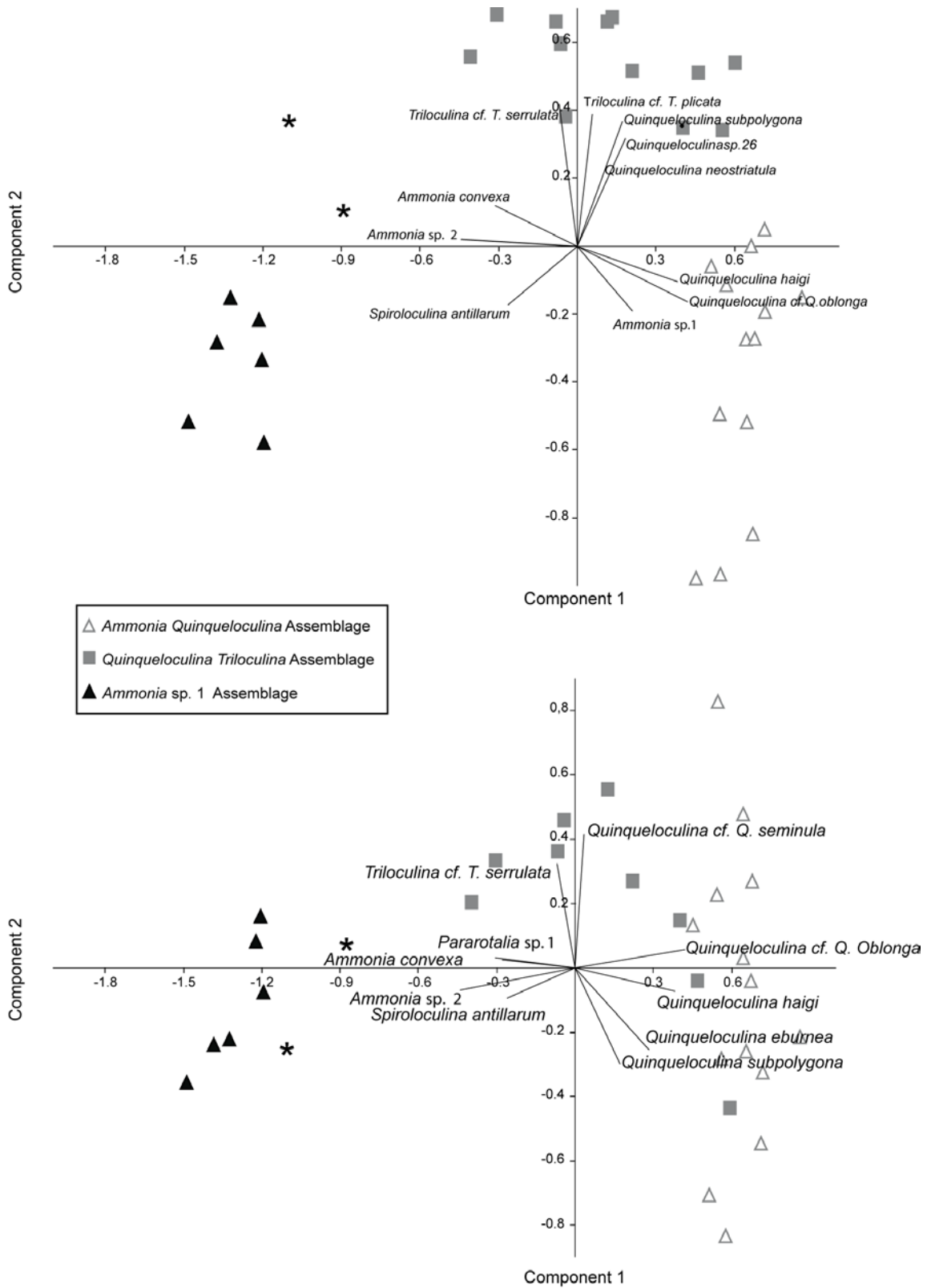


Fig. 4.10 Principal Component Analysis of the foraminiferal fauna of Core #16 showing principal components 1 and 2 and 1 and 3. Symbols refer to the assemblages defined in Fig. 4.9. The species abundances were log-normal transformed prior to analysis.

Diversity fluctuation along Core #19 is not as high as in Core #16 (Fig. 4.7). Diversity is lowest in the *Ammonia* sp. 2 Assemblage, but constant until ~5 kyrs BP (Shannon's $H \approx 3.0$). A transition to higher diversity takes place in the *Quinqueloculina-Triloculina* Assemblage when *Ammonia* sp. 2 decreases in abundances and the accumulation rate increases (Fig. 4.4b); it slightly declines again towards core top, when *Ammonia* sp.1 becomes more frequent in the samples. The courses of the diversity curves for the 30 most abundant species and the log-transformed species abundances in the core are similar (not shown), indicating a robust diversity signal.

Due to the virtual absence of agglutinated foraminifera, the assemblages of Core #19 plot towards the hyaline-porcelaneous line in the fields of normal marine lagoons Murray's (2006) triplot (Fig. 4.8b). They also plot in the field of the hyposaline field. In contrast to samples of Core #16, they plot in agreement with the encountered environment of the marginal reef at the sampling site. The high abundances up to 40% of *Ammonia* sp. 2 in the *Ammonia* sp. 2 Assemblage causes the samples to plot towards the hyaline corner until ~5.0 kyrs BP. Afterwards, miliolid species become more abundant and the samples plot towards the porcelaneous corner.

4.5 Discussion

Core #16 indicates an undisturbed sedimentological environment in the deeper lagoon after the onset of marine sedimentation at ~7.0 kyrs BP, and reveals a continuous transition from mollusk floatstone, to mollusk wackestone and to mudstone. Similarly, the record of Core #19 indicates a mostly undisturbed environment that was, however, interrupted by a coarser layer of mollusk-coral floatstone and rudstone that could be either interpreted as a tsunami- or a storm-induced layer.

The species records of lagoonal Core #16 and marginal reef Core #19 indicate that relatively stable conditions persisted at the core sites since sea level reached its present height. Since death assemblages were studied, taphonomical effects, lateral transport, the presence of deep dwelling infaunal taxa and time averaging might complicate any interpretations (Goldstein et al., 1995; Hippensteel et al., 2000; Horton, 2006; Murray, 2006). Taphonomical effects, such as in situ dissolution and transport processes that favour the preservation of more robust allochthonous specimens in the

samples, have to be considered to introduce bias. However, the effects of neomorphism and dissolution were not observed in the thin sections. The picked benthic foraminifera were mostly well-preserved and omitted specimens with significant test damage were very rare and therefore negligible. Moreover, thin walled species such as small miliolid species are abundant in most samples, and are in many samples more abundant than more robust species. The allochthonous component in the samples, i.e. shallow reef taxa (i.e., *Amphistegina*, *Cibicides*), is minor and does not exceed more than an estimated 3%. Since the occurrence of these shallow water taxa is rare and sporadic, it is not possible to further interpret their presence, although it is likely that some infrequent disturbance event (e.g., storm or tsunami) was responsible.

The problem of contamination by infaunal taxa is likely to be negligible as most of the identified species are epifaunal or at most shallow infaunal; typical infaunal foraminifera such as buliminids are rare. Sedimentological indicators for bioturbation, such as remains of burrowing organisms, e.g. callianassid crustaceans, are very rare. Still, the effect of time averaging via bioturbation, which might have dampened changes in diversity in the record, cannot be ruled out. This could be the case at the base where taxa occur in the same samples that do not coexist in life assemblages. For instance, textulariids, *Operculina* and *Nummulites* might have been mixed in the *Ammonia* sp. 1 Assemblage samples at the base of Core #16, while specimens of *Ammonia* sp. 1 might have been mixed as minor component above into the samples of the *Operculina-Textularia* Assemblage. The time averaging effect of changing sedimentation rates should be significant at the base of the cores where sedimentation rates are relatively low and less significant in upper core sections where sedimentation rates are higher. However, diversity is lowest at the base of each core and much higher near the top, where diversity fluctuates (Fig. 4.7). Based on sample spacing, the resolution of our record averages ~250 yrs, with longer spacing at the base and shorter spacing toward the top.

4.5.1. Foraminiferal assemblages and diversity

Core #16

The *Ammonia* sp. 1 Assemblage at the base of Core #16 appears to represent an early colonization phase that lasted from ~10 to ~7 kyrs BP. This is interpreted from the dominance of the single species, *Ammonia* sp. 1 and low diversity (Fig 4.4a, Table 4.1). *Ammonia* is an opportunistic genus and early colonizer of shallow water environments and the small test sizes indicate a continuous reproduction throughout the year (Alve, 1999; Debenay et al., 2009). The dominance of this species can be attributed to its tolerance to environmental stress such as changes in water temperature, salinity, and organic matter during shallow water and brackish conditions and is typically encountered in restricted environments like hyposaline lagoons and estuaries (Debenay, 2000; Langer and Lipps, 2003; Murray, 2006; Cheng et al., 2012). It typically co-occurs with small miliolid taxa in environments of elevated salinity, or small organic-walled agglutinated foraminifera in environments of reduced salinity. This suggests that during the Early Holocene (~10 to 7 kyrs BP), while sea-level rose to its present position, conditions at the site of Core #16 were as in a shallow brackish swamp.

The *Operculina-Textularia* Assemblage coincides with the slowdown of the sea-level rise and the transition to a deep lagoon site might reflect a long stable phase. The presence of *Operculina*, *Nummulites* and other open shelf taxa (e.g. *Schlumbergeriana* and *Neouvigerina*) suggest high circulation of the bottom waters, and the decline of these taxa may indicate quietening of the bottom waters from ~5.5 to ~2.5 kyrs BP. This change follows a gradual faunal shift that leads to the dominance of *Textularia foliacea* (Fig. 4.4a).

The abundance peak of the genus *Triloculina*, dominated by *Triloculina* sp. 1 in the samples between 3.0 and 4.0 kyrs BP, is enigmatic (Fig. 4.4a): it shows a normal distribution and may be related to a bloom of this species due to a period of favorable environmental conditions or available niches.

Parker and Gischler (2011) reported high abundances (up to 40%) of agglutinating species in the surface samples of the lagoon in water depths of >30 m. However, the abundance of agglutinated species never exceeded that of the *Textularia foliacea* Assemblage (up to 70%; Fig. 4.8a). Samples from the core with elevated

agglutinated foraminifera might represent an environmental niche that no longer exists in the modern Rasdhoo Atoll, or was not sampled by Parker and Gischler (2011). The plot of these samples in the field of normal marine marches instead of normal marine lagoons also indicates that this environmental niche is also not adequately represented in Murray's (2006) triplot.

The increasing dominance of *T. foliacea* and the interval of dominance of this species could be explained by the factor time. The precondition is the assumption of stable environmental conditions in the deeper lagoon until the Late Holocene. Water depths of >30 m in the western lagoon are too deep for direct influence of tidal currents, but tidal exchange is too high to develop a temperature or salinity driven circulation in the lagoon. Connell's (1978) Intermediate Disturbance Hypothesis (IDH) considers time as a factor that influences diversity: it explains low diversity in a habitat with infrequent disturbances and the progressive loss of diversity in a given habitat with a significant temporal distance to a disturbance or new colonization. This leads to the dominance of few species due to competitive exclusion and the prevalence of a climax community. The IDH does not apply to communities with a high complexity of habitats due to a reduced competitive exclusion, such as well-oxygenated marine sediments that are enabling species to partition space in three dimensions (Hughes, 2012; and references therein). It does apply, however, to shallow and less complex environments such as firmground surfaces of boulders (Sousa, 1979), and possibly to restricted low-relief lagoon floors.

The lagoon bottom at Rasdhoo has an epibenthic to shallow endobenthic infaunal fauna of foraminifera and also low abundances of autochthonous sediment producers (Gischler, 2006; Parker and Gischler, 2011) that might indicate a shallow sediment redox interface. The IDH could explain the progressive loss of diversity and species richness and the increasing dominance of *T. foliacea* in Core #16 with the prevalence of stable and undisturbed environmental conditions. Richardson-White and Walker (2011) suggest that unlike metazoans, protists behave differently to environmental disturbances and do not react as predicted by the IDH. Our data indicate that the IDH applies to benthic foraminifera in a low-relief habitat on centennial to millennial scales.

The abrupt recovery of diversity after ~1.4 kyrs BP is accompanied by a distinct decrease in foraminiferal accumulation rate, which indicates the depletion of foraminifera in the sediment (Figs. 4.4a, 4.7), and a change in composition of the fauna. The transition to the *Cymbaloporetta* Assemblage reflects this faunal turnover. Samples of this assemblage are statistically similar to Parker and Gischler's (2011) modern surface samples from near the site of Core #16. The decrease of the previously dominant *T. foliacea* after ~1.4 kyrs BP coincides with the decline of foraminiferal accumulation rate.

Increasing percentages of *C. bradyi* and of the rare *Cymbaloporetta squamosa* in the samples after ~1.4 kyrs BP are therefore the effect of the depletion of other species, such as *T. foliacea*, at the deep lagoon site. This could indicate an environmental change that was tolerated by *Cymbaloporetta*. This taxon is also reported to dwell under low oxygen content or high flux of organic matter from high surface productivity (Sarkar and Gupta, 2009). *Cymbaloporetta* is known as a taxon with a planktic stage that can disperse broadly and creates seasonal bloomings with small tests (personal observation of J. Parker). However, tests of *Cymbaloporetta* belong to the largest picked in the samples, do not show float chambers and indicate no direct evidence for single events, but for permanent colonization.

The reoccurrence of *Ammonia* sp. 1 with small tests in the fauna at ~0.5 kyrs BP can also be attributed to a decrease in the oxygen content and also increased nutrient levels in the bottom water, typical for species with an r-strategy life mode (Alve, 1999). The small test size could indicate rapid reproduction and blooming during either a single colonization or several colonization events. The occurrence of the symbiont-bearing *O. ammonoides* under such conditions could then be explained by its adaption to semi-eutrophic conditions (e.g., Havach and Collins, 1997). These findings could indicate the permanent decrease in bottom water oxygen at the deep lagoon site after ~1.4 kyrs BP.

Core #19

Similar to Core #16, the base of the marginal lagoon Core #19 is dominated by *Ammonia*. Here, *Ammonia* sp. 2 (Fig. 4.7) dominates the fauna of the Early to Middle Holocene until ~4.0 kyrs BP. In modern surface samples of Parker and Gischler (2011),

Ammonia sp. 2 is found only as a minor component in the fauna. *Ammonia* sp. 2 is also rare throughout Core #16. The high abundance of *Ammonia* sp. 2 until ~4.0 kyrs BP in Core #19 could reflect environmental conditions that no longer exist in the present, and indicates a different environmental tolerance compared to *Ammonia* sp. 1: *Ammonia* sp. 2 resembles the morphotype of *Ammonia parkinsoniana*, and *Ammonia* sp. 1 resembles the morphotype of *Ammonia tepida*, respectively. *A. parkinsoniana* and *A. tepida* were originally described from the Caribbean, and while the relationship between the Caribbean *A. parkinsoniana* and similar morphotypes from the Indo-Pacific is unclear, *A. tepida* has been shown to be cosmopolitan (Hayward et al., 2004). Both species comes from restricted environments, but *A. tepida* is a highly tolerant species, compared to *A. parkinsoniana*, which is indicative for more normal marine environments. The decrease of *Ammonia* sp. 2 after ~4.0 kyrs BP and the simultaneous rise of foraminiferal accumulation mark the onset of a more even fauna that could indicate a change in the environmental conditions at the site of Core #19. The increase of *Ammonia* sp. 1 and porcelaneous species such as the small miliolid taxa *Q.* cf. *Q. oblonga* and *Q. haigi* suggests a shift to similar conditions in which Parker and Gischler's (2011) modern Lagoon Assemblage 1 (Fig. 4.2) was deposited.

The faunal transition in Core #19 at ~4.0 kyrs BP occurs at the time when the present position of the sea level was reached at Rasdhoo Atoll (Gischler et al., 2008). It is likely that after ~4.0 kyrs BP the prominent long sand spit in the north and northwest of the lagoon has begun to form. The site of Core #19 then became increasingly restricted from the main lagoon. Parker and Gischler (2011) suggested that high abundances of *Ammonia* sp. 1 in the modern Lagoon Assemblage 1 reflect a stressed environment that is subject to fluctuations in temperature, salinity or low oxygen and organic matter in the bottom water. Permanent changes of these environmental parameters might explain the prevalence of an even and diverse fauna after ~4.0 kyrs BP in the *Ammonia-Quinqueloculina* and *Quinqueloculina-Triloculina* Assemblages: according to the IDH of Connell (1978), a moderately disturbed environment does not lead to a significant loss of diversity and prevents the dominance of single taxa due to the balance between r- and k-strategists.

4.5.2 Foraminiferal diversity and changes in the bottom water circulation of the lagoon

The sand spit formation after ~4.0 kyrs BP could be one of the major causes of changes in diversity and assemblages of benthic foraminifera in the Late Holocene. The tidal channels in the reef margin of Rasdhoo are shallower (10 m) than the lagoon (40 m) which would cause restricted lagoonal circulation. For comparison, van Arx (1954) reported resident times of the lagoon water in Bikini Atoll in the Pacific in the order of weeks to months. Ocean water flows in an atoll lagoon over the windward reef, and the restricted circulation in the lagoon favours the development of a bottom current in opposite direction to the surface currents. Using this as a model, seawater would flow into the Rasdhoo Atoll lagoon over the windward reef in the west; the bottom current would flow westwards over the western, northern or southern reef back into the adjacent ocean (Fig. 4.11a). A constant and relatively short residence time of the bottom water would explain stable conditions in the deep lagoon, thereby favoring the development of low oxygen conditions and/or high nutrient levels.

Sand spit formation would have increased restriction since ~4.0 kyrs BP in the northern and later on in the northern and western lagoons: at the site of Core #19 it would have caused a reduced eastward flow of surface currents and a restricted circulation on a smaller scale in a secondary, marginal lagoon (Fig. 4.11b). The weaker exchange of water with the main lagoon would have led to stronger environmental fluctuations and an increase of disturbances in the secondary lagoon. This would have supported, according to the IDH, the development of a higher diverse fauna of benthic foraminifera in the Late Holocene of Core #19. The major disturbance at ~1.4 kyrs BP in the foraminiferal fauna in the main lagoon (Core #16) could have marked the time when the sand spit reached the western lagoon and acted as an obstacle for both the eastward surface and the westward flowing bottom currents. As a consequence, the transport of bottom water decreased and its residence time increased. This would have caused the formation of low-oxygen and increased nutrient conditions in the bottom waters of the deep lagoon the faunal change at the site of Core #16, and, as a consequence the increase in abundance of *C. bradyi* and *Ammonia* sp. 1.

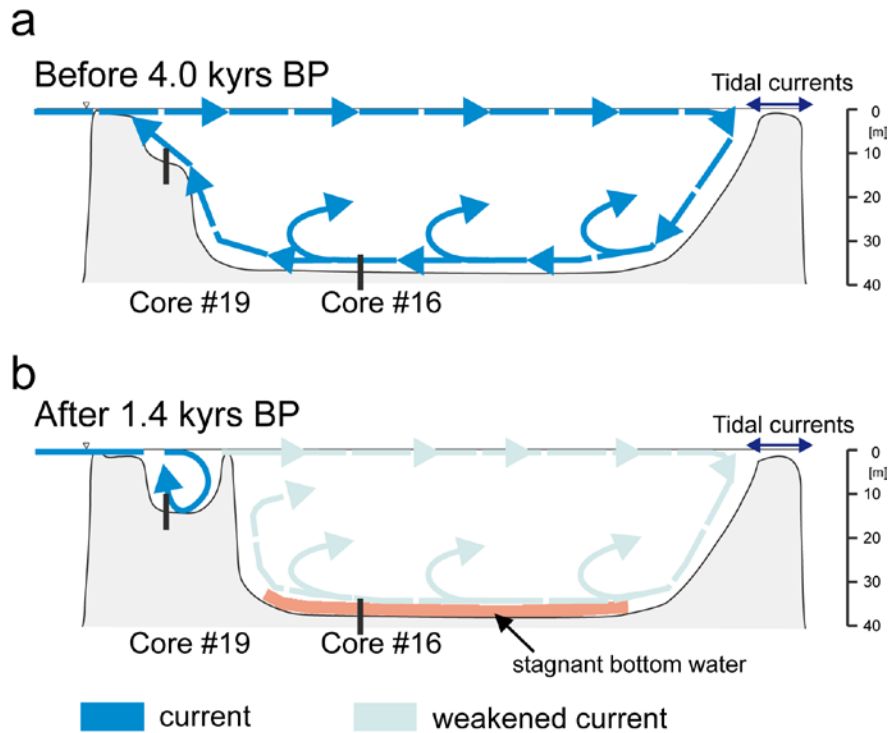


Fig. 4.11 Schematic illustration of the van Arx's (1954) model of restricted circulation applied for Rasdhoo Atoll. (a) Lagoon circulation before the sand spit development in the Late Holocene after 4.0 kyrs BP. (b) Lagoon circulation after the development of the sand spit in the northwestern lagoon.

4.6 Conclusions

This is the first high-resolution study on diversity and assemblages of benthic foraminifera in Holocene sediment cores from shallow marine environments in the Indian Ocean.

Core #16 shows a transition from an early colonization phase with the dominance of a single species (*Ammonia* sp. 1) in the Early Holocene with the onset of marine sedimentation during the rapid sea-level rise. This low diverse fauna was succeeded by a diverse fauna with the onset of a stable environmental in the deep lagoon after the sea-level slowdown at ~7.0 kyrs BP. Foraminiferal assemblages during this phase show a continuous shift towards the dominance of a single agglutinating species (*T. foliacea*) and a decrease in diversity until the Late Holocene. A continuing environmental change after ~1.4 kyrs BP caused the fauna to become more even, a recovery of diversity and a permanent decline of foraminiferal accumulation rate. The decline of diversity during

the Middle to Late Holocene until ~1.4 kyrs BP under stable environmental conditions stresses the impact of the factor time on diversity. It could be interpreted with Connell's (1978) Intermediate Disturbance Hypothesis that attributes the dominance of single taxa at a given habitat to the lack of significant disturbances that otherwise increases diversity.

Core #19 shows a transition at ~4.0 kyrs BP from a restricted *Ammonia* sp. 2-dominated fauna to a more even and diverse fauna that is dominated by *Quinqueloculina*, *Triloculina* and *Ammonia* sp. 1 that indicates stronger restriction. This change coincides with the time when the sea level reached its present position. Changes in the faunas in Core #19 (~4.0 kyrs BP) and Core #16 (~1.4 kyrs BP) could be explained with the sand spit formation in the northwestern and western lagoon. The sand spit has apparently acted as an obstacle in lagoonal circulation and might have caused unstable environmental conditions due to a more rapid circulation at the shallow marine site of Core #19 and a slowdown of bottom water circulation in the main lagoon leading to higher residence times and to lower oxygen and higher nutrient concentrations.

This study indicates that changes in diversity and assemblages at different reef sites and environments in a coral reef could be linked to a single geomorphological process. Both cores illustrate the impact of changes in lagoon circulation and bottom water residence times on diversity of benthic foraminifera. This has important implications for reef ecology and reef monitoring: it gives insight into the long term effects of modification to spits/sand bars with reference to man-made structures that change localized circulation patterns.

Chapter 5. Summary and conclusion

This study describes the Holocene sedimentary lagoonal deposition history, including event sedimentation and benthic foraminiferal analyzes, from about 10 kyrs BP until today. This is the first study describing the sedimentation of a Maldivian atoll lagoon in such detail. Thirty-nine sediment cores have been recovered from the deep Rasdhoo Atoll lagoon of the Maldives (4°N/73°W). Seventeen sediment cores were opened, described, and 296 sediment samples have been collected and analyzed. Different methods have been used to evaluate the coarse- and fine-grained carbonate components and a total of fifty-eight samples have been dated radiometrically by Beta Analytic Inc., Miami, Florida. In general, the Rasdhoo Atoll lagoon sediments can be divided into (1) a Late Pleistocene soil, (2) an early Holocene peat layer composed of mangrove deposits which mark the beginning inundation of the atoll lagoon by the rising Holocene sea-level at $10,320 \pm 100$ yrs BP, and (3) carbonate sediments starting to fill up the lagoon 7850 ± 140 yrs BP until today. The transition from peat to carbonate is characterized by a considerable hiatus. Six different carbonate sediment facies are classified by statistical analyses, listed in decreasing abundance:

- (1) mollusk-coral-algal floatstone to rudstone (30%)
- (2) mollusk-coral-red algae rudstone (23%)
- (3) mollusk-coral-algal wackestone to floatstone (23%)
- (4) mollusk-coral wackestone (13%)
- (5) mollusk-coral mudstone to wackestone (9%)
- (6) mollusk mudstone (2%)

Based on grain-sizes in combination with coral identification, the facies represent both lagoonal background sedimentation (mostly fine-grained sediments (matrix >50%)) and event sedimentation (coarse-grained sediment layers composing reefal components).

Six coarser grained layers in muddy background sediments of the Rasdhoo Atoll lagoon were interpreted as Holocene tsunami events, based on the increase of allochthonous skeletal material with shallow-water reef affinity such as fragments of shallow-water coral species, coralline red algae, and reef-dwelling foraminifera in these layers, as well as AMS dating:

- Event 1: 420 - 890 yrs BP (655 yrs BP)
- Event 2: 890 - 1560 yrs BP (1225 yrs BP)
- Event 3: 2040 - 2340 yrs BP (2190 yrs BP)
- Event 4: 2420 - 3380 yrs BP (2900 yrs BP)
- Event 5: 3890 - 4330 yrs BP (4110 yrs BP)
- Event 6: 5480 - 5760 yrs BP (5620 yrs BP)

Five of the six layers may be correlated to previously published tsunami events at adjacent coastal research sites. The mid-late Holocene atoll lagoon archive is incomplete though based on the assumption that major earthquakes at the Indonesian subduction zone generated more than six major tsunamis during the past 6.5 kyrs.

According to Gischler (2006), the sediments of the Rasdhoo Atoll lagoon can be divided into two areas: (1) a central to marginal deep lagoon with a lateral west-to-east gradient of sediment facies distribution, visible in sections <4 kyrs BP with sedimentary facies of mudstone to wackestone in the western part (e.g., cores 16, 18, and 34) and coarse-grained coral and algal-rich sediments in the eastern part of the lagoon (e.g., cores 30 and 31). (2) A northern enclosed and shallow area between the sand apron and the sand spit accumulating “sandy” sediments of wackestone facies (cores 2, 19, 25, and 26).

Comparing the sediment accumulation data of the lagoon with two reconstructed local sea-level curves, three different sequence-stratigraphical systems tracts are visible: (1) a lowstand systems tract (LST) >10 kyrs BP. Pleistocene brownish soil superposing subaerially exposed Pleistocene reef limestone. (2) A transgressive systems tract (TST) 10-6.5 kyrs BP. A peat layer marks the beginning of the inundation, and the carbonate sedimentation starts with very low sedimentation rates of 0.02 m/kyr. (3) A highstand systems tract (HST) 6.5-0 kyrs BP, further divided into three stages (6.5-3, 3-1, 1-0 kyrs BP). The sea-level rise slowed down, sedimentation rates are increasing continuously up to a maximum of 1.4 m/kyr, the sand spit developed some 4 kyrs BP, the lagoonal circulation got restricted, and the lateral west-to-east gradient of grain-size accumulation started. From 1-0 kyrs BP the sedimentation rates slowed down to modern mean sedimentation rates of 0.6 m/kyr.

Two cores, one core from the center of the lagoon (core 16) and one core from the northern margin of the lagoon (core 19), have been analyzed on diversity and assemblages of benthic foraminifera in high-resolution. The transitions of *Ammonia* spp. to a more even and diverse fauna marks a significant environmental change at 7.0 kyrs BP in core 16 (onset of a stable environment in the deep lagoon after the sea-level rise slowed down at HST stage 1) and at 4.0 kyrs BP in core 19. A continuing environmental change after 1.4 kyrs BP in core 16 caused the fauna to become more even, a recovery of diversity and a permanent decline of foraminiferal accumulation rate. The changes in the faunas at 4.0 kyrs BP and at 1.4 kyrs BP could be explained with the sand spit formation in the northwestern and western lagoon. The sand spit has apparently acted as an obstacle in lagoonal circulation and might have caused unstable environmental conditions due to a more rapid circulation at the shallow marine site of core 19 and a slowdown of bottom water circulation in the main lagoon (core 16) leading to higher residence times and to lower oxygen and higher nutrient concentrations.

Zusammenfassung

Die Untersuchung von holozänen Lagunensedimenten aus dem Rasdhoo Atoll im zentralen, westlichen Bereich der Malediven (4°N/73°W) ist Forschungsgegenstand der Arbeit. Sedimentkerne aus einer Atolllagune können bedeutende Auskünfte hinsichtlich (1) der Entwicklung und der natürlichen Auffüllung einer Atolllagune mit Karbonatsedimenten liefern, (2) aufzeigen, wie sich niedrig gelegene Landflächen zum Meeresspiegelanstieg verhalten und (3) die Aufzeichnung von Tsunami-Ereignissen in der jüngsten geologischen Vergangenheit vervollständigen.

Die Inselkette der Malediven befindet sich auf einem der größten geologischen Kalksteingebiete der Erde. Sie liegt im zentralen Norden des Indischen Ozean, südwestlich von Indien (7°N bis 1°S entlang 73°E). Die Malediven bestehen aus 1300 Inseln verteilt auf 21 Atolle (Gischler et al., 2013), die sich über 1000 km Länge erstrecken und eine Fläche von 107.500 km² umfassen. Karbonatgesteine lagern sich seit dem frühen Eozän auf dem Chagos-Laccadiven-Rücken ab, der durch eine Kette von Vulkanen eine erhöhte Struktur unter dem Meeresspiegel ausbildet. Bis heute hat sich eine ca. 3 km mächtige Kalksteinplattform gebildet (Belopolsky und Droxler, 2004). Das heutige Riff reicht bis maximal 5 m über den Meeresspiegel und bildet typische Atollstrukturen. Ein Atoll besteht aus einem Randriff, das meist bis zum Meeresspiegel, innerhalb des Gezeitenbereichs, reicht. An der dem Meer zugewandten Seite des Riffs brechen die Wellen. Die vom Randriff umgebene Lagune stellt einen strömungsarmen, geschützten Bereich dar und wird durch einen oder mehrere Kanäle am Randriff mit dem umgebenden Meer verbunden. Die Kanäle stellen Gebiete des Randriffs dar, die unter dem Meeresspiegel liegen. An anderen Stellen beträgt die Tiefe der Kanäle bis zu 10 m. Durch die Gezeitenkraft, die auf den Malediven zwischen 0,5 und 1,0 m beträgt (Kench et al., 2006), entstehen Strömungen, die ein Wasseraustausch der Lagune mit dem Meerwasser bewirken. Die nahezu kreisrunde Struktur des Randriffs um eine tiefere Lagune erinnert an einen mit Wasser gefüllten Eimer (Ladd, 1949, 1950; Schlager, 1981, 1993). Die Riffe des Atolls werden durch physikalische (Wellenenergie), chemische (Regenwasser) und biologische (z.B. durch Fische, Würmer und Algen) Kräfte erodiert und kalkige Sedimente entstehen. Die Lagune ("Eimer") wird

durch Sedimente vom Riff langsam gefüllt und es entsteht eine Sandschürze ("sand apron") an der Innenseite des Randriffs, welche die Lagune von Außen nach Innen auffüllt (Purdy und Gischler, 2005; Schlager und Purkis, 2013). Sedimente die in der strömungsarmen Lagune entstehen, werden auf dem Lagunenboden abgelagert. Keine oder nur sehr wenige Sedimente werden durch die Kanäle ins Meer transportiert (Gischler, 2006). Eine Lagune, bzw. ein solcher mit Wasser gefüllter Eimer, stellt damit eine Art Sedimentfalle dar, die seit dem letzten glazialen Meerwassertiefstand (LGM) die Holozäne sedimentäre Geschichte der Malediven aufzeichnet (Purdy und Gischler, 2005).

Das annähernd kreisrunde Rasdhoo Atoll hat einen Durchmesser von 9,25 km und erstreckt sich über eine Fläche von 62 km². Die Lagune beinhaltet eine Vielzahl von Fleckenriffen ("patch reefs") und wird durch drei Kanäle mit dem Meer verbunden. Die moderne Rifffazies besteht aus Korallen-Algen grainstone, die Sedimentfazies der Lagune umfasst mudstone, wackestone und grobe Korallenfragmente ohne feine Sedimente im Bereich der Kanäle (Gischler, 2006). Zwischen dem Randriff und der Lagune befindet sich eine Sandschürze, die im Westen (Luvseite) des Atolls die größte Fläche bedeckt. Eine Sandbank verläuft parallel zum Randriff im Norden und Nordosten des Atolls und teilt die Lagune in einen flachen, eingeschlossenen Bereich mit Wassertiefen <15 m und in einen tieferen Bereich mit Wassertiefen bis zu 40 m.

Mithilfe von Meeresspiegelkurven aus zwei Atollen der Malediven und unter Berücksichtigung der Wachstumsraten der Riffe aus dem Rasdhoo Atoll (Gischler et al., 2008; Kench et al., 2009), wurde die geologische, sedimentäre Geschichte des Atolls anhand von holozänen Lagunensedimenten untersucht. Vom 12. November bis zum 04. Dezember 2010 wurden im Rasdhoo Atoll an zweiundvierzig Stationen, insgesamt neununddreißig Kerne mit einem elektrischen Rossfelder Vibrationsbohrer gebohrt. Siebzehn Kerne wurden aufgrund ihrer Länge und ihrer Lage in der Lagune ausgewählt und sedimentologisch, mineralogisch und chronologisch untersucht. Neun der siebzehn Kerne stammen aus dem Zentrum der Lagune und acht Kerne vom Randbereich der Lagune. Die Wassertiefen der Kernstationen am Randbereich betragen 10,7-20,0 m (Kerne: 1, 2, 11, 12, 18, 19, 25 und 26) und im Zentrum der Lagune 21,6-37,6 m (Kerne: 8, 13, 16, 24, 27, 29, 30, 31 und 34). Es wurden keine Kerne auf der Sandschürze oder

im flachen Randbereich der Lagune (Karbonatbank) gebohrt, da der Rossfelder Vibrationsbohrer nur in Wassertiefen >10 m eingesetzt werden kann.

In den Laboren der Goethe-Universität Frankfurt wurden die Sedimentkerne geöffnet, beschrieben und Sedimentproben entnommen. Die Proben wurden aus einer Hälfte der Kerne genommen, die andere Hälfte wurde verpackt und archiviert. Insgesamt wurden 296 Sedimentproben bearbeitet und analysiert. Neuundvierzig Sedimentproben wurden mit einem Massenspektrometer (AMS) radiometrisch datiert und neun Korallen wurden mithilfe der standardisierten C-14-Altersbestimmung datiert (Bard, 1998). Beide Datierungsmethoden wurden von Beta Analytic Inc. in Miami, Florida durchgeführt.

Die Lagunensedimente können in drei Sedimenttypen unterteilt werden: (1) Einen spät-pleistozänen Boden, (2) eine früh-holozäne Torf-Lage, bestehend aus Mangroven-Ablagerungen, die den steigenden Meeresspiegel und die damit zusammenhängende Überschwemmung der Atolllagune vor 10.320 ± 100 yrs BP kennzeichnet und (3) in Karbonatsedimente, die vor 7.850 ± 140 yrs BP anfangen auf dem Lagunenboden abzulagern. Torf-Lagen, die eine beginnende Überschwemmung von Lagunen und Küstengebieten kennzeichnen, sind auch in den Kernen von Mayotte (Elmoutaki et al., 1992; Zinke et al., 2001, 2003a, b, 2005), Belize (Shinn et al., 1982; Gischler, 2003), den Bahamas (Newell et al., 1959), Süd Florida (Scholl, 1964; Dodd and Siemers, 1971) und dem Great Barrier Reef (Larcombe and Carter, 1998) zu beobachten. Der Übergang von der Torf-Lage zu den ersten Karbonatsedimenten beschreibt eine Schichtlücke von rund 2.500 Jahren, die den verzögerten Prozess der Sedimentbildung durch das erst anlaufende Korallenwachstum in einer kürzlich gefluteten Lagune darstellt (Tipper, 1997; Gischler, 2003; Schultz et al., 2010). Sechs unterschiedliche Karbonatsedimentfazies wurden mithilfe von verschiedenen statistischen Verfahren (u.a. Punktzählverfahren, Cluster-Analyse) klassifiziert und werden folgend mit abnehmender Häufigkeit aufgelistet: (1) Mollusken-Korallen-Algen floatstone zu rudstone (30%), (2) Mollusken-Korallen-Rotalgen rudstone (23%), (3) Mollusken-Korallen-Algen wackestone zu floatstone (23%), (4) Mollusken-Korallen wackestone (13%), (5) Mollusken-Korallen mudstone zu wackestone (9%) und Mollusken mudstone (2%). Begründet durch die Größe der Komponenten (Korngröße) sowie der taxonomischen Bestimmung der Korallen repräsentieren die Sedimentfazies

die Hintergrund-Sedimentbildung (meist feinkörnige Sedimente mit >50% Matrix) und die Ereignis-Sedimentation (Sedimentlagen mit groben Riff-Komponenten).

In einer ansonsten feinkörnigen Sedimentabfolge wurden sechs grobkörnige Sedimentlagen als Relikte von holozänen Tsunami-Ereignissen gedeutet und datiert:

- Ereignis 1: 420 - 890 yrs BP (655 yrs BP)
- Ereignis 2: 890 - 1560 yrs BP (1225 yrs BP)
- Ereignis 3: 2040 - 2340 yrs BP (2190 yrs BP)
- Ereignis 4: 2420 - 3380 yrs BP (2900 yrs BP)
- Ereignis 5: 3890 - 4330 yrs BP (4110 yrs BP)
- Ereignis 6: 5480 - 5760 yrs BP (5620 yrs BP)

Die Ereignis-Lagen weisen einen erhöhten Anteil von allochthonem Skelettmaterial auf, die der Flachwasser-Rifffazies entsprechen. Dazu gehören zum Beispiel Arten von Flachwasser-Korallen, koralline Rotalgen und am Riff lebende benthische Foraminiferen. Fünf der sechs Lagen wurden vorangegangenen publizierten Tsunami-Ereignissen aus benachbarten Küstenregionen zugeordnet (Klostermann, 2014). Es wird angenommen, dass mehr als sechs starke Erdbeben an der Indonesischen Subduktionszone innerhalb der letzten 6500 Jahre stattgefunden haben, sodass die Aufzeichnung der Paläo-Tsunami-Ereignisse durch weitere Untersuchungen vervollständigt werden muss.

Übereinstimmend mit Gischler (2006) kann die Lagunensedimentfazies des Rasdhoo Atolls in zwei Gebiete unterteilt werden: (1) Eine relativ zentral gelegene, tiefe Lagune mit einem von Westen (fein) nach Osten (grob) folgenden Verlauf der Korngrößenverteilung der Sedimente: Die Fazies der westlichen Gebiete entsprechen mudstone und wackestone (z.B. Kerne 16, 18 und 34) und werden Richtung Osten der Lagune grobkörniger mit korallen- und algenreichen Sedimenten (z.B. Kerne 30 und 31). (2) Ein nördliches, eingeschlossenes und seichtes Gebiet zwischen der Sandschürze und der Sandbank mit überwiegend sandigen Sedimenten entspricht der Fazies wackestone (Kerne 2, 19, 25 und 26).

Ein Vergleich der Sedimentationsraten in der Lagune mit zwei lokalen, Meeresspiegelkurven lässt eine Unterteilung in drei unterschiedliche sequenzstratigraphische Systeme zu: (1) Ein Niedrigwasserstand-System (LST) vor

>10 kyrs BP. Ein pleistozäner, brauner Boden überlagert pleistozänen Riff-Kalkstein. (2) Ein Transgressions-System (TST) vor 10-6,5 kyrs BP. Eine Torf-Lage markiert die beginnende Überschwemmung der Lagune und die Ablagerung von Karbonatsedimenten beginnt mit sehr niedrigen Sedimentationsraten von 0,02 m/kyr. (3) Ein Hochwasserstand-System (HST) vor 6,5-0 kyrs BP. Diese Phase kann in kürzere Abschnitte unterteilt werden (6,5-3, 3-1, 1-0 kyrs BP). Der Anstieg des Meeresspiegels wird langsamer, die Sedimentationsraten steigen kontinuierlich bis zu einem Maximum von 1,4 m/kyr an. Die Sandbank bildete sich vor <4 kyrs BP (Storz et al., 2014), die Wasserzirkulation in der Lagune änderte sich und die Unterteilung in grobe Sedimente im Osten sowie feinere Sedimente im Westen bildete sich aus. Vor rund 1000 Jahren bis heute verlangsamte sich die Sedimentationsrate zu dem aktuell beobachteten, mittleren Wert von 0,6 m/kyr (z.B. Yamano et al., 2002; Gischler, 2003).

Kern 16 aus dem Zentrum der Lagune und Kern 19 vom nördlichen Randbereich der Lagune, wurden mit einer hohen Auflösung auf die Verteilung und Vergesellschaftung von benthischen Foraminiferen untersucht. Der starke Rückgang der dominierenden *Ammonia* Spezies zu einer Foraminiferen-Fauna mit einem hohen Vorkommen von Spezies der Gattungen *Quinqueloculina* und *Triloculina* markiert eine signifikante Umweltveränderung vor ca. 7,0 kyrs BP, erkennbar in Kern 16. Das Datum markiert den Beginn des Hochwasserstands (HST) nach dem sich der Meeresspiegelanstieg verlangsamte und sich die Fauna in der Lagune der veränderten Umwelt anpasste. Ähnliches wurde in Kern 19 vor ca. 4,0 kyrs BP und <1,4 kyrs BP festgestellt. Die Veränderungen der Foraminiferen-Fauna kann durch die Bildung der Sandbank im Nordwesten und Westen der Lagune erklärt werden (Storz et al., 2014). Die Sandbank behinderte möglicherweise die Wasserzirkulation in der Lagune und veränderte somit die Umweltbedingungen hin zu einer verstärkten Wasserzirkulation in den seichten Randbereichen der Lagune (Kern 19) und reduzierte die Tiefenwasserzirkulation im Zentrum der Lagune (Kern 16). Die Aufenthaltszeit des Tiefenwassers wurde erhöht, die Konzentration von Sauerstoff in der Wassermasse nahm mit der Zunahme an Nährstoffen ab, womit die Änderungen und Anzahl der dominierenden Arten von benthischen Forminiferen erklärt werden kann (Havach und Collins, 1997; Alve, 1999; Sarkar und Gupta, 2009).

References

- Alve, E., 1995. Benthic foraminiferal responses to estuarine pollution: review. *J. Foramin. Res.* 25, 190–185.
- Alve, E., 1999. Colonization of new habitats by benthic foraminifera: a review. *Earth-Sci. Rev.* 46, 167–185.
- Araoka, D., Yokoyama, Y., Suzuki, A., Goto, K., Miyago, K., Miyazawa, K., Matsuzaki, H., Kawahata, H., 2013. Tsunami recurrence revealed by *Porites* coral boulders in the southern Ryukyu Islands, Japan. *Geology* 41, 919–922.
- Aronson, R.B., Precht, W.F., 1995. Landscape patterns of reef coral diversity: A test of the intermediate disturbance hypothesis. *J. Exp. Mar. Biol. Ecol.* 192, 1–14.
- Aubert, O., Droxler, A., 1996. General Cenozoic evolution of the Maldives carbonate system (equatorial Indian Ocean). *Bull Centr Rech Explor-Prod Aquitaine* 16, 113–136.
- Bahlburg, H., and Spiske, M., 2012. Sedimentology of tsunami inflow and backflow deposits: key differences revealed in a modern example. *Sedimentology* 59, 1063–1086.
- Banakar, V.K., Mahesh, B., Burr, G., 2010. Climatology of the Eastern Arabian Sea during the last glacial cycle reconstructed from paired measurement of foraminiferal $\delta^{18}\text{O}$ and Mg/Ca. *Quat. Res.* 73, 535–540.
- Bard, E., Rostek, F., Sonzogni, C., 1997. Interhemispheric synchrony of the last deglaciation inferred from alkenone palaeothermometry. *Nature* 385, 707–710.
- Bard, E., 1998. Geochemical and geophysical implications of the radiocarbon calibration. *Geochim Cosmochim Acta* 62, 2025–2038.
- Beavington-Penney, S.J., Racey, A., 2004. Ecology of extant nummulitids and other large benthic foraminifera: application in palaeoenvironmental analysis. *Earth-Sci. Rev.* 67, 219–265.
- Betzler, C., Hübscher, C., Lindhorst, S., Reijmer, J.J.G., Römer, M., Droxler, A.W., Fürstenau, J., Lüdmann, T., 2009. Monsoon-induced partial carbonate platform drowning (Maldives, Indian Ocean). *Geology* 37, 867–870.
- Betzler, C., Fürstenau, J., Lüdmann, T., Hübscher, C., Lindhorst, S., Paul, A., Reijmer, J.J.G., Droxler, A.W., 2012. Sea-level and ocean-current control on carbonate-platform growth, Maldives, Indian Ocean. *Basin Res.* 25, 172–196.
- Betzler, C., Lüdmann, T., Hübscher, C., Fürstenau, J., 2013. Current and sea-level signals in periplatform ooze (Neogene, Maldives, Indian Ocean). *Sediment. Geol.* 290, 126–137.
- Bianchi, C.N., Colantoni, P., Geister, J., Morri, C., 1997. Reef geomorphology, sediments and ecological zonation at Felidu Atoll, Maldivian Islands (Indian Ocean). *Proc. 8th Int. Coral Reef Symp. Panama* 1, 431–436.

References

- Bicchi, E., Debenay, J.P., Pages, J. 2002. Relationship between benthic foraminiferal assemblages and environmental factors in atoll lagoons of the central Tuamotu Archipelago (French Polynesia). *Coral Reefs* 21, 275–290.
- Boudagher-Fadel, M., 2008. Evolution and Geological Significance of Larger Benthic Foraminifera. Elsevier, 544 pp.
- Brill, D., Brückner, H., Jankaew, K., Kelletat, D., Scheffers, A., Scheffers, S., 2011. Potential predecessors of the 2004 Indian Ocean Tsunami– Sedimentary evidence of extreme wave events at Ban Bang Sak, SW Thailand. *Sedimentary Geology* 239, 146–161.
- Cabioch, G., Montaggioni, L.F., Faure, G., Ribaud-Laurenti, A., 1999. Reef corallgal assemblages as recorders of paleobathymetry and sea level changes in the Indo-Pacific province. *Quaternary Science Reviews* 19, 1681–1695.
- Camoin, G.F., Colonna, M., Montaggioni, L.F., Casanova, J., Faure, G., Thomassin, B.A., 1997. Holocene sea level changes and reef development in the southwestern Indian Ocean. *Coral Reefs* 16, 247–259.
- Camoin, G.F., Montaggioni, L.F., Braithwaite, C.J.R., 2004. Late glacial to post glacial sea levels in the western Indian Ocean. *Mar. Geol.* 206, 119–146.
- Chasens, S.A., 1981. Foraminifera of the Kenya coastline. *J. Foramin. Res.* 11, 191–202.
- Cheng, J., Collins, L.S., Homes, C., 2012. Four thousand years of habitat change in Florida Bay, as indicated by benthic foraminifera. *J. Foramin. Res.* 42, 3–17.
- Ciarapica, G., Passeri, L., 1993. An overview of the Maldivian coral reefs in Felidu and North Malé Atoll (Indian Ocean): Platform drowning and ecological crisis. *Facies* 28, 33–66.
- Ciarapica, G., 1995. Preliminary notes of the Maldivian Foraminifera from Ari and Felidu Atoll (Maldives, Indian Ocean). *Rev. Paléobiol.* 14, 321–347.
- Cockey, E.M., Hallock, P.M., Lidz, B.H., 1996. Decadal-scale changes in benthic foraminiferal assemblages off Key Largo, Florida. *Coral Reefs* 15, 237–248.
- Connell, J.H., 1978. Diversity in tropical rainforests and coral reefs. *Science* 199, 1302–1310.
- Dawson, A.G., and Stewart, I., 2007. Tsunami deposits in the geological record. *Sedimentary Geology* 200, 166–183.
- Debenay, J.P., 2000. Foraminifera of paralic tropical environments. *Micropaleontol.* 46, 153–160.
- Debenay, JP, Patrona, D., Goguenheim, H., 2009. Colonization of coastal environments by foraminifera: insight from shrimp ponds in New Caledonia (SW Pacific). *J. Foramin. Res.* 39, 249–266.
- Dennison, J.M., Hay, W.W., 1967. Estimating the needed sampling area for subaquatic ecologic studies. *J. Paleont.* 41, 706–708.

- Dodd, J.R., Siemers, C.T., 1971. Effect of Late Pleistocene karst topography on Holocene sedimentation and biota, lower Florida Keys. *Bull. Geol. Soc. Am.* 82, 211–218.
- Dullo, W.C., Blomeier, D., Camoin, G.F., Casanova, J., Colonna, M., Eisenhauer, A., Faure, G., Thomassin, B.A., 1998. Sediments and sea level changes of the foreslopes of Mayotte, Comoro Islands: direct observations from a submersible. In: Camoin, G., Bergerson, D. (eds) *Reefs and carbonate platforms of the Indian and Pacific Oceans*. IAS Spec. Publ. 25, 219–236.
- Dunham, R.J., 1962. Classification of carbonate rocks according to depositional texture. In: Ham, W.E. (eds) *Classification of Carbonate Rocks. A Symposium*, Am. Assoc. of Pet. Geol. Mem. 1, 108–121.
- Einsele, G., Chough, S.K., Shiki, T., 1996. Depositional events and their records – an introduction. *Sedimentary Geology* 104, 1–9.
- Eisenhauer, A., Wasserburg, G.J., Chen, J.H., Bonani, G., Collins, L.B., Zhu, Z.R., Wyrwoll, K.H., 1993. Holocene sea-level determination relative to the Australian continent: U/Th (TIMS) and ^{14}C (AMS) dating of coral cores from the Abrolhos Islands. *Earth Planet. Sci. Lett.* 114, 529–547.
- Elmoutaki, S., Lezine, A.M., Thomassin, B.A., 1992. Vegetational and climatic evolution during the last glacial-interglacial transition and during the Holocene. *CR Acad. Sci.* 314, 237–244.
- Ellis, B.F., Messina, A., 1940. *Catalogue of Foraminifera. et seq* American Museum of Natural History, New York. 1940 and supplements.
- Embry, A.F., Klovan, J.E., 1971. A late Devonian reef tract on northeastern Banks Island. *N.T.W. Bull. Canadian Petrol. Geol.* 19, 730–781.
- Embry, A.F., Klovan, J.E., 1972. Absolute water depths limits of late Devonian paleoecological zones. *Geol. Rundsch.* 61, 672–686.
- Flessa, K.W., and Kowalewski, M., 1994. Shell survival and time-averaging in nearshore and shelf environments: estimates from the radiocarbon literature. *Lethaia* 27, 153–165.
- Fujino, S., Naruse, H., Matsumoto, D., Jarupongsakul, T., Sphawajruksakul, A., Sakakura, N., 2009. Stratigraphic evidence for pre-2004 tsunamis in southwestern Thailand. *Marine Geology* 262, 25–28.
- Gardiner, J.S., Murray, J., 1906. Lagoon deposits. In: Gardiner, J.S. (ed) *The fauna and geography of the Maldive and Laccadive Archipelagos*. University Press Cambridge 2, 581–588.
- Gischler, E., and Lomando, A.J., 2000. Isolated carbonate platforms of Belize, Central America: sedimentary facies, late Quaternary history and controlling factors, in: Insalaco, E., Skelton, P.W., Palmer, T.J. (Eds.), *Carbonate platform systems: components and interactions*. Geological Society London, Special Publication 178, pp. 135–146.
- Gischler, E., 2003. Holocene lagoonal development in the isolated carbonate platforms off Belize. *Sediment. Geol.* 159, 113–132.

References

- Gischler, E., Hauser, I., Heinrich, K., Scheitel, U., 2003. Characterization of depositional environments in carbonate platforms based on benthic foraminifera, Belize, Central America. *Palaios* 18, 236–255.
- Gischler, E., 2006. Sedimentation on Rasdhoo and Ari atolls, Maldives, Indian Ocean. *Facies* 52, 341–360.
- Gischler, E., and Kikinger, R., 2006. Effects on the tsunami of 26 December 2004 on Rasdhoo and Ari Atolls, Maldives. *Atoll Research Bulletin* 561, 61–74.
- Gischler, E., Hudson, J.H., Pisera, A., 2008. Late Quaternary reef growth and sea level in the Maldives (Indian Ocean). *Mar. Geol.* 250, 104–113.
- Gischler, E., Shinn, E.A., Oschmann, W., Fiebig, J., Buster, N.A., 2008. A 1,500 year Holocene Caribbean climate archive from the Blue Hole, Lighthouse Reef, Belize. *Journal of Coastal Research* 24, 1495–1505.
- Gischler, E., Anselmetti, F.S., Shinn, E.A., 2013. Seismic stratigraphy of the Blue Hole sediments (Lighthouse Reef, Belize), a late Holocene climate and storm archive. *Marine Geology* 344, 155–162.
- Gischler, E., Storz, D., Schmitt, D., 2014. Sizes, shapes, and patterns of coral reefs in the Maldives, Indian Ocean: the influence of wind, storms, and precipitation on a major tropical carbonate platform. *Carbonates Evaporites* 29, 73–87.
- Goff, J., Chagué-Goff, C., Nichol, S., Jaffe, B., Dominey-Howes, D., 2012. Progress in palaeotsunami research. *Sedimentary Geology* 243–244, 70–88.
- Goldberg, E.D., Griffin, J.J., 1970. The sediments of the northern Indian Ocean. *Deep Sea Res. and Oceanogr. Abstr.*, 17, 513–537.
- Goldstein, S.T., Watkins, G.T., Kuhn, R.M., 1995. Microhabitats of salt marsh foraminifera: St. Catherines Island, Georgia, USA. *Mar. Micropal.* 26, 17–29.
- Haig, D.W., 1988. Miliolid foraminifera from inner neritic and mud facies of the Papuan Lagoon. *J. Foramin. Res.* 18, 203–236.
- Haig, D.W., 1993. Buliminid foraminifera from inner neritic and mud facies of the Papuan Lagoon. *J. Foramin. Res.* 23, 162–179.
- Hammer, O., Harper, D.A.T., Ryan, P.D., 2001. Paleontological statistics software package for Education and data analysis. *Palaeontol. Electron.* 4, 1–9.
- Harmelin-Vivien, M.L., 1994. The effects of storms and cyclones on coral reefs: a review. *Journal of Coastal Research*, special issue no. 12, 211–231.
- Harper, S.B., 2005. Bedded shell deposit at Ao Nang, Krabi Province, southern Thailand: a record of a prehistoric tsunami event or extreme storm event or neither. *Geological Society of America, Abstracts* 37, 75.
- Havach, S.M., Collins, L.S., 1997. The distribution of Recent benthic foraminifera across habitats of Bocas del Toro, Caribbean Panama. *J. Foramin. Res.* 27, 232–249.

- Hayward, B.W., Holzmann, M., Grenfell, H.R., Pawlowski, J., Triggs, C.M., 2004. Morphological distinction of molecular types in *Ammonia* - towards a taxonomic revision of the world's most commonly misidentified foraminifera. *Mar. Micropaleontol.* 50, 237–271.
- Heron-Allen, E., Earland, A., 1915. The foraminifera of the Kerimba Archipelago (Portuguese East Africa). Part II. *Trans. Zool. Soc. London* 20, 43–795.
- Hippensteel, S.P., Martin, R.E., Nikitina, D., Pizzuto, J.E., 2000. The formation of Holocene marsh foraminiferal assemblages, middle Atlantic coast, U.S.A.: implications for Holocene sea-level change. *J. Foram. Res.* 30, 272–293.
- Hoegh-Guldberg, O., 2011. Coral reef ecosystems and anthropogenic climate change. *Reg. Environ. Change* 11, 215–227.
- Horton, B.P., 2006. Quantifying Holocene sea level change using intertidal foraminifera: Lessons from the British Isles. *Cushman Found. Foram. Res., Spec. Publ.* 40, 97 pp.
- Hottinger, L., Haliz, E., Reiss, Z., 1993. Recent foraminifera from the Gulf of Aqaba. *Slovenska Akademija Znanosti in Umetnosti, Ljubljana*.
- Hughes, A., 2012. Disturbance and diversity: An ecological chicken and egg problem. *Nature Edu. Knowl.* 3, 48.
- Jankaew, K., Atwater, B.F., Sawai, Y., Choowong, M., Charoentitirat, T., Martin, M.E., Prendergast, A., 2008. Medieval forewarning of the 2004 Indian Ocean tsunami in Thailand. *Nature* 455, 1228–1231.
- Kan, H., Ali, M., Riyat, M., 2007. The 2004 Indian Ocean tsunami in the Maldives: scale of the disaster and topographic effects on atoll reefs and islands. *Atoll Research Bulletin* 555, 1–65.
- Kench, P.S., 1998. Physical controls on development of lagoon sand deposits and lagoon infilling in an Indian Ocean atoll. *J. Coast. Res.* 14, 1014–1024.
- Kench, P.S., McLean, R.F., Nichol, S.L., 2005. New model of reef island evolution: Maldives, Indian Ocean. *Geology* 33, 145–148.
- Kench, P.S., Brander, R.W., 2006. Response of reef island shorelines to seasonal climate oscillations: South Maalhosmadulu Atoll, Maldives. *J. Geophys. Res.* 111, F01001.
- Kench, P.S., Nichol, S.L., Smithers, S.G., McLean, R.F., Brander, R.W., 2008. Tsunami as agents of geomorphic change in mid-ocean reef islands. *Geomorphology* 95, 361–383.
- Kench, P.S., Smithers, S.G., McLean, R.F., Nichol, S.L., 2009. Holocene reef growth in the Maldives: evidence of a mid-Holocene sea-level highstand in the central Indian Ocean. *Geol.* 37, 455–458.
- Klostermann, L., Gischler, E., Storz, D., Hudson, J.H., 2014. Sedimentary record of late Holocene event beds in a mid-ocean atoll lagoon, Maldives, Indian Ocean: Potential for deposition by tsunamis. *Mar. Geol.* 348, 37–43.

References

- Lambeck, K., 1990. Late Pleistocene, Holocene and present sea-levels: constraints on future change. *Palaeogeogr. Palaeoclimatol. Palaeoecol.* 89, 205–217.
- Langer, M., 2008. Assessing the contribution of foraminiferan protists to global ocean carbonate production. *J. Eukaryot. Microbiol.* 55, 63–169.
- Langer, M., Hottinger, L., 2000. Biogeography of selected “larger” foraminifera. *Micropal* 46, 105–127.
- Langer, M., Lipps, J.H., 2003. Foraminiferal distribution and diversity, Madang Lagoon, Papua New Guinea. *Coral Reefs* 22, 143–154.
- Langer, M., Silk, M.T., Lipps, J.H., 1997. Global ocean carbonate and carbon dioxide production; the role of reef Foraminifera. *J. Foramin. Res.* 27, 271–277.
- Larcombe, P., Carter, R.M., 1998. Sequence architecture during the Holocene transgression: an example from the Great Barrier Reef shelf, Australia. *Sediment. Geol.* 117, 97–121.
- Levy, A., Mathieu, R., Poignant, A., Rosset-Moulinier, M., Ambroise, D., 1996. Foraminifères benthiques des îles Maldives (Océan Indien). *Mem. Soc. Géol. France* 169, 129–138.
- Loeblich, A., Tappan, H., 1994. Foraminifera of the Sahul Shelf. *Cushman Found. Foramin. Res. Spec. Publ.* 31, 1–661.
- Lüdmann, T., Kavelage, C., Betzler, C., Fürstenau, J., Hübscher, C., 2013. The Maldives, a giant isolated carbonate platform dominated by bottom currents. *Mar. Petrol. Geol.* 43, 326–340.
- Makled, W.A., Langer, M., 2011. Benthic Foraminifera from the Chuuk Lagoon Atoll System (Caroline Islands, Pacific Ocean). *N. Jb. Geol. Pal. Abh.* 259, 231–249.
- Malik J., Banerjee, C., Shishikura, M., 2010. Paleo-tsunami and land-level change evidence from the west coast of South Andaman, Andaman Nicobar Island, India. *Geophysical Research, Abstracts* 12.
- Mamo, B., Strotz, L., Dominey-Howes, D., 2009. Tsunami sediments and foraminiferal assemblages. *Earth-Sci. Rev.* 96, 263–278.
- Marshall, J.F., Davies, P.J., 1982. Internal structure and Holocene evolution of One Tree Reef, southern Great Barrier Reef. *Coral Reefs* 1, 21–28.
- Miller, M.W., Sulka, R.D., 1999. Patterns of seagrass and sediment nutrient distribution suggest anthropogenic enrichment in Laamu Atoll, Republic of Maldives. *Mar. Pollut. Bull.* 38, 1152–1156.
- Milliman, J.D., 1974. *Marine Carbonates*. Springer, New York. 375 pp.
- Monecke, K., Finger, W., Klarer, D., Kongko, W., McAdoo, B.G., Moore, A.L., Sudrajat, S.U., 2008. A 1,000-year sediment record of tsunami recurrence in northern Sumatra. *Nature* 455, 1232–1234.
- Montaggioni, L., 1988. Holocene reef growth in mid-plate high volcanic islands. *Proc. of the 6th Int. Coral Reef Symp.* 3, 455–460.

References

- Morton, R.A., Gelfenbaum, G., Jaffe, B.E., 2007. Physical criteria for distinguishing sandy tsunami and storm deposits using modern examples. *Sedimentary Geology* 200, 184–207.
- Mossadegh, Z., Parker, J., Gischler, E., 2012. Biodiversity and community structure of Late Pleistocene foraminifera from Kish Island, Persian Gulf (Iran). *Facies* 58, 339–365.
- Murray, J.W., 2006. Ecology and applications of benthic foraminifera. Cambridge University Press, Cambridge. 426 pp.
- Natawidjaja, D.H., Sieh, K., Chlieh, M., Galetzka, J., Suwargadi, B.W., Cheng, H., Edwards, R.L., Avouac, J.-P., Ward, S.N., 2006. Source parameters of the great Sumatran megathrust earthquakes of 1797 and 1833 inferred from coral microatolls. *Journal of Geophysical Research* 111, 1–37.
- Newcomb, K., and McCann, W., 1987. Seismic history and seismotectonics of the Sunda Arc. *Journal of Geophysical Research* 92, 421–439.
- Newell, N.D., Imbrie, J., Purdy, E.G., Thurber, D.L., 1959. Organism communities and bottom facies, Great Bahama Bank. *Bull. Am. Mus. Nat. Hist.* 117, 181–228.
- Nott, J., 2011. A 6000 year tropical cyclone record from Western Australia. *Quaternary Science Reviews* 30, 713–722.
- Nott, J., and Forsyth, A., 2012. Punctuated global tropical cyclone activity over the past 5,000 years. *Geophysical Research Letter* 39, L14703.
- Parker, J., 2009. Foraminifera from Ningaloo Reef, Western Australia. *Mem. Assoc. Aust. Palaeont.* 36; 810 pp.
- Parker, J.H., and Gischler, E., 2011. Modern foraminiferal distribution and diversity in two atolls from the Maldives, Indian Ocean. *Marine Micropaleontology* 78, 30–49.
- Parker, J., Gischler, E., Eisenhauer, A., 2012. Biodiversity of foraminifera from Late Pleistocene to Holocene coral reefs, South Sinai, Egypt. *Mar. Micropal.* 86, 59–75.
- Paul, A., Reijmer, J.J.G., Fürstenau, J., Kinkel, H., Betzler, C., 2012. Relationship between late Pleistocene sea-level variations, carbonate platform morphology and aragonite production (Maldives, Indian Ocean). *Sedimentology* 59, 1640–1658.
- Perry, C.T., Kench, P.S., Smithers, S.G., Yamano, H., O’Leary, M., Gulliver, P., 2013. Time scales and modes of reef lagoon infilling in the Maldives and controls on the onset of reef island formation. *Geology* 41, 1111–1114.
- Pillai, C.S.G., and Scheer, G., 1976. Report on the stony corals from the Maldivian Archipelago. *Zoologica* 126, 1–81.
- Preu, C., Engelbrecht, A., 1991. Patterns and processes shaping the present morphodynamics of coral reef islands - Case study from North-Malé Atoll, Maldives (Indian Ocean). In: Bruckner H, Radtke U (Eds), from the North Sea to the Indian Ocean. Franz Steiner, Stuttgart, p. 209–200.

References

- Purdy, E.G., Bertram, G.T., 1993. Carbonate concepts from the Maldives, Indian Ocean. *Am. Assoc. Pet. Geol. Studies Geol.* 34, 1–56.
- Purdy, E.G., Gischler, E., 2005. The transient nature of the empty bucket model of reef sedimentation. *Sed. Geol.* 175, 35–47.
- Rajendran, C.P., Rajendran, K., Machado, T., Satyamurthy, T., Aravazhi, P., Jaiswal, M., 2006. Evidence of ancient sea surges at the Mamallapuram coast of India and implications for previous Indian Ocean tsunami events. *Current Science* 91, 1242–1247.
- Rankey, E.C., Garza-Pérez, J.R., 2012. Seascape metrics of shelf-margin reefs and reef sand aprons of Holocene carbonate platforms. *J. Sed. Res.* 82, 53–71.
- Rhodes, B.P., Kirby, M.E., Jankaew, K., Choowong, M., 2011. Evidence for a mid-Holocene tsunami deposit along the Andaman coast of Thailand preserved in a mangrove environment. *Marine Geology* 282, 255–267.
- Richarson-White, S., Walker, S.E., 2011. Diversity, taphonomy and behavior of encrusting foraminifera on experimental shells deployed along a shelf-to-slope bathymetric gradient, Lee Stocking Island, Bahamas. *Palaeogeogr. Palaeoclimatol. Palaeoecol.* 312, 305–324.
- Sanders, H.L., 1969. Benthic marine diversity and the stability-time hypothesis. *Brookhaven Symp. Biol.* 22, 71–81.
- Saraswat, R., Nigam, R., Weldeab, S., Mackensen, A., Naidu, P.D., 2005. A first look at past sea surface temperatures in the equatorial Indian Ocean from Mg/Ca in foraminifera. *Geophys. Res. Lett.* 32, L24605, doi:10.1029/2005GL024093.
- Sarkar, S., Gupta, A.K., 2009. Deep-sea paleoceanography of the Maldives Islands (ODP Hole 716A), equatorial Indian Ocean during MIS 12–6. *J. Biosci.* 34, 749–764.
- Schlager, W., Purkis, S.J., 2013. Bucket structure in carbonate accumulations of the Maldivian, Chagos and Laccadive archipelagos. *Int. J. Earth. Sci.* 102, 2225–2238.
- Scholl, D.W., 1964. Recent sedimentary record in mangrove swamps and rise in sea level over the southern coast of Florida: Part 1. *Mar. Geol.* 1, 344–366.
- Schott, F.A., McCready, J.P., 2001. The monsoon circulation of the Indian Ocean. *Progr. Oceanogr.* 51, 1–123.
- Schultz, S., Gischler, E., Oschmann, W., 2010. Diversity, distribution, and assemblages of benthic foraminifera in atoll lagoons during the Holocene, Belize, Central America. *Facies* 56, 323–336.
- Scoffin, T.P., 1993. The geological effects of hurricanes on coral reefs and the interpretation of storm deposits. *Coral Reefs* 12, 203–221.
- Scott, D.B., Medioli, F.S., Schafer, C.T., 2001. Monitoring in coastal environments using foraminifera and thecamoebian indicators. *Cambridge Univ. Press* 177 pp.
- Shinn, E.A., Hudson, J.H., Halley, R.B., Lidz, B., Robbin, D.M., Macintyre, I.G., 1982. Geology and sediment accumulation rates at Carrie Bow Cay, Belize. In: Rützler, K., Macintyre,

References

- I.G., (eds) The Atlantic barrier reef ecosystem at Carrie Bow Cay, Belize: I. Structure and communities, Belize Science Report 1. *Smithson Contrib. to Mar. Sci.* 12, 63–75.
- Sing, O.P., Ali Khan, T.M., Rahman, M.S., 2000. Changes in the frequency of tropical cyclones over the North Indian Ocean. *Meteorol. and Atmos. Phys.* 75, 11–20.
- Smithers, S.G., Woodroffe, C.D., McLean, R.F., Wallensky, E.P., 1992. Lagoonal sedimentation in the Cocos (Keeling) Islands, Indian Ocean. *Proc. 7th Int. Coral Reef Symp.* 1, 273–288.
- Sousa, W.P., 1979. Disturbance in marine intertidal boulder fields: the nonequilibrium maintenance of species diversity. *Ecology* 60, 1225–1239.
- Storz, D., Gischler, E., 2011a. Coral extension rates in the NW Indian Ocean I: reconstruction of 20th century SST variability and monsoon current strength. *Geo-Mar. Lett.* 31, 141–154.
- Storz, D., Gischler, E., 2011b. Coral extension rates in the NW Indian Ocean II: reconstruction of 20th century Indian monsoon strength and rainfall over India. *Geo-Mar. Lett.* 31, 155–162.
- Storz, D., Gischler, E., Parker, J., Klostermann, L., 2014. Changes in diversity and assemblages of foraminifera through the Holocene in an atoll from the Maldives, Indian Ocean, *Mar. Micropaleontol.* 106, 40–54.
- Tipper, J.C., 1997. Modeling carbonate platform sedimentation - lag comes naturally. *Geology* 25, 495–498.
- Toomey, M.R., Donnelly, J.P., Woodruff, J.D., 2013. Reconstructing mid–late Holocene cyclone variability in the central Pacific using sedimentary records from Tahaa, French Polynesia. *Quat. Sci. Rev.* 77, 181–189.
- Tudhope, A.W., and Scoffin, T.P., 1984. The effects of *Callianassa* bioturbation on the preservation of carbonate grains in Davies Reef lagoon, Great Barrier Reef, Australia. *J. Sed. Petrol.* 54, 1091–1096.
- Tudhope, A.W., 1989. Shallowing-upwards sedimentation in a coral reef lagoon, Great Barrier Reef of Australia. *J. Sed. Petrol.* 59, 1036–1051.
- van Arx, W.S., 1954. Circulation systems of Bikini and Rongelap lagoons. *US Geol. Surv. Prof. Pap.* 260-B, 265–273.
- van der Plaas, L., Tobi, A.C., 1965. A chart for judging the reliability of point-counting results. *Amer. J. Sci.* 263, 87–90.
- Verma, M., and Bansal, B.K., 2013. Seismic hazard assessment and mitigation in India: an overview. *International Journal of Earth Sciences* 102, 1203–1218.
- Veron, J.E.N., 2000. *Corals of the world*, 3 volumes. Australian Institute of Marine Science and CRR Qld. Pty. Ltd., Townsville.
- Webster, P.J., Holland, G.J., Curry, J.A., Chang, H.-R., 2005. Changes in tropical cyclone number, duration, and intensity in a warming environment. *Science* 309, 1844–1846.

- Woodroffe, C.D., 1992. Morphology and evolution of reef islands in the Maldives. Proc. of the 7th Int. Coral Reef Symp. 2, 1217–1226.
- Woodroffe, C.D., McLean, R.F., Wallensky, E., 1994. Geomorphology of the Cocos (Keeling) Islands. Atoll Res. Bull. 402, 1–33.
- Yamano, H., Miyajima, T., Koike, I., 2001. Importance of foraminifera for the formation and maintenance of a coral sand cay: Green Island, Australia. Coral Reefs 19, 51–58.
- Yamano, H., Kayanne, H., Matsuda, F., Tsuji, Y., 2002. Lagoonal facies, ages, and sedimentation in three atolls in the Pacific. Mar. Geol. 185, 233–247.
- Yu, K.F., Zhao, J.X., Shi, Q., Meng, Q.S., 2009. Reconstruction of storm/tsunami records over the last 4000 years using transported coral blocks and lagoon sediments in the southern South China Sea. Quat. Int. 195, 128–137.
- Zinke, J., Reijmer, J.J.G., Taviani, M., Dullo, W.C., Thomassin, B., 2005. Facies and faunal assemblage changes in response to the Holocene transgression in the Lagoon of Mayotte (Comoro Archipelago, SW Indian Ocean). Facies 50, 391–408.
- Zinke, J., Reijmer, J.J.G., Thomassin, B.A., 2001. Seismic architecture and sediment distribution within the Holocene barrier reef-lagoon complex of Mayotte (Comoro archipelago, SW Indian Ocean). Palaeogeogr. Palaeoclimatol. Palaeoecol. 175, 343–368.
- Zinke, J., Reijmer, J.J.G., Thomassin, B.A., 2003a. Systems tracts sedimentology in the lagoon of Mayotte associated with the Holocene transgression. Sed. Geol. 160, 57–79.
- Zinke, J., Reijmer, J.J.G., Thomassin, B.A., Dullo, W.C., Grootes, P.M., Erlenkeuser, H., 2003b. Postglacial flooding history of Mayotte Lagoon (Comoro Archipelago, southwest Indian Ocean). Mar. Geol. 194, 181–196.

Danksagung/Acknowledgements

Vor allem möchte ich mich ganz herzlich bei Herrn Prof. Dr. Eberhard Gischler bedanken. Sowohl für die Vergabe der Dissertation, als auch für die Möglichkeit die Arbeit an der Goethe-Universität Frankfurt schreiben und nicht zuletzt für die sehr gute Betreuung und die vielen Anregungen. Ich danke Prof. Dr. Christian Betzler von der Universität Hamburg für die Zweitbegutachtung der Arbeit sowie der Deutschen Forschungsgemeinschaft und der Vereinigung von Freunden und Förderern der Goethe-Universität Frankfurt, die dieses Projekt finanziell unterstützt haben.

Für die Röntgen-Diffraktometrie Messungen (XRD) der Karbonat- und Bodenproben möchte ich mich bei Herrn Dr. Reiner Petschick bedanken sowie bei Anja Isaack und Nils Prawitz für die viele praktische Hilfe in den Laboren und der Präparation der Goethe-Universität Frankfurt. Des Weiteren möchte ich mich bei meinem Zimmerkollegen David Storz für seine fachlichen und kompetenten Hilfestellungen und bei meiner Zimmernachbarin Fiederike Adomat für die anregenden Diskussionsrunden während den Mittagspausen bedanken.

Zuletzt gilt mein Dank der Exkursionsteilnehmer Harold Hudson (Miami), Stefan Haber (Bad Karlshafen), Gabi Gischler (Frankfurt) und Kaptain Haneef mit seiner Dhoni Besatzung von der Insel Rasdhoo, die uns während der Feldarbeit im Rasdhoo Atoll stets hilfsbereit unterstützt haben.

Appendix Table 2.5 Correlation matrices of sediment data

Sample depth [cm]	<125 µm [wt.%]	>2 mm [wt.%]	Mollusk [%]	Coral [%]	Foram. [%]	Echino. [%]	Halimeda [%]	Red algae [%]	Crustacea [%]	Peloids [%]	Opaque [%]	ARA [wt.%]	LMC [wt.%]	HMC [wt.%]
	0.004	0.031	0.028	0.001	0.520	0.120	0.240	0.001	0.000	0.813	0.000	0.000	0.309	0.000
<125µm [wt.%]		0.000	0.000	0.000	0.000	0.000	0.000	0.000	0.511	0.000	0.268	0.943	0.000	0.094
>2mm [wt.%]	-0.894		0.261	0.000	0.000	0.616	0.000	0.000	0.542	0.000	0.296	0.710	0.000	0.002
Mollusk [%]	-0.368	0.078		0.000	0.000	0.127	0.000	0.000	0.000	0.029	0.189	0.657	0.115	0.000
Coral [%]	-0.229	0.267	0.343		0.001	0.000	0.000	0.000	0.248	0.008	0.021	0.014	0.435	0.332
Foram. [%]	-0.045	0.310	0.347	0.584		0.000	0.066	0.000	0.024	0.000	0.088	0.510	0.000	0.002
Echino. [%]	0.108	0.217	0.106	0.225	0.526		0.554	0.000	0.006	0.001	0.995	0.243	0.000	0.001
Halimeda [%]	-0.082	0.035	0.423	0.307	0.128	-0.041		0.583	0.778	0.247	0.314	0.041	0.001	0.032
Red algae [%]	-0.222	0.437	0.240	0.430	0.678	0.425	0.038	0.000	0.025	0.000	0.236	0.398	0.000	0.002
Crustacea [%]	0.454	-0.043	0.285	0.080	0.157	0.192	-0.020	-0.155	0.112	0.107	0.002	0.657	0.177	0.000
Peloids [%]	0.017	0.437	-0.324	-0.183	-0.303	-0.232	-0.081	-0.459	0.209	-0.072	0.303	0.343	0.573	0.356
Opaque [%]	0.418	-0.073	0.091	-0.161	-0.118	0.000	-0.070	-0.083	0.209	-0.072	0.303	0.000	0.019	0.000
ARA [wt.%]	-0.314	-0.005	-0.026	0.031	0.046	-0.081	0.142	-0.059	-0.031	0.066	-0.833	0.000	0.713	0.002
LMC [wt.%]	-0.071	0.448	-0.110	-0.054	0.253	0.363	-0.222	0.357	-0.094	-0.039	-0.162	-0.026	0.000	0.000
HMC [wt.%]	-0.262	-0.116	0.211	-0.368	0.211	0.219	-0.148	0.217	-0.281	0.064	-0.523	0.215	0.515	0.000

Statistically significant correlations ($p < 0.05$, top right half of the table) are marked in bold. Percentages of constituent particles (<125 µm and >2 mm) were used. *ARA*: aragonite, *LMC*: low-magnesium calcite, *HMC*: high-magnesium calcite

Appendix

Appendix Table 2.6 Texture, composition, and mineralogy of soil facies

Sample no.	<125 µm [wt.%]	>2 mm [wt.%]	Mollusk [%]	Coral [%]	Foram. [%]	Echino. [%]	Halimeda [%]	Red algae [%]	Crustacean [%]	Peloid [%]	Opaque [%]	ARA [wt.%]	LMC [wt.%]	HMC [wt.%]
#16 415-420	83.06	5.41	9.43	0.00	0.56	0.28	0.06	0.00	0.96	0.00	5.65	70.39	2.68	3.42
#16 425-430	86.47	3.41	6.18	0.00	0.51	0.34	0.00	0.00	0.34	0.00	6.18	32.91	2.04	0.89
#16 435-440	81.69	4.29	11.55	0.16	0.16	0.24	0.00	1.14	0.49	0.00	4.56	0.00	0.00	0.00
#16 445-450	78.06	7.26	8.49	1.06	0.35	0.00	0.00	3.89	0.35	0.00	7.79	0.00	0.00	0.00
mean	82.32	5.09	8.91	0.31	0.40	0.22	0.01	1.26	0.54	0.00	6.04	25.82	1.18	1.08
SD	3.48	1.66	2.23	0.51	0.18	0.15	0.03	1.84	0.29	0.00	1.34	33.51	1.39	1.62

Appendix Table 2.7 Texture, composition, and mineralogy of mollusk-coral-algal floatstone-rudstone (mcaFR) facies

Sample no.	<125 µm [wt.%]	>2 mm [wt.%]	Mollusk [%]	Coral [%]	Foram. [%]	Echino. [%]	Halimeda [%]	Red algae [%]	Crustacean [%]	Peloid [%]	Opaque [%]	ARA [wt.%]	LMC [wt.%]	HMC [wt.%]
#19 235-240	59.76	31.90	16.63	14.35	2.68	1.07	3.89	0.80	0.54	0.27	0.00	86.22	5.27	8.51
#19 245-250	36.32	34.86	21.84	10.05	3.49	0.15	6.55	0.87	0.58	0.15	0.00	91.25	1.17	7.57
#19 255-260	51.24	32.43	28.44	10.40	3.09	0.33	3.74	0.81	1.79	0.16	0.00	90.77	2.27	6.96
#34 110-120	60.25	30.15	3.50	2.11	0.96	0.43	0.00	2.40	0.19	0.00	0.00	86.49	2.72	10.79
#34 150-160	55.16	29.95	6.78	2.75	1.19	0.60	0.00	3.42	0.15	0.00	0.00	85.46	2.99	11.56
#34 270-275	61.63	17.96	5.51	5.82	3.27	0.20	0.20	5.31	0.10	0.00	0.00	84.28	4.79	10.93
#34 350-360	54.89	13.27	10.67	7.48	5.58	1.59	0.00	6.05	0.48	0.00	0.00	68.86	7.66	23.48
#34 380-390	46.46	24.08	8.10	6.63	5.60	1.18	0.00	7.66	0.29	0.00	0.00	83.02	3.72	13.26
#8 10-20	33.40	33.40	1.75	2.54	1.33	0.73	0.73	4.84	0.18	0.00	0.00	85.74	3.16	11.10
#8 50-60	58.43	28.05	3.79	3.18	2.43	0.61	0.34	3.11	0.07	0.00	0.00	82.95	4.21	12.84
#8 130-140	58.95	20.38	4.75	4.24	3.20	0.41	0.21	7.75	0.10	0.00	0.00	82.97	3.59	13.44
#8 170-180	57.25	20.42	4.35	6.59	2.57	1.67	0.22	6.59	0.33	0.00	0.00	82.92	3.72	13.36
#29 80-90	62.12	24.04	4.64	3.25	1.25	0.21	0.00	4.29	0.21	0.00	0.00	83.22	3.76	13.02
#13 30-40	43.38	30.01	4.79	8.52	4.12	0.40	3.33	5.06	0.40	0.00	0.00	86.38	2.79	10.83
#13 60-70	47.64	26.45	5.31	12.05	2.33	0.39	4.02	1.81	0.00	0.00	0.00	86.92	3.30	9.78
#13 107-116	51.41	15.07	7.21	10.56	3.69	0.34	5.87	5.53	0.34	0.00	0.00	86.67	2.66	10.67
#13 116-125	43.88	25.54	5.81	9.48	3.67	0.31	7.19	3.98	0.15	0.00	0.00	86.28	3.34	10.38
#13 125-135	50.06	15.77	4.44	10.76	3.59	1.88	10.76	2.73	0.00	0.00	0.00	86.41	3.32	10.27
#13 145-155	42.01	11.16	5.39	14.29	3.28	0.47	12.41	11.01	0.00	0.00	0.00	86.73	2.93	10.34
#18 288-295	56.06	32.05	6.24	1.66	0.65	0.00	0.59	2.56	0.18	0.00	0.00	88.77	1.67	9.56
#24 27-35	66.11	20.16	4.26	2.47	1.10	0.62	1.17	4.05	0.07	0.00	0.00	86.56	3.21	10.22
#24 50-60	58.23	30.21	3.87	2.25	1.27	0.29	0.58	3.06	0.23	0.00	0.00	84.70	2.73	12.57
#24 90-100	52.27	33.90	3.73	2.90	1.45	0.62	0.48	4.50	0.14	0.00	0.00	84.87	2.98	12.14
#24 120-130	63.04	23.66	4.86	1.73	2.20	0.13	0.07	4.32	0.00	0.00	0.00	81.55	3.25	15.20
#31 10-20	54.03	24.52	6.44	2.90	2.57	0.00	1.18	8.37	0.00	0.00	0.00	82.48	3.57	13.95
#31 40-50	56.12	23.53	6.00	5.19	3.05	0.41	0.61	4.99	0.10	0.00	0.00	82.82	3.65	13.53
#31 70-80	56.67	23.28	8.12	3.01	3.71	0.00	0.50	4.71	0.00	0.00	0.00	83.54	2.91	13.54
#31 100-110	52.27	21.15	11.43	3.19	3.19	0.66	0.13	7.84	0.13	0.00	0.00	82.92	3.68	13.40
#31 120-126	41.99	27.04	12.39	4.96	2.32	0.00	0.15	11.15	0.00	0.00	0.00	81.58	8.11	10.31
#27 25-30	59.21	20.37	7.86	5.72	1.74	0.51	0.51	4.49	0.00	0.00	0.00	88.34	2.04	9.62
#30 5-10	29.84	21.98	14.94	13.25	6.75	0.72	0.00	11.57	0.96	0.00	0.00	87.17	3.14	9.69
#30 20-27	25.89	36.80	15.48	9.89	4.85	0.56	0.19	6.34	0.00	0.00	0.00	84.45	3.50	12.05
#30 50-59	24.07	38.89	15.75	7.60	2.59	0.56	0.93	9.26	0.37	0.00	0.00	82.73	7.88	9.39
#1 220-230	40.68	6.88	27.53	9.44	2.88	0.00	4.46	8.13	0.00	0.00	0.00	90.48	2.53	6.98
#11 50-60	31.06	29.17	22.67	7.16	2.39	0.00	1.99	5.57	0.00	0.00	0.00	91.19	2.30	6.51
#25 145-148	43.41	10.21	30.85	2.55	0.00	0.00	10.90	2.09	0.00	0.00	0.00	92.45	1.10	6.44
#25 166-181	30.67	22.05	21.99	2.13	0.24	0.00	21.99	0.71	0.00	0.00	0.24	87.98	2.69	9.33
#26 130-135	53.58	16.90	7.82	13.73	3.10	0.00	3.69	1.18	0.00	0.00	0.00	89.74	1.60	8.66
mean	50.28	24.41	10.16	6.49	2.72	0.46	2.88	4.97	0.21	0.02	0.01	85.47	3.42	11.11
SD	10.77	7.64	7.81	4.01	1.47	0.48	4.61	2.94	0.34	0.05	0.04	4.02	1.58	3.04

Appendix Table 2.8 Texture, composition, and mineralogy of mollusk-coral-red algae rudstone (mcrR) facies

Sample no.	<125 µm [wt.%]	>2 mm [wt.%]	Mollusk [%]	Coral [%]	Foram. [%]	Echino. [%]	Halimeda [%]	Red algae [%]	Crustacean [%]	Peloid [%]	Opaque [%]	ARA [wt.%]	LMC [wt.%]	HMC [wt.%]
#34 160-170	48.95	35.24	6.09	3.95	1.03	0.87	0.00	3.72	0.16	0.00	0.00	86.75	2.71	10.54
#8 20-30	48.76	33.68	3.78	2.28	3.16	0.44	0.97	6.41	0.53	0.00	0.00	83.92	3.65	12.42
#8 125-130	37.85	48.28	4.65	2.91	2.15	0.21	1.60	2.36	0.00	0.00	0.00	82.76	4.82	12.42
#8 140-150	40.88	44.64	3.91	2.82	1.52	0.29	0.51	5.29	0.07	0.00	0.07	82.75	3.33	13.92
#29 10-20	46.96	42.27	2.05	2.91	1.13	0.11	0.27	4.09	0.22	0.00	0.00	83.44	3.49	13.07
#29 30-35	32.50	44.08	3.75	11.36	1.76	0.12	1.29	4.80	0.12	0.00	0.00	85.81	2.86	11.33
#29 42-55	50.93	42.08	1.61	2.80	0.52	0.10	0.35	1.57	0.00	0.00	0.03	85.56	3.18	11.26
#29 61-66	48.32	36.77	3.43	5.14	1.34	0.75	0.15	3.80	0.30	0.00	0.00	83.70	4.28	12.02
#29 73-80	48.49	38.00	2.77	6.35	1.82	0.54	0.34	1.69	0.00	0.00	0.00	83.70	3.97	12.33
#29 90-98	46.03	41.95	3.73	4.15	1.92	0.18	0.06	1.80	0.18	0.00	0.00	85.16	3.29	11.55
#29 120-130	41.13	47.07	3.24	3.07	1.83	0.29	0.12	3.19	0.06	0.00	0.00	83.51	3.09	13.40
#13 10-23	30.26	49.84	3.19	5.67	2.49	0.30	1.79	6.37	0.10	0.00	0.00	87.32	2.33	10.35
#13 50-60	35.61	44.23	2.92	7.96	1.51	0.60	3.53	3.63	0.00	0.00	0.00	86.43	2.67	10.91
#13 80-90	38.42	41.60	4.20	7.99	2.10	0.20	2.70	2.70	0.10	0.00	0.00	74.89	4.73	20.38
#18 300-310	41.62	47.44	5.58	1.04	0.87	0.38	0.55	2.35	0.16	0.00	0.00	89.22	1.70	9.08
#18 325-337	44.65	42.90	6.04	1.49	0.87	0.12	0.37	3.17	0.37	0.00	0.00	89.22	1.78	9.00
#24 70-80	48.57	37.44	3.78	1.89	0.98	0.56	1.33	5.25	0.21	0.00	0.00	84.72	2.79	12.49
#24 105-112	38.81	52.62	2.78	1.37	0.69	0.39	0.04	3.21	0.09	0.00	0.00	82.74	3.12	14.14
#24 140-152	23.13	65.40	3.96	2.75	0.52	0.46	0.00	3.79	0.00	0.00	0.00	77.48	7.10	15.42
#31 30-40	38.83	46.65	5.08	2.54	2.40	0.29	0.44	3.56	0.22	0.00	0.00	83.89	3.38	12.73
#31 60-70	45.91	37.09	8.50	1.45	1.79	0.34	0.43	4.42	0.00	0.00	0.09	82.00	4.20	13.80
#31 90-100	35.51	47.72	6.45	2.51	1.34	0.17	0.42	5.78	0.08	0.00	0.00	81.97	4.72	13.31
#27 40-50	47.90	35.72	6.06	3.27	0.65	0.33	0.33	5.49	0.25	0.00	0.00	86.76	3.10	10.14
#27 70-80	32.02	55.85	5.28	2.85	1.03	0.12	0.06	2.67	0.12	0.00	0.00	85.69	2.84	11.46
#30 35-40	18.26	59.20	9.36	4.85	2.59	0.45	0.11	4.96	0.23	0.00	0.00	85.82	5.46	8.72
#30 40-50	8.90	78.68	2.92	5.03	1.12	0.25	0.12	2.86	0.12	0.00	0.00	84.93	6.13	8.94
#2 184-195	19.27	69.94	5.99	0.81	0.22	0.00	1.56	1.89	0.32	0.00	0.00	89.60	1.62	8.78
#26 135-145	33.62	44.20	7.32	10.20	1.11	0.00	2.66	0.89	0.00	0.00	0.00	86.84	1.85	11.31
#26 155-165	31.48	44.12	8.42	10.61	1.34	0.00	2.20	1.34	0.37	0.00	0.12	91.65	0.95	7.40
#26 175-185	27.36	45.50	9.36	11.54	2.04	0.14	2.04	1.49	0.54	0.00	0.00	91.47	1.29	7.25
mean	37.70	46.67	4.87	4.45	1.46	0.30	0.87	3.48	0.16	0.02	0.02	84.99	3.35	11.66
SD	10.56	10.36	2.12	3.16	0.70	0.21	0.97	1.55	0.15	0.00	0.04	3.55	1.41	2.62

Appendix Table 2.9 Texture, composition, and mineralogy of mollusk-coral-algal wackestone-floatstone (mcaWF) facies

Sample no.	<125 µm [wt.%]	>2 mm [wt.%]	Mollusk [%]	Coral [%]	Foram. [%]	Echino. [%]	Halimeda [%]	Red algae [%]	Crustacean [%]	Peloid [%]	Opesque [%]	ARA [wt.%]	LMC [wt.%]	FMC [wt.%]
#19 225-230	72.33	13.98	13.47	7.75	0.92	0.28	2.77	0.74	0.83	0.83	0.09	89.30	1.35	9.35
#34 180-190	64.60	15.80	6.17	5.00	2.35	0.88	0.00	5.00	0.20	0.00	0.00	85.33	2.76	11.91
#34 190-200	71.18	8.21	7.42	5.05	2.27	0.62	0.00	5.15	0.10	0.00	0.00	85.70	3.18	11.12
#34 210-220	64.86	13.65	6.55	4.94	3.33	1.18	0.00	5.37	0.11	0.00	0.00	85.75	2.61	11.64
#34 230-240	66.81	11.11	7.62	5.19	3.86	0.77	0.00	4.53	0.11	0.00	0.00	86.08	2.37	11.55
#34 250-260	64.25	12.59	7.06	6.25	3.36	0.46	0.35	4.98	0.69	0.00	0.00	85.74	3.04	11.21
#34 280-290	71.13	6.57	6.80	4.46	4.13	0.89	0.11	5.58	0.33	0.00	0.00	83.82	3.75	12.43
#34 320-330	67.41	8.55	6.01	6.37	3.37	0.36	0.00	7.69	0.24	0.00	0.00	84.65	3.24	12.11
#8 40-50	69.12	15.81	3.77	5.35	2.79	0.00	0.00	2.94	0.23	0.00	0.00	83.51	3.70	12.80
#8 70-75	73.99	7.84	5.18	6.91	1.55	0.36	0.27	3.82	0.09	0.00	0.00	84.20	3.07	12.73
#8 95-105	66.92	12.98	5.73	4.12	2.11	0.50	0.40	6.93	0.30	0.00	0.00	82.32	6.06	11.63
#8 115-125	68.15	7.82	6.85	6.01	2.40	1.44	0.36	6.97	0.00	0.00	0.00	84.18	3.06	12.76
#29 110-120	73.50	6.84	5.11	5.21	1.87	0.79	0.20	6.29	0.20	0.00	0.00	83.79	3.93	12.29
#18 275-280	75.46	10.56	9.36	1.33	0.35	0.28	1.12	1.54	0.00	0.00	0.00	88.63	1.42	9.95
#18 317-325	71.12	6.22	10.43	5.10	1.36	0.11	2.04	3.29	0.23	0.00	0.11	88.09	1.87	10.04
#27 2-6	64.98	10.01	12.51	5.75	1.38	0.50	0.38	4.38	0.13	0.00	0.00	86.58	3.11	10.31
#27 14-17	65.66	10.69	8.87	7.57	1.30	0.00	1.06	4.26	0.59	0.00	0.00	86.58	3.11	10.31
#1 30-40	64.76	4.18	13.36	12.89	0.47	0.31	0.00	4.04	0.00	0.00	0.00	90.66	1.81	7.52
#1 40-47	68.44	3.10	9.96	12.81	1.57	0.00	0.57	3.56	0.00	0.00	0.00	89.99	2.09	7.92
#1 47-52	65.68	3.54	12.46	12.62	1.69	0.77	0.77	1.85	0.62	0.00	0.00	90.31	1.69	8.00
#1 110-120	66.78	4.11	19.94	3.06	1.46	0.29	1.46	2.91	0.00	0.00	0.00	90.25	1.91	7.83
#2 143-145	72.75	6.92	11.59	1.32	1.12	0.00	3.66	2.64	0.00	0.00	0.00	89.26	1.51	9.23
#2 160-170	74.95	3.99	9.79	2.11	1.47	0.00	2.63	4.84	0.21	0.00	0.00	88.56	1.40	10.04
#11 15-25	62.51	1.20	23.95	4.35	2.90	0.18	1.63	3.27	0.00	0.00	0.00	90.46	1.76	7.78
#25 20-30	75.22	0.63	9.90	1.09	1.45	0.00	8.69	3.02	0.00	0.00	0.00	90.36	0.95	8.69
#25 34-37	72.42	1.08	12.06	1.85	1.72	0.00	9.80	1.06	0.00	0.00	0.00	90.12	1.17	8.72
#25 90-100	65.21	2.13	16.66	2.61	0.82	0.00	10.94	0.98	0.65	0.00	0.00	90.36	1.82	7.82
#26 37-42	64.92	8.36	9.08	11.09	1.34	0.00	1.60	3.34	0.13	0.00	0.13	88.94	2.30	8.76
#26 42-44	68.25	5.23	12.07	6.76	2.65	0.00	0.93	3.85	0.27	0.00	0.00	94.94	0.81	4.25
#26 44-46	67.03	9.79	10.54	7.42	1.16	0.00	1.51	2.43	0.12	0.00	0.00	89.01	1.92	9.07
#26 80-90	68.21	7.37	15.02	2.20	1.95	0.61	3.18	1.47	0.00	0.00	0.00	88.68	1.35	9.97
mean	68.66	7.77	10.17	5.63	1.95	0.37	1.82	3.83	0.21	0.03	0.01	87.62	2.39	9.99
SD	3.74	4.29	4.47	3.25	0.97	0.39	2.86	1.82	0.24	0.15	0.03	2.89	1.10	2.01

Appendix Table 2.10 Texture, composition, and mineralogy of mollusk-coral wackestone (mcW) facies

Sample no.	<125 µm [wt.%]	>2 mm [wt.%]	Mollusk [%]	Coral [%]	Foram. [%]	Echino. [%]	Halimeda [%]	Red algae [%]	Crustacean [%]	Peloid [%]	Opaque [%]	ARA [wt.%]	LMC [wt.%]	HMC [wt.%]
#16 365-370	86.03	6.85	11.32	0.00	0.98	0.47	0.00	0.00	0.65	0.05	0.51	87.62	3.70	8.68
#16 375-380	80.81	10.42	12.09	0.45	2.62	0.83	0.06	0.00	1.73	0.19	1.22	87.92	4.33	7.75
#16 385-390	83.78	5.76	11.62	0.05	1.35	1.14	0.38	0.00	1.57	0.00	0.11	81.88	3.56	9.65
#16 395-400	81.35	12.03	11.06	1.49	2.24	0.75	0.06	0.00	1.86	0.12	1.06	86.36	2.80	6.69
#16 405-410	83.02	8.44	11.94	0.00	1.02	0.51	0.06	0.00	1.02	0.00	2.43	81.91	3.24	5.65
#16 305-310	87.74	4.42	9.73	0.00	1.10	0.25	0.00	0.00	0.49	0.65	0.04	86.90	3.03	10.07
#16 315-320	87.18	5.02	9.83	0.00	1.75	0.47	0.00	0.00	0.56	0.21	0.00	87.04	2.76	10.20
#16 335-340	85.63	6.87	11.68	0.00	1.29	0.19	0.14	0.00	0.72	0.19	0.14	87.70	2.81	9.48
#34 90-100	82.52	4.48	7.31	1.27	1.32	0.86	0.00	1.68	0.56	0.00	0.00	86.58	3.39	10.03
#34 130-140	76.77	5.26	7.28	2.61	2.79	1.08	0.00	3.95	0.27	0.00	0.00	87.16	3.07	9.77
#12 19-20	79.07	0.07	6.26	10.43	1.04	0.21	0.21	2.71	0.00	0.00	0.00	91.69	2.67	5.64
#29 35-42	77.56	15.06	1.59	2.18	1.48	0.18	0.04	1.74	0.04	0.00	0.00	84.57	3.96	11.48
#18 270-275	81.15	5.53	8.73	1.33	0.80	0.07	0.40	1.73	0.27	0.00	0.00	88.21	2.13	9.66
#18 280-288	78.21	7.83	7.68	3.21	0.56	0.00	0.14	2.30	0.07	0.00	0.00	88.58	1.62	9.80
#18 310-317	81.50	10.14	4.22	1.34	0.54	0.08	0.29	1.84	0.04	0.00	0.00	88.78	1.98	9.24
#24 21-24	80.60	6.82	3.90	1.57	0.94	0.50	1.38	4.21	0.06	0.00	0.00	86.79	3.15	10.06
#24 40-50	77.18	8.10	3.90	3.09	1.54	0.51	1.03	4.56	0.07	0.00	0.00	85.87	2.68	11.45
#24 100-105	78.17	3.83	6.75	2.88	1.53	0.63	0.45	5.67	0.09	0.00	0.00	83.58	3.61	12.81
#26 30-37	80.43	0.36	6.53	6.24	2.88	0.10	2.69	0.77	0.00	0.00	0.00	89.04	1.38	9.58
#19 95-100	83.38	5.41	7.59	4.99	1.16	0.06	1.27	0.50	0.28	0.78	0.00	87.37	1.93	10.69
#19 115-120	83.67	3.59	6.97	4.24	1.09	0.05	1.74	0.54	1.25	0.44	0.00	87.65	1.54	10.80
#19 145-150	80.53	6.30	4.61	8.37	1.43	0.00	3.70	0.39	0.58	0.39	0.00	87.46	1.55	10.99
#19 195-200	81.37	5.63	5.59	7.14	1.62	0.00	2.11	0.56	1.06	0.56	0.00	90.32	1.70	7.98
#19 215-220	82.12	3.32	7.99	6.32	0.95	0.18	1.13	0.42	0.48	0.42	0.00	89.02	1.68	9.30
#19 265-270	79.66	4.32	8.47	6.03	0.95	0.07	3.12	0.47	1.22	0.00	0.00	89.68	1.26	9.06
#12 170-180	80.20	3.76	5.93	6.25	1.12	0.00	0.32	2.16	0.24	0.00	0.00	90.01	2.27	7.72
#12 190-200	82.13	2.06	7.35	3.16	1.74	0.24	0.00	3.00	0.32	0.00	0.00	90.33	2.23	7.44
#18 230-240	80.62	2.27	10.27	2.99	0.86	0.17	0.60	1.54	0.68	0.00	0.00	87.81	2.09	10.10
#125-30	79.03	0.39	10.70	6.58	1.03	0.00	0.31	1.95	0.00	0.00	0.00	90.02	1.61	8.37
mean	81.43	5.76	7.79	3.25	1.37	0.33	0.75	1.47	0.56	0.14	0.19	87.51	2.54	9.32
SD	2.84	3.43	2.86	2.89	0.61	0.34	1.02	1.58	0.54	0.23	0.53	2.33	0.85	1.67

Appendix Table 2.11 Texture, composition, and mineralogy of mollusk-coral mudstone-wackestone (mcMW) facies

Sample no.	<125 µm [wt.%]	>2 mm [wt.%]	Mollusk [%]	Coral [%]	Foram. [%]	Echino. [%]	Halimeda [%]	Red algae [%]	Crustacean [%]	Peloid [%]	Opaque [%]	ARA [wt.%]	LMC [wt.%]	HMC [wt.%]
#16 215-220	93.41	2.90	5.23	0.00	0.46	0.02	0.00	0.00	0.11	0.73	0.04	84.91	4.34	10.75
#16 295-300	92.80	2.63	5.40	0.00	0.00	0.24	0.00	0.00	0.29	0.09	0.05	85.09	2.75	12.16
#16 325-330	91.85	1.97	6.12	0.00	1.25	0.19	0.00	0.00	0.49	0.08	0.03	88.09	3.34	8.57
#16 345-350	92.91	3.31	4.40	1.11	0.52	0.31	0.17	0.00	0.54	0.05	0.00	86.82	3.22	9.96
#16 355-360	89.77	3.05	5.70	3.14	0.48	0.07	0.00	0.00	0.85	0.00	0.00	87.96	2.71	9.33
#19 5-10	91.22	0.50	2.43	3.86	0.73	0.03	1.29	0.12	0.12	0.09	0.00	87.73	1.51	10.76
#19 15-20	89.07	0.41	1.79	5.32	0.95	0.00	2.44	0.18	0.22	0.04	0.00	87.84	1.63	10.53
#19 25-30	87.83	0.77	1.99	5.76	1.46	0.12	1.87	0.32	0.32	0.28	0.04	87.47	1.83	10.71
#19 35-40	89.68	0.19	2.55	4.09	1.00	0.00	2.13	0.24	0.21	0.10	0.00	86.99	2.18	10.82
#19 45-50	88.26	0.30	2.39	5.48	1.29	0.12	1.88	0.35	0.12	0.12	0.00	86.77	1.52	11.70
#19 55-60	90.92	0.52	2.48	3.69	0.58	0.03	1.42	0.09	0.30	0.48	0.00	86.64	1.68	11.69
#19 65-70	92.16	0.29	2.48	2.90	0.71	0.00	1.05	0.18	0.24	0.00	0.00	86.80	1.52	11.67
#19 75-80	89.45	1.61	3.73	3.80	0.42	0.04	1.20	0.25	0.53	0.60	0.00	87.54	1.81	10.66
#19 85-90	88.73	0.72	2.74	4.47	1.05	0.00	1.47	0.34	0.38	0.83	0.00	86.56	1.69	11.76
#19 105-110	87.45	2.48	3.64	5.23	1.30	0.00	1.38	0.25	0.46	0.29	0.00	87.05	1.67	11.28
#19 125-130	86.72	2.60	4.56	4.69	0.89	0.00	2.70	0.13	0.04	0.27	0.00	87.14	2.18	10.68
#19 135-140	86.60	1.55	4.87	5.09	0.85	0.00	1.52	0.27	0.49	0.31	0.00	88.08	1.54	10.38
#19 155-160	86.69	2.53	5.77	4.35	1.02	0.00	1.15	0.31	0.22	0.31	0.18	88.72	1.60	9.68
#19 165-170	88.16	1.03	4.07	5.01	0.71	0.04	1.22	0.71	0.04	0.04	0.00	89.22	1.53	9.25
#19 175-180	84.63	2.81	5.38	5.89	1.33	0.26	1.64	0.61	0.26	0.00	0.00	88.71	1.48	9.81
#19 185-190	86.16	1.35	5.44	4.84	0.78	0.18	1.61	0.51	0.05	0.42	0.00	89.21	1.67	9.12
#19 205-210	87.70	1.71	4.26	4.55	0.70	0.25	1.52	0.45	0.25	0.33	0.00	89.54	1.73	8.73
#19 275-280	87.13	2.00	3.69	4.46	0.73	0.00	3.30	0.21	0.47	0.00	0.00	90.44	1.28	8.28
#19 285-290	91.01	1.79	3.57	2.13	0.84	0.06	1.50	0.30	0.54	0.00	0.06	88.81	1.99	9.20
#19 295-300	92.42	0.84	3.13	1.39	0.86	0.08	0.88	0.61	0.58	0.00	0.05	89.67	1.47	8.86
#19 305-310	93.50	0.29	1.56	1.73	0.74	0.00	1.11	0.91	0.46	0.00	0.00	89.71	1.77	8.52
#19 315-320	93.57	0.28	1.86	1.61	0.64	0.00	0.99	0.79	0.54	0.00	0.00	89.38	1.67	8.95
#34 10-20	85.71	1.23	7.78	1.57	0.85	0.52	0.26	0.91	0.85	0.33	0.00	88.13	2.13	9.74
#34 40-50	92.26	1.67	3.19	0.70	0.61	0.30	0.03	1.09	0.09	0.00	0.06	86.45	3.72	9.83
#34 60-70	91.05	1.72	4.12	1.12	0.47	0.58	0.00	0.80	0.14	0.00	0.00	86.13	2.97	10.90
#12 0-10	92.91	0.32	2.07	2.57	0.47	0.07	0.00	1.59	0.00	0.00	0.00	90.69	1.99	7.32
#12 30-40	93.23	0.09	2.50	2.20	0.77	0.03	0.00	1.10	0.07	0.00	0.00	90.71	1.85	7.44
#12 50-60	91.89	0.27	2.94	3.25	0.27	0.00	0.00	1.03	0.15	0.00	0.00	90.21	2.55	7.23
#12 70-80	89.58	1.29	4.57	2.28	0.73	0.14	0.00	1.37	0.00	0.00	0.05	90.13	1.95	7.92
#12 110-120	89.82	0.64	3.67	3.72	0.62	0.05	0.10	1.14	0.24	0.00	0.00	90.33	1.96	7.71
#12 130-140	83.82	2.48	5.55	4.86	1.03	0.00	0.00	1.85	0.41	0.00	0.00	89.93	1.68	8.39
#18 20-30	84.77	1.24	6.64	2.24	1.40	0.07	1.82	1.82	0.00	0.00	0.00	88.13	1.57	10.30
#18 60-70	93.37	1.06	2.51	0.81	0.67	0.08	0.47	0.98	0.03	0.00	0.03	87.94	2.20	9.86
#18 80-90	93.60	1.27	1.72	1.34	0.41	0.05	0.26	1.23	0.13	0.00	0.00	87.64	1.97	10.39
#18 120-130	93.09	1.16	2.42	1.01	0.72	0.09	0.32	1.21	0.00	0.00	0.00	76.48	3.20	20.32
#18 145-150	88.51	3.81	4.03	1.61	0.50	0.08	0.42	1.04	0.00	0.00	0.00	87.78	1.89	10.32
#18 170-180	92.20	1.46	3.74	0.44	0.76	0.03	0.19	1.14	0.03	0.00	0.00	87.83	1.75	10.42
#18 210-220	86.55	4.66	4.92	1.06	0.88	0.13	0.22	1.19	0.40	0.00	0.00	87.06	2.38	10.56
#18 250-260	85.39	4.11	5.67	2.57	0.26	0.10	0.47	1.21	0.21	0.00	0.00	87.92	1.70	10.37
#24 0-10	84.88	2.46	3.73	3.29	0.63	0.82	0.51	3.42	0.06	0.19	0.00	87.63	2.39	9.98
#2 70-80	87.76	1.04	6.38	0.34	1.12	0.00	2.18	1.12	0.00	0.00	0.06	88.58	2.03	9.39
mean	89.57	1.58	3.90	2.86	0.79	0.11	0.93	0.73	0.26	0.14	0.01	87.88	2.07	10.05
SD	2.95	1.12	1.52	1.78	0.29	0.17	0.86	0.65	0.22	0.21	0.03	2.23	0.66	1.99

Appendix Table 2.12 Texture, composition, and mineralogy of mollusk mudstone (mM) facies

Sample no.	<125 µm [wt.%]	>2 mm [wt.%]	Mollusk [%]	Coral [%]	Foram. [%]	Echino. [%]	Halimeda [%]	Red algae [%]	Crustacean [%]	Peloid [%]	Opaque [%]	ARA [wt.%]	LMC [wt.%]	HMC [wt.%]
#16 5-10	97.81	0.03	1.68	0.00	0.03	0.06	0.00	0.00	0.01	0.40	0.01	85.46	3.42	11.12
#16 15-20	97.62	0.28	1.51	0.00	0.01	0.04	0.00	0.00	0.02	0.80	0.00	86.15	2.95	10.90
#16 25-30	98.6	0.19	1.24	0.00	0.02	0.01	0.01	0.00	0.02	0.09	0.00	84.89	3.31	11.80
#16 35-40	97.02	1.31	2.27	0.01	0.06	0.06	0.00	0.00	0.02	0.56	0.00	84.65	3.47	11.89
#16 45-50	97.45	1.13	1.96	0.00	0.16	0.05	0.01	0.00	0.00	0.37	0.00	84.64	3.44	11.92
#16 55-60	97.36	0.47	2.03	0.00	0.18	0.02	0.00	0.00	0.00	0.41	0.00	84.19	3.59	12.22
#16 65-70	96.98	0.34	2.20	0.00	0.20	0.02	0.00	0.00	0.01	0.58	0.00	84.58	3.22	12.20
#16 75-80	97.41	0.42	1.85	0.00	0.29	0.11	0.00	0.00	0.00	0.43	0.00	83.98	4.82	11.21
#16 85-90	96.89	0.59	2.46	0.00	0.32	0.11	0.00	0.00	0.00	0.22	0.00	84.67	3.20	12.13
#16 95-100	96.33	1.59	2.61	0.00	0.75	0.01	0.00	0.00	0.00	0.31	0.00	84.32	3.42	12.26
#16 105-110	97.49	0.65	2.05	0.00	0.28	0.03	0.00	0.00	0.02	0.13	0.00	84.81	3.36	11.83
#16 115-120	97.79	0.45	1.77	0.00	0.31	0.03	0.00	0.00	0.00	0.10	0.00	84.63	3.61	11.76
#16 125-130	97.56	0.54	1.98	0.00	0.32	0.02	0.00	0.00	0.00	0.12	0.00	84.92	3.32	11.76
#16 135-140	97.3	0.37	2.24	0.00	0.27	0.03	0.00	0.00	0.00	0.15	0.01	84.82	3.50	11.68
#16 145-150	97.16	0.95	2.40	0.00	0.22	0.07	0.00	0.00	0.00	0.15	0.00	84.38	4.30	11.32
#16 155-160	95.7	1.52	3.51	0.00	0.50	0.07	0.00	0.00	0.01	0.20	0.00	85.25	3.32	11.43
#16 165-170	95.13	1.86	3.93	0.00	0.37	0.05	0.00	0.03	0.06	0.42	0.00	84.61	3.41	11.98
#16 175-180	95.76	1.22	3.35	0.00	0.37	0.04	0.00	0.00	0.06	0.42	0.00	84.93	3.67	11.40
#16 185-190	96.98	0.99	2.57	0.00	0.26	0.03	0.00	0.00	0.03	0.12	0.00	86.50	3.15	10.35
#16 195-200	95.41	1.11	3.84	0.00	0.28	0.00	0.00	0.00	0.03	0.44	0.00	85.63	3.01	11.36
#16 205-210	96.76	0.88	2.60	0.00	0.40	0.00	0.00	0.00	0.00	0.24	0.00	85.06	3.44	11.50
#16 225-230	95.19	1.70	3.81	0.00	0.40	0.02	0.00	0.00	0.06	0.46	0.05	85.66	3.11	11.23
#16 235-240	96.8	0.50	2.50	0.00	0.31	0.05	0.00	0.00	0.14	0.20	0.00	85.50	3.47	11.04
#16 245-250	96.73	1.09	2.38	0.00	0.54	0.07	0.00	0.00	0.01	0.21	0.05	85.60	3.41	10.99
#16 255-260	96.01	1.10	3.16	0.00	0.31	0.19	0.00	0.00	0.01	0.25	0.07	85.98	3.78	10.25
#16 265-270	96.21	0.95	2.84	0.00	0.35	0.20	0.00	0.00	0.00	0.33	0.06	85.34	3.31	11.35
#16 275-280	95.6	0.96	3.58	0.00	0.29	0.16	0.00	0.00	0.26	0.09	0.01	85.16	3.77	11.08
#16 285-290	96.01	0.75	3.10	0.00	0.52	0.12	0.00	0.00	0.05	0.16	0.04	84.51	3.40	12.09
#19 325-328	98.91	0.02	1.97	0.28	0.19	0.01	0.18	0.09	0.06	0.00	0.00	88.31	1.88	9.81
#18 0-10	95.44	0.03	1.97	0.50	0.68	0.09	0.54	0.68	0.07	0.00	0.00	88.38	1.47	10.15
mean	96.78	0.80	2.46	0.03	0.31	0.06	0.02	0.03	0.03	0.28	0.01	85.25	3.35	11.40
SD	0.98	0.51	0.83	0.10	0.17	0.05	0.10	0.12	0.05	0.19	0.02	1.03	0.58	0.64

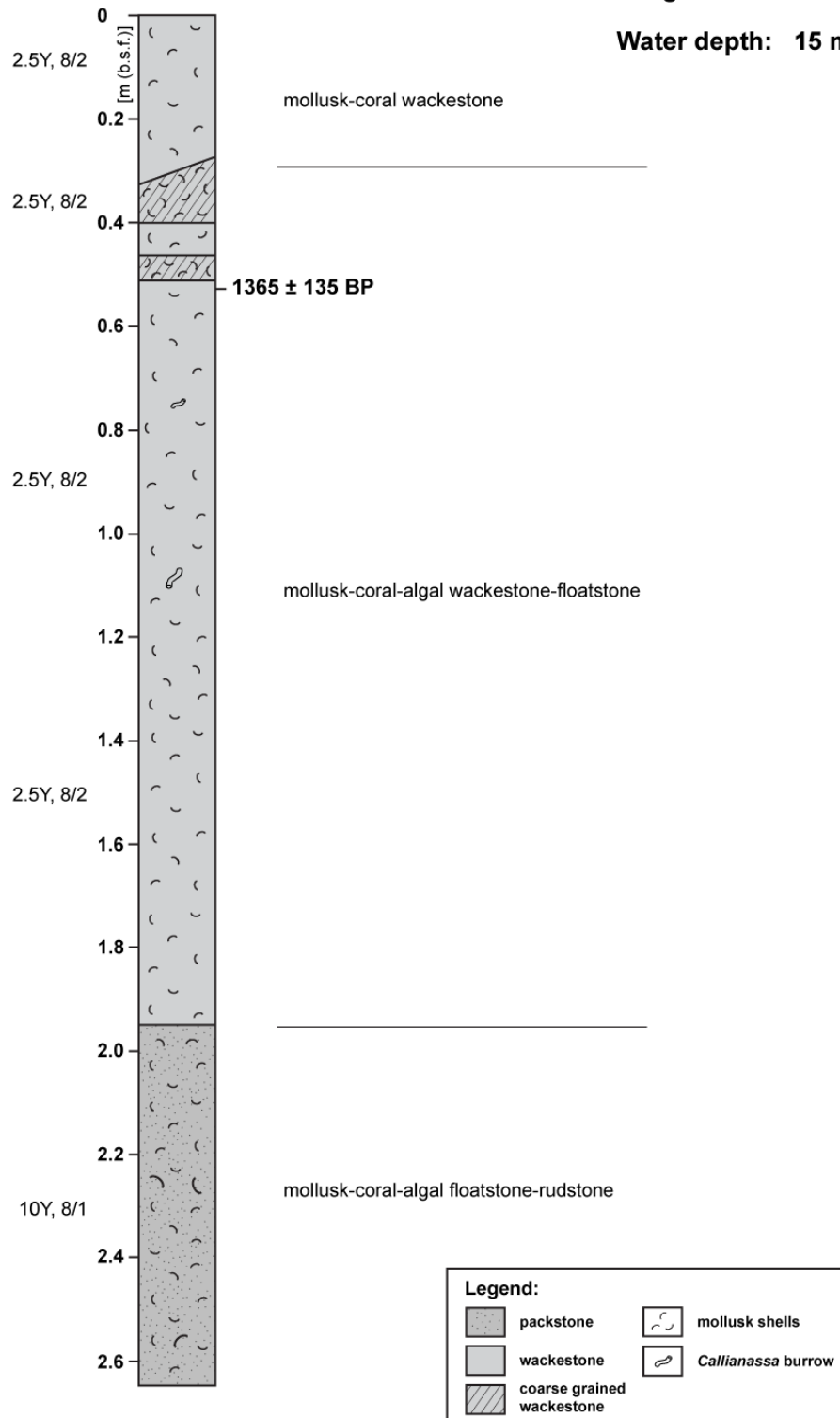
Appendix 4.2 Core #19 species data

Species	0-5	10-15	20-25	30-35	40-45	50-55	60-65	70-75	80-85	90-95	100-105	110-115	120-125	130-135	140-145	150-155	160-165	170-175	180-185	190-195	200-205	210-215	220-225	230-235	240-245	250-255	260-265	270-275	280-285	290-295	300-305	310-315	320-325	Grand Total	Structure			
<i>Eigeneria</i> sp. 1	0	0	0	0	0	0	0	0	0	0	0	0	0	0	0	0	0	0	0	0	0	0	0	0	0	0	0	0	0	0	0	0	0	0	1 agglutinated			
<i>Textularia candelina</i>	0	0	0	0	0	0	0	0	0	0	0	0	0	0	0	0	0	0	0	0	0	0	0	0	0	0	0	0	0	0	0	0	0	0	1 agglutinated			
<i>Textularia</i> cf. <i>Q. keribaensis</i>	0	0	0	0	0	0	0	0	0	0	0	0	0	0	0	0	0	0	0	0	0	0	0	0	0	0	0	0	0	0	0	0	0	0	1 agglutinated			
<i>Textularia</i> cf. <i>T. cushmani</i>	0	0	0	0	0	0	0	0	0	0	0	0	0	0	0	0	0	0	0	0	0	0	0	0	0	0	0	0	0	0	0	0	0	0	1 agglutinated			
<i>Textularia crenata</i>	0	0	0	0	0	0	0	0	0	0	0	0	0	0	0	0	0	0	0	0	0	0	0	0	0	0	0	0	0	0	0	0	0	0	5 agglutinated			
<i>Textularia foliacea</i>	0	1	0	0	1	2	1	0	0	1	2	0	2	2	2	2	1	0	0	1	0	0	0	0	0	0	0	0	0	0	0	0	0	0	0	25 agglutinated		
<i>Textularia</i> sp. 1	0	0	0	1	0	0	0	0	0	1	3	0	2	0	0	0	0	0	0	0	0	0	0	0	0	0	0	0	0	0	0	0	0	0	18 agglutinated			
<i>Abdodentrix</i> sp. 1	0	1	2	3	2	3	3	1	2	3	2	2	3	4	3	1	3	7	6	4	8	11	6	8	4	16	15	9	18	11	9	13	11	196	hyaline			
<i>Ammonia convexa</i>	60	44	55	46	57	59	50	41	43	57	58	44	35	24	28	27	32	32	16	25	22	25	24	18	26	13	17	12	14	24	14	28	1094	hyaline				
<i>Ammonia</i> sp. 1	25	13	19	18	19	25	18	14	13	19	18	29	19	19	21	29	37	28	27	27	42	41	37	31	51	56	83	127	128	126	126	120	114	1519	hyaline			
<i>Amphistegina lessona</i>	0	0	1	0	0	1	0	0	1	1	0	0	1	3	2	0	0	0	0	0	0	0	0	0	0	0	0	0	0	0	0	0	0	0	23	hyaline		
<i>Amphistegina lobifera</i>	0	0	0	0	0	0	0	0	0	0	0	0	0	0	0	0	0	0	0	0	0	0	0	0	0	0	0	0	0	0	0	0	0	0	9	hyaline		
<i>Amphistegina papillosa</i>	0	0	0	0	0	0	0	0	0	0	0	0	0	0	0	0	0	0	0	0	0	0	0	0	0	0	0	0	0	0	0	0	0	0	5	hyaline		
<i>Amphistegina radiata</i>	0	0	0	0	0	0	0	0	0	0	0	0	0	0	0	0	0	0	0	0	0	0	0	0	0	0	0	0	0	0	0	0	0	0	0	5	hyaline	
<i>Amphistegina</i> sp. 1	1	1	2	0	0	1	2	0	0	1	3	0	2	0	0	0	0	0	0	0	0	0	0	0	0	0	0	0	0	0	0	0	0	0	0	32	hyaline	
<i>Anomalina</i> sp. 1	0	0	0	0	0	0	0	0	0	0	0	0	0	0	0	0	0	0	0	0	0	0	0	0	0	0	0	0	0	0	0	0	0	0	0	4	hyaline	
<i>Anomalina</i> sp. 2	0	0	0	0	0	0	0	0	0	0	0	0	0	0	0	0	0	0	0	0	0	0	0	0	0	0	0	0	0	0	0	0	0	0	0	1	hyaline	
<i>Asanonella tubifera</i>	0	0	0	0	0	0	0	0	0	0	0	0	0	0	0	0	0	0	0	0	0	0	0	0	0	0	0	0	0	0	0	0	0	0	0	1	hyaline	
<i>Bolivina striatula</i>	0	0	0	0	0	0	0	0	0	0	0	0	0	0	0	0	0	0	0	0	0	0	0	0	0	0	0	0	0	0	0	0	0	0	0	2	hyaline	
<i>Calcarina</i> sp. 1	0	0	0	0	0	0	0	0	0	0	0	0	0	0	0	0	0	0	0	0	0	0	0	0	0	0	0	0	0	0	0	0	0	0	0	2	hyaline	
<i>Caribbeanella</i> sp. 1	0	0	0	0	0	0	0	0	0	0	0	0	0	0	0	0	0	0	0	0	0	0	0	0	0	0	0	0	0	0	0	0	0	0	0	2	hyaline	
<i>Cibicides</i> cf. <i>C. lobatus</i>	0	0	0	0	0	0	0	0	0	0	0	0	0	0	0	0	0	0	0	0	0	0	0	0	0	0	0	0	0	0	0	0	0	0	0	0	3	hyaline
<i>Cibicides</i> sp. 2	0	0	0	0	0	0	0	0	0	0	0	0	0	0	0	0	0	0	0	0	0	0	0	0	0	0	0	0	0	0	0	0	0	0	0	0	4	hyaline
<i>Cibicides</i> sp. 3	0	0	0	0	0	0	0	0	0	0	0	0	0	0	0	0	0	0	0	0	0	0	0	0	0	0	0	0	0	0	0	0	0	0	0	0	4	hyaline
<i>Cibicides</i> cf. <i>basilianensis</i>	0	0	0	0	0	0	0	0	0	0	0	0	0	0	0	0	0	0	0	0	0	0	0	0	0	0	0	0	0	0	0	0	0	0	0	0	10	hyaline
<i>Cibicides</i> sp. 1	1	0	0	0	0	1	0	0	0	2	0	0	0	0	0	0	0	0	0	0	0	0	0	0	0	0	0	0	0	0	0	0	0	0	0	0	6	hyaline
<i>Cibicides</i> sp. 2	0	0	0	0	0	0	0	0	0	0	0	0	0	0	0	0	0	0	0	0	0	0	0	0	0	0	0	0	0	0	0	0	0	0	0	0	6	hyaline
<i>Cibicides</i> sp. 3	0	1	1	0	0	0	0	0	0	0	0	0	0	0	0	0	0	0	0	0	0	0	0	0	0	0	0	0	0	0	0	0	0	0	0	0	4	hyaline
<i>Cibicides</i> sp. 5	2	1	1	0	1	3	0	1	0	1	1	1	0	3	0	0	0	0	0	0	0	0	0	0	0	0	0	0	0	0	0	0	0	0	0	0	8	hyaline
<i>Cymbaloporella tabelliformis</i>	1	0	1	2	0	3	1	0	0	0	0	1	3	1	0	0	0	0	0	0	0	0	0	0	0	0	0	0	0	0	0	0	0	0	0	0	19	hyaline
<i>Cymbaloporella bradyi</i>	11	6	6	2	10	8	10	3	11	7	7	6	5	5	8	2	8	4	8	4	8	5	7	6	4	6	2	3	1	2	4	0	0	0	183	hyaline		
<i>Cymbaloporella</i> sp. 1	4	2	0	0	1	0	0	0	0	0	0	0	0	0	0	0	0	0	0	0	0	0	0	0	0	0	0	0	0	0	0	0	0	0	0	12	hyaline	
<i>Cymbaloporella squamosa</i>	0	0	0	0	0	0	0	0	0	0	0	0	0	0	0	0	0	0	0	0	0	0	0	0	0	0	0	0	0	0	0	0	0	0	0	34	hyaline	
<i>Discorbina</i> cf. <i>bertheloti</i>	1	0	0	0	0	0	0	0	0	0	0	0	0	0	0	0	0	0	0	0	0	0	0	0	0	0	0	0	0	0	0	0	0	0	0	7	hyaline	
<i>Elphidium batavum</i>	0	0	0	0	0	0	0	0	0	0	0	0	0	0	0	0	0	0	0	0	0	0	0	0	0	0	0	0	0	0	0	0	0	0	0	4	hyaline	
<i>Elphidium</i> cf. <i>E. advenum</i>	0	0	0	0	0	0	0	0	0	0	0	0	0	0	0	0	0	0	0	0	0	0	0	0	0	0	0	0	0	0	0	0	0	0	0	7	hyaline	
<i>Elphidium</i> cf. <i>E. jensenii</i>	0	0	0	0	0	0	0	0	0	0	0	0	0	0	0	0	0	0	0	0	0	0	0	0	0	0	0	0	0	0	0	0	0	0	0	5	hyaline	
<i>Elphidium craticulatum</i>	0	0	0	0	0	0	0	0	0	0	0	0	0	0	0	0	0	0	0	0	0	0	0	0	0	0	0	0	0	0	0	0	0	0	0	3	hyaline	
<i>Elphidium crispum</i>	0	0	0	0	0	0	0	0	0	0	0	0	0	0	0	0	0	0	0	0	0	0	0	0	0	0	0	0	0	0	0	0	0	0	0	0	3	hyaline
<i>Elphidium</i> sp. 1	3	3	0	3	2	4	1	0	0	5	1	3	1	2	2	1	1	1	3	0	0	0	0	0	0	0	0	0	0	0	0	0	0	0	0	0	26	hyaline
<i>Elphidium</i> sp. 2	1	1	0	0	0	1	0	0	0	1	0	1	0	1	0	0	0	0	0	0	0	0	0	0	0	0	0	0	0	0	0	0	0	0	0	0	75	hyaline
<i>Elphidium</i> sp. 3	0	0	0	0	0	0	0	0	0	0	0	0	0	0	0	0	0	0	0	0	0	0	0	0	0	0	0	0	0	0	0	0	0	0	0	9	hyaline	
<i>Elphidium</i> sp. 4	0	0	0	0	0	0	0	0	0	0	0	0	0	0	0	0	0	0	0	0	0	0	0	0	0	0	0	0	0	0	0	0	0	0	0	2	hyaline	
<i>Elphidium</i> sp. 5	0	0	0	0	0	0	0	0	0	0	0	0	0	0	0	0	0	0	0	0	0	0	0	0	0	0	0	0	0	0	0	0	0	0	0	8	hyaline	
<i>Elphidium</i> sp. 6	0	0	0	0	0	0	0	0	0	0	0	0	0	0	0	0	0	0	0	0	0	0	0	0	0	0	0	0	0	0	0	0	0	0	0	10	hyaline	
<i>Elphidium</i> sp. 7	0	0	0	0	0	0	0	0	0	0	0	0	0	0	0	0	0	0	0	0	0	0	0	0	0	0	0	0	0	0	0	0	0	0	0	9	hyaline	
<i>Elphidium</i> sp. 8	3	0	0	0	0	0	0	0	0	0	0	0	0	0	0	0	0	0	0	0	0	0	0	0	0	0	0	0	0	0	0	0	0	0	0	10	hyaline	
<i>Elphidium</i> sp. 9	0	0																																				

Core log #1

Length: 2.65 m

Water depth: 15 m

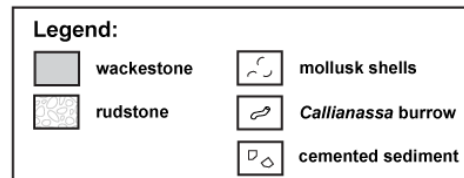
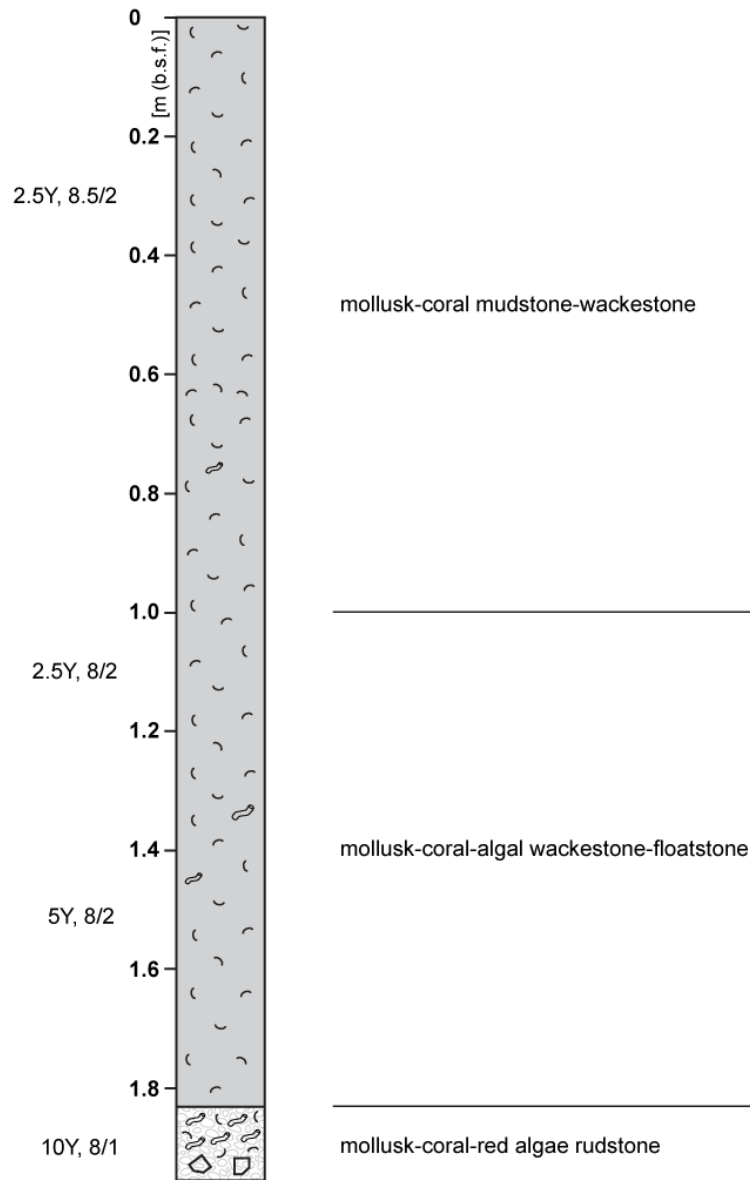


Core log #1: Core #1 starts with a packstone unit. The rest of the core is classified as wackestone with two visually coarser layers between 50 and 30 cm. The color of the packstone unit is light greenish gray (GLE Y1, 10Y, 8/1), the wackestone unit is pale yellow (WHITE, 2.5Y, 8/2).

Core log #2

Length: 1.95 m

Water depth: 10.7 m

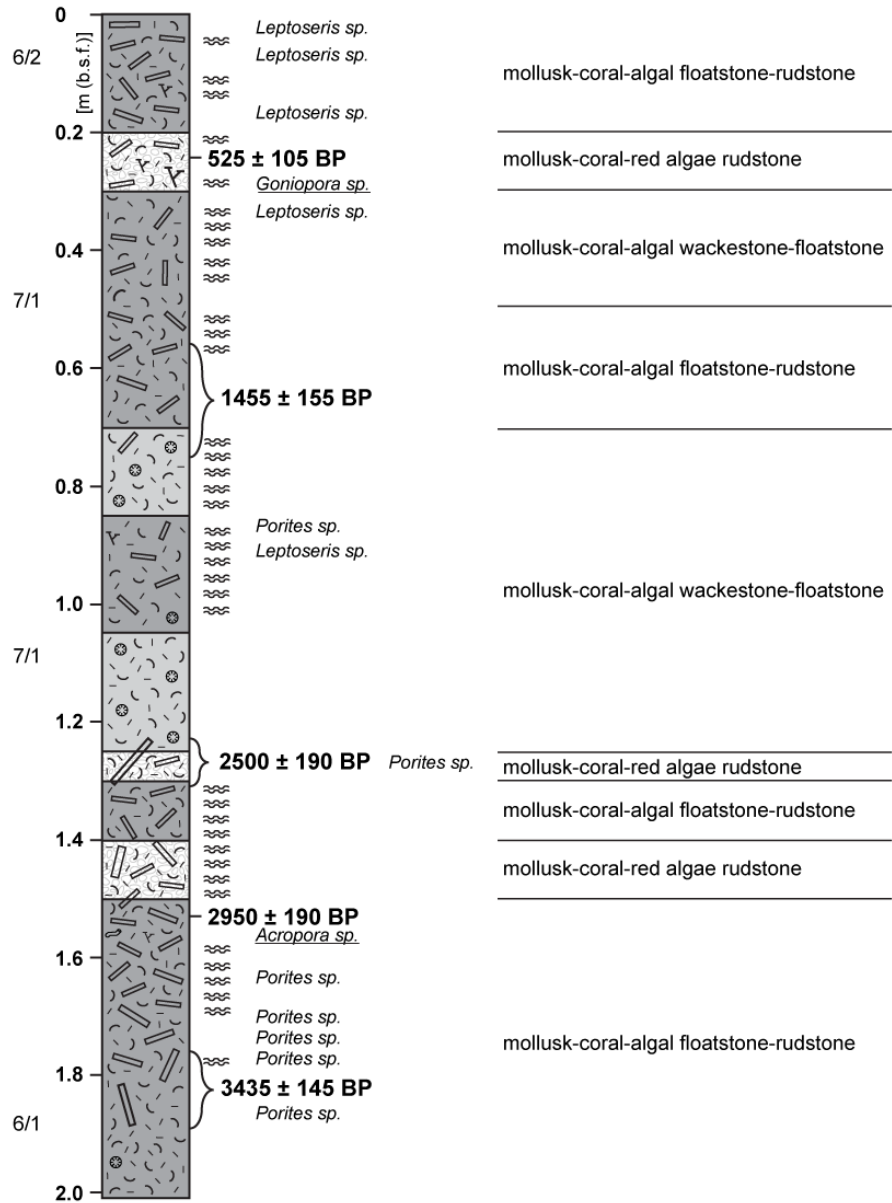


Core log #2: At the base of core #2 cemented sediment clasts occurs. The color of the rudstone unit is light greenish gray (GLE Y1, 10Y, 8/1). The core becomes lighter towards the top with colors of pale yellow (WHITE, 5Y, 8/2 - 2.5Y, 8.5/2).

Core log #8

Length: 2.01 m

Water depth: 36.8 m



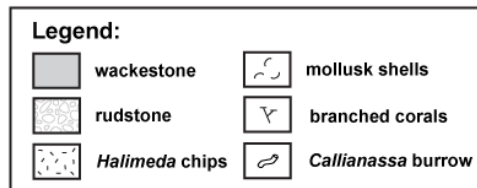
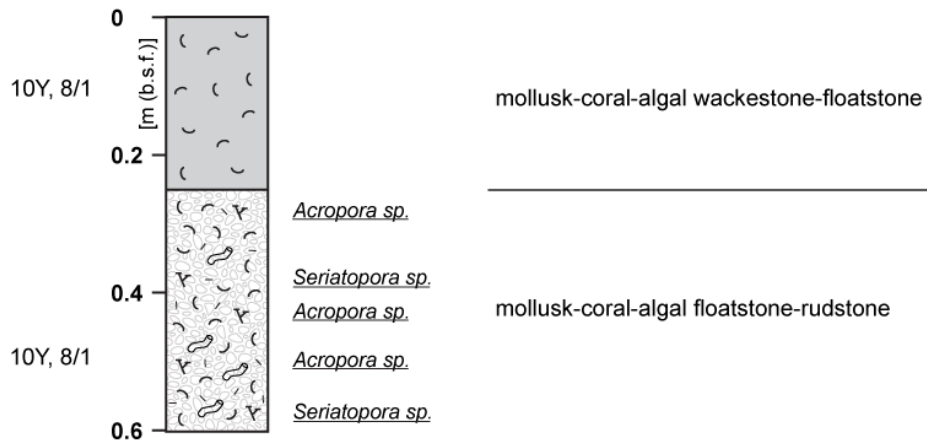
Legend:

Core log #8: Generally coarse grained core, floatstone is alternating with wacke- and rudstone. The colors range from greenish gray (GLEY1, 10Y, 6/1) over light greenish gray (GLEY1, 10Y, 7/1) to light grayish olive (10Y, 6/2). Underlined coral ID marks redeposition.

Core log #11

Length: 0.6 m

Water depth: 18 m

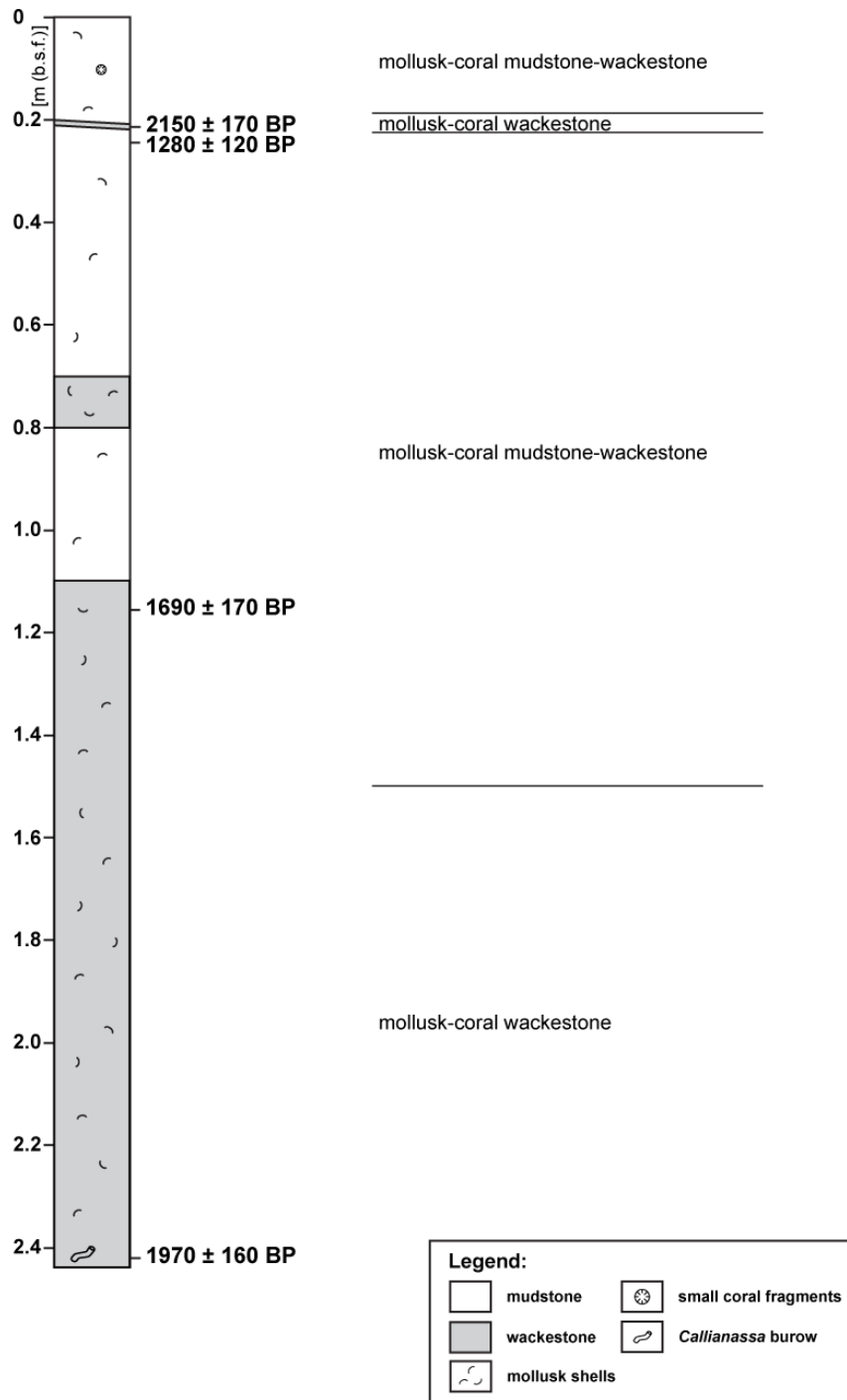


Core log #11: Core #11 is a very short core with a rudstone unit composed of shallow water corals, mollusk shells, Halimeda chips and *Callianassa* burrows, and a wackestone unit mainly composed of mollusk shells. The color of the rudstone and wackestone unit is light greenish gray (GLE Y1, 10Y, 8/1). Underlined coral ID marks redeposition.

Core log # 12

Length: 2.44 m

Water depth: 20 m

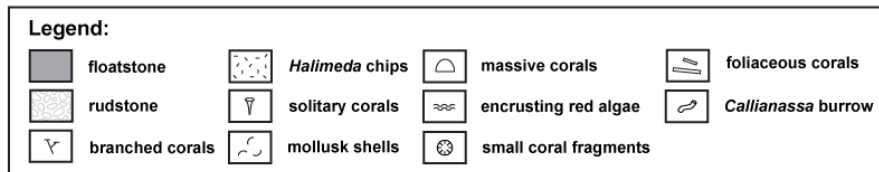
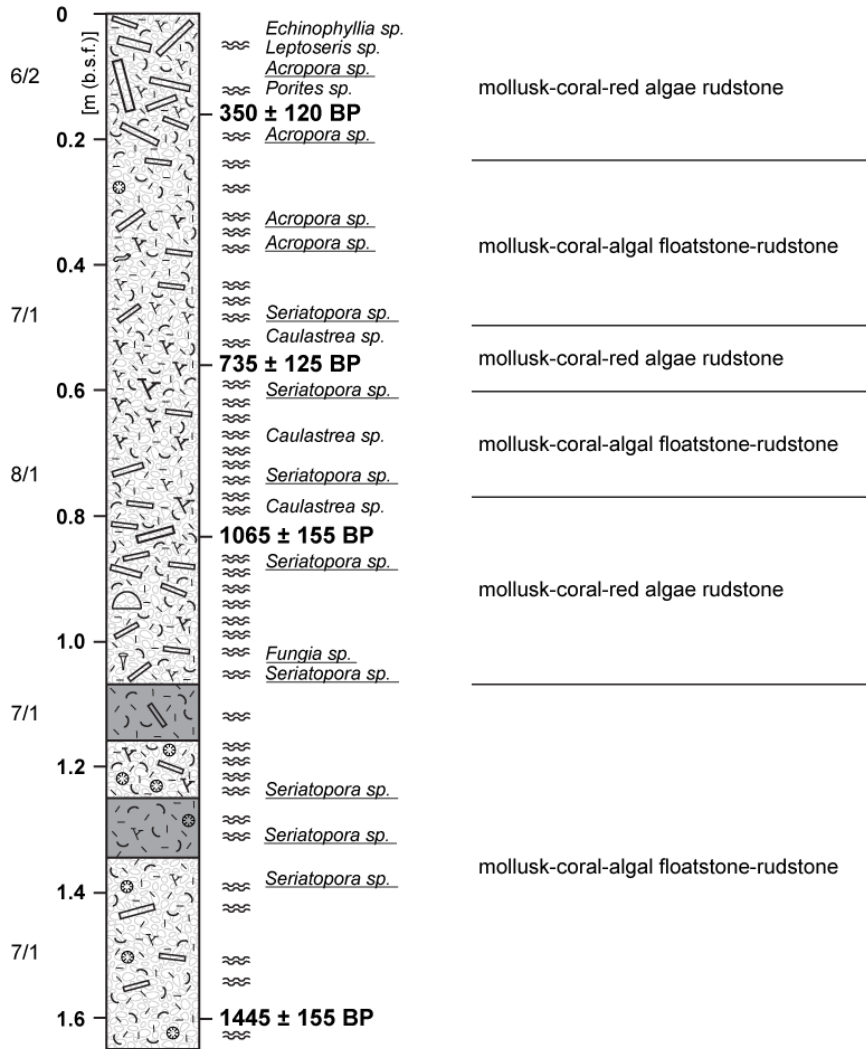


Core log #12: Generally fine grained core (mudstone, wackestone) including some shell fragments. The color of the whole core is white (5Y, 8/1). The coarser layer around 20 cm marks a sedimentary event.

Core log #13

Length: 1.65 m

Water depth: 29.5 m

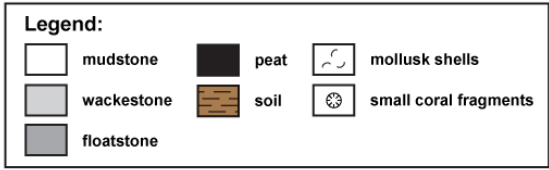
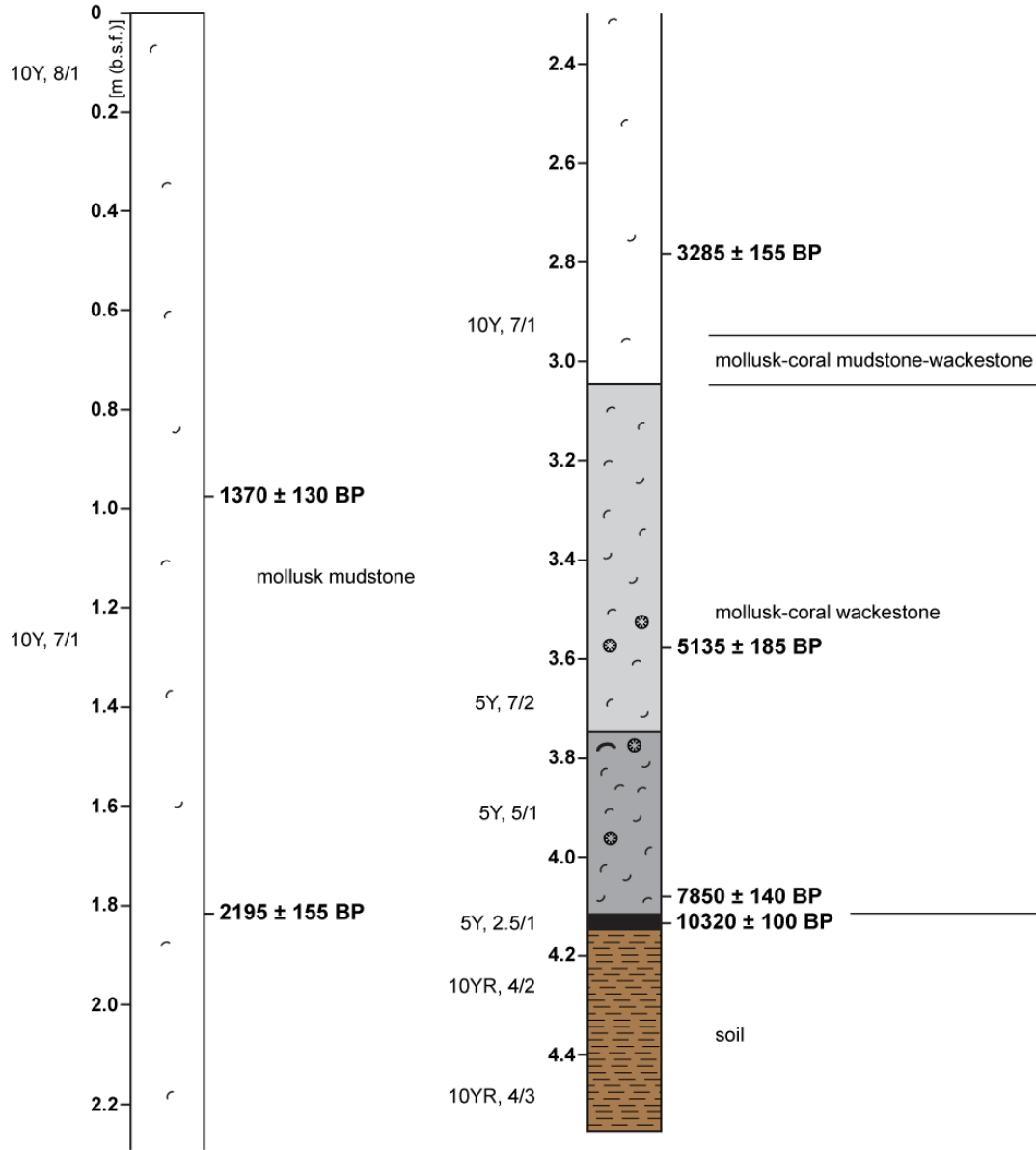


Core log #13: Core #13 contains coarse and muddy sediment including different species of coral fragments. Halimeda chips interspersed throughout the whole core. The color ranges from light greenish gray (GLE Y1, 10Y, 7/1 - 8/1) to light grayish olive (10Y, 6/2) towards the top. Underlined coral ID marks redeposition.

Core log #16

Length: 4.56 m

Water depth: 34.5 m

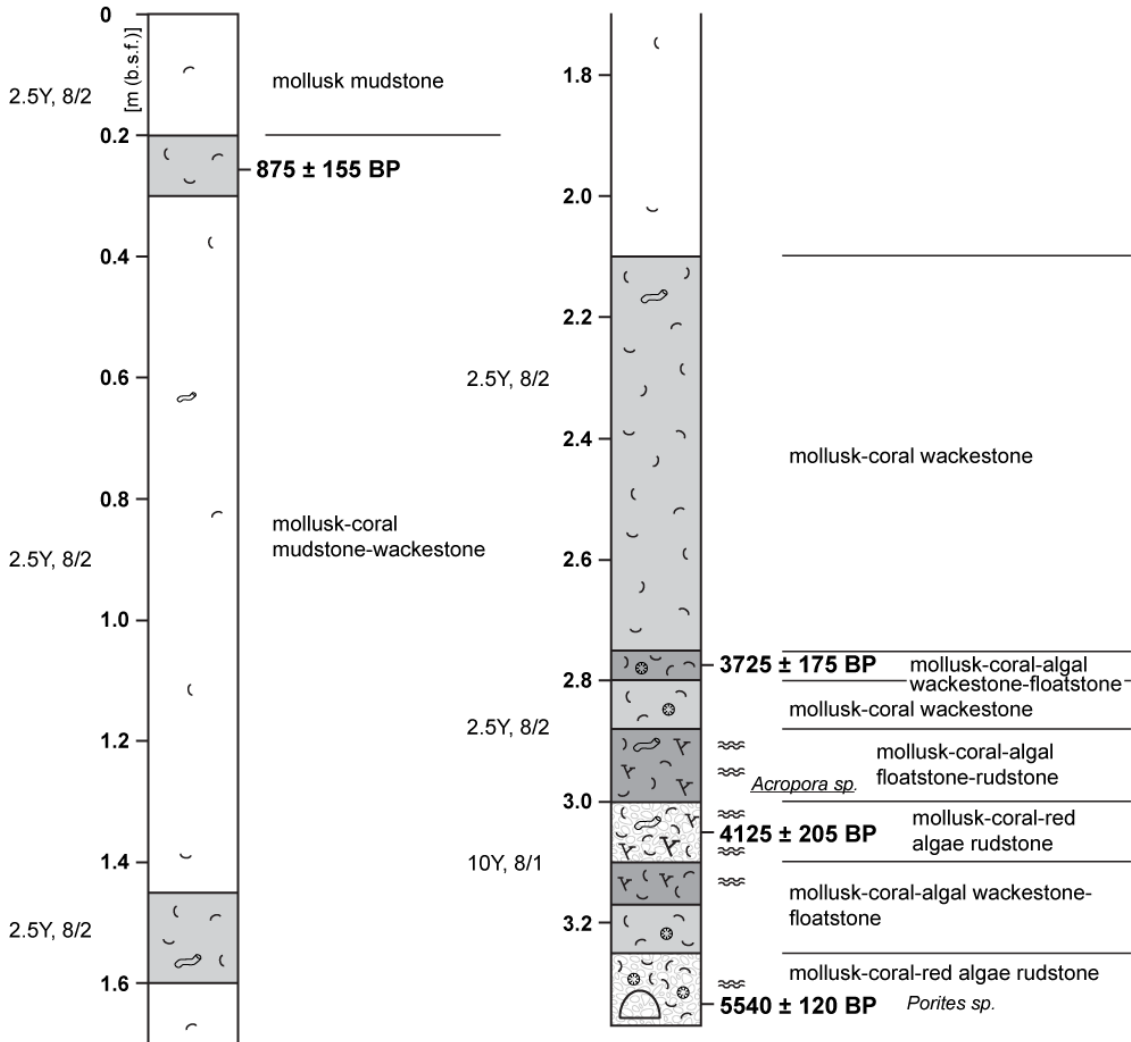


Core log #16: Core #16 is composed of 6 units, with two significant units at the base. The sharp contact of the 3 cm thick layer of peat to the gray lagoon sediment marks the beginning of the marine sedimentation. The color of the core varies at the base from brown (10YR, 4/3) over black (5Y, 2.5/1) to gray (5Y, 5/1). The marine sediment color becomes lighter towards the top, starting with gray (5Y, 5/1) above the peat, over light gray (5Y, 7/2) to light greenish gray (GLE1, 10Y, 7/1 - 8/1).

Core log #18

Length: 3.37 m

Water depth: 14.3 m

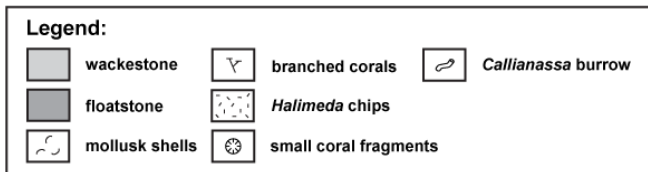
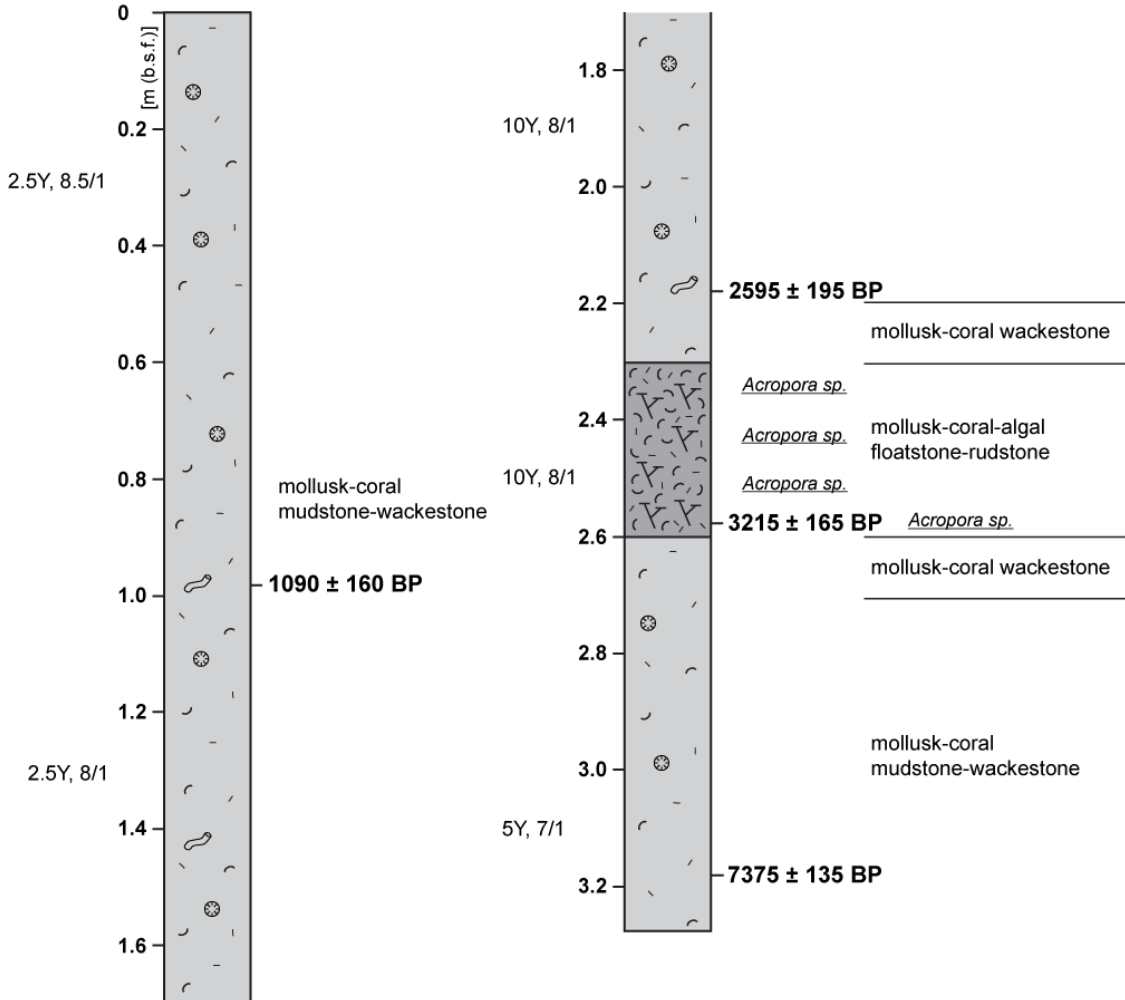


Core log #18: Core #18 starts with alternating coarser and finer units consisting of mollusk shells and in-crusting coral fragments. Mollusk shells are dominant throughout the whole core. At the base, the color is light greenish gray (GLE Y1, 10Y, 8/1). Towards the top, the core becomes finer and white in color (WHITE, 2.5Y, 8/2). Underlined coral ID marks redeposition.

Core log #19

Length: 3.28 m

Water depth: 13.6 m

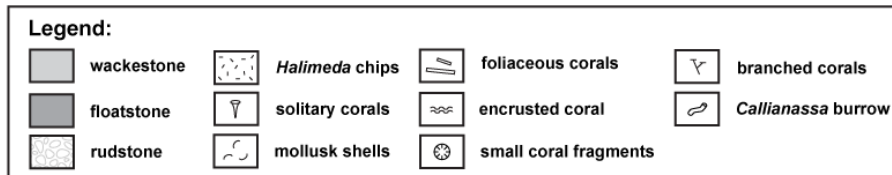
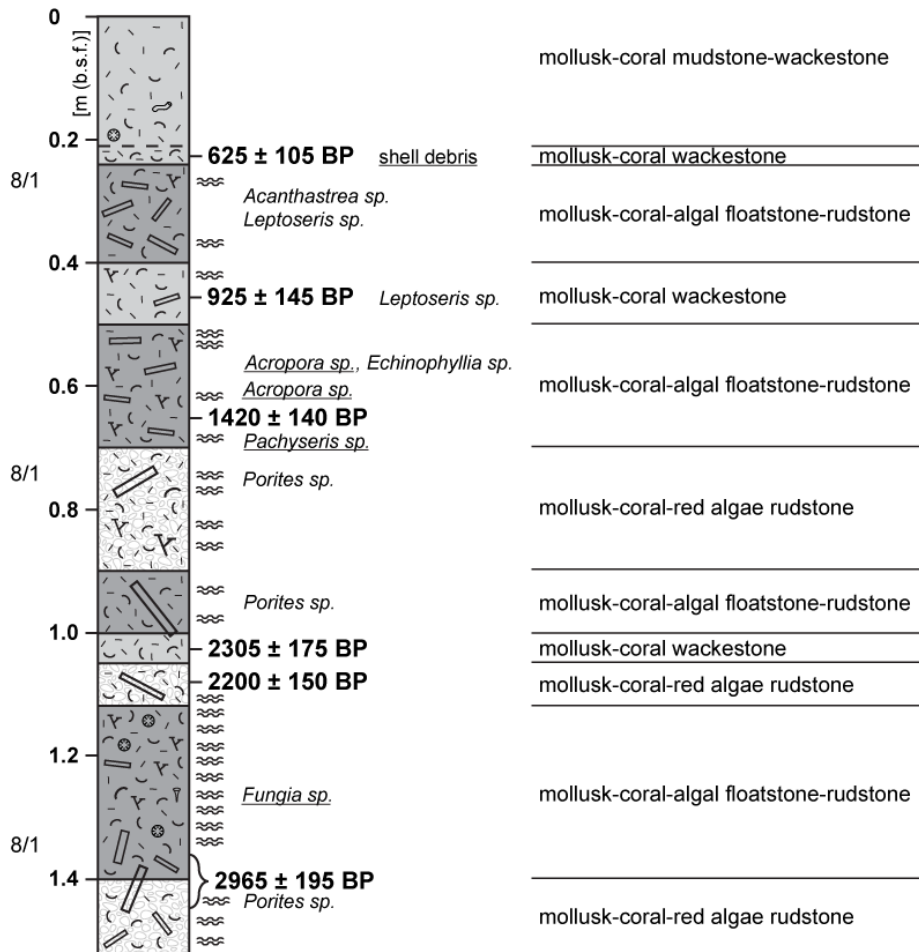


Core log #19: Core #19 is relatively uniform in color and components. Two of the four units mainly consist of coral fragments, mollusk shells, *Halimeda* and some foraminifera. Unit two and three are significantly coarser, with large branches of *Acropora sp.* and mollusk shells. Generally, the color becomes lighter towards the top, ranging from light gray (5Y, 7/1) over light greenish gray (GLE Y1, 10Y, 8/1) to white (WHITE, 2.5Y, 8/1 - 8.5/1). Underlined coral ID marks redeposition.

Core log #24

Length: 1.52 m

Water depth: 28.5 m

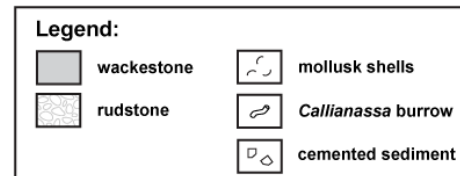
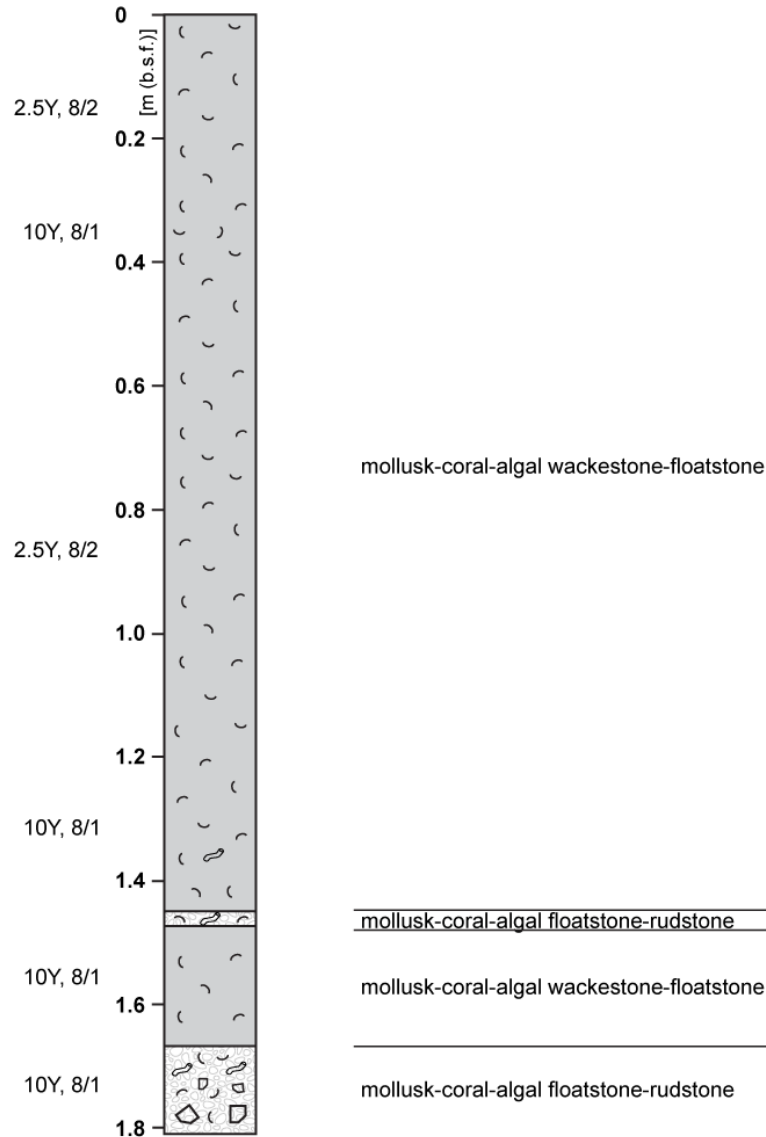


Core log #24: Generally coarse grained core with a consistent color of light greenish gray (GLE1, 10Y, 8/1). Mollusk floatstone is alternating with mollusk wacke- and rudstone. The amount of *Halimeda* chips is increasing at the base up to 105 cm within the core and stays relative stable towards the top. Underlined coral ID marks redeposition.

Core log #25

Length: 1.81 m

Water depth: 11.7 m

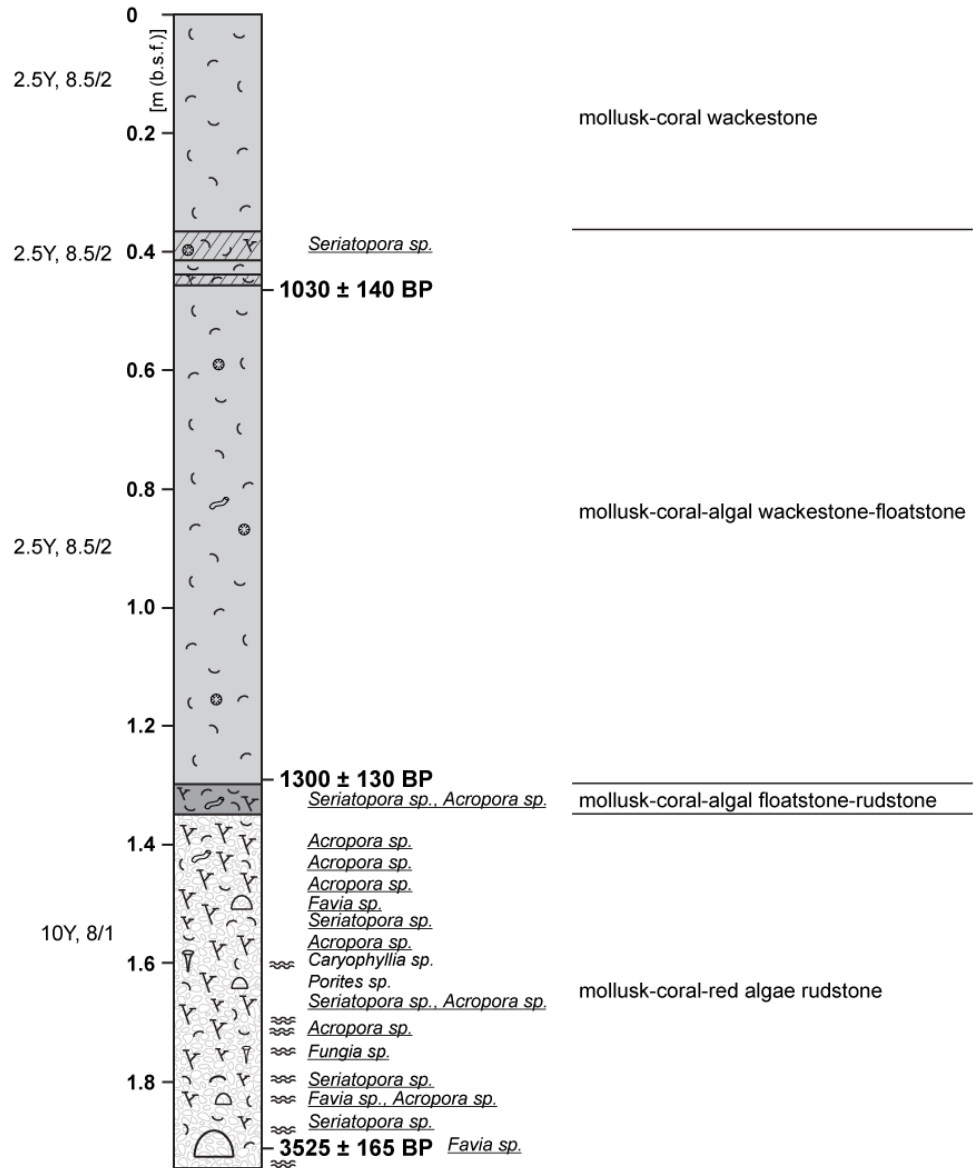


Core log #25: At the base of core #25 cemented sediment clasts occur within a rudstone unit, similar to core #2. The rest of the core is classified as a wackestone with a small rudstone layer around 145 cm. The color of the rudstone unit is light greenish gray (GLE Y1, 10Y, 8/1) and the wackestone unit becomes lighter towards the top to pale yellow (WHITE 2.5Y, 8.5/2).

Core log #26

Length: 1.95 m

Water depth: 12.6 m



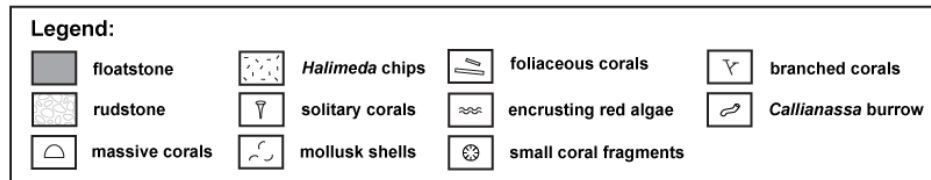
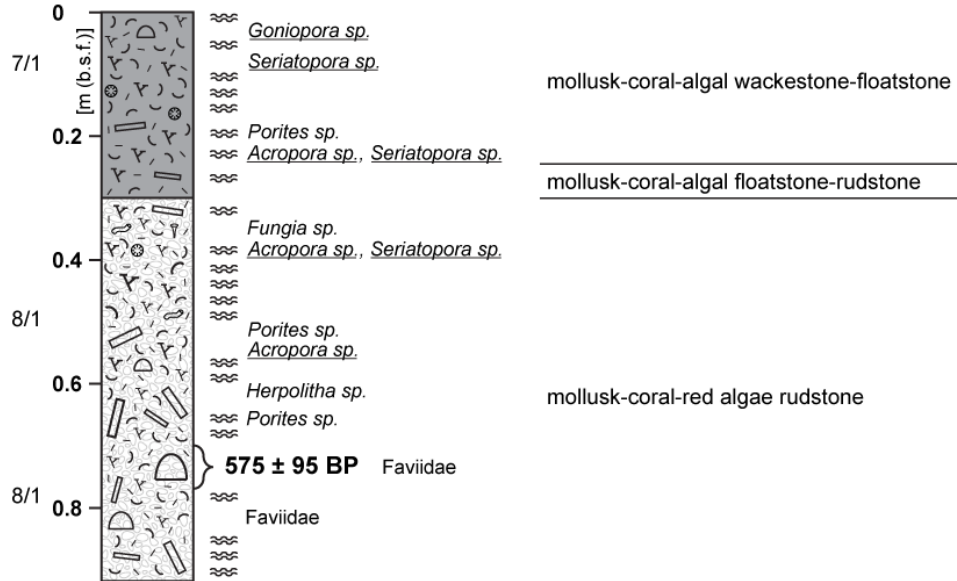
Legend:			
	wackestone		rudstone
	coarse grained wackestone		massive corals
	floatstone		Callianassa burrow
	mollusk shells		branched corals
	small coral fragments		encrusting red algae
			solitary corals

Core log #26: Core #26 is composed of a coral rich rudstone to floatstone unit and a wackestone unit. Two slightly coarser layers around 40 cm marks a possible sedimentary event. The color of the rudstone unit is light greenish gray (GLE Y1, 10Y, 8/1) and the wackestone unit is pale yellow (WHITE 2.5Y, 8.5/2). Underlined coral ID marks redeposition.

Core log #27

Length: 0.92 m

Water depth: 21.6 m

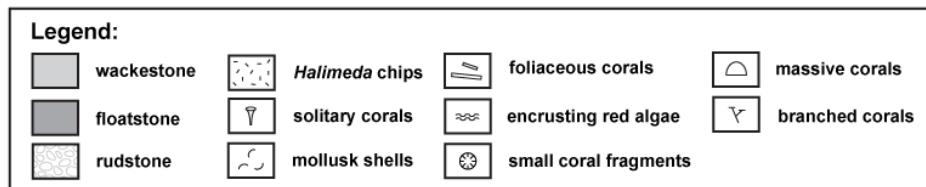
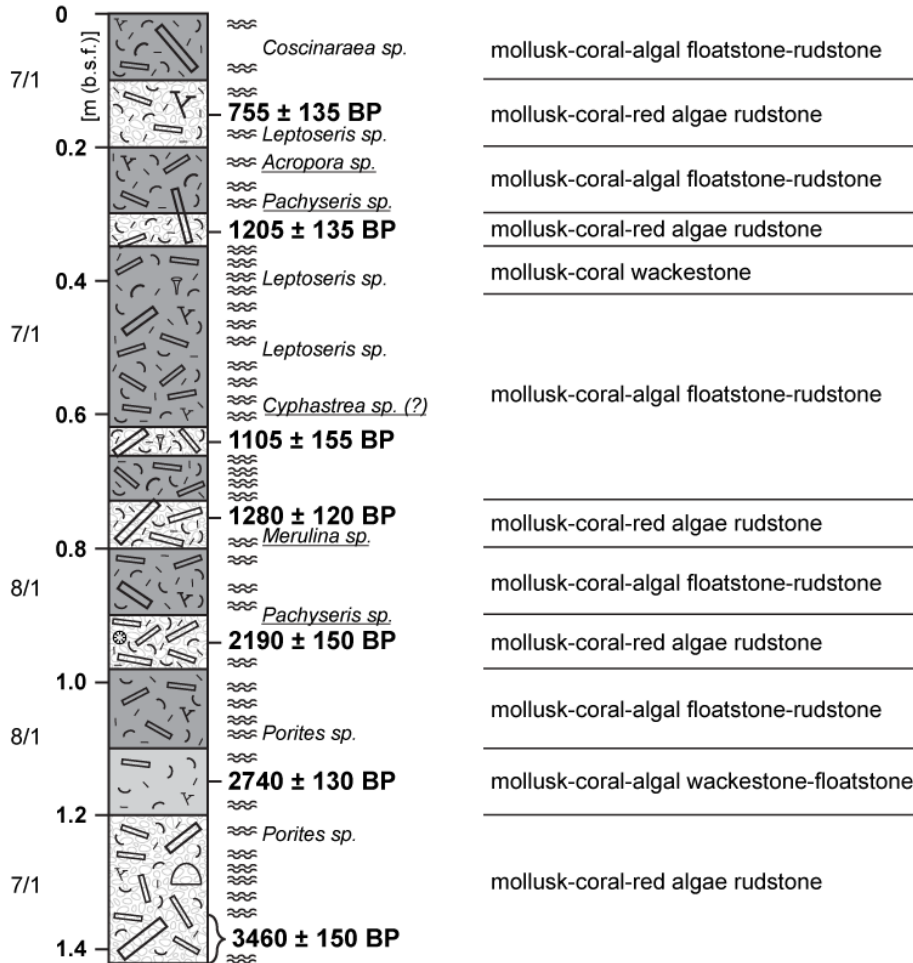


Core log #27: Generally coarse grained core with alternating coarser and finer layers within the floatstone. The colors are light greenish gray (GLE Y1, 10Y, 7/1 - 8/1). Underlined coral ID marks redeposition.

Core log #29

Length: 1.42 m

Water depth: 37.5 m

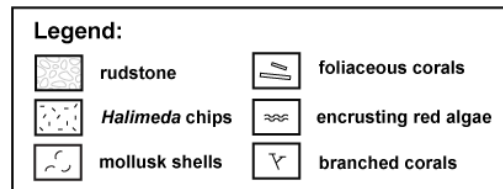
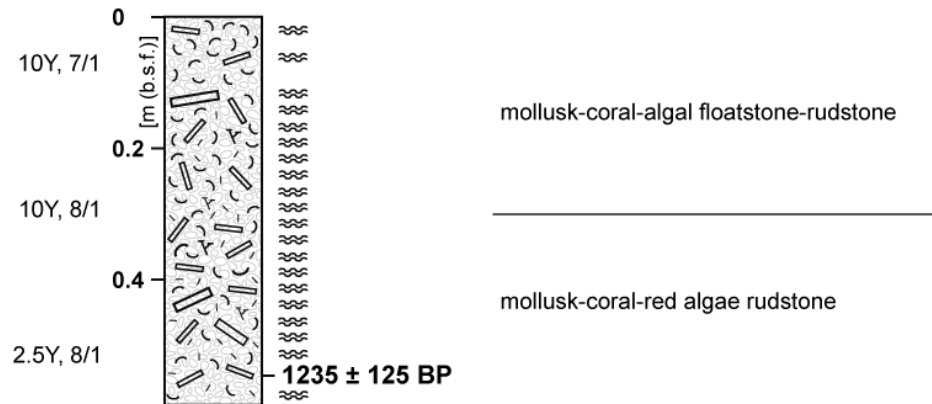


Core log #29: Mainly foliaceous coral fragments in muddy matrix with colors of light greenish gray (GLE1, 10Y, 7/1 - 8/1). Floatstone is alternating with rudstone. Fewer *Halimeda* chips at the base. Underlined coral ID marks redeposition.

Core log #30

Length: 0.59 m

Water depth: 37.6 m

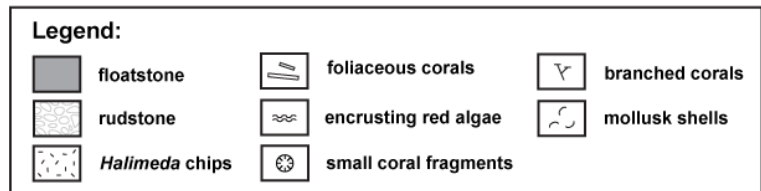
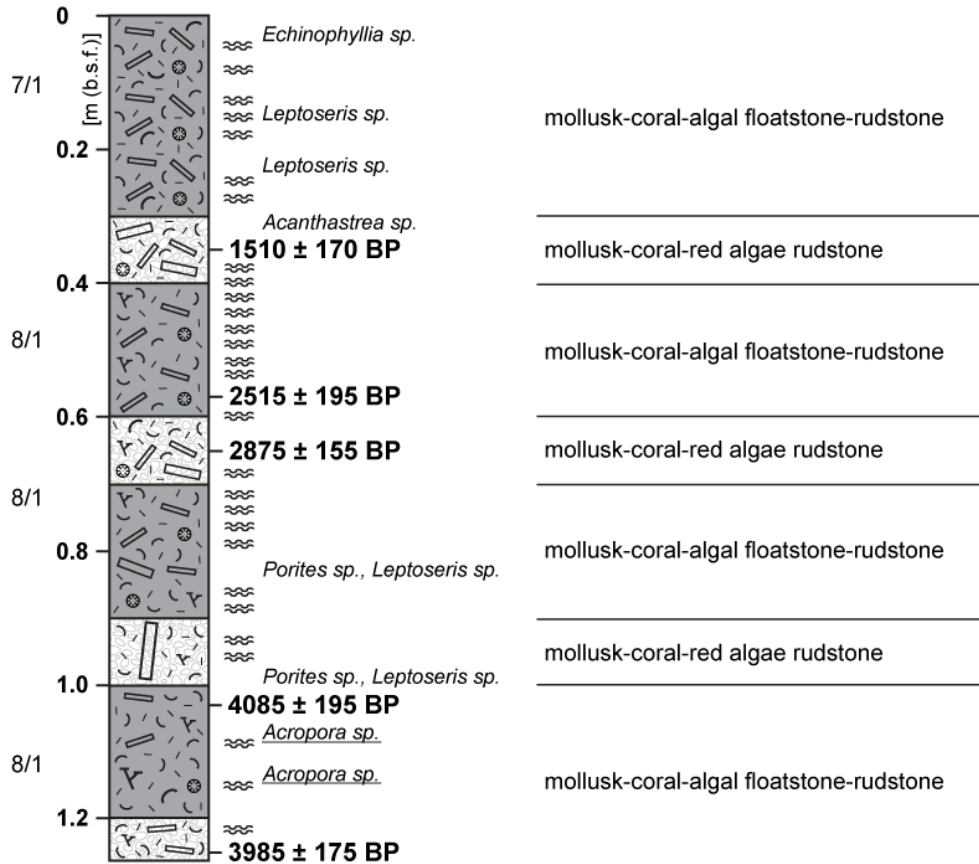


Core log #30: Consistently coarse core with colors of white (WHITE, 2.5Y, 8/1) to light greenish gray (GLE Y1, 10Y, 7/1 - 8/1) towards the top. Sediment was lost at the base of the core from 59 to 40 cm. The dashed line marks a sharp boundary to a slightly darker and greener sediment color towards the top. Underlined coral ID marks redeposition.

Core log #31

Length: 1.26 m

Water depth: 37 m

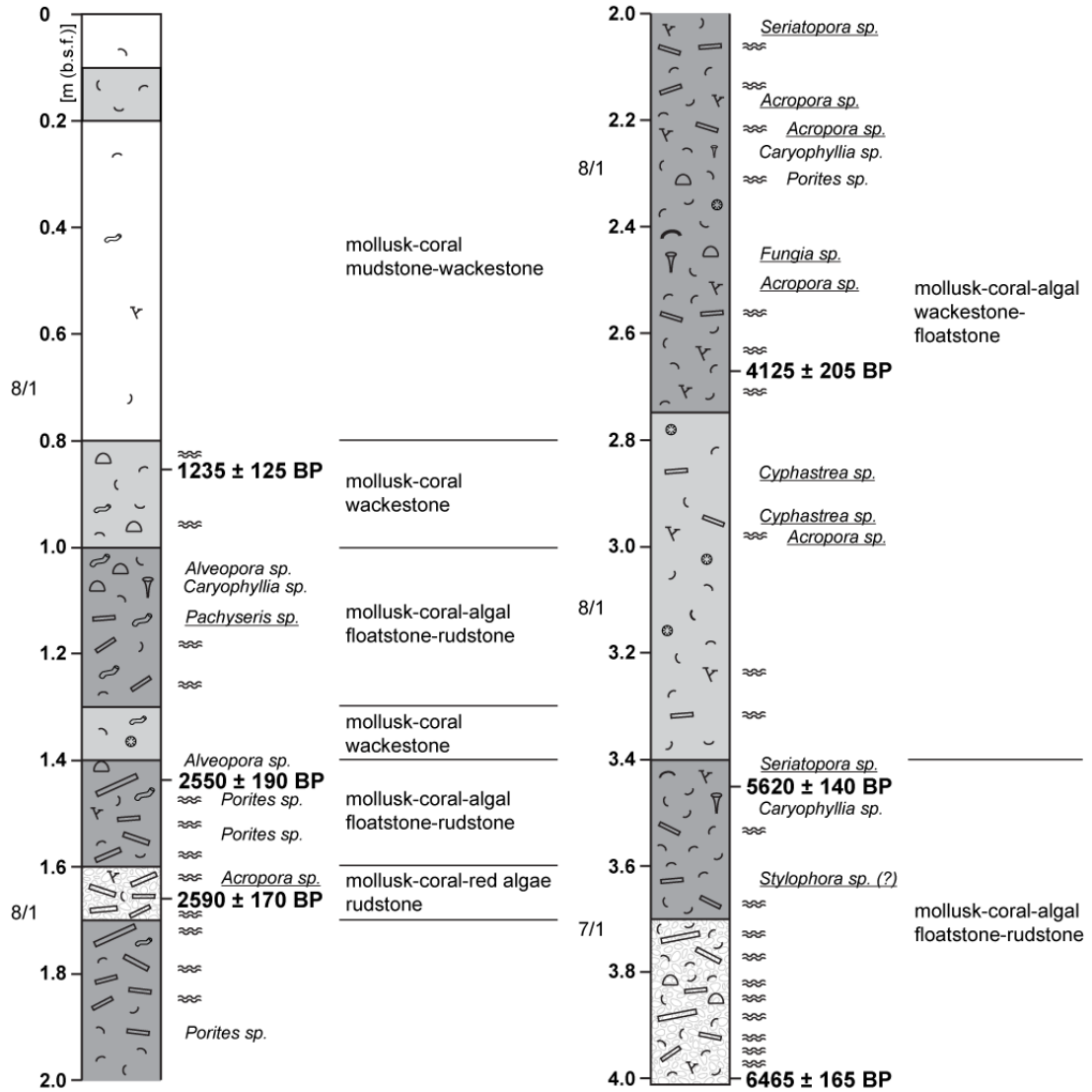


Core log #31: Generally coarse grained core with a consistent color of light greenish gray (GLE Y1, 10Y, 8/1). The first 10 cm at the top are slight greener than the rest (GLE Y1, 10Y, 7/1). Mollusk floatstone is alternating with mollusk rudstone. Underlined coral ID marks redeposition.

Core log #34

Length: 4.01 m

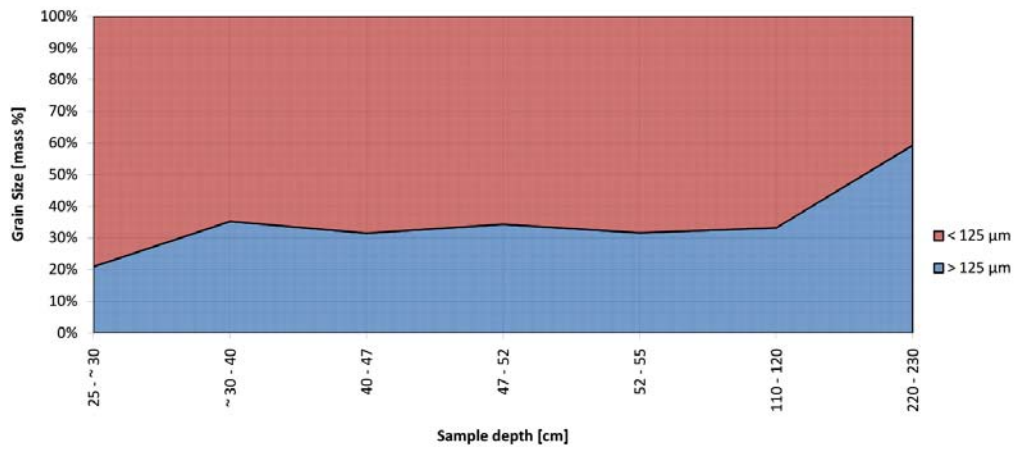
Water depth: 30 m



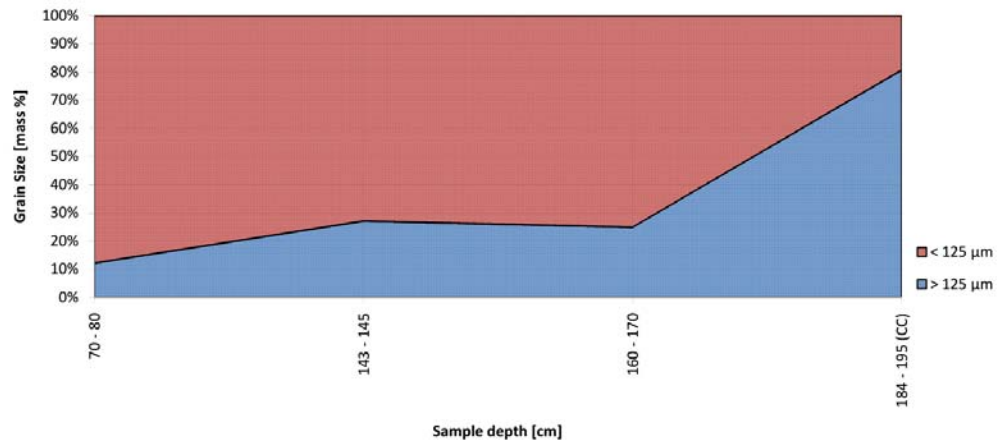
Legend:			

Core log #34: Core #34 is divided into ten different units mainly consisting of muddy sediment with mollusk shells and some coral fragments. Most of the corals are encrusted by calcareous red algae. Generally, the sediment becomes less coarse towards the top with colors of light greenish gray (GLE Y1, 10Y, 7/1 - 8/1). Underlined coral ID marks redeposition.

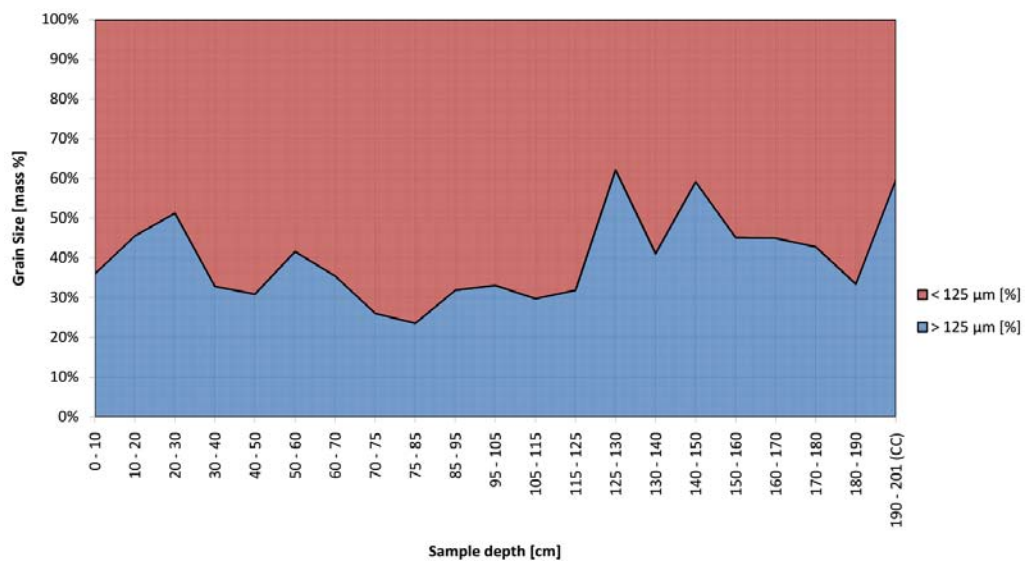
MV Core # 1



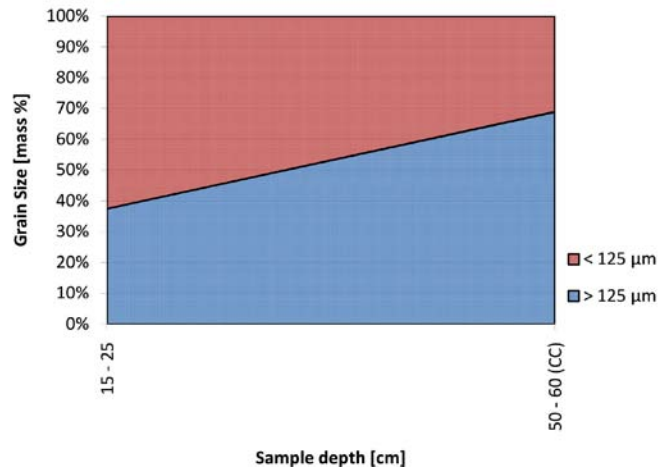
MV Core # 2



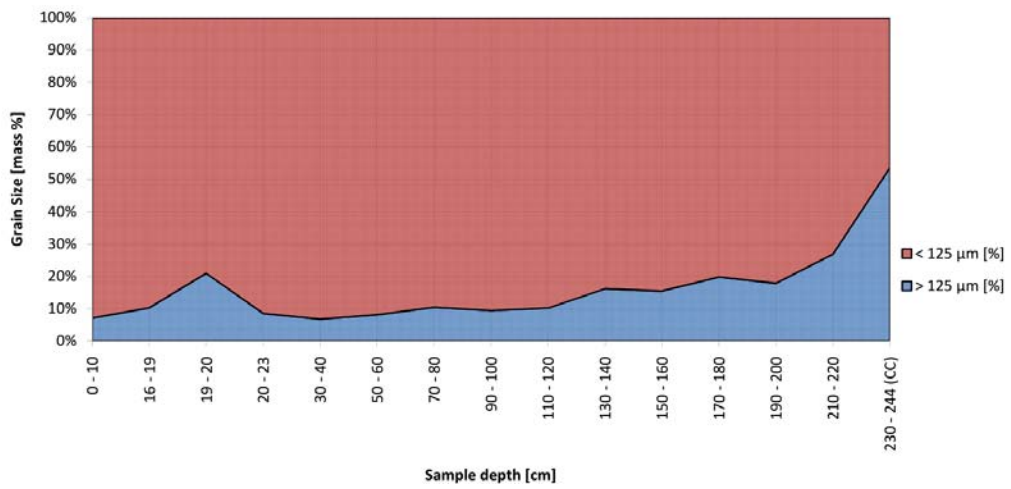
MV Core # 8



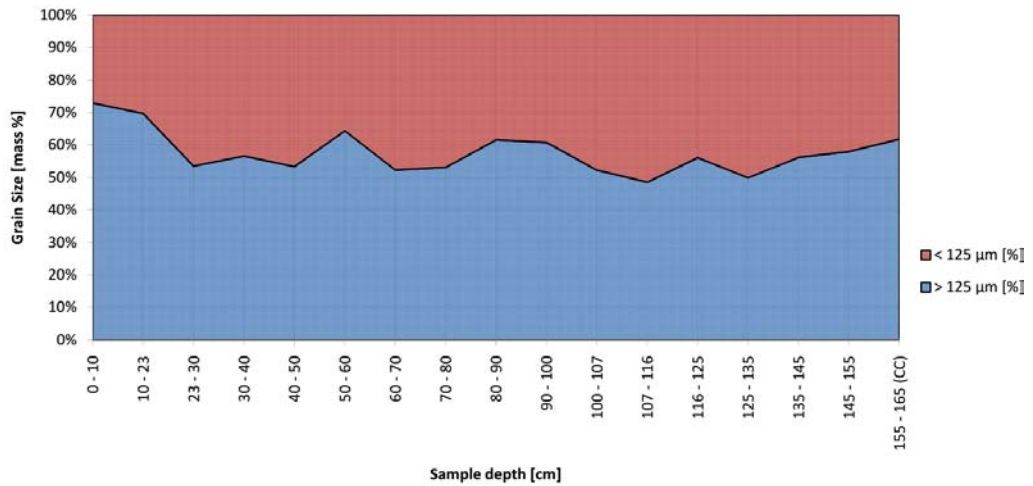
MV Core # 11



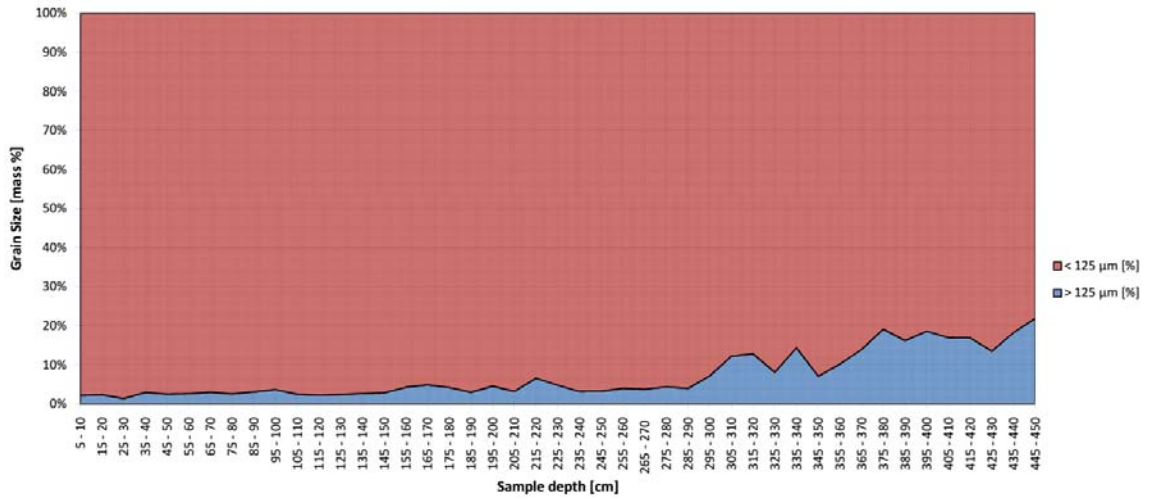
MV Core # 12



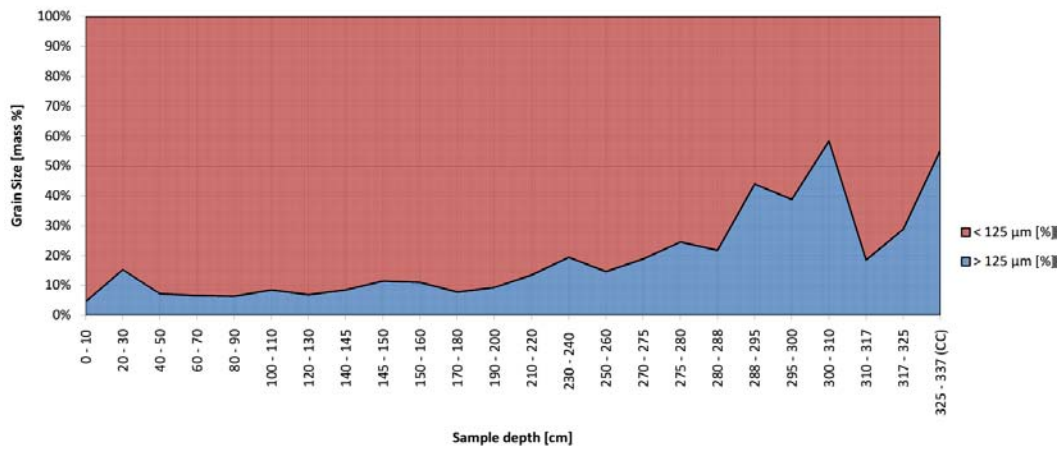
MV Core # 13



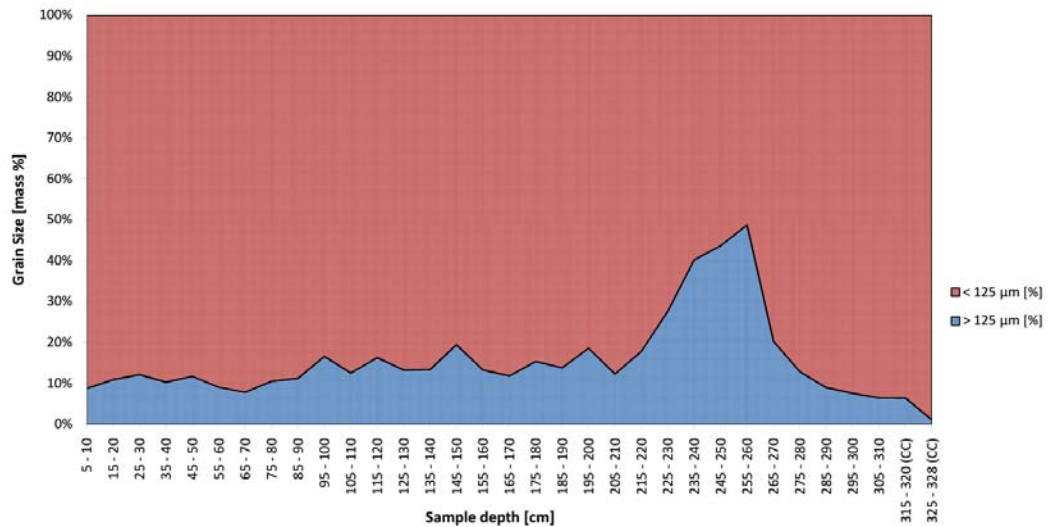
MV Core # 16



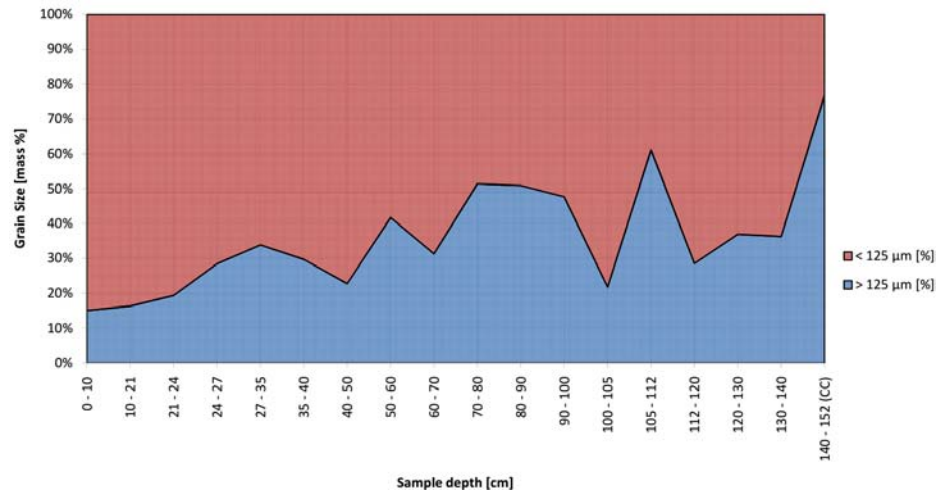
MV Core # 18



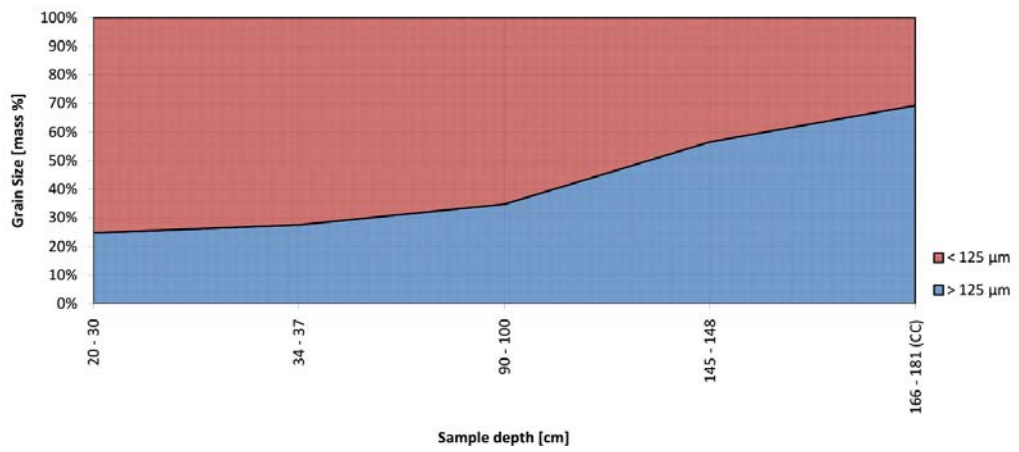
MV Core # 19



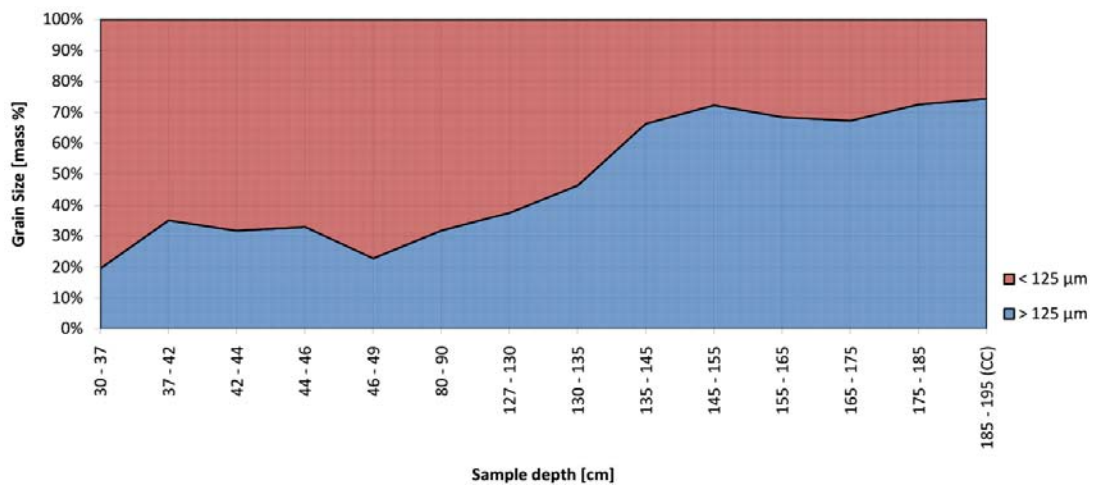
MV Core # 24



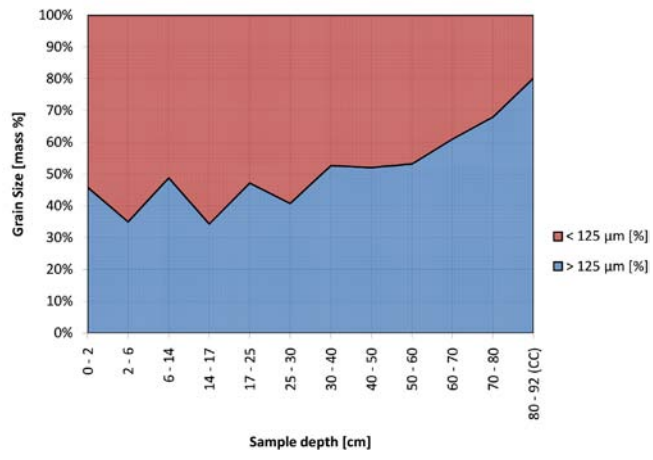
MV Core # 25



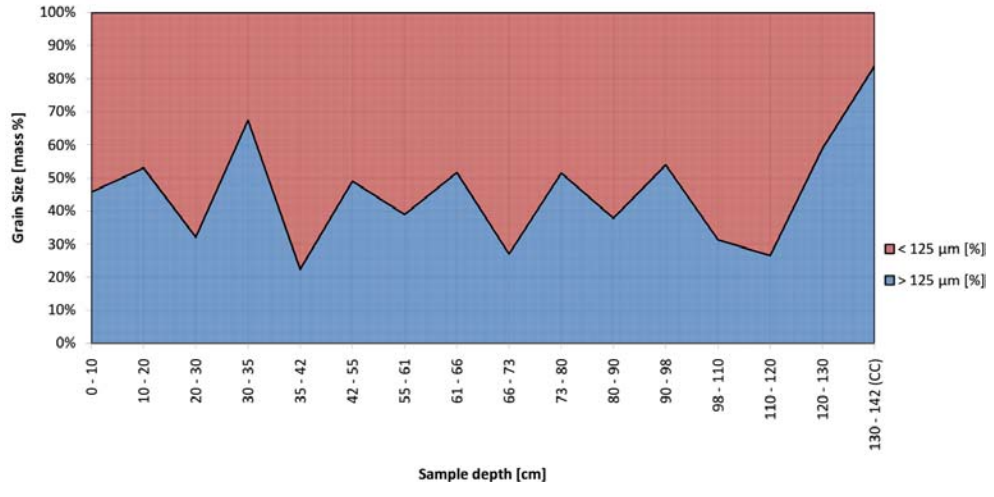
MV Core # 26



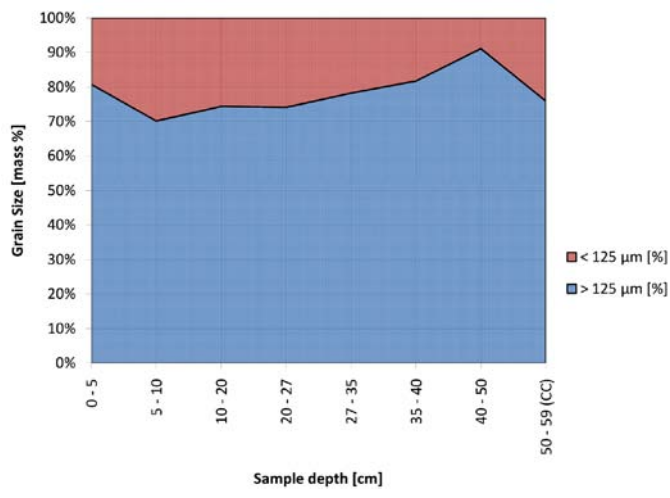
MV Core # 27



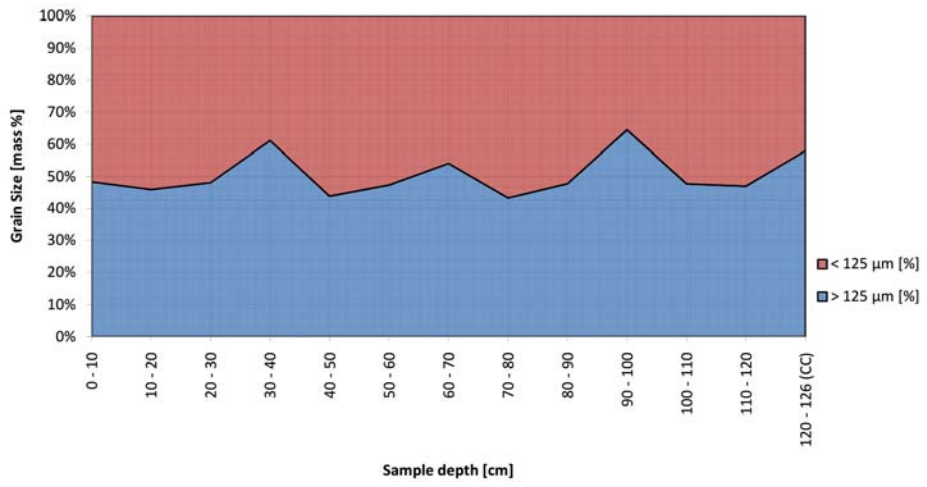
MV Core # 29



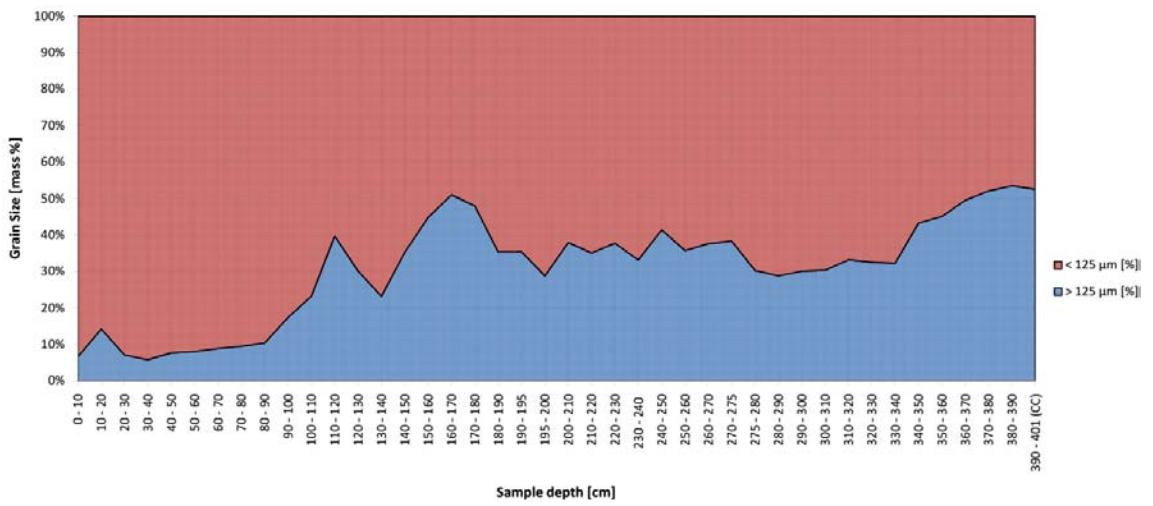
MV Core # 30



MV Core # 31



MV Core # 34



Appendix

Rasdhoor Atoll: Cores & Samples

Core #	Local Date	Local Time	Water Depth [m]	Penetration [m]	Core length [m]	Sample depth [cm]	Dry weight > 2 mm [g]	Dry weight 125 µm - 2 mm [g]	Dry weight > 125 µm [g]	Dry weight < 125 µm [g]	Total dry weight [g]	> 2 mm [%]	125 µm - 2 mm [%]	> 125 µm [%]	< 125 µm [%]	Thin Section	Facies
16	25.11.2010	14:50	34.5	5.49	4.56	5 - 10	0.04	2.60	2.64	117.92	120.56	0.03	2.16	2.19	97.81	x	Mudstone
16	25.11.2010	14:50	34.5	5.49	4.56	15 - 20	0.32	2.39	2.71	111.12	113.83	0.28	2.10	2.38	97.62	x	Mudstone
16	25.11.2010	14:50	34.5	5.49	4.56	25 - 30	0.21	1.33	1.54	108.51	110.05	0.19	1.21	1.40	98.60	x	Mudstone
16	25.11.2010	14:50	34.5	5.49	4.56	35 - 40	1.49	1.89	3.38	110.03	113.41	1.31	1.67	2.98	97.02	x	Mudstone
16	25.11.2010	14:50	34.5	5.49	4.56	45 - 50	1.41	1.78	3.19	121.72	124.91	1.13	1.43	2.55	97.45	x	Mudstone
16	25.11.2010	14:50	34.5	5.49	4.56	55 - 60	0.58	2.66	3.24	119.72	122.96	0.47	2.16	2.64	97.36	x	Mudstone
16	25.11.2010	14:50	34.5	5.49	4.56	65 - 70	0.44	3.43	3.87	124.41	128.28	0.34	2.67	3.02	96.98	x	Mudstone
16	25.11.2010	14:50	34.5	5.49	4.56	75 - 80	0.54	2.77	3.31	124.29	127.6	0.42	2.17	2.59	97.41	x	Mudstone
16	25.11.2010	14:50	34.5	5.49	4.56	85 - 90	0.77	3.29	4.06	126.5	130.56	0.59	2.52	3.11	96.89	x	Mudstone
16	25.11.2010	14:50	34.5	5.49	4.56	95 - 100	1.93	2.53	4.46	117.05	121.51	1.59	2.08	3.67	96.33	x	Mudstone
16	25.11.2010	14:50	34.5	5.49	4.56	105 - 110	0.83	2.38	3.21	124.87	128.08	0.65	1.86	2.51	97.49	x	Mudstone
16	25.11.2010	14:50	34.5	5.49	4.56	115 - 120	0.60	2.37	2.97	131.49	134.46	0.45	1.76	2.21	97.79	x	Mudstone
16	25.11.2010	14:50	34.5	5.49	4.56	125 - 130	0.77	2.69	3.46	138.16	141.62	0.54	1.90	2.44	97.56	x	Mudstone
16	25.11.2010	14:50	34.5	5.49	4.56	135 - 140	0.51	3.20	3.71	133.53	137.24	0.37	2.33	2.70	97.30	x	Mudstone
16	25.11.2010	14:50	34.5	5.49	4.56	145 - 150	1.23	2.43	3.66	125.28	128.94	0.95	1.88	2.84	97.16	x	Mudstone
16	25.11.2010	14:50	34.5	5.49	4.56	155 - 160	2.07	3.78	5.85	130.27	136.12	1.52	2.78	4.30	95.70	x	Mudstone
16	25.11.2010	14:50	34.5	5.49	4.56	165 - 170	2.07	3.74	6.04	117.88	123.92	1.86	3.02	4.87	95.13	x	Mudstone
16	25.11.2010	14:50	34.5	5.49	4.56	175 - 180	1.60	3.96	5.56	125.58	131.14	1.22	3.02	4.24	95.76	x	Mudstone
16	25.11.2010	14:50	34.5	5.49	4.56	185 - 190	1.22	2.48	3.70	118.95	122.65	0.99	2.02	3.02	96.98	x	Mudstone
16	25.11.2010	14:50	34.5	5.49	4.56	195 - 200	1.48	4.62	6.10	126.74	132.84	1.11	3.48	4.59	95.41	x	Mudstone
16	25.11.2010	14:50	34.5	5.49	4.56	205 - 210	1.15	3.09	4.24	126.66	130.9	0.88	2.36	3.24	96.76	x	Mudstone
16	25.11.2010	14:50	34.5	5.49	4.56	215 - 220	3.76	4.79	8.55	121.14	129.69	2.90	3.69	6.59	93.41	x	Mudstone
16	25.11.2010	14:50	34.5	5.49	4.56	225 - 230	1.86	3.41	5.27	104.4	109.67	1.70	3.11	4.81	95.19	x	Mudstone
16	25.11.2010	14:50	34.5	5.49	4.56	235 - 240	0.63	3.37	4.00	120.91	124.91	0.50	2.70	3.20	96.80	x	Mudstone
16	25.11.2010	14:50	34.5	5.49	4.56	245 - 250	1.39	2.77	4.16	123.18	127.34	1.09	2.18	3.27	96.73	x	Mudstone
16	25.11.2010	14:50	34.5	5.49	4.56	255 - 260	1.42	3.71	5.13	123.53	128.66	1.10	2.88	3.99	96.01	x	Mudstone
16	25.11.2010	14:50	34.5	5.49	4.56	265 - 270	1.18	3.53	4.71	119.61	124.32	0.95	2.84	3.79	96.21	x	Mudstone
16	25.11.2010	14:50	34.5	5.49	4.56	275 - 280	1.22	4.38	5.60	121.77	127.37	0.96	3.44	4.40	95.60	x	Mudstone
16	25.11.2010	14:50	34.5	5.49	4.56	285 - 290	0.87	3.78	4.65	111.79	116.44	0.75	3.25	3.99	96.01	x	Mudstone
16	25.11.2010	14:50	34.5	5.49	4.56	295 - 300	3.46	6.00	9.46	121.92	131.38	2.63	4.57	7.20	92.80	x	Mudstone
16	25.11.2010	14:50	34.5	5.49	4.56	305 - 310	6.30	11.17	17.47	124.98	142.45	4.42	7.84	12.26	87.74	x	Wackestone
16	25.11.2010	14:50	34.5	5.49	4.56	315 - 320	6.37	9.89	16.26	110.58	126.84	5.02	7.80	12.82	87.18	x	Wackestone
16	25.11.2010	14:50	34.5	5.49	4.56	325 - 330	2.22	6.95	9.17	103.28	112.45	1.97	6.18	8.15	91.85	x	Mudstone
16	25.11.2010	14:50	34.5	5.49	4.56	335 - 340	9.02	9.85	18.87	112.48	131.35	6.87	7.50	14.37	85.63	x	Wackestone
16	25.11.2010	14:50	34.5	5.49	4.56	345 - 350	4.31	4.93	9.24	121.01	130.25	3.31	3.79	7.09	92.91	2x	Mudstone
16	25.11.2010	14:50	34.5	5.49	4.56	355 - 360	4.26	10.04	14.30	125.45	139.75	3.05	7.18	10.23	89.77	2x	Wackestone
16	25.11.2010	14:50	34.5	5.49	4.56	365 - 370	9.19	9.55	18.74	115.38	134.12	6.85	7.12	13.97	86.03	x	Wackestone
16	25.11.2010	14:50	34.5	5.49	4.56	375 - 380	14.13	11.88	26.01	109.56	135.57	10.42	8.76	19.19	80.81	x	Floatstone
16	25.11.2010	14:50	34.5	5.49	4.56	385 - 390	6.14	11.16	17.30	89.36	106.66	5.76	10.46	16.22	83.78	x	Wackestone
16	25.11.2010	14:50	34.5	5.49	4.56	395 - 400	9.91	5.45	15.36	67.01	82.37	12.03	6.62	18.65	81.35	2x	Floatstone
16	25.11.2010	14:50	34.5	5.49	4.56	405 - 410	7.52	7.61	15.13	73.96	89.09	8.44	8.54	16.98	83.02	x	Wackestone
16	25.11.2010	14:50	34.5	5.49	4.56	415 - 420	3.78	8.06	11.84	58.05	69.89	5.41	11.53	16.94	83.06	x	Soil
16	25.11.2010	14:50	34.5	5.49	4.56	425 - 430	2.40	7.12	9.52	60.82	70.34	3.41	10.12	13.53	86.47	x	Soil
16	25.11.2010	14:50	34.5	5.49	4.56	435 - 440	2.34	7.64	9.98	44.54	54.52	4.29	14.01	18.31	81.69	x	Soil
16	25.11.2010	14:50	34.5	5.49	4.56	445 - 450	3.79	7.67	11.46	40.77	52.23	7.26	14.69	21.94	78.06	x	Soil
19	26.11.2010	10:30	13.6	5.18	3.28	5 - 10	0.62	10.18	10.80	112.15	122.95	0.50	8.28	8.78	91.22	3x	Mudstone
19	26.11.2010	10:30	13.6	5.18	3.28	15 - 20	0.57	14.72	15.29	124.59	139.88	0.41	10.52	10.93	89.07	x	Wackestone
19	26.11.2010	10:30	13.6	5.18	3.28	25 - 30	0.94	13.91	14.85	107.17	122.02	0.77	11.40	12.17	87.83	x	Wackestone
19	26.11.2010	10:30	13.6	5.18	3.28	35 - 40	0.23	12.40	12.63	109.74	122.37	0.19	10.13	10.32	89.68	x	Wackestone
19	26.11.2010	10:30	13.6	5.18	3.28	45 - 50	0.39	14.72	15.11	113.64	128.75	0.30	11.43	11.74	88.26	2x	Wackestone
19	26.11.2010	10:30	13.6	5.18	3.28	55 - 60	0.60	9.95	10.55	105.64	116.19	0.52	8.56	9.08	90.92	x	Mudstone
19	26.11.2010	10:30	13.6	5.18	3.28	65 - 70	0.35	9.00	9.35	109.91	119.26	0.29	7.55	7.84	92.16	x	Mudstone
19	26.11.2010	10:30	13.6	5.18	3.28	75 - 80	1.97	10.97	12.94	109.72	122.66	1.61	8.94	10.55	89.45	x	Wackestone
19	26.11.2010	10:30	13.6	5.18	3.28	85 - 90	0.81	11.79	12.60	99.18	111.78	0.72	10.55	11.27	88.73	x	Wackestone
19	26.11.2010	10:30	13.6	5.18	3.28	95 - 100	6.48	13.44	19.92	99.93	119.85	5.41	11.21	16.62	83.38	x	Wackestone
19	26.11.2010	10:30	13.6	5.18	3.28	105 - 110	3.01	12.20	15.21	106	121.21	2.48	10.07	12.55	87.45	x	Wackestone
19	26.11.2010	10:30	13.6	5.18	3.28	115 - 120	4.56	16.18	20.74	106.29	127.03	3.59	12.74	16.33	83.67	x	Wackestone
19	26.11.2010	10:30	13.6	5.18	3.28	125 - 130	3.05	12.51	15.56	101.58	117.14	2.60	10.68	13.28	86.72	x	Wackestone
19	26.11.2010	10:30	13.6	5.18	3.28	135 - 140	1.73	13.26	14.99	96.84	111.83	1.55	11.86	13.40	86.60	x	Wackestone
19	26.11.2010	10:30	13.6	5.18	3.28	145 - 150	7.81	16.33	24.14	99.82	123.96	6.30	13.17	19.47	80.53	x	Wackestone
19	26.11.2010	10:30	13.6	5.18	3.28	155 - 160	2.64	11.26	13.90	90.57	104.47	2.53	10.78	13.31	86.69	x	Wackestone
19	26.11.2010	10:30	13.6	5.18	3.28	165 - 170	1.15	12.13	13.28	98.87	112.15	1.03	10.82	11.84	88.16	x	Wackestone
19	26.11.2010	10:30	13.6	5.18	3.28	175 - 180	3.12	13.96	17.08	94.05	111.13	2.81	12.56	15.37	84.63	x	Wackestone
19	26.11.2010	10:30	13.6	5.18	3.28	185 - 190	1.55	14.33	15.88	98.9	114.78	1.35	12.48	13.84	86.16	x	Wackestone
19	26.11.2010	10:30	13.6	5.18	3.28	195 - 200	6.65	15.37	22.02	96.18	118.2	5.63	13.00	18.63	81.37	x	Wackestone
19	26.11.2010	10:30	13.6	5.18	3.28	205 - 210	1.99	12.29	14.28	101.82	116.1	1.71	10.59	12.30	87.70	x	Wackestone
19	26.11.2010	10:30	13.6	5.18	3.28	215 - 220	4.10	18.01	22.11	101.52	123.63	3.32	14.57	17.88	82.12	x	Wackestone
19	26.11.2010	10:30	13.6	5.18	3.28	225 - 230	18.48	18.10	36.58	95.6	132.18	13.98	13.69	27.67	72.33	x	Floatstone
19	26.11.2010	10:30</															

Appendix

Rasdhoor Atoll: Cores & Samples (continued)

Core #	Local Date	Local Time	Water Depth [m]	Penetration [m]	Core length [m]	Sample depth [cm]	Dry weight > 2 mm [g]	Dry weight 125 µm - 2 mm [g]	Dry weight > 125 µm [g]	Dry weight < 125 µm [g]	Total dry weight [g]	> 2 mm [%]	125 µm - 2 mm [%]	> 125 µm [%]	< 125 µm [%]	Thin Section	Facies
34	30.11.2010	16:35	30	5.80	4.01	195-200	9.81	24.64	34.45	85.07	119.52	8.21	20.62	28.82	71.18	x	Wackestone
34	30.11.2010	16:35	30	5.80	4.01	200-210	46.53	54.52	101.05	165.3	266.35	17.47	20.47	37.94	62.06		Floatstone
34	30.11.2010	16:35	30	5.80	4.01	210-220	37.36	58.82	96.18	177.55	273.73	13.65	21.49	35.14	64.86	x	Floatstone
34	30.11.2010	16:35	30	5.80	4.01	220-230	50.50	56.42	106.92	176.22	283.14	17.84	19.93	37.76	62.24		Floatstone
34	30.11.2010	16:35	30	5.80	4.01	230-240	31.20	62.00	93.20	187.62	280.82	11.11	22.08	33.19	66.81	x	Floatstone
34	30.11.2010	16:35	30	5.80	4.01	240-250	69.15	67.15	136.30	192.6	328.9	21.02	20.42	41.44	58.56		Floatstone
34	30.11.2010	16:35	30	5.80	4.01	250-260	39.24	72.13	111.37	200.19	311.56	12.59	23.15	35.75	64.25	x	Floatstone
34	30.11.2010	16:35	30	5.80	4.01	260-270	48.13	76.00	124.13	205.47	329.6	14.60	23.06	37.66	62.34		Floatstone
34	30.11.2010	16:35	30	5.80	4.01	270-275	26.89	30.55	57.44	92.25	149.69	17.96	20.41	38.37	61.63	x	Floatstone
34	30.11.2010	16:35	30	5.80	4.01	275-280	11.43	31.49	42.92	98.75	141.67	8.07	22.23	30.30	69.70		Wackestone
34	30.11.2010	16:35	30	5.80	4.01	280-290	19.98	67.82	87.80	216.32	304.12	6.57	22.30	28.87	71.13	x	Wackestone
34	30.11.2010	16:35	30	5.80	4.01	290-300	26.49	55.83	82.32	191.12	273.44	9.69	20.42	30.11	69.89		Wackestone
34	30.11.2010	16:35	30	5.80	4.01	300-310	20.39	66.56	86.95	199.13	286.08	7.13	23.27	30.39	69.61		Wackestone
34	30.11.2010	16:35	30	5.80	4.01	310-320	21.24	70.15	91.39	183.52	274.91	7.73	25.52	33.24	66.76		Wackestone
34	30.11.2010	16:35	30	5.80	4.01	320-330	23.59	66.28	89.87	185.88	275.75	8.55	24.04	32.59	67.41	x	Wackestone
34	30.11.2010	16:35	30	5.80	4.01	330-340	21.91	64.72	86.63	181.49	268.12	8.17	24.14	32.31	67.69		Wackestone
34	30.11.2010	16:35	30	5.80	4.01	340-350	61.52	69.28	130.80	171.2	302	20.37	22.94	43.31	56.69		Floatstone
34	30.11.2010	16:35	30	5.80	4.01	350-360	38.18	91.65	129.83	157.95	287.78	13.27	31.85	45.11	54.89	x	Floatstone
34	30.11.2010	16:35	30	5.80	4.01	360-370	48.26	112.67	160.93	163.91	324.84	14.86	34.68	49.54	50.46		Floatstone
34	30.11.2010	16:35	30	5.80	4.01	370-380	67.16	103.24	170.40	156.52	326.92	20.54	31.58	52.12	47.88		Rudstone
34	30.11.2010	16:35	30	5.80	4.01	380-390	70.54	86.28	156.82	136.07	292.89	24.08	29.46	53.54	46.46	x	Rudstone
34	30.11.2010	16:35	30	5.80	4.01	390-401 (CC)	40.93	64.37	105.30	95.1	200.40	20.42	32.12	52.54	47.46		Rudstone
12	24.11.2010	17:20	20	3.58	2.44	0-10	0.81	17.28	18.04	236.43	254.47	0.32	6.77	7.09	92.91	x	Mudstone
12	24.11.2010	17:20	20	3.58	2.44	16-19	0.51	4.09	4.60	40.15	44.75	1.14	9.14	10.28	89.72		Wackestone
12	24.11.2010	17:20	20	3.58	2.44	19-20	0.03	9.11	9.14	34.52	43.66	0.07	20.87	20.93	79.07	x	Wackestone
12	24.11.2010	17:20	20	3.58	2.44	20-23	0.05	6.70	6.75	72.63	79.38	0.06	8.44	8.50	91.50		Mudstone
12	24.11.2010	17:20	20	3.58	2.44	30-40	0.26	18.72	18.98	261.57	280.55	0.09	6.67	6.77	93.23	x	Mudstone
12	24.11.2010	17:20	20	3.58	2.44	50-60	1.27	20.58	21.85	247.44	269.29	0.47	7.64	8.11	91.89	x	Mudstone
12	24.11.2010	17:20	20	3.58	2.44	70-80	3.50	24.71	28.21	242.4	270.61	1.29	9.13	10.42	89.58	x	Wackestone
12	24.11.2010	17:20	20	3.58	2.44	90-100	1.12	23.86	24.98	240.35	265.33	0.42	8.99	9.41	90.59		Mudstone
12	24.11.2010	17:20	20	3.58	2.44	110-120	1.80	26.86	28.66	252.94	281.60	0.64	9.54	10.18	89.82	x	Wackestone
12	24.11.2010	17:20	20	3.58	2.44	130-140	6.55	36.23	42.78	221.69	264.47	2.48	13.70	16.18	83.82	x	Wackestone
12	24.11.2010	17:20	20	3.58	2.44	150-160	4.02	36.49	40.51	221.67	262.18	1.53	13.92	15.45	84.55		Wackestone
12	24.11.2010	17:20	20	3.58	2.44	170-180	10.30	43.86	54.16	219.44	273.60	3.76	16.03	19.80	80.20	x	Wackestone
12	24.11.2010	17:20	20	3.58	2.44	190-200	5.72	43.97	49.69	228.43	278.12	2.06	15.81	17.87	82.13	x	Wackestone
12	24.11.2010	17:20	20	3.58	2.44	210-220	13.29	58.97	72.26	196.69	268.95	4.94	21.93	26.87	73.13		Wackestone
12	24.11.2010	17:20	20	3.58	2.44	230-244 (CC)	70.72	81.66	152.38	131.9	284.28	24.88	28.73	53.60	46.40		Rudstone
8	24.11.2010	11:40	36.8	2.23	2.01	0-10	60.87	27.01	87.88	156.37	244.25	24.92	11.06	35.98	64.02		Floatstone
8	24.11.2010	11:40	36.8	2.23	2.01	10-20	75.81	27.47	103.28	123.71	226.99	33.40	12.10	45.50	54.50	x	Floatstone
8	24.11.2010	11:40	36.8	2.23	2.01	20-30	110.55	57.64	168.19	160.08	328.27	33.68	17.56	51.24	48.76	x	Rudstone
8	24.11.2010	11:40	36.8	2.23	2.01	30-40	43.54	29.96	73.50	150.61	224.11	19.43	13.37	32.80	67.20		Floatstone
8	24.11.2010	11:40	36.8	2.23	2.01	40-50	34.14	32.54	66.68	149.28	215.96	15.81	15.07	30.88	69.12	x	Floatstone
8	24.11.2010	11:40	36.8	2.23	2.01	50-60	69.30	33.41	102.71	144.35	247.06	28.05	13.52	41.57	58.43	x	Floatstone
8	24.11.2010	11:40	36.8	2.23	2.01	60-70	40.55	43.40	83.95	153.06	237.01	17.11	18.31	35.42	64.58		Floatstone
8	24.11.2010	11:40	36.8	2.23	2.01	70-75	10.55	24.47	35.02	99.6	134.62	7.84	18.18	26.01	73.99	x	Wackestone
8	24.11.2010	11:40	36.8	2.23	2.01	75-85	15.45	36.06	51.51	167.72	219.23	7.05	16.45	23.50	76.50		Wackestone
8	24.11.2010	11:40	36.8	2.23	2.01	85-95	35.13	43.37	78.50	167.87	246.37	14.26	17.60	31.86	68.14		Floatstone
8	24.11.2010	11:40	36.8	2.23	2.01	95-105	31.28	48.43	79.71	161.22	240.93	12.98	20.10	33.08	66.92	x	Floatstone
8	24.11.2010	11:40	36.8	2.23	2.01	105-115	14.43	57.67	72.10	170.57	242.67	5.95	23.76	29.71	70.29		Wackestone
8	24.11.2010	11:40	36.8	2.23	2.01	115-125	19.44	59.78	79.22	169.52	248.74	7.82	24.03	31.85	68.15	x	Wackestone
8	24.11.2010	11:40	36.8	2.23	2.01	125-130	66.49	19.11	85.60	52.13	137.73	48.28	13.87	62.15	37.85	x	Rudstone
8	24.11.2010	11:40	36.8	2.23	2.01	130-140	46.55	47.22	93.77	134.65	228.42	20.38	20.67	41.05	58.95	x	Floatstone
8	24.11.2010	11:40	36.8	2.23	2.01	140-150	114.28	37.08	151.36	104.65	256.01	44.64	14.48	59.12	40.88	x	Floatstone
8	24.11.2010	11:40	36.8	2.23	2.01	150-160	75.11	52.59	127.70	155.49	283.19	26.52	18.57	45.09	54.91		Floatstone
8	24.11.2010	11:40	36.8	2.23	2.01	160-170	69.00	54.75	123.75	151.69	275.44	25.05	19.88	44.93	55.07		Floatstone
8	24.11.2010	11:40	36.8	2.23	2.01	170-180	53.00	57.95	110.95	148.6	259.55	20.42	22.33	42.75	57.25	x	Floatstone
8	24.11.2010	11:40	36.8	2.23	2.01	180-190	30.54	68.72	99.26	197.69	296.95	10.28	23.14	33.43	66.57		Floatstone
8	24.11.2010	11:40	36.8	2.23	2.01	190-201 (CC)	51.55	65.16	116.71	78.82	195.53	26.36	33.32	59.69	40.31		Rudstone
29	28.11.2010	13:25	37.5	2.27	1.42	0-10	61.75	25.67	87.42	103.63	191.05	32.32	13.44	45.76	54.24		Floatstone
29	28.11.2010	13:25	37.5	2.27	1.42	10-20	100.78	25.68	126.46	111.98	238.44	42.27	10.77	53.04	46.96	x	Rudstone
29	28.11.2010	13:25	37.5	2.27	1.42	20-30	42.29	33.67	75.96	160.38	236.34	17.89	14.25	32.14	67.86		Floatstone
29	28.11.2010	13:25	37.5	2.27	1.42	30-35	63.38	11.96	97.05	46.72	143.77	44.08	23.42	67.50	32.50	x	Floatstone
29	28.11.2010	13:25	37.5	2.27	1.42	35-42	24.39	26.47	36.35	125.61	161.96	15.06	7.38	22.44	77.56	x	Floatstone
29	28.11.2010	13:25	37.5	2.27	1.42	42-55	159.39	44.48	185.86	192.88	378.74	42.08	6.99	49.07	50.93	x	Floatstone
29	28.11.2010	13:25	37.5	2.27	1.42	55-61	27.99	25.31	72.47	113.47	185.94	15.05	23.92	38.97	61.03		Floatstone
29	28.11.2010	13:25	37.5	2.27	1.42	61-66	62.42	18.83	87.73	82.03	169.76	36.77	14.91	51.68	48.32	x	Floatstone
29	28.11.2010	13:25	37.5	2.27	1.42	66-73	33.06	30.44	51.89	139.96	191.85	17.23	9.81	27.05	72.95		Floatstone
29	28.11.2010	13:25	37.5	2.27	1.42	73-80	85.64	24.58	116.08	109.27	225.35	38.00	13.51	51.51	48.49	x	Floatstone

Appendix

Rasdhoor Atoll: Cores & Samples (continued)

Core #	Local Date	Local Time	Water Depth [m]	Penetration [m]	Core length [m]	Sample depth [cm]	Dry weight > 2 mm [g]	Dry weight 125 µm - 2 mm [g]	Dry weight > 125 µm [g]	Dry weight < 125 µm [g]	Total dry weight [g]	> 2 mm [%]	125 µm - 2 mm [%]	> 125 µm [%]	< 125 µm [%]	Thin Section	Facies
18	26.11.2010	09:00	14.3	5.67	3.37	140-145	2.53	8.89	11.42	122.37	133.79	1.89	6.64	8.54	91.46		Mudstone
18	26.11.2010	09:00	14.3	5.67	3.37	145-150	5.67	11.44	17.11	131.8	148.91	3.81	7.68	11.49	88.51	x	Wackestone
18	26.11.2010	09:00	14.3	5.67	3.37	150-160	10.52	21.39	31.91	256.69	288.60	3.65	7.41	11.06	88.94		Wackestone
18	26.11.2010	09:00	14.3	5.67	3.37	170-180	3.72	16.10	19.82	234.39	254.21	1.46	6.33	7.80	92.20	x	Mudstone
18	26.11.2010	09:00	14.3	5.67	3.37	190-200	5.84	16.93	22.77	220.64	243.41	2.40	6.96	9.35	90.65		Mudstone
18	26.11.2010	09:00	14.3	5.67	3.37	210-220	10.49	19.79	30.28	194.79	225.07	4.66	8.79	13.45	86.55	x	Wackestone
18	26.11.2010	09:00	14.3	5.67	3.37	230-240	6.23	46.95	53.18	221.17	274.35	2.27	17.11	19.38	80.62	x	Wackestone
18	26.11.2010	09:00	14.3	5.67	3.37	250-260	11.20	28.58	39.78	232.5	272.28	4.11	10.50	14.61	85.39	x	Wackestone
18	26.11.2010	09:00	14.3	5.67	3.37	270-275	7.63	18.40	26.03	112.05	138.08	5.53	13.33	18.85	81.15	x	Wackestone
18	26.11.2010	09:00	14.3	5.67	3.37	275-280	13.88	18.36	32.24	99.16	131.40	10.56	13.97	24.54	75.46	x	Floestone
18	26.11.2010	09:00	14.3	5.67	3.37	280-288	14.39	25.67	40.06	143.8	183.86	7.83	13.96	21.79	78.21	x	Wackestone
18	26.11.2010	09:00	14.3	5.67	3.37	288-295	72.88	27.03	99.91	127.47	227.38	32.05	11.89	43.94	56.06	x	Floestone
18	26.11.2010	09:00	14.3	5.67	3.37	295-300	43.01	24.16	67.17	106.1	173.27	24.82	13.94	38.77	61.23		Floestone
18	26.11.2010	09:00	14.3	5.67	3.37	300-310	150.69	34.72	185.41	132.2	317.61	47.44	10.93	58.38	41.62	x	Rudstone
18	26.11.2010	09:00	14.3	5.67	3.37	310-317	37.52	30.94	68.46	301.51	369.97	10.14	8.36	18.50	81.50	x	Floestone
18	26.11.2010	09:00	14.3	5.67	3.37	317-325	11.23	40.95	52.18	128.51	180.69	6.22	22.66	28.88	71.12	x	Wackestone
18	26.11.2010	09:00	14.3	5.67	3.37	325-337(CC)	118.81	34.47	153.28	123.66	276.94	42.90	12.45	55.35	44.65	x	Rudstone
24	27.11.2010	14:15	28.5	2.64	1.52	0-10	5.82	29.94	35.76	200.77	236.53	2.46	12.66	15.12	84.88	x	Wackestone
24	27.11.2010	14:15	28.5	2.64	1.52	10-21	10.86	34.12	44.98	230.07	275.05	3.95	12.41	16.35	83.65		Wackestone
24	27.11.2010	14:15	28.5	2.64	1.52	21-24	4.72	8.71	13.43	55.8	69.23	6.82	12.58	19.40	80.60	x	Wackestone
24	27.11.2010	14:15	28.5	2.64	1.52	24-27	11.71	9.36	21.07	52.81	73.88	15.85	12.67	28.52	71.48		Floestone
24	27.11.2010	14:15	28.5	2.64	1.52	27-35	33.89	23.08	56.97	111.12	168.09	20.16	13.73	33.89	66.11	x	Floestone
24	27.11.2010	14:15	28.5	2.64	1.52	35-40	16.56	13.99	30.55	72.12	102.67	16.13	13.63	29.76	70.24	x	Floestone
24	27.11.2010	14:15	28.5	2.64	1.52	40-50	18.86	34.24	53.10	179.63	232.73	8.10	14.71	22.82	77.18	x	Wackestone
24	27.11.2010	14:15	28.5	2.64	1.52	50-60	87.70	35.56	121.26	169.03	290.29	30.21	11.56	41.77	58.23	x	Floestone
24	27.11.2010	14:15	28.5	2.64	1.52	60-70	47.95	37.69	85.64	187.58	273.22	17.55	13.79	31.34	68.66		Floestone
24	27.11.2010	14:15	28.5	2.64	1.52	70-80	92.27	34.50	126.77	119.7	246.47	37.44	14.00	51.43	48.57	x	Rudstone
24	27.11.2010	14:15	28.5	2.64	1.52	80-90	65.70	60.38	126.08	121.54	247.62	26.53	24.38	50.92	49.08		Rudstone
24	27.11.2010	14:15	28.5	2.64	1.52	90-100	98.66	40.26	138.92	152.12	291.04	33.90	13.83	47.73	52.27	x	Floestone
24	27.11.2010	14:15	28.5	2.64	1.52	100-105	4.65	21.82	26.47	94.81	121.28	3.83	17.99	21.83	78.17	x	Wackestone
24	27.11.2010	14:15	28.5	2.64	1.52	105-112	98.30	16.00	114.30	72.5	186.80	52.62	8.57	61.19	38.81	x	Rudstone
24	27.11.2010	14:15	28.5	2.64	1.52	112-120	30.33	30.06	60.39	150.81	211.20	14.36	14.23	28.59	71.41		Floestone
24	27.11.2010	14:15	28.5	2.64	1.52	120-130	66.43	37.36	103.79	177.03	280.82	23.66	13.30	36.96	63.04	x	Floestone
24	27.11.2010	14:15	28.5	2.64	1.52	130-140	51.64	40.99	92.63	162.36	254.99	20.25	16.08	36.33	63.67		Floestone
24	27.11.2010	14:15	28.5	2.64	1.52	140-152(CC)	123.78	21.72	145.50	43.78	189.28	65.40	11.48	76.87	23.13	x	Rudstone
31	30.11.2010	11:40	37	2.04	1.26	0-10	49.84	43.67	93.51	99.96	193.47	25.76	22.57	48.33	51.67		Floestone
31	30.11.2010	11:40	37	2.04	1.26	10-20	61.52	53.84	115.36	135.57	250.93	24.52	21.46	45.97	54.03	x	Wackestone
31	30.11.2010	11:40	37	2.04	1.26	20-30	72.00	49.13	121.13	130.75	251.88	28.59	19.51	48.09	51.91		Floestone
31	30.11.2010	11:40	37	2.04	1.26	30-40	123.56	38.48	162.04	102.84	264.88	46.65	14.53	61.17	38.83	x	Rudstone
31	30.11.2010	11:40	37	2.04	1.26	40-50	52.01	44.98	96.99	124.05	221.04	23.53	20.35	43.88	56.12	x	Floestone
31	30.11.2010	11:40	37	2.04	1.26	50-60	60.07	41.42	101.49	112.76	214.25	28.04	19.33	47.37	52.63		Floestone
31	30.11.2010	11:40	37	2.04	1.26	60-70	109.77	50.32	160.09	135.87	295.96	37.09	17.00	54.09	45.91	x	Rudstone
31	30.11.2010	11:40	37	2.04	1.26	70-80	52.42	45.16	97.58	127.64	225.22	23.28	20.05	43.33	56.67	x	Floestone
31	30.11.2010	11:40	37	2.04	1.26	80-90	56.16	42.20	98.36	107.46	205.82	27.29	20.50	47.79	52.21		Floestone
31	30.11.2010	11:40	37	2.04	1.26	90-100	103.72	36.43	140.15	77.18	217.33	47.72	16.76	64.49	35.51	x	Rudstone
31	30.11.2010	11:40	37	2.04	1.26	100-110	47.27	59.42	106.69	116.82	223.51	21.15	26.58	47.73	52.27	x	Floestone
31	30.11.2010	11:40	37	2.04	1.26	110-120	40.17	65.53	105.70	119.12	224.82	17.87	29.15	47.02	52.98		Floestone
31	30.11.2010	11:40	37	2.04	1.26	120-126(CC)	25.55	29.26	54.81	39.67	94.48	27.04	30.97	58.01	41.99	x	Rudstone
27	28.11.2010	09:45	21.6	1.49	0.92	0-2	8.81	7.29	16.10	18.97	35.07	25.12	20.79	45.91	54.09		Floestone
27	28.11.2010	09:45	21.6	1.49	0.92	2-6	6.57	16.42	22.99	42.65	65.64	10.01	25.02	35.02	64.98	x	Floestone
27	28.11.2010	09:45	21.6	1.49	0.92	6-14	46.14	31.03	77.17	80.91	158.08	29.19	19.63	48.82	51.18		Floestone
27	28.11.2010	09:45	21.6	1.49	0.92	14-17	7.36	16.28	23.64	45.2	68.84	10.69	23.65	34.34	65.66	x	Floestone
27	28.11.2010	09:45	21.6	1.49	0.92	17-25	44.36	29.48	73.84	82.62	156.46	28.35	18.84	47.19	52.81		Floestone
27	28.11.2010	09:45	21.6	1.49	0.92	25-30	17.91	17.96	35.87	52.06	87.93	20.37	20.43	40.79	59.21	x	Floestone
27	28.11.2010	09:45	21.6	1.49	0.92	30-40	69.70	31.17	100.87	90.58	191.45	36.41	16.28	52.69	47.31		Rudstone
27	28.11.2010	09:45	21.6	1.49	0.92	40-50	82.64	37.88	120.52	110.82	231.34	35.72	16.37	52.10	47.90	x	Rudstone
27	28.11.2010	09:45	21.6	1.49	0.92	50-60	92.89	34.89	127.78	112.29	240.07	38.69	14.53	53.23	46.77		Rudstone
27	28.11.2010	09:45	21.6	1.49	0.92	60-70	94.16	26.38	120.54	76.97	197.51	47.67	13.36	61.03	38.97		Rudstone
27	28.11.2010	09:45	21.6	1.49	0.92	70-80	104.97	22.80	127.77	60.18	187.95	55.85	12.13	67.98	32.02	x	Rudstone
27	28.11.2010	09:45	21.6	1.49	0.92	80-92(CC)	73.99	14.42	88.41	21.8	110.21	67.14	13.08	80.22	19.78		Rudstone
30	30.11.2010	10:20	37.6	0.70	0.59	0-5	64.73	88.47	153.20	36.48	189.68	34.13	46.64	80.77	19.23		Rudstone
30	30.11.2010	10:20	37.6	0.70	0.59	5-10	30.53	66.95	97.48	41.45	138.93	21.98	48.19	70.16	29.84	x	Rudstone
30	30.11.2010	10:20	37.6	0.70	0.59	10-20	110.92	81.61	192.53	66.3	258.83	42.85	31.53	74.38	25.62		Rudstone
30	30.11.2010	10:20	37.6	0.70	0.59	20-27	76.24	77.28	153.52	53.64	207.16	36.80	37.30	74.11	25.89	x	Rudstone
30	30.11.2010	10:20	37.6	0.70	0.59	27-35	131.89	97.92	229.81	63.91	293.72	44.90	33.34	78.24	21.76		Rudstone
30	30.11.2010	10:20	37.6	0.70	0.59	35-40	80.50	30.66	111.16	24.83	135.99	59.20	22.55	81.74	18.26	x	Rudstone
30	30.11.2010	10:20	37.6	0.70	0.59	40-50	166.51	26.29	192.80	18.83	211.63	78.68	12.42	91.10	8.90	x	Rudstone
30	30.11.2010	10:20	37.6	0.70	0.59	50-59(CC)	34.32	32.70	67.02	21.24	88.26	38.89					

Appendix

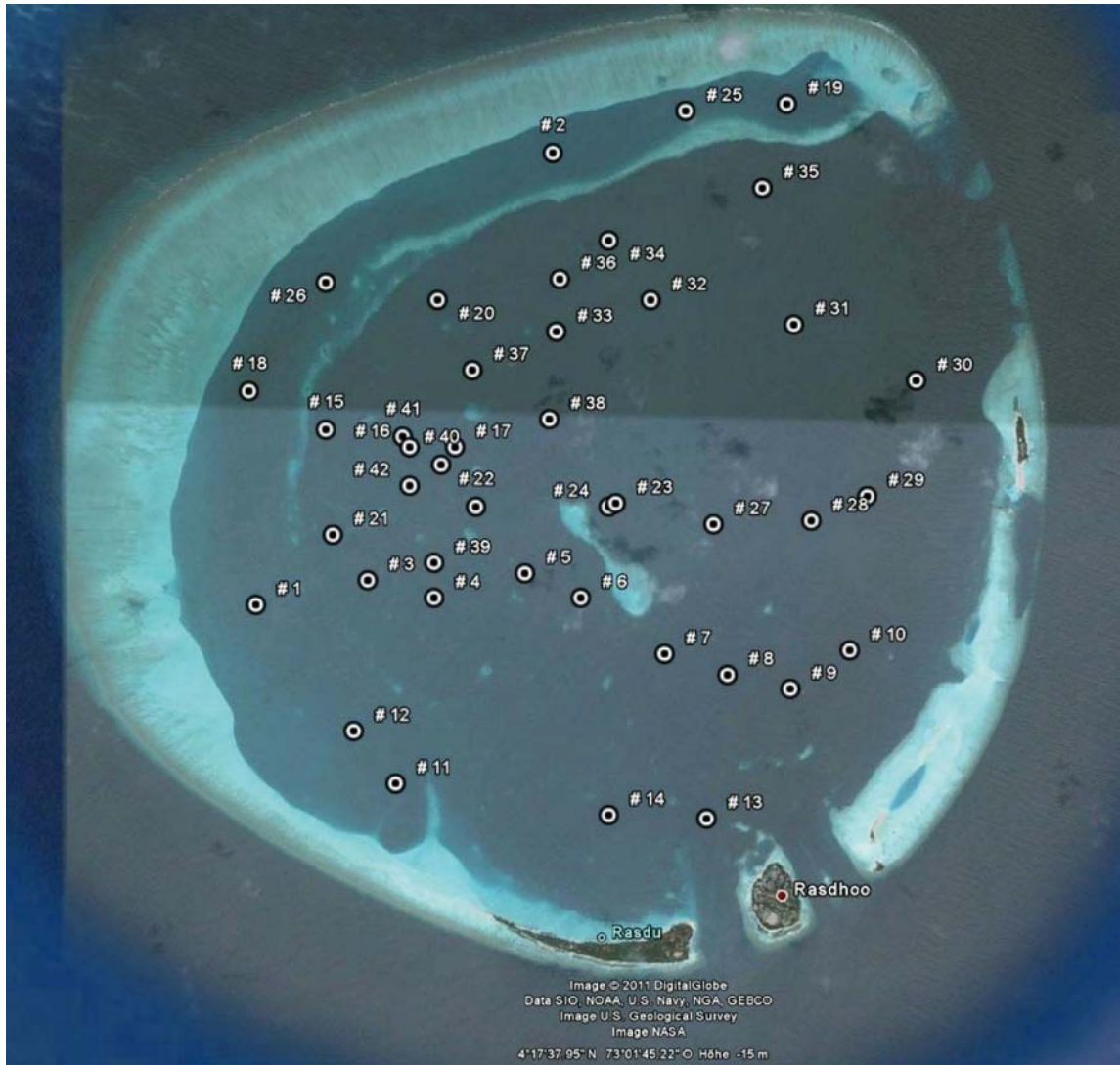
Thin Section Point Counting Data																			
Core #	Sample depth (cm)	Foraminifera	Red Algae	Fecal Pellets	Echinodermata	Corals	Mollusca	Assini	Pteropoda	Bivalvia	Gastropoda	Nautiloida	Aggregates	?	Opaque	Miliolid Forams	Cymbaloporetta	Crustacea	Total
		n %	n %	n %	n %	n %	n %	n %	n %	n %	n %	n %	n %	n %	n %	n %	n %	n %	n %
16	5-10	3 1.00	0 0.00	55 18.33	8 2.67	0 0.00	153 51.00	0 0.00	2 0.67	15 5.00	60 20.00	0 0.00	0 0.00	0 0.00	0 0.00	0 0.00	0 0.00	0 0.00	300 100
16	15-20	1 0.33	0 0.00	101 33.67	5 1.67	0 0.00	124 41.33	0 0.00	11 3.67	6 2.00	49 16.33	0 0.00	0 0.00	0 0.00	0 0.00	0 0.00	0 0.00	0 0.00	3 1.00
16	25-30	4 1.33	0 0.00	19 6.33	3 1.00	0 0.00	152 50.67	0 0.00	5 1.67	30 10.00	79 26.33	2 0.67	0 0.00	0 0.00	0 0.00	0 0.00	0 0.00	0 0.00	5 1.67
16	35-40	5 1.67	0 0.00	56 18.67	6 2.00	1 0.33	175 58.33	0 0.00	2 0.67	15 5.00	37 12.33	0 0.00	0 0.00	0 0.00	0 0.00	0 0.00	0 0.00	0 0.00	1 0.33
16	45-50	18 6.00	0 0.00	44 14.67	6 2.00	0 0.00	180 60.00	0 0.00	8 2.67	4 1.33	38 12.67	1 0.33	0 0.00	0 0.00	0 0.00	0 0.00	0 0.00	0 0.00	0 0.00
16	55-60	19 6.33	0 0.00	47 15.67	2 0.67	0 0.00	137 45.67	0 0.00	7 2.33	28 9.33	59 19.67	0 0.00	0 0.00	0 0.00	0 0.00	0 0.00	0 0.00	0 0.00	0 0.00
16	65-70	18 6.00	0 0.00	58 19.33	2 0.67	0 0.00	137 45.67	0 0.00	10 3.33	29 9.67	43 14.33	0 0.00	0 0.00	0 0.00	0 0.00	0 0.00	0 0.00	0 0.00	2 0.67
16	75-80	33 11.00	0 0.00	50 16.67	2 0.67	0 0.00	147 49.00	0 0.00	9 3.00	23 7.67	35 11.67	0 0.00	0 0.00	0 0.00	0 0.00	0 0.00	0 0.00	0 0.00	1 0.33
16	85-90	28 9.33	0 0.00	21 7.00	11 3.67	0 0.00	137 45.67	0 0.00	18 6.00	47 15.67	35 11.67	0 0.00	0 0.00	0 0.00	0 0.00	0 0.00	0 0.00	0 0.00	3 1.00
16	95-100	59 19.67	0 0.00	25 8.33	1 0.33	0 0.00	159 53.00	0 0.00	8 2.67	20 6.67	26 8.67	0 0.00	0 0.00	0 0.00	0 0.00	0 0.00	0 0.00	0 0.00	1 0.33
16	105-110	30 10.00	0 0.00	16 5.33	3 1.00	0 0.00	155 51.67	0 0.00	10 3.33	32 10.67	48 16.00	0 0.00	0 0.00	0 0.00	0 0.00	0 0.00	0 0.00	0 0.00	3 1.00
16	115-120	38 12.67	0 0.00	14 4.67	4 1.33	0 0.00	160 53.33	0 0.00	15 5.00	33 11.00	52 17.33	0 0.00	0 0.00	0 0.00	0 0.00	0 0.00	0 0.00	0 0.00	1 0.33
16	125-130	31 10.33	0 0.00	15 5.00	3 1.00	0 0.00	144 48.00	0 0.00	20 6.67	22 7.33	57 19.00	0 0.00	0 0.00	0 0.00	0 0.00	0 0.00	0 0.00	0 0.00	0 0.00
16	135-140	23 7.67	0 0.00	17 5.67	3 1.00	0 0.00	159 53.00	0 0.00	14 4.67	24 8.00	52 17.33	0 0.00	0 0.00	0 0.00	0 0.00	0 0.00	0 0.00	0 0.00	1 0.33
16	145-150	19 6.33	0 0.00	16 5.33	7 2.33	0 0.00	131 43.67	0 0.00	12 4.00	19 6.33	92 30.67	0 0.00	0 0.00	0 0.00	0 0.00	0 0.00	0 0.00	0 0.00	4 1.33
16	155-160	24 8.00	0 0.00	14 4.67	5 1.67	0 0.00	139 46.33	0 0.00	12 4.00	26 8.67	68 22.67	0 0.00	0 0.00	0 0.00	0 0.00	0 0.00	0 0.00	0 0.00	10 3.33
16	165-170	16 5.33	2 0.67	26 8.67	3 1.00	0 0.00	116 38.67	0 0.00	2 0.67	34 11.33	90 30.00	0 0.00	0 0.00	0 0.00	0 0.00	0 0.00	0 0.00	0 0.00	5 1.67
16	175-180	21 7.00	0 0.00	30 10.00	3 1.00	0 0.00	131 43.67	0 0.00	2 0.67	26 8.67	78 26.00	0 0.00	0 0.00	0 0.00	0 0.00	0 0.00	0 0.00	0 0.00	5 1.67
16	185-190	21 7.00	0 0.00	12 4.00	3 1.00	0 0.00	140 46.67	1 0.33	9 3.00	19 6.33	88 29.33	0 0.00	0 0.00	0 0.00	0 0.00	0 0.00	0 0.00	0 0.00	3 1.00
16	195-200	12 4.00	0 0.00	29 9.67	0 0.00	0 0.00	152 50.67	0 0.00	6 2.00	25 8.33	68 22.67	0 0.00	0 0.00	0 0.00	0 0.00	0 0.00	0 0.00	0 0.00	2 0.67
16	205-210	25 8.33	0 0.00	22 7.33	0 0.00	0 0.00	97 32.33	6 2.00	3 1.00	30 10.00	111 37.00	0 0.00	0 0.00	0 0.00	0 0.00	0 0.00	0 0.00	0 0.00	5 1.67
16	215-220	13 4.33	0 0.00	33 11.00	1 0.33	0 0.00	144 48.00	2 0.67	7 2.33	19 6.33	68 22.67	0 0.00	0 0.00	0 0.00	0 0.00	0 0.00	0 0.00	0 0.00	6 2.00
16	225-230	22 7.33	0 0.00	29 9.67	1 0.33	0 0.00	129 43.00	0 0.00	11 3.67	30 10.00	68 22.67	0 0.00	0 0.00	0 0.00	0 0.00	0 0.00	0 0.00	0 0.00	2 0.67
16	235-240	19 6.33	0 0.00	19 6.33	5 1.67	0 0.00	111 37.00	5 1.67	10 3.33	29 9.67	84 28.00	0 0.00	0 0.00	0 0.00	0 0.00	0 0.00	0 0.00	0 0.00	3 1.00
16	245-250	33 11.00	0 0.00	19 6.33	6 2.00	0 0.00	125 41.67	3 1.00	9 3.00	10 3.33	75 25.00	0 0.00	0 0.00	0 0.00	0 0.00	0 0.00	0 0.00	0 0.00	5 1.67
16	255-260	12 4.00	0 0.00	19 6.33	14 4.67	0 0.00	143 47.67	3 1.00	6 2.00	27 9.00	62 20.67	0 0.00	0 0.00	0 0.00	0 0.00	0 0.00	0 0.00	0 0.00	5 1.67
16	265-270	23 7.67	0 0.00	26 8.67	16 5.33	0 0.00	126 42.00	0 0.00	10 3.33	30 10.00	59 19.67	0 0.00	0 0.00	0 0.00	0 0.00	0 0.00	0 0.00	0 0.00	5 1.67
16	275-280	16 5.33	0 0.00	6 2.00	11 3.67	0 0.00	180 60.00	2 0.67	3 1.00	6 2.00	55 18.33	0 0.00	0 0.00	0 0.00	0 0.00	0 0.00	0 0.00	0 0.00	1 0.33
16	285-290	19 6.33	0 0.00	12 4.00	9 3.00	0 0.00	153 51.00	11 3.67	5 1.67	25 8.33	50 16.67	0 0.00	0 0.00	0 0.00	0 0.00	0 0.00	0 0.00	0 0.00	3 1.00
16	295-300	16 5.33	0 0.00	12 4.00	10 3.33	0 0.00	147 49.00	14 4.67	11 3.67	21 7.00	46 15.33	0 0.00	0 0.00	0 0.00	0 0.00	0 0.00	0 0.00	0 0.00	2 0.67
16	305-310	11 3.67	0 0.00	16 5.33	6 2.00	0 0.00	128 42.67	7 2.33	5 1.67	34 11.33	71 23.67	0 0.00	0 0.00	0 0.00	0 0.00	0 0.00	0 0.00	0 0.00	3 1.00
16	315-320	20 6.67	0 0.00	5 1.67	11 3.67	0 0.00	139 46.33	11 3.67	5 1.67	38 12.67	48 16.00	0 0.00	0 0.00	0 0.00	0 0.00	0 0.00	0 0.00	0 0.00	10 3.33
16	325-330	3 1.00	0 0.00	7 2.33	3 1.00	0 0.00	144 48.00	15 5.00	4 1.33	19 6.33	59 19.67	0 0.00	0 0.00	0 0.00	0 0.00	0 0.00	0 0.00	0 0.00	9 3.00
16	335-340	7 2.33	0 0.00	4 1.33	4 1.33	0 0.00	120 40.00	8 2.67	8 2.67	48 16.00	68 22.67	3 1.00	0 0.00	0 0.00	0 0.00	0 0.00	0 0.00	0 0.00	3 1.00
16	345-350	7 2.33	0 0.00	2 0.67	13 4.33	47 15.67	91 30.33	11 3.67	0 0.00	18 6.00	77 25.67	7 2.33	0 0.00	0 0.00	0 0.00	0 0.00	0 0.00	0 0.00	4 1.33
16	355-360	9 3.00	0 0.00	0 0.00	2 0.67	92 30.67	71 23.67	5 1.67	1 0.33	69 23.00	26 8.67	0 0.00	0 0.00	0 0.00	0 0.00	0 0.00	0 0.00	0 0.00	25 8.33
16	365-370	7 2.33	0 0.00	1 0.33	10 3.33	0 0.00	126 42.00	7 2.33	8 2.67	22 7.33	87 29.00	0 0.00	0 0.00	0 0.00	0 0.00	0 0.00	0 0.00	0 0.00	14 4.67
16	375-380	19 6.33	0 0.00	3 1.00	13 4.33	7 2.33	137 45.67	16 5.33	6 2.00	7 2.33	39 13.00	1 0.33	0 0.00	0 0.00	0 0.00	0 0.00	0 0.00	0 0.00	27 9.00
16	385-390	5 1.67	0 0.00	0 0.00	21 7.00	1 0.33	80 26.67	18 6.00	13 4.33	92 30.67	30 10.00	7 2.33	0 0.00	0 0.00	0 0.00	0 0.00	0 0.00	0 0.00	29 9.67
16	395-400	16 5.33	0 0.00	2 0.67	12 4.00	24 8.00	117 39.00	12 4.00	8 2.67	32 10.67	21 7.00	1 0.33	0 0.00	0 0.00	0 0.00	0 0.00	0 0.00	0 0.00	30 10.00
16	405-410	7 2.33	0 0.00	0 0.00	9 3.00	0 0.00	99 33.00	7 2.33	1 0.33	41 13.67	70 23.33	1 0.33	0 0.00	0 0.00	0 0.00	0 0.00	0 0.00	0 0.00	18 6.00
16	415-420	7 2.33	0 0.00	0 0.00	5 1.67	0 0.00	92 30.67	0 0.00	0 0.00	56 18.00	21 7.00	1 0.33	0 0.00	0 0.00	0 0.00	0 0.00	0 0.00	0 0.00	17 5.67
16	425-430	6 3.75	0 0.00	0 0.00	4 2.50	0 0.00	57 35.63	0 0.00	0 0.00	10 3.33	6 2.00	0 0.00	0 0.00	0 0.00	0 0.00	0 0.00	0 0.00	0 0.00	4 2.50
16	435-440	1 0.44	14 6.22	0 0.00	3 1.33	2 0.89	67 25.78	0 0.00	2 0.89	48 16.00	25 8.33	0 0.00	0 0.00	0 0.00	0 0.00	0 0.00	0 0.00	0 0.00	6 2.67
16	445-450	1 1.61	11 17.74	0 0.00	0 0.00	3 4.84	14 22.58	0 0.00	0 0.00	8 2.67	2 3.23	0 0.00	0 0.00	0 0.00	0 0.00	0 0.00	0 0.00	0 0.00	1 1.61
19	5-10	18 6.00	8 2.67	3 1.00	1 0.33	132 44.00	77 25.67	0 0.00	1 0.33	1 0.33	44 14.67	0 0.00	0 0.00	0 0.00	0 0.00	0 0.00	0 0.00	0 0.00	4 1.33
19	15-20	14 4.67	5 1.67	1 0.33	0 0.00	146 48.67	45 15.00	0 0.00	1 0.33	0 0.00	3 1.00	67 22.33	0 0.00	2 0.67	0 0.00	12 4.00	0 0.00	0 0.00	4 1.33
19	25-30	14 4.67	8 2.67	7 2.33	3 1.00	142 47.33	35 11.6												

Appendix

Thin Section Point Counting Data (continued)

Core #	Sample depth (cm)	Foraminifera n %	Red Algae n %	Fecal Pellets n %	Echinodermata n %	Corals n %	Mollusca n %	Assimina n %	Pteropoda n %	Bivalvia n %	Gastropoda n %	Holimeda n %	Aggregates n %	?	Opaque n %	Miliolid Foram n %	Cymbaloporetta n %	Crustacea n %	Total n %	
8	10-20	18 9.00	80 40.00	0 0.00	12 6.00	42 21.00	26 13.00	0 0.00	0 0.00	0 0.00	3 1.50	12 6.00	0 0.00	0 0.00	0 0.00	4 2.00	0 0.00	3 1.50	200 100	
8	20-30	21 10.50	73 36.50	0 0.00	5 2.50	26 13.00	31 15.50	9 4.50	0 0.00	2 1.00	10 5.00	11 5.50	0 0.00	0 0.00	0 0.00	6 3.00	0 0.00	6 3.00	200 100	
8	40-50	24 12.00	39 19.50	0 0.00	0 0.00	71 35.50	40 20.00	7 3.50	0 0.00	2 1.00	8 4.00	0 0.00	0 0.00	0 0.00	0 0.00	6 3.00	0 0.00	3 1.50	200 100	
8	50-60	25 12.50	46 23.00	0 0.00	9 4.50	47 23.50	43 21.50	9 4.50	1 0.50	4 2.00	8 4.00	5 2.50	0 0.00	0 0.00	0 0.00	1 0.50	1 0.50	1 0.50	200 100	
8	70-75	10 5.00	42 21.00	0 0.00	4 2.00	76 38.00	45 22.50	4 2.00	0 0.00	0 0.00	12 6.00	3 1.50	0 0.00	0 0.00	0 0.00	3 1.50	0 0.00	1 0.50	200 100	
8	95-105	16 8.00	69 34.50	0 0.00	5 2.50	41 20.50	47 23.50	2 1.00	0 0.00	0 0.00	8 4.00	4 2.00	0 0.00	0 0.00	0 0.00	3 1.50	0 0.00	3 1.50	200 100	
8	115-125	11 5.50	58 29.00	0 0.00	12 6.00	50 25.00	50 25.00	2 1.00	0 0.00	0 0.00	7 3.50	3 1.50	0 0.00	0 0.00	0 0.00	6 3.00	1 0.50	0 0.00	200 100	
8	125-130	23 11.50	34 17.00	0 0.00	3 1.50	42 21.00	67 33.50	7 3.50	0 0.00	0 0.00	0 0.00	23 11.50	0 0.00	0 0.00	0 0.00	1 0.50	0 0.00	0 0.00	200 100	
8	130-140	25 12.50	75 37.50	0 0.00	4 2.00	41 20.50	43 21.50	0 0.00	1 0.50	0 0.00	2 1.00	2 1.00	0 0.00	0 0.00	0 0.00	6 3.00	0 0.00	1 0.50	200 100	
8	140-150	14 7.00	73 36.50	0 0.00	4 2.00	39 19.50	51 25.50	3 1.50	0 0.00	1 0.50	2 1.00	7 3.50	0 0.00	0 0.00	1 0.50	4 2.00	0 0.00	1 0.50	200 100	
8	170-180	19 9.50	59 29.50	0 0.00	15 7.50	59 29.50	34 17.00	1 0.50	0 0.00	1 0.50	4 2.00	2 1.00	0 0.00	0 0.00	0 0.00	3 1.50	0 0.00	3 1.50	200 100	
29	10-20	14 7.00	76 38.00	0 0.00	2 1.00	54 27.00	28 14.00	4 2.00	2 1.00	1 0.50	7 3.50	5 2.50	0 0.00	0 0.00	0 0.00	4 2.00	0 0.00	4 2.00	200 100	
29	30-35	12 6.00	41 20.50	0 0.00	2 1.00	97 48.50	27 13.50	0 0.00	0 0.00	2 1.00	3 1.50	11 5.50	0 0.00	0 0.00	0 0.00	1 0.50	3 1.50	0 0.00	1 0.50	200 100
29	35-42	27 13.50	47 23.50	0 0.00	5 2.50	59 29.50	36 18.00	4 2.00	0 0.00	4 2.00	3 1.50	1 0.50	0 0.00	0 0.00	0 0.00	9 4.50	0 0.00	5 2.50	200 100	
29	42-55	12 6.00	45 22.50	0 0.00	3 1.50	80 40.00	43 21.50	0 0.00	0 0.00	0 0.00	0 0.00	3 1.50	0 0.00	0 0.00	0 0.00	1 0.50	3 1.50	0 0.00	0 0.00	200 100
29	61-66	17 8.50	51 25.50	0 0.00	10 5.00	69 34.50	36 18.00	0 0.00	0 0.00	1 0.50	9 4.50	2 1.00	0 0.00	0 0.00	0 0.00	0 0.00	1 0.50	4 2.00	2.00	200 100
29	73-80	20 10.00	25 12.50	0 0.00	8 4.00	94 47.00	39 19.50	1 0.50	0 0.00	0 0.00	2 1.00	5 2.50	0 0.00	0 0.00	0 0.00	6 3.00	0 0.00	0 0.00	0 0.00	200 100
29	80-90	10 5.00	62 31.00	0 0.00	3 1.50	47 23.50	41 20.50	0 0.00	0 0.00	4 2.00	22 11.00	0 0.00	0 0.00	0 0.00	0 0.00	8 4.00	0 0.00	3 1.50	200 100	
29	90-98	25 12.50	30 15.00	0 0.00	3 1.50	69 34.50	58 29.00	1 0.50	0 0.00	2 1.00	2 1.00	1 0.50	0 0.00	0 0.00	0 0.00	6 3.00	0 0.00	3 1.50	200 100	
29	110-120	11 5.50	64 32.00	0 0.00	8 4.00	53 26.50	39 19.50	4 2.00	0 0.00	1 0.50	12 6.00	2 1.00	0 0.00	0 0.00	0 0.00	3 1.50	1 0.50	2 1.00	200 100	
29	120-130	21 10.50	54 27.00	0 0.00	5 2.50	52 26.00	52 26.00	3 1.50	0 0.00	1 0.50	2 1.00	2 1.00	0 0.00	0 0.00	0 0.00	7 3.50	0 0.00	1 0.50	200 100	
13	10-23	19 9.50	64 32.00	0 0.00	3 1.50	57 28.50	27 13.50	5 2.50	0 0.00	0 0.00	5 2.50	18 9.00	0 0.00	0 0.00	0 0.00	1 0.50	0 0.00	1 0.50	200 100	
13	30-40	19 9.50	38 19.00	0 0.00	3 1.50	64 32.00	34 17.00	8 4.00	0 0.00	2 1.00	0 0.00	25 12.50	0 0.00	1 0.50	0 0.00	4 2.00	0 0.00	2 1.00	200 100	
13	50-60	7 3.50	36 18.00	0 0.00	6 3.00	79 39.50	27 13.50	2 1.00	0 0.00	0 0.00	2 1.00	35 17.50	0 0.00	0 0.00	0 0.00	9 4.50	0 0.00	5 2.50	200 100	
13	60-70	14 7.00	24 12.00	0 0.00	3 1.50	93 46.50	37 18.50	1 0.50	0 0.00	0 0.00	4 2.00	31 15.50	0 0.00	0 0.00	0 0.00	3 1.50	0 0.00	0 0.00	0 0.00	200 100
13	80-90	15 7.50	27 13.50	0 0.00	2 1.00	80 40.00	36 18.00	2 1.00	1 0.50	0 0.00	5 2.50	27 13.50	0 0.00	0 0.00	0 0.00	4 2.00	0 0.00	1 0.50	200 100	
13	107-116	16 8.00	33 16.50	0 0.00	2 1.00	63 31.50	37 18.50	1 0.50	0 0.00	0 0.00	6 3.00	35 17.50	0 0.00	0 0.00	0 0.00	5 2.50	0 0.00	2 1.00	200 100	
13	116-125	16 8.00	26 13.00	0 0.00	2 1.00	62 31.00	32 16.00	5 2.50	0 0.00	3 1.50	3 1.50	47 23.50	0 0.00	0 0.00	0 0.00	3 1.50	0 0.00	1 0.50	200 100	
13	125-135	18 9.00	16 8.00	0 0.00	11 5.50	63 31.50	24 12.00	1 0.50	0 0.00	1 0.50	1 0.50	63 31.50	0 0.00	0 0.00	0 0.00	2 1.00	0 0.00	0 0.00	0 0.00	200 100
13	145-155	11 5.50	47 23.50	0 0.00	2 1.00	61 30.50	20 10.00	0 0.00	0 0.00	0 0.00	3 1.50	53 26.50	0 0.00	0 0.00	0 0.00	3 1.50	0 0.00	0 0.00	0 0.00	200 100
18	0-10	20 10.00	30 15.00	0 0.00	4 2.00	22 11.00	78 39.00	0 0.00	0 0.00	2 1.00	7 3.50	24 12.00	0 0.00	0 0.00	0 0.00	10 5.00	0 0.00	3 1.50	200 100	
18	20-30	10 5.00	26 13.00	0 0.00	1 0.50	32 16.00	86 43.00	0 0.00	0 0.00	6 3.00	3 1.50	26 13.00	0 0.00	0 0.00	0 0.00	10 5.00	0 0.00	0 0.00	0 0.00	200 100
18	60-70	13 6.50	35 17.50	0 0.00	3 1.50	29 14.50	79 39.50	1 0.50	0 0.00	3 1.50	8 4.00	17 8.50	0 0.00	0 0.00	1 0.50	10 5.00	0 0.00	1 0.50	200 100	
18	80-90	7 3.50	42 21.00	0 0.00	2 1.00	52 26.00	45 22.50	0 0.00	0 0.00	14 7.00	8 4.00	10 5.00	0 0.00	0 0.00	0 0.00	9 4.50	0 0.00	5 2.50	200 100	
18	120-130	20 10.00	42 21.00	0 0.00	3 1.50	35 17.50	62 31.00	0 0.00	1 0.50	4 2.00	17 8.50	11 5.50	0 0.00	0 0.00	0 0.00	5 2.50	0 0.00	0 0.00	0 0.00	200 100
18	145-150	6 3.00	27 13.50	0 0.00	2 1.00	42 21.00	78 39.00	0 0.00	0 0.00	10 5.00	17 8.50	11 5.50	0 0.00	0 0.00	0 0.00	7 3.50	0 0.00	0 0.00	0 0.00	200 100
18	170-180	9 4.50	36 18.00	0 0.00	1 0.50	14 7.00	90 45.00	1 0.50	1 0.50	7 3.50	20 10.00	6 3.00	0 0.00	0 0.00	0 0.00	13 6.50	1 0.50	1 0.50	200 100	
18	210-220	9 4.50	27 13.50	0 0.00	3 1.50	24 12.00	95 47.50	1 0.50	0 0.00	5 2.50	12 6.00	5 2.50	0 0.00	0 0.00	0 0.00	10 5.00	0 0.00	9 4.50	200 100	
18	230-240	4 2.00	18 9.00	0 0.00	2 1.00	35 17.50	86 43.00	0 0.00	0 0.00	8 4.00	26 13.00	7 3.50	0 0.00	0 0.00	0 0.00	6 3.00	0 0.00	8 4.00	200 100	
18	250-260	4 2.00	23 11.50	0 0.00	2 1.00	49 24.50	72 36.00	0 0.00	0 0.00	6 3.00	30 15.00	9 4.50	0 0.00	0 0.00	0 0.00	1 0.50	0 0.00	4 2.00	200 100	
18	270-275	9 4.50	26 13.00	0 0.00	1 0.50	20 10.00	95 47.50	0 0.00	0 0.00	10 5.00	26 13.00	6 3.00	0 0.00	0 0.00	0 0.00	3 1.50	0 0.00	4 2.00	200 100	
18	275-280	1 0.50	22 11.00	0 0.00	4 2.00	19 9.50	117 58.50	0 0.00	0 0.00	11 5.50	6 3.00	16 8.00	0 0.00	0 0.00	0 0.00	4 2.00	0 0.00	0 0.00	0 0.00	200 100
18	280-288	3 1.50	33 16.50	0 0.00	0 0.00	46 23.00	94 47.00	0 0.00	0 0.00	2 1.00	14 7.00	2 1.00	0 0.00	0 0.00	0 0.00	3 1.50	0 0.00	1 0.50	200 100	
18	288-295	9 4.50	43 21.50	0 0.00	0 0.00	28 14.00	82 41.00	0 0.00	0 0.00	11 5.50	10 5.00	10 5.00	0 0.00	0 0.00	0 0.00	2 1.00	0 0.00	3 1.50	200 100	
18	300-310	7 3.50	43 21.50	0 0.00	7 3.50	19 9.50	83 41.50	0 0.00	0 0.00	3 1.50	16 8.00	10 5.00	0 0.00	0 0.00	0 0.00	9 4.50	0 0.00	3 1.50	200 100	
18	310-317	9 4.50	44 22.00	0 0.00	2 1.00	32 16.00	74 37.00	0 0.00	0 0.00	7 3.50	20 10.00	7 3.50	0 0.00	0 0.00	0 0.00	4 2.00	0 0.00	1 0.50	200 100	
18	317-325	10 5.00	29 14.50	0 0.00	1 0.50	45 22.50	81 40.50	0 0.00	0 0.00	2 1.00	9 4.50	18 9.00	0 0.00	0 0.00	1 0.50	2 1.00	0 0.00	2 1.00	200 100	
18	325-337 (C)	7 3.50	51 25.50	0 0.00	2 1.00	24 12.00	83 41.50	0 0.00	0 0.00	4 2.00	10 5.00	6 3.00	0 0.00	0 0.00	0 0.00	7 3.50	0 0.00	6 3.00	200 100	
24	0-10	6 3.00	54 27.00	3 1.50	13 6.50	52 26.00	37 18.50	2 1.00	0 0.00	9 4.50	13 6.50	8 4.00	0 0.00	0 0.00	0 0.00	2 1.00	0 0.00	1 0.50	200 100	
24	21-24	6 3.00	67 33.50	0 0.00	8 4.00	25 12.50	40 20.00	5 2.50	0 0.00	3 1.50	19 9.50	22 11.00	0 0.00	0 0.00	0 0.00	4 2.00	0 0.00	1 0.50	200 100	
24	27-35	13 6.50	59 29.50	0 0.00	9 4.50	36 18.00	42 21.00	3 1.50	0 0.00	3 1.50	17 8.50	17 8.50	0 0.00	0 0.00	0 0.00	0 0.00	0 0.00	1 0.50	200 100	
24	40-50	9 4.50	62 31.00	0 0.00	7 3.50	42 21.00	50 25.00	5 2.50	0 0.00	0 0.00	3 1.50	14 7.00	0 0.00	0 0.00	0 0.00					

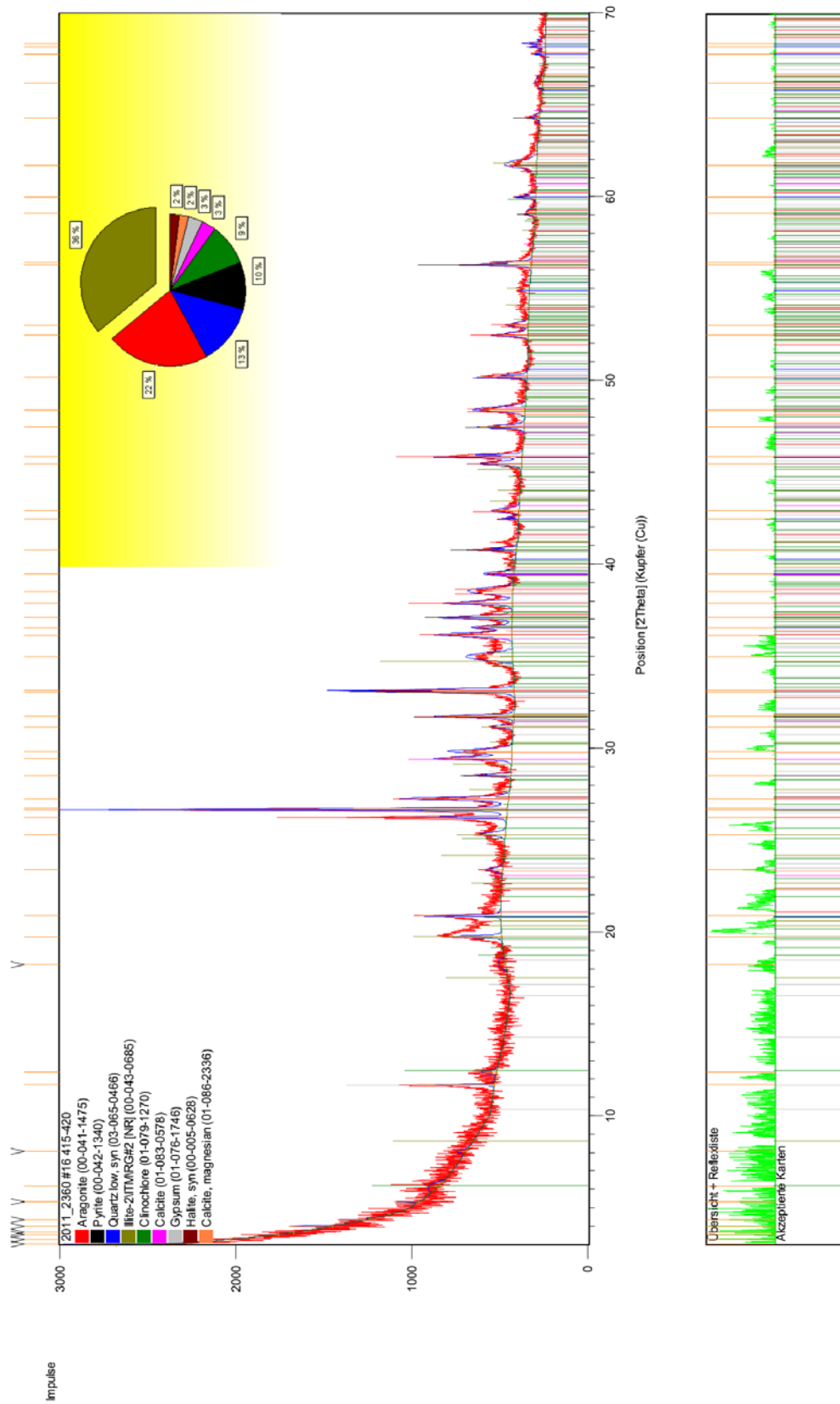
Rasdhoo Atoll map of stations



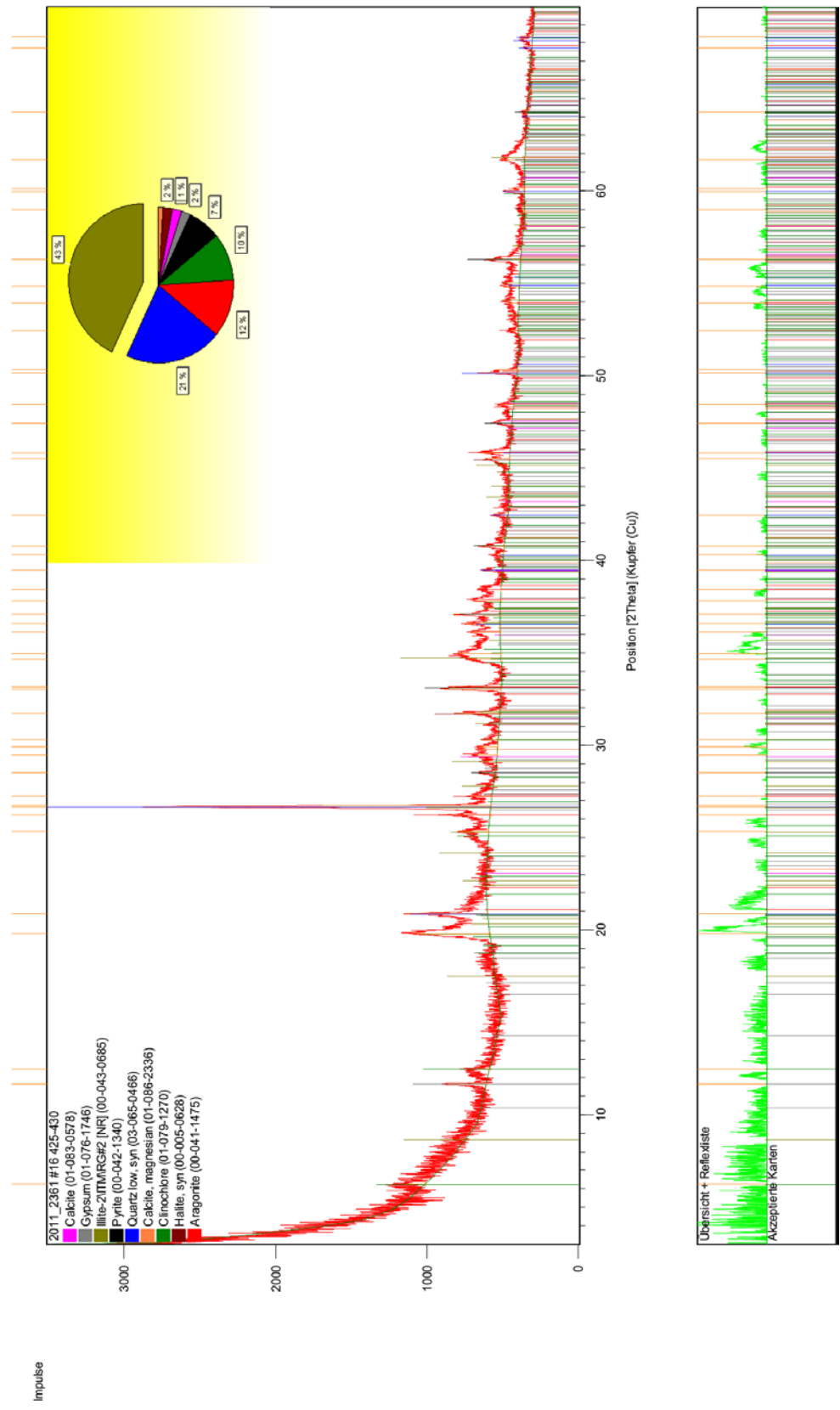
Rasdho Atoll: Station Coordinates & Recovery

Station #	Degree		Decimal		Core length [m]	Water depth [m]
	Latitude	Longitude	Latitude	Longitude		
1	04°17'11 N	72°57'03 E	4,286389	72,950833	2,65	15
2	04°19'20 N	72°58'28 E	4,322222	72,974444	1,95	10,7
3	04°17'18 N	72°57'35 E	4,288333	72,959722	0,94	21
4	04°17'13 N	72°57'54 E	4,286944	72,965	5,04	32
5	04°17'20 N	72°58'20 E	4,288889	72,972222	1,43	22,3
6	04°17'13 N	72°58'36 E	4,286944	72,976667	1,54	36
7	04°16'57 N	72°59'00 E	4,2825	72,983333	0,81	39,5
8	04°16'51 N	72°59'18 E	4,280833	72,988333	2,01	36,8
9	04°16'47 N	72°59'36 E	4,279722	72,993333	1,21	33,25
10	04°16'58 N	72°59'53 E	4,282778	72,998056	1,09	37,5
11	04°16'20 N	72°57'43 E	4,272222	72,961944	0,6	18
12	04°16'35 N	72°57'31 E	4,276389	72,958611	2,44	20
13	04°16'10 N	72°59'12 E	4,269444	72,986667	1,65	29,5
14	04°16'11 N	72°58'44 E	4,269722	72,978889	0	30
15	04°18'01 N	72°57'23 E	4,300278	72,956389	2,91	24,5
16	04°17'56 N	72°57'47 E	4,298889	72,963056	4,56	34,5
17	04°17'56 N	72°58'00 E	4,298889	72,966667	4,58	35
18	04°18'12 N	72°57'01 E	4,303333	72,950278	3,37	14,3
19	04°19'34 N	72°59'35 E	4,326111	72,993056	3,28	13,6
20	04°18'38 N	72°57'55 E	4,310556	72,965278	0,885	18,3
21	04°17'31 N	72°57'25 E	4,291944	72,956944	3,09	22
22	04°17'39 N	72°58'06 E	4,294167	72,968333	4,59	34
23	04°17'40 N	72°58'46 E	4,294444	72,979444	0	28
24	04°17'39 N	72°58'44 E	4,294167	72,978889	1,52	28,5
25	04°19'32 N	72°59'06 E	4,325556	72,985	1,81	11,7
26	04°18'43 N	72°57'23 E	4,311944	72,956389	1,95	12,6
27	04°17'34 N	72°59'14 E	4,292778	72,987222	0,92	21,6
28	04°17'35 N	72°59'42 E	4,293056	72,995	0,81	38,2
29	04°17'42 N	72°59'58 E	4,295	72,999444	1,42	37,5
30	04°18'15 N	73°00'12 E	4,304167	73,003333	0,59	37,6
31	04°18'31 N	72°59'37 E	4,308611	72,993611	1,26	37
32	04°18'38 N	72°58'56 E	4,310556	72,982222	2,85	35,6
33	04°18'29 N	72°58'29 E	4,308056	72,974722	0	33,4
34	04°18'55 N	72°58'44 E	4,315278	72,978889	4,01	30
35	04°19'10 N	72°59'28 E	4,319444	72,991111	1,23	36,3
36	04°18'44 N	72°58'30 E	4,312222	72,975	2,695	29,2
37	04°18'18 N	72°58'05 E	4,305	72,968056	4,71	33,8
38	04°18'04 N	72°58'27 E	4,301111	72,974167	1,5	34,4
39	04°17'23 N	72°57'54 E	4,289722	72,965	3,19	31,2
40	04°17'51 N	72°57'56 E	4,2975	72,965556	4,23	33
41	04°17'59 N	72°57'45 E	4,299722	72,9625	3,24	33,2
42	04°17'45 N	72°57'47 E	4,295833	72,963056	4,43	32,5

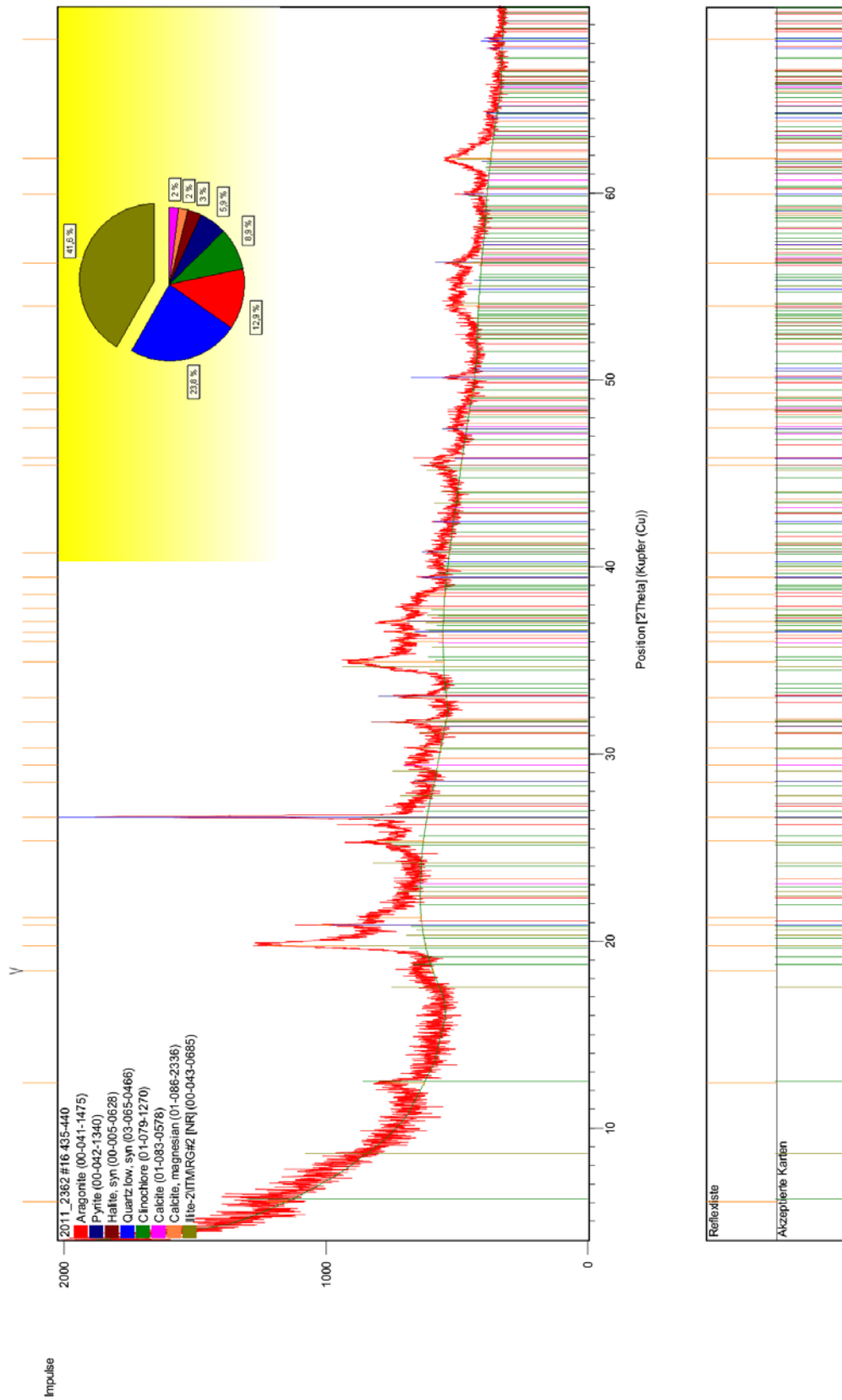
XRD results soil sample core #16 415-420



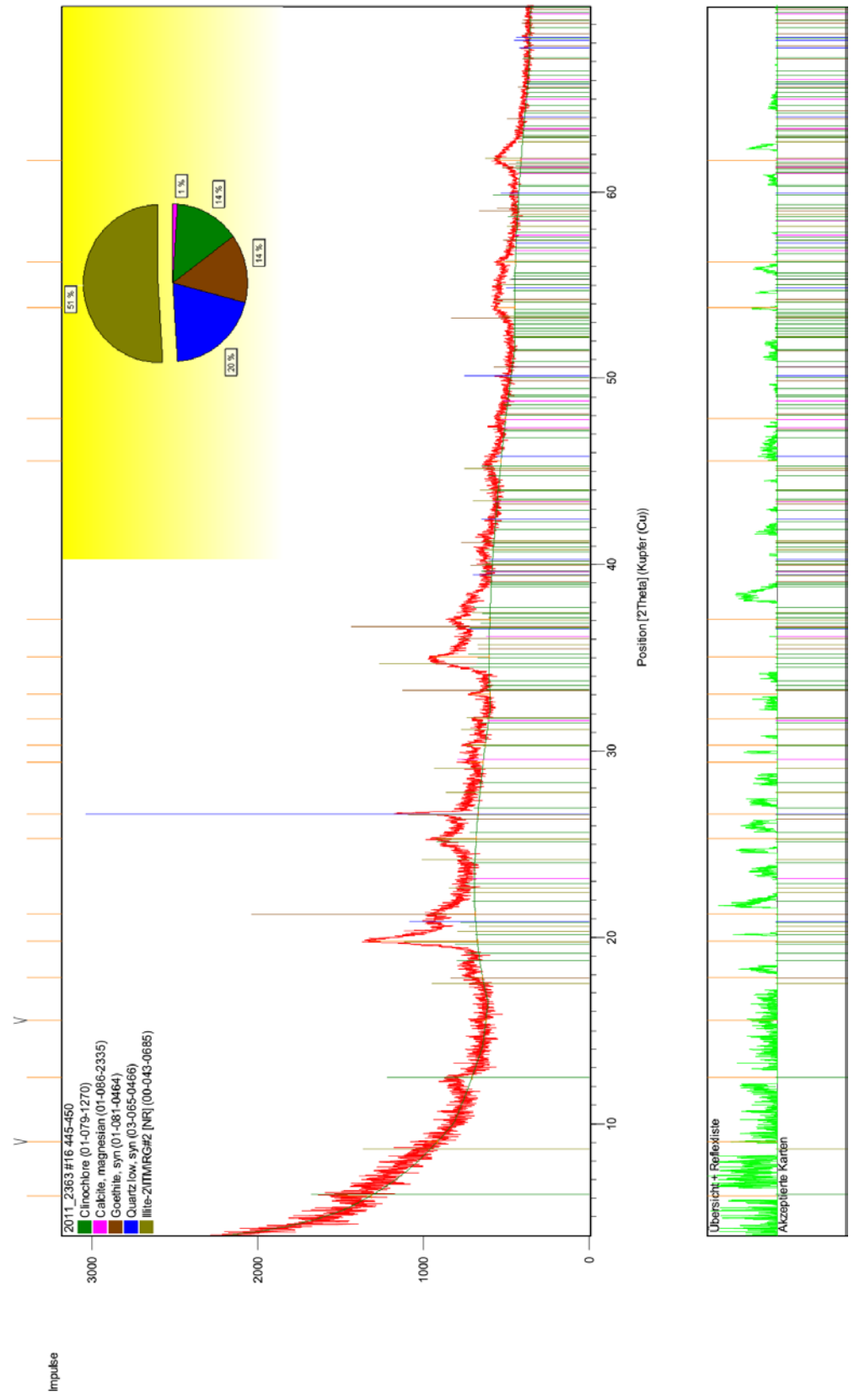
XRD results soil sample core #16 425-430



XRD results soil sample core #16 435-440



XRD results soil sample core #16 445-450



Karbonatgehaltsbestimmung nach Scheibler

Eichproben-Nr.	Gewicht Eichprobe [mg]	Skalenwert	mg/100 Skalenteile	
I (E1)	320	73,4	435,967	435,629
II (13)	370	85	435,291	
III (26)	310	67,2	461,31	

Probennummer	Gewicht Probe [mg]	Skalenwert	% Karbonat	
#16 415-420 (2)	256	16	27,23	27,905
#16 415-420 (5)	253	16,6	28,58	
#16 425-430 (6)	257	6,8	11,53	11,895
#16 425-430 (7)	263	7,4	12,26	
#16 435-440 (10)	256	4,7	8	8,29
#16 435-440 (11)	254	5	8,58	
#16 445-450 (17)	260	2,9	4,86	5,555
#16 445-450 (20)	258	3,7	6,25	